Panton–Valentine leucocidin colocalized with retinal neurons cells and incited early retinal inflammation through rabbit endophthalmitis and retinal explant models

Xuanli Liu

UNIVERSITÉ DE STRASBOURG

ÉCOLE DOCTORALE DES SCIENCES DE LA VIE ET DE LA SANTE

Virulence bactérienne précoce: EA 7290

THÈSE présentée par :

Xuanli LIU

soutenue le : **28 Septembre 2018**

Pour obtenir le grade de : **Docteur de l'université de Strasbourg**

Discipline/ Spécialité : Sciences médicales- médecine

Rôle de la leucocidine de Panton-Valentine dans l'infection oculaire *staphylococcique*

Etude des cibles cellulaires et des conséquences inflammatoires tissulaires rétiniennes sur des modèles d'endophtalmie *in vivo* et *ex vivo* chez le lapin

THÈSE dirigée par :

Mr GAUCHER David	Professeur, Université de Strasbourg
Mr PREVOST Gilles	Docteur, Université de Strasbourg

RAPPORTEURS :

Mr RENDON Alvaro	Docteur émérite, Sorbonne Université
Mr WOLFENSBERGER Thomas Jona	Professeur, Université de Lausanne

AUTRES MEMBRES DU JURY :

Mme TOTI Florence	Docteur, Université de Strasbourg

Remerciements

Mes plus vifs remerciements vont au Dr Gilles Prévost et au Pr David Gaucher, qui m'ont accueilli dans leur laboratoire à l'Université de Strasbourg, me permettant de soutenir ma thèse en science. Je leur sais grée de l'aide qu'ils m'ont apporté dans l'obtention de la bourse de l'état Chinois.

Merci au Dr Gilles Prévost qui m'a fait confiance, encourageant mes initiatives tout en me guidant pendant 3 années en me prodiguant de précieux conseils utiles pour ma carrière de chercheuse.

Au Pr David Gaucher, qui m'a connu dans le Service d'Ophtalmologie des HUS pendant mon stage dans un cadre du programme d'échange avec l'Université Médicale de Chongqing (en Chine). Particulièrement merci pour tous les conseils sur les aspects relatifs à l'œil du lapin, pour les collaborations extérieures, pour la rédaction des différents écrits, vous m'avez constamment soutenue pour ma thèse.

Au Pr Thomas Jona Wolfensberger, qui m'a fait l'honneur d'accepter de présider mon jury de thèse, et de se déplacer de Lausanne à Strasbourg et d'être mon rapporteur extérieur. Votre compétence dans le domaine des maladies rétiniennes est reconnue.

Au Dr Alvaro Rendon, qui m'a fait honneur d'être également rapporteur externe et venir de l'Institut de la Vision de Paris pour participer à mon jury de thèse. Vos travaux de recherche sur les pathologies de la rétine font de vous un expert dans le domaine.

Au Pr Florence TOTI, qui a accepté d'examiner ma de thèse au nom de l'Université de Strasbourg
et dont l'expertise s'étend entre autres à la physiopathologie vasculaire.

Que tous les membres du jury trouvent ici l'expression de ma gratitude.

A M. Daniel Keller, le technicien de notre laboratoire, qui m'a donné beaucoup de conseils pendant les manipulations sur la paillasse. Merci pour ta patience et tes explications qui m'ont permis de mieux m'intégrer pendant mon séjour en France.
A Mme Elodie Collin, pour ta disponibilité et tes aides pour certaines manipulations.

Merci à mes collègues de laboratoire :
A Mme le Dr. Pauline Heitz, qui m'a précédé sur le sujet et m'a transmis les résultats de ses travaux et qui m'a initié à la chirurgie sur l'œil du lapin.
A Mlle Gaëlle Zimmermann-Meisse, qui m'a donné des conseils concernant les anticorps et utilisation du microscope.

Merci à Emmanuel Jover, Xavier Argemi, Chimène Nanoukon, Viola Mazzoleni, Kevin Prola, Elodie Olivares, Margaux Dreyer, Jimmy Chammas, pour leur amitié, leur aide, leurs encouragements et leur disponibilité.
Merci au « Chinese Scholarship Council », au Gouvernement Chinois, qui m'a attribué la bourse pour mes études et mon séjour en France.
Merci à mes parents, à mon frère en Chine, qui m'ont soutenu pendant ma thèse en France. Grâce à leur soutien et leur compréhension, j'ai pu faire ma thèse sereinement en France.

List of abbreviations

BRB, blood-retina barrier
CA-MRSA, community-associated methicillin-resistant *S. aureus*
CGRP, calcitonin gene-related peptide
CHIPS, chemotaxis inhibitory protein of *staphylococci*
Clf A, B, clumping factor A, B;
CoNS, coagulase-negative staphylococci
EVS, Endophthalmitis Vitrectomy Study
FnBPA, fibronectin-binding protein A.
GCL: ganglion cell layer;
GFAP: glial fibrillary acidic protein
HA-MRSA, hospital-acquired methicillin-resistant *S. aureus*
INL: inner nuclear layer;
IOFB, intraocular foreign body
LPS, lipopolysaccharides
MGE, mobile genetic elements
MHC-II, histocompatibility complex-II
MSCRAMMs, microbial surface components recognizing adhesive matrix molecules;
MSSA, methicillin-susceptible *Staphylococcus aureus*
NFL: nerve fiber layer;
NLRs, NOD-like receptors
NO, nitric oxides
ONL: outer nuclear layer;
PMN, polymorphonuclear leukocytes
PVL: Panton-Valentine leukocidin
RGCs: retinal ganglion cells
RPE: retinal pigment epithelium
SCCmec, staphylococcal chromosomal cassette *mec*
SCIN, staphylococcal complement inhibitor;
TLRs, Toll-like receptors
TSST-1, toxic shock syndrome toxin-1
RPE, retinal pigment epithelium
VEGF, vascular endothelial growth factor
VRSA, vancomycin-resistant *Staphylococcus aureus*

Table of Content

1. Introduction

1.1 *Staphylococcus aureus*

Staphylococcus aureus was first discovered in 1871. It was identified as bacteria responsible for purulent infection in 1880. *S. aureus* is Gram positive, ubiquitous pathogen and commensal to human being. About 20%-25% of the population permanently carry *S. aureus* and at least 60% carry transiently *S. aureus*[1]. It colonizes in wet areas, such as mucosa from the anterior nostrils to nasopharynx, axilla, wrist and perineum. *S. aureus* together with *Escherichia coli* and *Pseudomonas aeruginosa* are the most common isolated bacteria from hospital environment. It is also the second bacteria responsible for nosocomial infections, after *E. coli*. The diseases caused by *S. aureus* vary greatly, from dermal or mucosal infection (folliculitis, boil, impetigo and sinusitis) to visceral organ infections (endophthalmitis, pneumonia, endocarditis and osteomyelitis), and some life-threatening syndromes, such as septicemia and toxic shock syndrome[2].
S. aureus is a great burden for health care system, because of its significant morbidity and mortality worldwide. It is hazardous for people that have chronic diseases such as diabetes, eczema, or immune system deficiency (old people, AIDS) and those who are foreign material implant carrier. *S. aureus* infection can rapidly jeopardize the general health condition and threaten the life, mostly due to its multiple antibiotic resistances and various virulence factors.
S. aureus is frequently found in ocular infections, in which retina can be severely damaged despite prompt and appropriate treatments.

1.1.1 Methicillin-resistant *S. aureus*

Antibiotic resistance makes *S. aureus* survive from the antibiotic treatment and spread in hospital and community acquired strains. *S. aureus* can pass genes of antibiotic resistance and virulence through horizontal transfer among the strains and can adapt rapidly to the new treatment.
β-lactams is the first antibiotic to treat *S. aureus* infection. The methicillin, one derivative of penicillin of β-lactam antibiotic family, was introduced to clinical usage in 1960. The first methicillin-resistant *S. aureus* (MRSA) isolate was discovered one year later. Then MRSA prevailed throughout the world as a multi-resistant hospital pathogen. MRSA strains encode a novel specific penicillin-binding protein (PBP2a), which has a low affinity with all β-lactams and makes MRSA resistant to β-lactam antibiotics. This novel PBP2a is encoded by methicillin resistance gene (*mec*A), which is carried by a variable mobile element, called staphylococcal cassette chromosome *mec* (SCCmec). SCCmec can be inserted into the chromosome. It is constituted by two complexes, a cassette chromosome recombinase (*ccr*) gene complex and *mec* complex. The *ccr* complex controls the insertion site and integration of SCCmec into the staphylococcal chromosome. The *mec* complex contains

mecA gene and is classified into six different classes, i.e. A, B, C1, C2, D and E. SCCmec could also encode β-lactamases to cleave β-lactams. SCCmec is classified into 9 types according to the classes of *ccr* and *mec* complexes[3]. The type I SCCmec was identified in 1961, type II and III in 1980s, type IV and V in 2000s. The other types of SCCmec were less frequent and identified later. SCCmec varies in size. The type I, II and III are larger than those of type IV and V. The larger SCCmec, such as SCCmec II and III, contains other antibiotic resistances genes.

1.1.2 HA-MRSA and CA-MRSA

Table 1. The differences between HA-MRSA and CA-MRSA

HA-MRSA	CA-MRSA
health care systems	general population
carry a large staphylococcal chromosomal cassette *mec* (SCCmec) belonging to type I, II, or III.	carry small SSCmec type IV or V
resistant to many classes of non-β-lactam antimicrobials	susceptible to non-β-lactam classes of antimicrobials
seldom carry PVL gene	frequently carry PVL gene; the percentage continues rising, due to horizontal transfer of genes

MRSA spreads rapidly and is continuously developing its capacity of resistance to antimicrobial drugs. Considering its ubiquity, virulence and multi-antibiotic resistance, MRSA is a great burden to health care systems. At beginning, MRSA strains were confined to hospitals and other health care systems. However, MRSA infections were reported in healthy populations without exposure to health care system since 1990s. This new emergent MRSA is called as community associated (CA)-MRSA, the previous MRSA as hospital acquired (HA)-MRSA. CA-MRSA is defined as any MRSA infection diagnosed for outpatients or within 48 h of hospitalization without HA-MRSA risk factors.

CA-MRSA strains are different from HA-MRSA strains in terms of genotypic, epidemiological and clinical features[4] (Table 1). HA-MRSA strains harbor SCCmec type I, II, or III and are resistant to many classes of β-lactam and non-β-lactam antibiotics. CA-MRSA strains carry small SCCmec type IV or type V and are susceptible to non-β-lactam antibiotics. The difference in types of SCCmec could well explain the multi-resistance antibiotics of HA-MRSA and the susceptibility of CA-MRSA to non-β-lactam antibiotics[5]. The gene encoding PVL can spread from strain to strain by some bacteriophages. About 60 to 100% of CA-MRSA strains carry gene encoding PVL[6, 7], while HA-MRSA or

methicillin-susceptible *staphylococcus aureus* (MSSA) are rarely discovered carrying gene encoding PVL. The percentage of CA-MRSA has significantly increased in MRSA infection isolates and may continue to rise in the future. One hypothesis for this increase is due to the horizontal transfer of SCCmec elements and PVL gene to the genomes of MSSA[5].
PVL is highly expressed in CA-MRSA strains. The combination of antibiotic resistance and virulent toxin expression might be a great burden in treating *S. aureus* infection.

1.1.3 Vancomycin-resistant *S. aureus*

The percentage of MRSA increases and accounts for more than half of *S. aureus* infections. For severe MRSA infections, such as bacteremia, endocarditis and osteomyelitis, the effective antibiotic treatment is prompt intravenous vancomycin. The adjunctive therapies can also improve the treatment, such as drainage of abscesses or infected lesions, removal of catheters and infected valves[8].
Vancomycin is a glycopeptide antibiotic and works by blocking the construction of bacterial cell wall. Vancomycin binds to the precursors of peptidoglycan on the outer surface of bacterial cytoplasmic membrane, preventing the synthesis of peptidoglycan in bacterial cell wall. The mechanism of vancomycin-resistant *enterococci* is to produce low-affinity precursors of peptidoglycan to eliminate high-affinity precursors. The first vancomycin-resistant clinical isolates were found in *Enterococcus* in 1988. Since then, vancomycin-resistant *enterococci* spread rapidly worldwide. In 1997, clinical *S. aureus* isolates susceptibly resistant to vancomycin was found, called vancomycin-resistant *Staphylococcus aureus* (VRSA). Then, more evident VRSA strains were found later. Vancomycin resistance genes, such as *VanA, VanR, VanH* and *VanB,* are located in plasmid and transferred to MRSA by conjugation to *Enterococcus sp*[9].
Vancomycin is the last therapy for infection caused by multi-resistant strains of *staphylococci*, *streptococci* and *enterococci*. The emergence of resistance to vancomycin means that the bacterial strains can develop resistance to all the antibiotics.
In recent years, alternatives to vancomycin for the treatment of MRSA infection are identified and used. The most effective and wildly used are daptomycin and linezolid. The other alternatives to vancomycin include quinupristin-dalfopristin, tigecycline, trimethoprim-sulfamethoxazole, clindamycin, and tetracyclines. Linezolid is a synthetic oxazolidinone antibiotic, which inhibits the synthesis of bacterial proteins. Linezolid is recommended to treat skin and soft-tissue infections. There was outbreak of linezolid resistance in MRSA strains, which was associated with nosocomial transmission and the extensive usage of linezolid. MRSA strains in patients receiving daptomycin are more likely to develop resistance to daptomycin. Thereby, vancomycin is still the first choice of antibiotic to MSRA infection[10].
Other strategies, such as surveillance cultures, more strict usage of antibiotic, and decolonization of *S. aureus* in bodies, are proposed to control MRSA development in hospital environment.

1.1.4 Horizontal transfer

S. aureus could acquire adaptation and evolution very rapidly due to horizontal transfer of mobile genetic elements (MGEs). They could gain new antibiotic resistance and new virulence factors, which facilitate them to escape from immune system and improve their pathogenesis.

MGEs are segments of DNA, which can move around within a genome and be transferred from one stain to another. MGEs encode proteins for antibiotic resistance, virulence and host-adaptation. MGEs include plasmids, bacteriophages and transposons. Plasmids and bacteriophages are the classic MGEs. They are transferred by 3 genetic transfer mechanisms: conjugation (transmission of plasmid), transduction (by the intermediate of viral vector), and/or transformation (that can integrate a DNA fragment into the bacterial genome)[11].

SCCmec elements are transferred by bacteriophage, for this reason the prevalence of MRSA increases continuously. VRSA has emerged through the transposons of vancomycin resistance genes; *S. aureus* pathogenicity islands (SaPIs) carry genes encoding the toxic shock toxin 1 and superantigens. Horizontal transfer of SaPIs relies on the specific "helper" bacteriophages. PVL and staphylococcal enterotoxin A (sea) are found on inserted bacteriophage. PVL gene is frequently found in CA-MRSA, which might be due to selective transfer of PVL-carrying prophages to CA-MRSA[12].

1.2 Virulence of *S. aureus*

S. aureus expresses various virulence factors, including adhesive factors, exoenzymes and toxins (Figure 1). Adhesive factors help *S. aureus* to adhere to cells and the extracellular matrix, and exoenzymes control colonization and dissemination of *S. aureus*. The colonization to host tissue is the first stage of microbial infection, which is associated with its structural components and ability to bypass the host defense mechanisms. The dissemination of bacteria can promote the spread of bacteria and enlarge the infection. Whereas, the toxins have a more offensive function, attacking directly the immune system and other cells of the host. For instance, staphylococcal complement inhibitor (SCIN) and chemotaxis inhibitory protein of *staphylococci* (CHIPS) can modulate neutrophil chemotaxis and phagocytosis. Superantigenes, another type of toxin, can induce activation of lymphocytes, which is responsible for various symptoms, such as toxic shock. Enterotoxins target the intestine cells and are responsible for staphylococcal food poisoning. Hemolysins are able to lyse erythrocytes and lymphocytes. Leukotoxins also lyse other leukocytes. At last, PVL is one of better characterized leukotoxins and is an important virulence factor of *S. aureus*. This study of its effects on organic tissue and especially retina could help to find new therapeutic solutions to fight *S. aureus* infection.

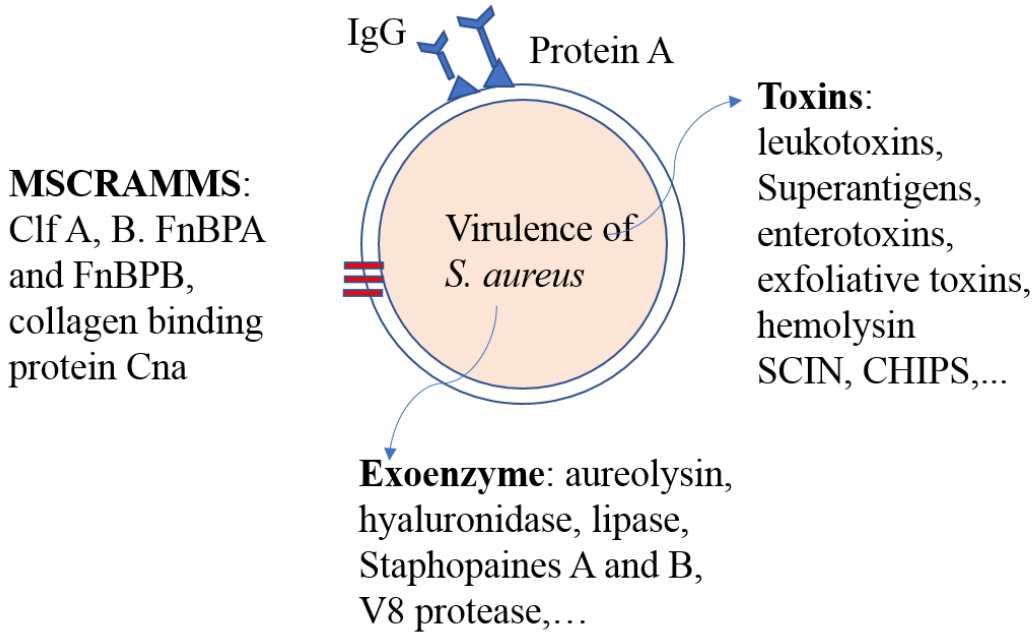

Figure 1: The virulence of *S. aureus*

The virulence of *S. aureus* includes MSCRAMMs, exoenzyme and toxins. MSCRAMMs and exoenzyme have passive functions on *S. aureus* colonization and dissemination, while toxins target actively immune system or cells of host. CHIPS, chemotaxis inhibitory protein of *staphylococci*; SCIN, staphylococcal complement inhibitor; Clf A, B, clumping factor A, B; MSCRAMMs, microbial surface components recognizing adhesive matrix molecules; FnBPA, fibronectin-binding protein A.

1.2.1 Adhesive factors

S. aureus adheres to extracellular matrix to form colonization, which is the primary step before opportunistic infection. This adherent ability is relied on microbial surface components recognizing adhesive matrix molecules (**MSCRAMMs**) on *S. aureus* surface, including fibronectin-binding protein A and B (FnBPA and FnBPB), a collagen binding protein Cna, a fibrinogen-binding protein and protein A.

FnBPA and **FnBPB**, expressed by two close genes in most *S. aureus* strains, attach to immobilized fibronectin. They are responsible for mediating *S. aureus* adhering to plasma clots and foreign body surface. The **collagen-binding protein Cna** adheres to collagen substrates and collagenous tissues. It is expressed by 38%-56% of *S. aureus* strains and mediates *S. aureus* binding to cartilage. It is associated with bone and joint infections[13]. Clumping factor A (**ClfA**) and B (**Clf B**) are the major fibrinogen (Fg) binding proteins of *S. aureus*. They recognize different parts of fibrinogen. ClfA binds to the carboxyl terminus of the γ chain of fibrinogen, while ClfB binds α and β chains of fibrinogen. They mediate *S. aureus* clumping in blood plasma during arthritis and endocarditis. **Protein A** is expressed by 90% of *S. aureus* stains. Unlikely to other molecules which binds to collagen, fibrinogen or fibronectin, protein A binds to the Fc region of immunoglobulin, which inhibits the opsonization, thus impairing phagocytosis of PMNs[13].

1.2.2 Exoenzymes

S. aureus secretes many exoenzymes to control its colonization and dissemination. The dissemination of bacteria can promote the spread of the infections. Those enzymes include nuclease, protease, lipase, hyaluronidase and collagenase. The proteases from *S. aureus* include serine, cysteine and metalloenzymes, and are not sensitive to most human inhibitors of plasma protease[14].

Aureolysin is a metalloproteinase of *S. aureus*. It can transform precursor of V8 protease into an active form. It inactivates ClfB by cleaving the N-terminal domain of ClfB. ClfB is membrane protein. The activation of ClfB can modify bacterial cell surface proteins, leading to tear off bacteria from colonization and promote the spread of infection. **Hyaluronate lyase** cleaves acid residues in hyaluronan, a component of extracellular matrix. This cleavage can dissociate extracellular matrix and promote bacterial dissemination and migration. **Staphylocoagulase** binds and activates prothrombin, leading to the cleavage of fibrinogen to fibrin. It promotes the abscess formation and lethal bacteremia of *S. aureus*. **V8 protease** is a serine protease, which cleaves specifically peptide bonds formed by aspartate and glutamate residues. It degrades the bacterial cell surface fibronectin-binding protein, facilitating bacterial dissemination. It can also promote the maturation of other virulence factors, such as staphostatins. **Lipase** can release a large quantity of fatty acids, which can help *S. aureus* to survive in the fatty human or mammalian skin. **Staphopains A and B** are the major secreted cysteine proteases of *S. aureus*, which may promote the invasion and metastatic infections of *S. aureus*. Staphostatin A and B may inhibit Staphopains A and B, respectively, through binding the active sites of these protease[14].

1.2.3 Toxins

Bacteria can secret toxic substances, which can directly damage host tissue or disable host immune system to protect bacteria against host defenses. *S. aureus* could produce a large repertoire of toxins, including CHIPS and SCIN, superantigens, enterotoxins, exfoliative toxin, hemolysins and leukotoxins. *S. aureus* strains express partially those toxins, presenting various degree of virulence.

1.2.3.1 CHIPS and SCIN

CHIPS and SCIN are toxins simultaneously expressed during the early (exponential) growth stage of *S. aureus* and can both modulate neutrophil chemotaxis, phagocytosis and cell killing[15].

CHIPS is a 121-residue protein excreted by about 60% of *S. aureus* strains. It is potent inhibitor of chemotaxis of neutrophils and monocytes toward C5a and the N-formylmethionyl-leucyl-phenylalanine (fMLP). Indeed, CHIPS binds directly to the receptors of C5a and fMLP with high affinity and selectivity. Thereby, it prevents C5a and fMLP from binding to their receptors and activating transduction pathways[16].

SCIN, an 85-residue protein secreted by *S. aureus*, has an anti-inflammatory action during *S. aureus* infection. It can inhibit the formation of lytic membrane attack complex (C5b-9 deposition) through disrupting alternative pathway-mediated and classical/lectin opsonization (C3b deposition). Thereby, it reduces phagocytosis following the opsonization and blocks efficiently the functions of the downstream effectors.

1.2.3.2 Superantigens and enterotoxins

Superantigens are proteins that cause non-specific activation of T-cells resulting in polyclonal T cell activation and massive cytokine release. *S. aureus* produces various superantigens, including the staphylococcal enterotoxins (SEs), the staphylococcal enterotoxin-like (SEls) proteins, and toxic shock syndrome toxin-1 (TSST-1).
Genes encoding superantigens are located on mobile genetic elements, which are carried by about 80% of *S. aureus* strains. In adaptive immune system, antigen presenting cells present antigens to CD4+ T cells by histocompatibility complex (MHC)-II. TSST-1 can bind to the invariant regions of MHC-II and interact with the β-chains of T cell receptors (Vβ-TCR), which can abnormally make cross-bridge between MHC-II and Vβ2-TCRs of subtype T-cells without specific antigens. This subpopulation of T cells is non-specifically activated and multiplies, resulting in massive release of inflammatory cytokines and toxic shock syndrome. By the same mechanism, superantigens cause other less severe syndromes, neonatal toxic shock syndrome-like exanthematous disease (NTED) and recalcitrant erythematous desquamating disorder (REDD). NTED is found in newborns and REDD is found in patients with AIDS[17].
An enterotoxin is an exotoxin released by a microorganism that targets the intestine. Staphylococcal enterotoxins have 20 distinct members, such as SEA, SEB, SED, SEE and SEF. They are responsible for the Staphylococcal food poisoning. Staphylococcal food poisoning, characterized by nausea and vomiting, is usually self-limited and resolves typically within 24-48 h after onset, albeit a few cases may result in a lethal toxin shock-like symptom. Enterotoxins can cause this disease even without the presence of *S. aureus*[18].

1.2.3.3 Exfoliative toxins

S. aureus produces exfoliative toxins (ETs) A, B, D, which cause a blistering of the skin. ETs target desmoglein-1 and act as serine proteases, resulting in mid-epidermal cleavage. ETs can cause dermal diseases ranging from blisters to severe exfoliation, such as bullous impetigo and staphylococcal scalded skin syndrome. About 5% of *S. aureus* strains carry ETs genes, but only a small proportion cause severe exfoliation. Some authors argued that ETs can act also as superantigens to cause autoimmune dermal disease[19].

1.2.3.4 Hemolysins

Hemolysins are lipids and proteins that lyse red blood cells by destroying their cell membrane. *S. aureus* expresses β-hemolysin, δ-hemolysin.

β-Hemolysin, also called beta-toxin, is a sphingomyelinase of *S. aureus*. It is encoded by a bacteriophage in a small percentage of *S. aureus*. It lyses erythrocytes and human lymphocytes by cleaving sphingomyelin in cell membranes to scavenge nutrients and escape from immune system. Its structure shows the characteristics of DNase I. However, instead of functioning as DNase, it precipitates extracellular DNA. The precipitated DNA forms non-specifically cross-linking with hemolysin β and other proteins, an insoluble nucleoprotein matrix, which contributes to biofilm formation[20].

δ-hemolysin is an alpha-helical and amphipathic 26-amino acid peptide, expressed in 97% of the *S. aureus* isolates. It is soluble in water and organic solvents. It can perturb the membrane after binding to it, resulting in cell lysis. It can lyse erythrocytes of many species[20].

1.2.3.5 Leukotoxins

Leukotoxins kills leukocytes, permitting bacteria to escape from host immune surveillance. Some of them are also hemolytic. Some of them are associated with severe infectious diseases. PVL is one well characterized leukotoxin, which is associated with necrotizing infections. We will review the members of leukotoxins from human isolated *S. aureus*, to better understand pathogenesis of *S. aureus*.

1.2.3.5.1 The prevalence of leukotoxins

Leukotoxins are composed of two distinct proteins, a class S (31–32 kDa) and a class F component (33–34 kDa). S component binds initially to the cytoplasmic membrane of target cells, then triggering the subsequent F component binding, which organize as alternate octamers, called prepores, then form the pore (Figure 2).

Human *S. aureus* isolates can produce five leukotoxins: γ-hemolysin consisting of two leukotoxins (HlgA/HlgB and HlgC/HlgB), LukAB, PVL and LukED[21]. The genes of HlgA/HlgB, HlgC/HlgB, and LukAB are located in the core genome on chromosome and are presented in almost all human *S. aureus* isolates. In contrast, PVL and LukED genes are located on mobile gene elements and could be horizontally transferred in a selective way. *S. aureus* expressing of PVL and LukED is related to some specific infections[22]. PVL gene is located in the temperate bacteriophage and is found in 2%-10% of all clinical *S. aureus* isolates in Europe, about 60% in African or Asian developing countries; PVL gene is positive in 60-100% of CA-MRSA isolates, while it is rare in HA-MRSA strains. LukED gene is located in a stable *S. aureus* pathogenicity island (a mobile gene element) and is found in 50% -75% clinical *S. aureus* isolates. *S. aureus* expressing LukED is associated with bullous impetigo and post-antibiotic diarrhea[31].

1.2.3.5.2 The genomic characteristic of leukotoxins

The gene encoding γ-hemolysin (HlgA/ HlgB, HlgA /HlgC) is divided into two parts. The first part is the locus for HlgA, which is about 400 bases upstream of second part which encodes the HlgC and HlgB. In that second party, *hlgC* and *hlgB* are separated by a base "T" and are simultaneously co-transcribed. For PVL and LukED, the genes of two components also are separated by one base "T" and are simultaneously co-transcribed. The genes of the two components of LukAB are also co-transcribed together and separated by 21 bases[23, 24].

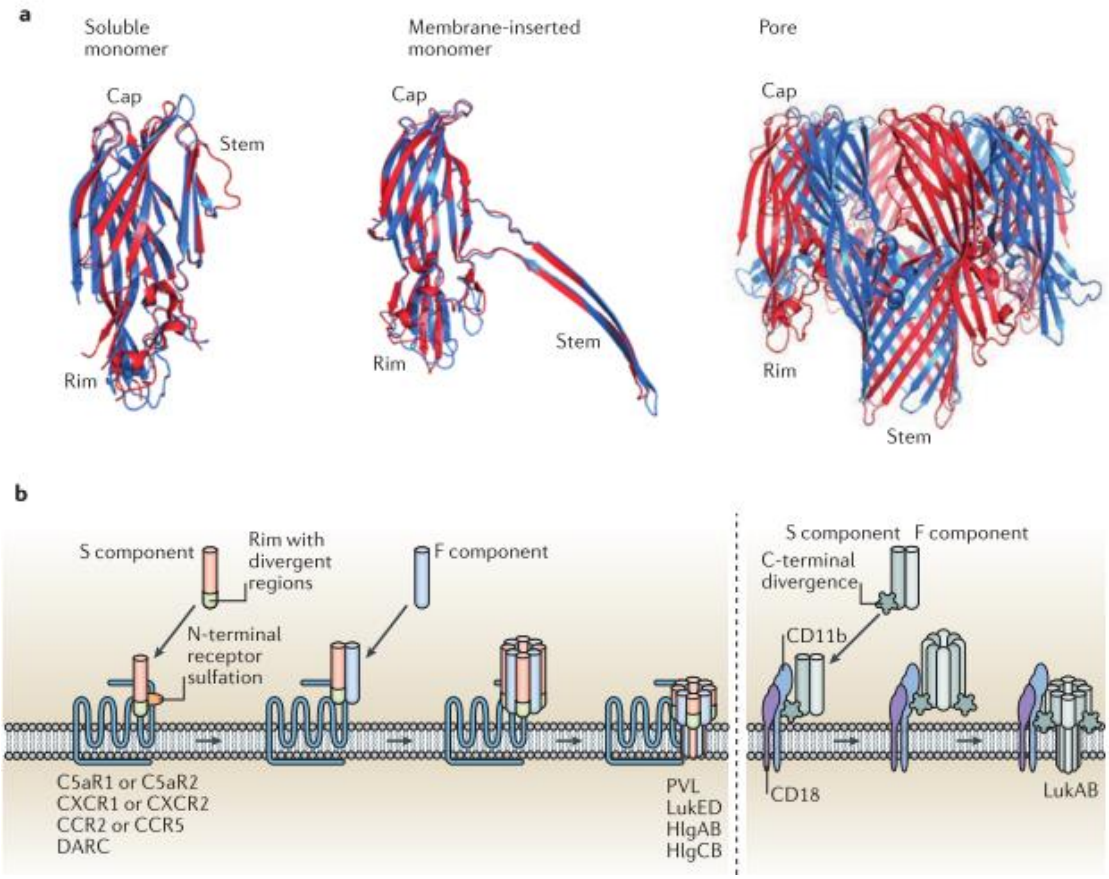

Figure 2: Crystal structure and pore formation of leukotoxins

(a) Crystal structures of leukotoxins: the soluble leukotoxin, leukotoxin in pre-pore formation, the hetero-octameric pore of leukotoxin. (b) The simple illustration of the processes of leukotoxin binding and pore formation. For PVL, LukED, HlgAB and HlgCB, the S component binds first to the receptor, then F component binds consecutively to the complex. Four S and four F components form a hetero-octameric pre-pore and then a pore. For LukA/B, S and F components form a dimer before binding to the receptor and forming the hetero-octameric pre-pore and pore. (Images in part a is from University Medical Center Utrecht, The Netherlands; images in part b is from András N. Spaan et al, 2017)

1.2.3.5.3 The spectra and receptors of leukotoxins

The leukotoxins of *S. aureus* have different cell-type and species-type targets. HlgA/HlgB could lyse lymphocytes and all the granule cells, while the other leukotoxins target granule

cells with different spectra. Also, PVL and HlgC/ HlgB could incite neurons to undergo calcium mobilization and glutamate release[25]. For a long time, cellular receptor was hypothesized to play a great role in the effect of leukotoxin. In recent years, the receptors of those leukotoxins are well identified, which can help to explain the spectra of target cells and species specificity of these toxins, and their cytotoxicity[22] (Table 2).

γ-Hemolysin

γ-Hemolysin consists of HlgA/HlgB and HlgC/HlgB. 99.5% of human *S. aureus* isolates express genes encoding γ-Hemolysin, which can aggravate septic arthritis and systemic infection. HlgA/HlgB has a large spectrum of target cells. It can lyse human and rabbit erythrocytes and target most leukocytes: T lymphocytes, granulocytes (neutrophil, basophil, eosinophil) and monocytes and their derivative cells (macrophages and dendritic cells). In contrast to HlgA/HlgB, HlgC/HlgB has a low capacity to lyse lymphocytes and does not lyse erythrocytes. HlgC/HlgB can target human granulocytes, monocytes macrophages and dendritic cells and cell line (HL-69) of the precursor of the neutrophils. To identify the specific receptors for HlgA/HlgB and HlgC/HlgB, human embryonic kidney cells were transfected with a collection of human chemokine receptors and were evaluated for the cytotoxic susceptibility to the two leukotoxins. It was shown that HlgA/HlgB bound to CXCR1, CXCR2 and CCR2, and HlgC/HlgB bound to C5aR and C5L2[22].

LukE/D

CCR5 is a receptor for LukE/D. Different cell lines (human T cell line, PMN-HL-69 osteosarcoma) are engineered to express CCR5 expression. LukE/D is cytotoxic toward cell lines in presence of CCR5, while the presence of other receptors (CCR1, CCR2, CCR3, CXCR4, CCR8, and CXCR6) does not make cell lines susceptible to LukE/D. The antagonist of CCR5 could effectively suppress LukE/D cytotoxicity. LukE/D can target human, rabbit and murine CCR5-bearing cells, and lyse neutrophils, monocytes and macrophages[26].

LukA/B

LukA/B is cytotoxic toward human and rabbit neutrophils, monocytes, macrophages and dendric cells, but not cytotoxic toward murine leukocytes. CD11b, α subunit of the αM/β2 integrin (CD11b/CD18), is known as macrophage-1 antigen or complement receptor 3. CD11b is identified as a host molecule required for LukA/B-mediated cell killing. LukA/B is the most divergent leukotoxin of staphylococcal leukotoxins. The amino acids sequences of LukA and LukB share about 30% and 40% with S component and F component of other leukotoxins, respectively. In contrast, other leukotoxins have 60%-80% similarity of amino acid sequence for S and F components. LukA/B needs to form a stable bicomponent before binding to its receptor, while S and F components of other leukotoxins bind separately and consecutively to the receptors[27] (Figure 2).

Table 2. The myeloid receptors, species activity and targeted leukocyte of leukotoxins of *S. aureus*

Leukotoxin names	Myeloid receptors	Species activity	Targeted leukocyte
PVL	LukS-PV:C5aR, C5L2 LukF-PV: CD45	Human (high) Rabbit (high) Mouse (none)	Monocytes Macrophages PMNs
HlgCB	HlgC:C5aR, C5L2	Human (high) Rabbit (medium) Mouse (low)	Monocytes Macrophages PMNs
HlgAB	HlgA: CCR2, CXCR1, CXCR2	Human (high) Mouse(medium)	Monocytes Macrophages Dendritic cells PMNs Lymphocyte T
LukED	LukE: CCR5	Human (high) Mouse (high)	Monocytes Macrophages PMNs
LukAB	LukAB: CD11b	Human (high) Rabbit (medium) Mouse (low)	Monocytes Macrophages Dendritic cells PMNs
LukMF´	LukM: CCR1	Bovine (high) Mouse (medium) Human (low)	PMNs Macrophages
LukPQ	LukP: CXCRA, CXCR2	Equine (high)	PMNs

Abbreviated symbols: PVL, Panton-Valentine leukocidin; C5aR, C5a receptor; C5L2, C5a receptor-like 2; PMNs, Polymorphonuclear leukocytes; CCR1, 2, 5, CC-chemokine receptor1, 2, 5; CXCR1, 2, A, CXC chemokine receptor 1, 2, A.

LukMF´ and LukPQ

Leukotoxin MF´ (LukMF´) and leukotoxin PQ (LukPQ) are associated with zoonotic infections and are rarely found in human *S. aureus* isolates. LukMF´ is associated to bovine mastitis, not in human infection[28]. The receptor for LukM is CCR1. LukMF´ targets actively bovine and murine neutrophils and macrophages, and human neutrophils to a lesser extent. LukPQ, a newly identified leukotoxin, targets mainly equine neutrophils through equine CXCRA and CXCR2[29].

PVL

Comparing to other leukotoxins, PVL has the smallest spectrum of target cells. PVL targets macrophages and neutrophils, not lymphocytes. In 2013, it was reported that human C5a receptors, C5aR and C5L2, were receptors for LukS-PV and mediators of PVL-induced cytotoxicity. The antibody against C5aR could effectively block PVL binding to neutrophils and macrophages. PVL has preference for animal species and does not recognize murine C5aR, which is determined by the second extracellular loop of C5aR[21]. Many previous studies used mice model to study PVL and might bring out some confusing results[30]. Recently, CD45 is identified as one receptor for LukF-PV, which influences the cytotoxicity of PVL towards neutrophils[31].

1.3 Leucocytes

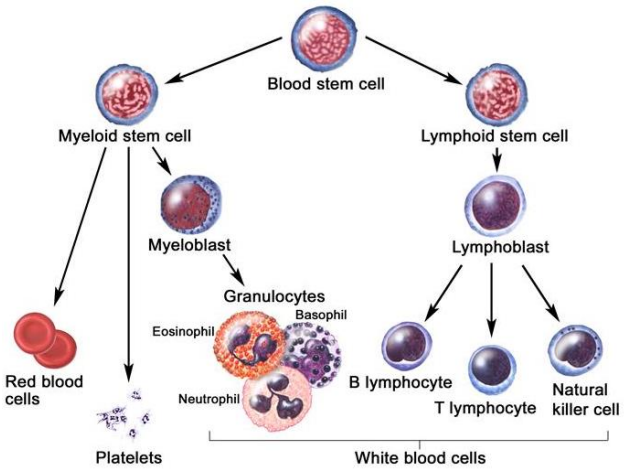

Figure 3: Hematopoietic differentiation tree

In the bone marrow, hematopoietic stem cells differentiate into two types of stem cells: one is myeloid stem cell, leading to the formation of red blood cells, platelets and myeloid cells; another is a lymphoid stem cell, leading to the formation of lymphocytes. (from website national cancer institute https://visualsonline.cancer.gov)

All the leukotoxins target and lyse leukocytes, which is the origin of their name. Leukocytes, the body's army of soldiers, are the cells of the immune system. They circulate in the body in blood vessels and lymphatic vessels. They fight the invading germs and prevent the infections. The leukotoxins kill leukocytes and help *S. aureus* to escape from immune defense and proliferate in human body. It's necessary to have an overview of leukocytes to understand well the cell targets of leukotoxins.

In the bone marrow, hematopoietic stem cell can differentiate into two types of stem cells: one is myeloid progenitor cell, leading to the formation of monocytes, red blood cells and neutrophils; another is lymphoid stem cell, leading to the formation of lymphocytes (Figure 3). Leukocytes circulate in the blood in a quiescent state with low adhesiveness, they have short life time about 7 to 12 h. They monitor the environment and can migrate into the tissues to defend against the invading microbes. Their main defensive functions are phagocytosis, degranulation and oxidative explosion[32].

1.3.1 Polynuclear neutrophils

Polynuclear neutrophils are the major cell type of granulocytes, occupying more than 40-75% of circulating leukocytes. Polynuclear neutrophils are the innate immune cells which react and migrate immediately to the lesion.

Migration

Neutrophils migrate from blood vessels to the tissues, through a process divided into four steps: rolling, activation, adhesion, and transendothelial migration. First, P-selectin ligand (PSGL-1) on neutrophils interacts with P-selectin expressed at the surface of endothelial cells. This interaction is of low-affinity, neutrophils poorly bind to the endothelial cells. Continuously being carried away by the blood flow, they roll on the vessel wall. During this rolling, neutrophils can be activated by the invading pathogens or proinflammatory products. Once being activated, neutrophils could express immediately more adhesive molecules on their surface, such as lymphocyte function-associated antigen 1 (LFA-1) which interacts with ligand intercellular adhesion molecule (ICAM-1) on endothelial cells. This high affinity adhesion allows neutrophils to attach firmly to blood vessels. Then, they transform, sneak through the endothelial cell layer and migrate to lesion[33].

Phagocytosis and degranulation

Neutrophils are effective phagocytes. They imprison pathogens inside an endosome, which is internalized into cytoplasm, called phagosome. The granules containing degradation enzymes come to merge with phagosome to degrade the contents.

Neutrophils are granulocytes and have four types of granules with different content. During the maturation of neutrophils, the primary granules are fused with phagosome. They contain myeloperoxidase, elastases, defensins, lysozymes and azurocidine, which digest phagocyted microorganisms. The other granules are formed later than primary granules. The second granules are rich in antimicrobial agents, which are released into extracellular medium. The third granules contain gelatinases, enzymes, and receptors, which are useful

for the neutrophils transendothelial migration. The fourth granules are secretory vesicles, which contain many receptors. They are rapidly secreted outside to modify the composition of the cytoplasmic membrane, promoting neutrophil activation and adhesion to the endothelium[34].

1.3.2 Eosinophils, basophils and mast cells

Eosinophils are circulating in blood, occupying normally less than 5% of circulating leukocytes. They produce and store biologically active molecules, including cytotoxic proteins, lipid mediators, chemotactic peptides and cytokines. They are associated with a series of disorders, such as asthma, tropical pulmonary eosinophilia. **Basophils** occupy normally less than 1% of circulating leukocytes and are associated with fatal asthma, acute and chronic allergy. They abundantly secrete cytokines after being activated to amplify the allergy. **Mast cells** are not flowing leukocytes, they reside in vascularized tissues. They have many granules, which contain histamine, proteases and cytokines. They can rapidly degranulate after interacting with IgE and release prostaglandins and leukotrienes during allergy[35].

1.3.3 Monocytes, macrophages and dendric cells

Monocytes constitute 3-10% of flowing leukocytes. Monocytes express many receptors, such as Toll-like receptors (TLRs), to monitor the environmental changes. In general, they flow in blood for 1-3 days, and then migrate into tissue and become resident macrophages or dendritic cells. In abnormal conditions, monocytes are activated and transform into inflammatory macrophages, which secrete cytokines, myeloperoxidase and superoxide, and help in phagocytosis to eliminate harmful materials. Monocytes and macrophages can eliminate pathogens, cancer cells and cellular debris by phagocytosis.
Dendritic cells are antigen-presenting cells in immune system. They reside in tissue which is in contact with external environment, such as skin and mucosa. Dendritic cells capture and present antigens to T-lymphocytes, which can activate them to undergo immune response. They also can promote B cell activation and differentiation by producing cytokines and other factors[36].

1.3.4 Lymphocytes T, B and NK

The flowing lymphocytes constitute 20-40% of the flowing leukocytes in adults and are divided into three types of lymphocytes in the peripheral blood: T, B and NK cells, representing about 80%, 10% and 10% of total lymphocytes, respectively. T lymphocyte is a major cell of the adaptive immune system and can be divided into $CD8^+$ and $CD4^+$ T cells. $CD8^+$ T cells are cytotoxic T lymphocytes. They bind to target cells and secrete molecules to destroy these cells. $CD4^+$ T cells bind to antigen fragment presented by CMH II from dendritic cell, macrophages and B lymphocyte. The $CD4^+$ T cells release cytokines or

chemokines and help to develop the clones of B cells which secrete antibodies against the presented antigens. B lymphocytes bind and engulf antigens, which are then presented to T-cells. Helper T cells can aid B cells to produce specific immunoglobulins to antigenic epitopes, called antibodies. Lymphocyte NK is component of innate host defense system. They can lyse virally infected cells and malignant cells[37].

1.4 PVL

In the early 1930s, PVL was first discovered by Panton and Valentine. It is a powerful leukotoxin secreted by *S. aureus*.

1.4.1 PVL-related clinical diseases

PVL is often found in necrotizing *S. aureus* infections, such as furuncles, acute necrotizing pneumonia and osteomyelitis. Here are a few examples of *S. aureus* infections potentially aggravated by PVL.

1.4.1.1 PVL pathophysiology in skin infection

The skin abscesses are often related to *S. aureus* infection. The rate of PVL expression in *S. aureus* strains isolated from skin infection is much higher than that from systemic infection[38]. A study included 43 *S. aureus* isolates from cutaneous infections, among which 12 (28%) strains expressed PVL gene. While only 1 strain among 49 (2%) isolates from systemic *S. aureus* infection was expressing PVL [39]. *S. aureus* expressing PVL is often related to primary skin infection, while the *S. aureus* non-expressing PVL is related to secondary infection after other dermal diseases such as bullous or pruritic diseases[39].
The skin lesion generated by PVL is dependent on PVL concentration. PVL concentration ranges from 0.27 mg/L to over 2 mg/L in pus of PVL-positive *S. aureus* skin abscess. When PVL concentration is superior 1 mg/L, large abscesses (diameter ≥5 cm) are observed[38]. Small PVL concentration (30 ng) induces dermal edema and erythema, high PVL concentration (300 ng) provokes widespread infiltrated erythema followed by skin necrosis after intradermal injection in rabbits[39]. In mice, skin does not react after intradermal injection PVL, even though the PVL doses reaches up to 3 µg[39].

1.4.1.2 PVL pathophysiology in pneumonia

CA-MRSA carrying PVL could cause severe and fatal pneumonia within a short time. PVL-positive *S. aureus* pneumonia is necrotizing pneumonia characterized by a bloody cough (haemoptysis) and a decrease of circulating leukocytes (leucopenia). Histopathological analysis shows extensive necrotic ulcerations and massive haemorrhagic necrosis in lung tissue[40]. This pneumonia is preceded by an influenza-like syndrome, then followed by high fever (above 39°C), tachycardia (>140 beats/min). The patients are healthy children or young adults.
This severity is associated with PVL. Purified PVL is directly instilled into rabbit lung and causes severe inflammation and injury by recruitment and subsequent lysis of PMNs in

lung during several hours. Damaged PMNs could release cytotoxic granules and/or reactive oxygen metabolites and significantly increase the level of IL-8 and MCP-1 in lung. These cytokines amplify the recruitment of leukocytes and damage the integrity of alveolus[41].

1.4.1.3 PVL aggravates osteomyelitis

S. aureus often induces infection in bone and joint. PVL aggravates osteomyelitis in both clinical and experimental observations. The osteomyelitis or arthritis caused by CA-MRSA carrying PVL have more severe damage and require longer antibiotic course and various surgical procedures. PVL-positive osteomyelitis or arthritis undergo rapid evolution toward multifocal osteomyelitis and/or multiple abscesses despite antibiotic treatment[42]. In experimental rabbit model, the bone is infected by PVL-positive CA-MRSA strain and its PVL-negative isogenic derivative. In presence of PVL, rabbit bone is deformed, muscle and joints are involved in infection, which is rarely found in PVL-negative strain osteomyelitis. The anti-PVL antibody significantly reduces the inflammation in osteomyelitis caused by PVL-positive *S. aureus*[43].

1.4.2 PVL effects

1.4.2.1 PVL inducing calcium mobilization

PVL induces an increase of intracellular calcium concentration in PMNs and neurons without membrane damages[25, 44]. This calcium mobilization is not associated with plasma membrane Ca^{2+} channels or pore formation, but with the sarcoendoplasmic reticulum calcium transport ATPase (SERCA)[45,46].

PVL induces an increase of intracellular calcium concentration after 100s, which increases linearly within 10 min. The extracellular calcium influences PVL effects in calcium mobilization. In presence of physiologic calcium concentration, PVL application incites an increase of the intracellular calcium concentration in PMNs. In absence of extracellular calcium, PVL forms pore on PMNs, while the intracellular calcium concentration is not affected[47].

PVL induces an increase of intracellular calcium concentration without pore-forming in primary cerebellar granular neurons and dorsal root sensory neurons. This calcium increase is accompanied by glutamate release from primary cerebellar granular neurons[25].

1.4.2.2 PVL inducing cell death

PVL can induce necrosis or apoptosis of PMNs, which are dependent on the PVL concentration. At high concentration, PVL induces necrosis by osmotic lysis, which might be due to pore formation on cytoplasmic membrane. At low concentration, PVL induces apoptosis by Bax-independent signaling pathway[48]. PVL is also related to neutrophil cell death during neutrophil extracellular traps (NETosis). NETosis is a recently described process of neutrophils trapping and killing of *S. aureus*, which leads to lytic cell death. PVL has been found to be associated to this process[49].

Cell apoptosis related to PVL is also demonstrated on keratinocytes: *S. aureus* strains are engulfed into endosomes by human epidermal keratinocytes (RHEK-1) within 1 h. PVL-positive *S. aureus* could successfully disrupt endosomes and replicate intracellularly. After 6 h, PVL induces significantly caspase-dependent keratinocyte apoptosis[50].

1.4.2.3 PVL inducing release of inflammatory factors

PVL is reported to target human and rabbit monocytes, macrophages and PMNs, but not to lymphocytes, which implies that PVL disturbs directly the innate immune system. PVL can also induce reactions on cerebral and radical ganglion neurons[25].

PVL induces different cell reactions in different cell types. PVL incites PMNs to secret granule content in a dose-dependent way. PVL induces proinflammatory factors release such as histamine, leukotriene B4 and IL-8 from neutrophils[51, 52]. Histamine is a potent vasodilator. Leukotriene B4 and IL-8 are chemokines which attract leukocytes to inflammatory sites. Those factors promote and facilitate PMNs-tissue infiltration. PVL influences the production of radical superoxide in PMNs: at low concentration, PVL induces PMNs to produce moderate superoxide anion; at high concentration, PVL inhibits radical superoxide formation. The production of free radical superoxide molecules could damage the tissues, while their inhibition could help *S. aureus* to spread[53].

PVL activates monocytes and macrophages to produce NLRP3 inflammasome, a signaling complex, which incites the release of IL-1β and IL-18[54]. IL-1β and IL-18 can further induce lung epithelial cells to secret chemokines and recruit leukocytes in PVL-positive MRSA necrotizing pneumonia[55].

PVL could incite neurons, resulting in calcium mobilization and glutamate release.

In total, PVL effects result in leukocyte recruitment and death, vasodilation, cells invasion and tissue necrosis.

1.4.2.4 PVL retrograde transport

After PVL binding to C5aR, the receptor is phosphorylated and PVL is internalized with the phosphorylated receptor[45]. Immunolabeling and confocal microscopic techniques were used to trace the PVL retrograde transport. It showed that PVL accumulated first in lysosomal compartments 10 min after PVL application and reached to Golgi network 3 h after PVL application. Cell apoptosis was observed 3 h and peaked 6 h after PVL application. PVL induced Ca^{2+} release from the ER within 10 min, unexpectedly not from lysosome, which indicated that PVL-induced calcium mobilization was not related to the pore formation. The initial process of interaction between PVL and C5aR seems to play great role in PVL-induced calcium mobilization and cytotoxicity, independently from pore formation[56].

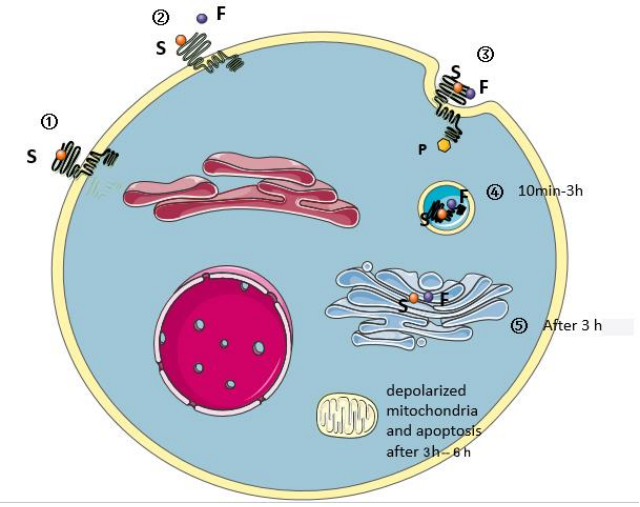

Figure 4: PVL retrograde transport

Step 1. LukS-PV binds to C5aR; Step 2. Recruitment of LukF-PV; Step 3. Internalization of PVL with phosphorylated C5aR; Step 4. Transfer to lysosome (10 min-3 h); Step 5. Transfer to Golgi (after 3h); Apoptosis occurs at 3 h and peaks at 6 h after PVL application.

1.4.3 PVL treatment

Considering the severity of *S. aureus* infection caused by PVL, PVL should be targeted as a new treatment. Different antibiotic families have very different effects in PVL secretion. Oxacillin enhances PVL release, while clindamycin, linezolid, fusidic acid and rifampicin inhibit PVL expression. The other antibiotics do not have influence on PVL expression. It has been proposed to combine clindamycin, linezolid, fusidic acid and rifampicin with other antibiotics to treat possible PVL-carrying *S. aureus* infection[43]. Those antibiotics could inhibit the production of many staphylococcal exotoxins *in vitro*. Combination those inhibitory antibiotics with other antibiotics needs be further studied in clinical studies.

Humanized heavy chain-only antibodies (HCAbs) against PVL two components (LukS and LukF) prevent PVL binding and pore formation. In a rabbit PVL-induced endophthalmitis *in vivo* model, HCAbs (anti-LukS-PV, anti-LukF-PV) prevent effectively ocular inflammation and show therapeutic potential[57].

Among a series of molecules tested to inhibit PVL, calixarenes show the property of inhibiting PVL. P-sulfonato-calix[n]arenes can abolish S protein binding to membrane. This inhibitory effect is also observed in a rabbit model of PVL-induced endophthalmitis[58]. All those PVL inhibitors are still in an experimental stage.

1.5 Retinal structure

1.5.1 General structure

1.5.1.1 The cell layers of retina

The retina is innermost, light-sensitive nervous layer that lines the inner surface of the back of the eyeball, in which stimulation by light occurs, initiating the sensation of vision. The light penetrates retina and is absorbed by photoreceptors. The photoreceptors transform the light into electrical message, which is sent to all the succeeding neurons of retina, reaching to central system by the visual pathway (Figure 5). The retina contains several structural layers, from the most inner layer to the most outer layer are as follows: the **inner limiting membrane (ILM**), which is constituted by a membrane and endfeet of Müller cells. ILM is the interface between retina and vitreous and functions as demi-barrier, which prevents large molecules from penetrating into retina; the **nerve fiber layer (NFL)**, which contains axons of ganglion cells which constitute optical nerve; the **ganglion cell layer (GCL)**, which contains two kinds of cells, ganglion cells and displaced amacrine cells; the **inner plexiform layer (IPL)**, which is neuropil containing the axons or synapses of nearby cells and some microglial cells; the **inner nuclear layer (INL)**, which is constituted by cellular soma of bipolar, horizontal, amacrine and Müller cells; the **outer plexiform layer (OPL)**, which is another neuropil containing process of bipolar cells and horizontal cells and synaptic pedicles of photoreceptors; the **outer nuclear layer (ONL)**, which contains rod and cone photoreceptors; the **outer limiting membrane (OLM)**, which is adherent junctions between Müller cells and photoreceptors; the **pigment epithelium layer**, which constitutes the outer ocular-blood barrier (Figure 6).

1.5.1.2 The retinal vasculature

The arterial intra-retinal branches supply three layers of capillary networks: the radial peripapillary capillaries, and the inner and the outer layers of capillaries (Figure 7). From NFL to OPL, the retinal structure is vascularized by retinal capillaries from central retinal artery. ONL is avascular and gets nutrients from the choriocapillaries which are supplied by choroidal arteria. The fovea is exceptional and avascular, in which cone photoreceptors are maximally concentrated and other retinal layers are absent.

1.5.1.3 The blood-retina barriers

The retina has two blood-retina barriers (BRB), the outer BRB, which is constituted by tight junctions among retinal pigment epithelium and inner BRB which is constituted by tight junctions among intra-retinal vessels. The molecules selectively pass through these BRBs, which is the principal mechanism to maintain retinal homeostasis and function.

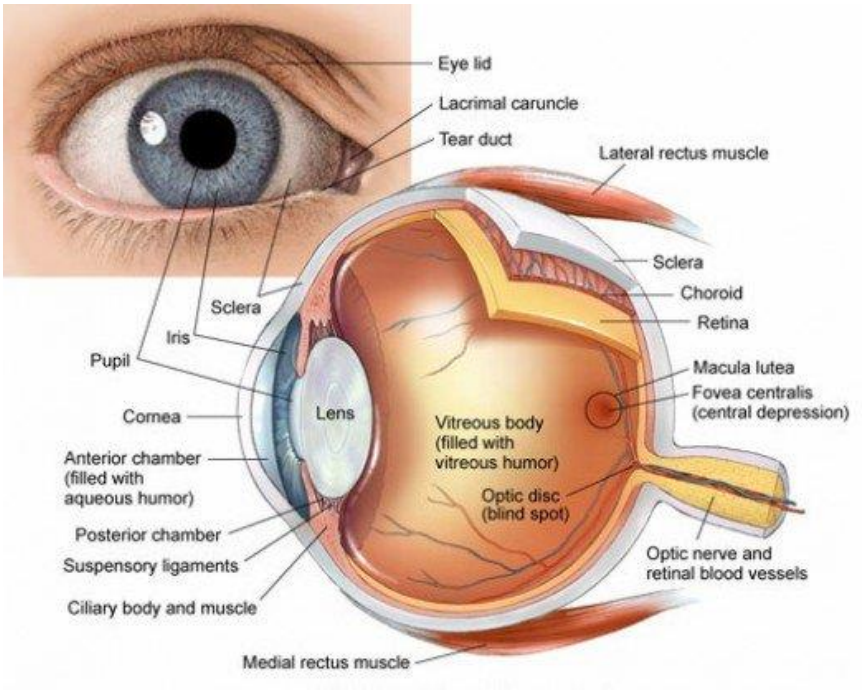

Figure 5: The structure of eye
(Gaurab Karki, 2018, Human Eye: Anatomy, parts and structure. http://www.onlinebiologynotes.com/human-eye-anatomy-parts-structure)

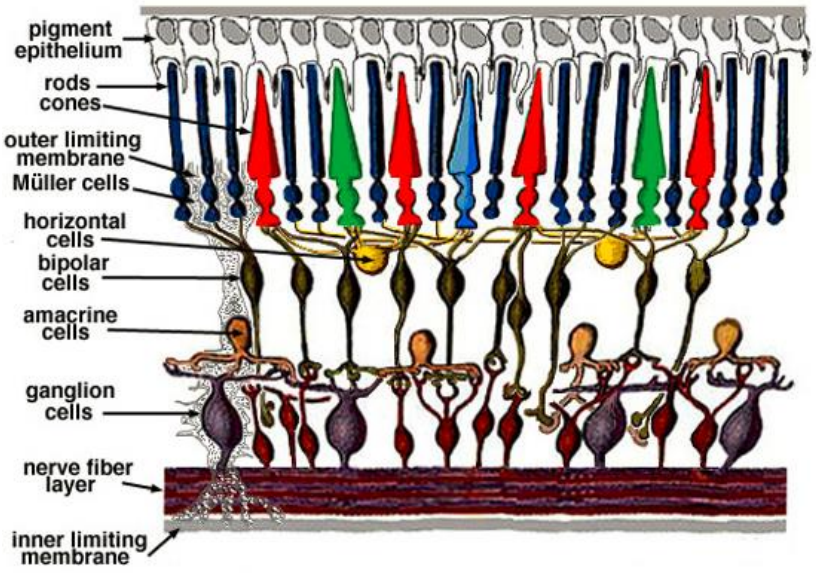

Figure 6: The organization of retina
(Helga Kolb, Webvision: Simple Anatomy of the Retina by Helga Kolb. https://webvision.med.utah.edu/book/part-i-foundations/simple-anatomy-of-the-retina/)

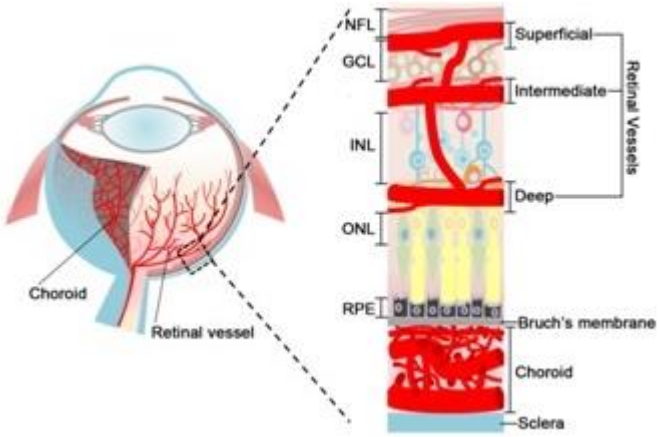

Figure 7: Simple illustration of ocular vasculature

Left: choroid and retinal vessels consist ocular vasculature. Right: retinal vessels are consisted in three layers: radial peripapillary capillaries (superficial), and the inner and the outer layer of capillaries (intermediate and deep). The choroidal vessels are under RPE and supply blood to the outer portion of the retina.

Abbreviation: GCL: ganglion cell layer; INL: inner nuclear layer; NFL: nerve fiber layer; ONL: outer nuclear layer; RPE: retinal pigment epithelium. (Image from Jing Chen Laboratory website).

1.5.2 Müller cells

1.5.2.1 Müller physiologic function

Müller cell population is intense and well organized in retina, which provides architectural support to retinal neurons. Their cell bodies are situated in the inner nuclear layer. Their processes extend through the entire retinal thickness, their endfeet forming the inner limiting membrane and their outer processes supporting photoreceptors. They also form endfeet on retinal large retinal blood vessels. Anatomically, Müller cells are tightly related to all retinal cells and blood vessels[59].

Müller cells participate in many retinal physiologic functions. They regulate retinal blood vessels and maintain blood-retinal barrier. They provide metabolic and nutritional support to retinal neurons, maintain retinal physiologic homeostasis (water/ion and pH), uptake or recycle neuronal transmitters, provide scaffold for neuronal cells orientation during retinal development, release neuroactive or vasoactive substances[59]. Müller cells secrete neuronal trophic molecules such as nerve growth factor to support neuronal survival and neuritogenesis[60].

1.5.2.2 Müller gliosis

In some species, Müller cells can regenerate retinal neurons after retinal damage. For example, zebrafish retinal Müller cells produce neural progenitor cells following neuronal damage and death[61]. While in mammalian, Müller cells undergo gliosis in response to retinal damages and infections, which is important for protecting and repairing neurons

from diverse harmful stimulus. The hallmark of retinal Müller cell gliosis is the shape change resulting from rapid upregulation of glial fibrillary acidic protein (GFAP) following acute retinal injury[62]. The time-dependent Müller cell gliosis is significantly associated with retinal functional impairment and alteration of retinal gene expression[63]. Human Müller cells may produce IL-6 mRNA and proteins after stimulation of IL-1β or LPS[64]. Müller gliosis modifies the expression of glutamine synthetase, reduces the K^+-conductance on their membrane, releases neurotrophic factors and antioxidants. The Müller gliosis can also release detrimental factors such as nitric oxide and VEGF, leading to detrimental glial scar, which could disturb the retinal function[59]. The increase of intermediate filament expression in Müller gliosis is correlated with cell stiffness, which could impede the nerve regeneration[65]. In retinal detachments, Müller cell processes migrate abnormally to the outer part of retina and undergo mitosis and gliosis, resulting in subretinal glial scar[66].

1.5.2.3 The inflammatory reaction of Müller cell

Müller cells express innate immune receptors and are capable to sense both pathogen- and host-derived ligands[67]. Müller cells express Toll-like receptors (TLRs) 1-10, the major family of pattern recognition receptors in innate immune response[68]. Müller cells express also intracellular NOD-like receptors (NLRs), which are correlated with TLRs and regulate inflammatory reaction[69]. After detecting these pathogens, Müller cells react intensely and release proinflammatory cytokines, chemokines and nitric oxide (NO). During *S. aureus* endophthalmitis, Müller cells are activated and secret proinflammatory cytokines (IL-6, TNF-α, and IL-1β), chemokines (IL-8), and antimicrobial peptide (IL-37)[70]. In endotoxin-induced uveitis, Müller cells express NO and TNF-α[71]. Müller cell-derived VEGF is the key factor in inducing retinal vascular lesions, vascular leakage and retinal cytokines productions[72].

1.5.2.4 Müller cell gliosis results in retinal edema

Müller cells express water transports coupled to potassium channels, which can be influenced during retinal inflammation. Kir4.1, the main potassium channel in retina, and Aquaporin 4 (AQP4), the predominant water channel colocalize on Müller cells. During uveitis, Kir4.1 and AQP4, 5 expressions are significantly decreased on cytoplasm membrane of Müller cells[73]. Aquaporin 11, expressed exclusively on Müller cells, decreases significantly during uveitis, which is related to Müller cell swelling and retinal edema[74]. When the homeostasis of ion and water influx is disturbed by inflammation, Müller cells undergo swelling and neurons suffer from the abnormal osmotic stress[59].
Müller gliosis is related to retinal swelling. In endotoxin (LPS)-induced ocular inflammation, Müller cells hypertrophy and increase the immunoactivity of GFAP. Electrophysiology shows the downregulation of inward K^+ currents and depolarization of Müller cell membrane. The intracellular Müller cell edema can increase extracellular fluid accumulation[75]. In retinal inflammation, retinal Müller cells are activated and transformed into gliosis, accompanied by decrease of potassium and water channel protein expression, which results in Müller cell swelling and dysfunction of retinal fluid absorption, leading to retinal edema and degeneration[74, 76].

1.5.3 Microglial cells

In retina, microglial cells have two origins: blood-cell born cells and mesodermal cells. In rabbit retina, microglial cells are located in nerve layer and inner plexiform layer, with small cell bodies and long ramified processes panning the around areas.

1.5.3.1 Microglial cell is sensitive to the changes of environment

Microglial cells monitor their environments and can migrate to damaged areas and phagocytize apoptotic cells and debris. In murine newborn, some retinal ganglion cells undergo physiological apoptosis. Microglial cells migrate to ganglion cell layer and transform into amoeboid phagocytic microglia[77]. In pathological condition when retina is injured, microglial cells are activated and transform into active amoeboid form to participate in inflammation, removal of cellular debris and glial scar[78].

Microglial cells have potential to act as macrophages and dendritic cells during immune responses[79]. Retinal microglial cells express CD45, CD68 and some macrophage antigens, suggesting that they are potential macrophages in retina[79]. Retinal microglial cells share many characteristics with dendritic antigen presenting cells. They express constitutive MHC class II antigens, HLA-DR, CD45 and nucleotidase[80]. Microglial cells are very sensitive to the changes of environment. Time-lapse confocal imaging shows that microglial cell processes are in dynamic movement (extension and retraction) and can rapidly transform their morphology and migrate in response to retinal injury[81]. In vitrectomy, microglial cells undergo reversible morphologic transformation without Müller cells activation or obvious neuronal damages[82].

1.5.3.2 Retinal microglial cell activation

Retinal microglial cell activation is a common hallmark of various retinal degenerative and inflammatory diseases and the early phenomenon in response to retinal injuries and inflammations[83]. Retinal microglial cells demonstrate a broad range of morphologic changes in different activated stages. Early activated changes include enlargement of the soma, retraction and shortening of processes, and increase of the expression of myeloid cell markers. Microglial cells are slightly activated but can easily resume to a resting state. At more activated state, microglial cells are transformed into amoeboid form, a round cellular soma without processes[84], which can turn into post-activated state with a reduced number of processes or undergo apoptosis by overactivation (Figure 8)[85]. Activated microglial cells can express proinflammatory cytokines, chemokines, growth factors, neurotrophins, reactive oxygen and nitrogen species. In autoimmune uveoretinitis, microglia migrate to the photoreceptor cell layer where they generate TNF-α and peroxynitrite[86]. Hypoxia induces microglial cells to express inflammatory factors, TNF-α and IL-1β, which can further cause ganglion cell apoptosis[87].

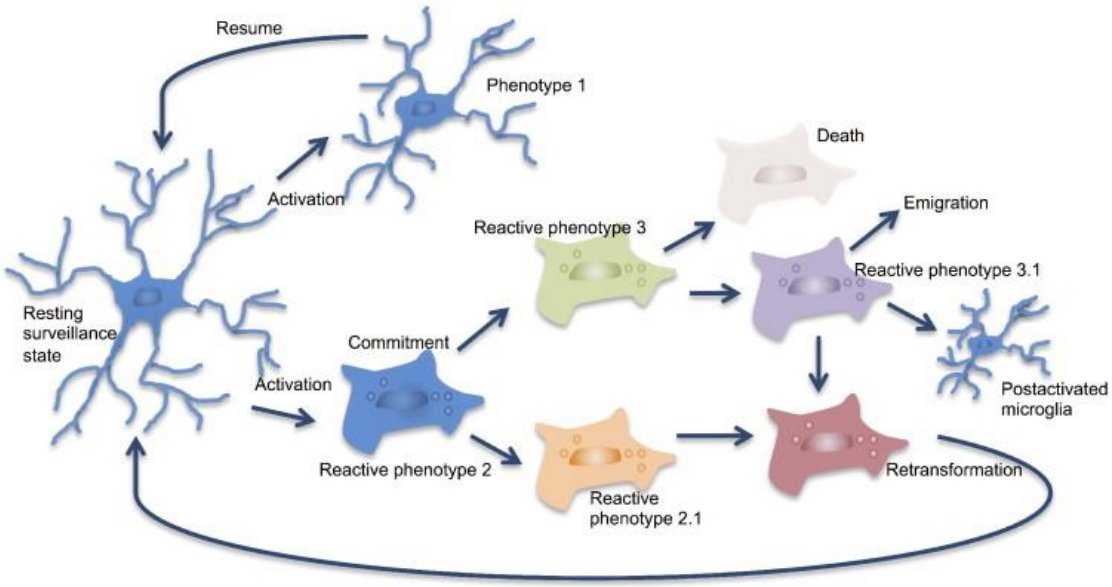

Figure 8: The activated states of microglial cell in response to various stimuli
Resting microglial cell is ramified and can transform into different activated states. Some active microglial cells reduce their processes but resume easily to resting state (phenotype 1). Some active microglial cells turn into amoeboid form (phenotype 2), which undergo death by overreaction (reactive phenotype 3) or migrate and return into post-activated state with a reduced number of processes (reactive phenotype 2.1 and 3.1). (F. RohanWalke et al, 2014).

1.5.3.3 The regulation of microglial cell activation

The activation and gene expression of microglial cells are influenced by two systems: receptors detecting pathogens and the balance between excitatory and inhibitory stimuli. The abnormal substances can be detected by an array of receptors expressed on microglial cells, such as Toll-like receptors (TLRs) detecting microbiological substances[85]. It is commonly admitted that microglial cells can monitor the overall neuronal condition by the balance between excitatory and inhibitory stimuli. The capacity of microglial cells to undergo inflammatory response is restrained by their microenvironment, especially those from neurons. It is widely proved that microglial cells are regulated by several ligand-receptor systems, such as CD200-CD200R, CD22–CD45, CX3CL1-CX3CR1, and neurotransmitters-receptors, such as TGFβ- TGFβ receptor and dopamine-dopamine receptor.

TGFβ predisposes retina to the IL-10 release[88]. CD200R is expressed on microglial cells. CD200, an inhibitory gland of CD200R, is wildly expressed on retinal cells and vascular endothelium. CD200 binds to CD200R on microglial cells, which incites inhibitory intracellular signaling cascade to block pro-inflammatory activation. When the balance of CD200:CD200R axis is disrupted, retinal microglial cells are activated[89]. CX3C chemokine receptor 1 (CX3CR1) can promote the dynamism of microglial cell process and cellular migration[90]. The chemokine [C-X3-C motif] ligand 1 (CX3CL1), a gland for CX3XCR1, is expressed on retinal neurons. The CX3CL1-CX3CR1 signaling regulates microglial

dynamism and maintains the microglial distribution in retina[91]. Retinal microglial morphology and dynamic behavior are also influenced by neurotransmitters such as glutamate and GABA release[92, 93].

1.5.3.4 Microglial cells interact with Müller cells

Activated microglial cells interact with activated Müller cells through neurotrophic factors, cytokines and chemokines, which influence further the neuronal survival. In response to retinal damage, microglial cells are activated and release neurotrophic factors such as nerve growth factor, ciliary neurotrophic factor, and glial cell line-derived neurotrophic factor (GDNF). Those neurotrophic factors can modulate Müller cells to release GDNF and basic fibroblast growth factor. Those neurotrophic factors influence photoreceptor survival[94]. In co-culture of activated microglial cells, Müller cells increase the expression of GDNF and leukemia inhibitory factor, which protect photoreceptors from oxidative stress and proinflammatory factors. Activated microglial cells can activate Müller cells, the activated Müller cells can further activate microglial cells[95].

1.5.4 Amacrine cells

Amacrine cells are interneurons, located at the second synaptic level of light pathways, which is consisted of the photoreceptor-bipolar-ganglion cell chain. Amacrine cells do not have true axons, only long processes. They play a role in modulating and interposing the signal transmitter[96]. Amacrine cells occupy more than 40% of the inner nuclear cells and are classified into more than 22 different morphological subtypes, only one type of amacrine cells makes up more than 5% of total amacrine cell population. The classification is based on cell shape, biochemistry and location in the inner plexiform layer. Amacrine cells from different classification connect with different bipolar cells and ganglion cells and contain different neurotransmitters[97]. Some amacrine cells are dopaminergic, some are glycinergic such as AII amacrine. "Starburst" amacrine cells use acetylcholine as excitatory neurotransmitter and GABA as inhibitory neurotransmitter[98]. Amacrine cells A2 contain substance P; some amacrine cells accumulate serotonin[99] (Table 3).
Neurobiotin injected to individual cell can diffuse across gap junctions to label neighboring neurons. This tracer coupling reveals the presence of gap junctions among coupled retinal neurons throughout the cellular network. In retina, except for starburst amacrine cells, amacrine cells are intensively coupled with other amacrine and ganglion cells. This coupling is directional: ganglion cells can pass neurobiotin to amacrine cells, but amacrine cells rarely can pass neurobiotin to ganglion cells[100]. AII amacrine cells are coupled with calbindin-positive bipolar cells[101].

1.5.5 Retinal ganglion cells

In retina, photoreceptors transform light into visual information and pass it to interneurons in retina. Retinal ganglion cells collect all the information and send it to the brain by their

axons through optical nerve. Retinal ganglion cells are divided into around 20 types according to their morphology, synaptic connections and light responses. Three major ganglion cells types (midget, parasol and small bistratified cells) occupy approximately 70% of all ganglion cells. The other ganglion cells are heterogenous[102]. In mammal retina, ganglion cells fail to regenerate and undergo apoptosis, when their axons are injured or cut[103].

1.5.6 Retinal neurotransmitters

Table 3. The distribution of neurotransmitters in retina

Neurotransmitters	Expressed on retinal cells	Principal role
Glutamate	AII photoreceptors, bipolar and ganglion cells	excitatory
GABA	amacrine cells which also contain other neurotransmitters and horizontal cells in center	inhibitory
Glycine	small-field types of amacrine cells (such as AII amacrine) and some bipolar cells	inhibitory
Acetylcholine	Starburst amacrine cells	Excitatory, co-localize GABA
Dopamine	one or more types of amacrine cells	Co-exists with other neurotransmitters, regulate gap junctions
Serotonin	A17 and A18 amacrine cells	Co-exists with GABA
Substance P	Some amacrine cells and some ganglion cells	SP amacrine cells co-localize GABA; SP ganglion cells colocalize glutamate
CGRP	Inner retina, ganglion cells	--
Others	Amacrine cells	--

Abbreviations: GABA: gamma-aminobutyric acid; SP, substance P; CGRP, Calcitonin gene-related peptide.

In retina, l-glutamate (excitatory), gamma-aminobutyric acid (GABA) and glycine (inhibitory) are the principal neurotransmitters in retinal synapses. Other neurotransmitters are acetylcholine, dopamine, serotonin and substance P. Glutamate immunoreactivity is in photoreceptor, bipolar and ganglion cells. GABA and glycine immunoreactivities are in amacrine and some bipolar, horizontal and ganglion cells[104]. Dopamine, acetylcholine and serotonin are in some amacrine cells. Glutamate is excitatory neurotransmitter. Glutamate release is largely mediated by calcium-dependent vesicular processes[105]. It is taken up by glutamate transporters expressed on Müller cells. Ganglion cells express glutamate receptors, the kainite/AMPA and NMDA. Müller cells increase ganglion cell survival through the increase of glutamate transporter expression[106]. GABA is the primary transmitter and substance P is the secondary transmitter in A22 amacrine cells. Substance P is also

expressed by some retinal ganglion cells. In rabbit, 25%-30% of retinal ganglion cells express substance P[107]. Calcitonin gene-related peptide (CGRP) immunoactivity is found in the whole retina, with more intense staining in some cells in INL and GCL[108].

1.5.7 The calcium channels on retinal cells

Voltage-dependent calcium channels (VDCCs) are involved in transmitter release, hormone secretion, gene transcription, cell regulation and synaptic plasticity in excitable cells[109]. VDCCs are transmembrane proteins consisted by three subunits: transmembrane α1 subunits, extracellular $\alpha_2\delta$ subunits and intracellular β subunits. VDCCs could be divided into two major families according to reaction in response to the voltages changes: high voltage-activated (HVA) channels such as the L-, P/Q-, N- and R-type channels and low voltage-activated (LVA) channels such as the T-type calcium channels [110]. Retinal ganglion cells express L-, N-. P/Q- and T- type VDCCs, as demonstrated by pharmacological blockades of these calcium channels[111].

There are also some non-VDCCs, which are activated by glandes or depletion of calcium store: the activation of receptor-operated calcium channels (ROCCs) depends on the activation of a range of receptors such as nicotinic acetylcholine receptors (nAChR). The store-operated calcium channels (SOCCs) are activated by depletion of the calcium store within the sarcoplasmic reticulum[112, 113].

The transient receptor potential channels (TRPs) are wildly expressed on cellular membrane and are divided into seven subfamilies: TRPC (canonical), TRPV (vanilloid), TRPM (melastatin), TRPP (polycystin), TRPML (mucolipin), TRPA (ankyrin) and TRPN. The TRPs are non-selective cation channels, except a few which are highly Ca^{2+} selective[114]. The TRPs can be activated by a variety of mechanisms, such as ligands, voltage changes, temperature and metabolic products. The activated TRPs cause depolarization and initiate immobilization of cations (such as Ca^{2+} and Mg^{2+}), which is involved in many physiological and pathological processes[115].

Cytoplasmic calcium is mostly stored in endoplasmic reticulum (ER) and mitochondria. Calcium is released from ER by activation of inositol trisphosphate receptors (IP_3R) and ryanodine receptors (RyR), which are mediated by other cytoplasmic membrane receptors, such as glutamate receptors[113, 116]. The calcium recharge in ER is mediated by the sarco-/endoplasmic reticulum calcium ATPase (SERCA)[117]. Mitochondria take up calcium through the calcium uniporter and release calcium by sodium-calcium exchange, which is much slower in physiological conditions[118]. The release of cytoplasmic calcium to extracellular compartment is through the plasma membrane calcium ATPase (PMCA) and the sodium-calcium exchanger (NCX)[119]. The lysosome can release calcium after being activated by nicotinic acid adenine dinucleotide phosphate (NAADP). NAADP is formed by ADP-ribosyl cyclase CD38 after transmembrane receptors being activated by their glands[120] (Figure 9).

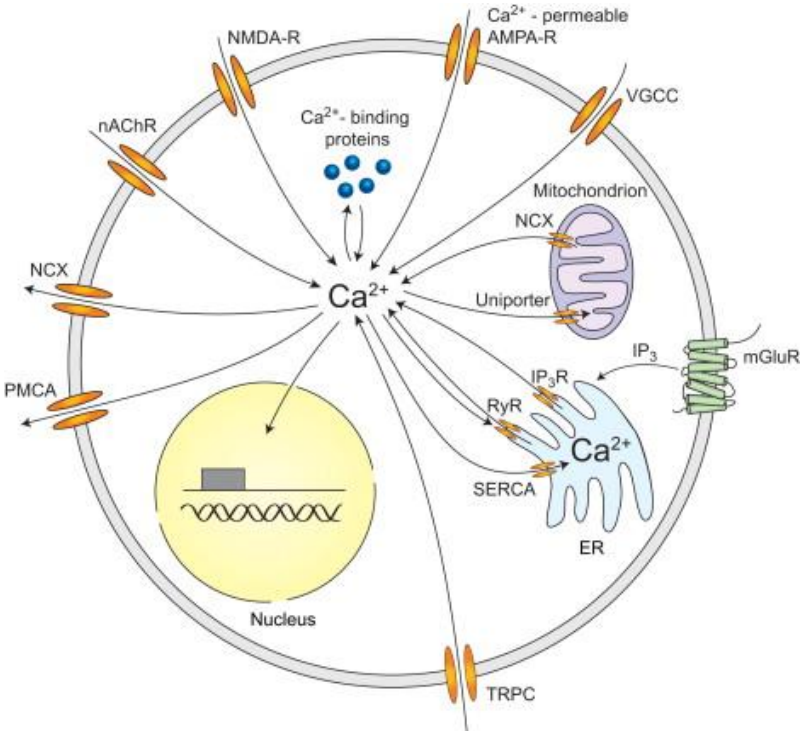

Figure 9: The sources of neuronal calcium mobilization

The extracellular calcium inflow after activating AMPA, NMDAR, VGCC and TRPC. The intracellular calcium is released from endoplasmic reticulum and mitochondrion after activating mGluR, RyR and IP_3R.

Abbreviations: AMPA, calcium-permeable α-amino-3-hydroxy-5-methyl-4-isoxazolepropionic acid; NMDAR, N-methyl-D-aspartate glutamate-type receptors; VGCC, voltage-gated calcium channels; nAChR, nicotinic acetylcholine receptors; TRPC, transient receptor potential type C channels; IP_3R, inositol trisphosphate receptors; RyR, ryanodine receptors; mGluR, metabotropic glutamate receptors. PMCA, plasma membrane calcium ATPase; NCX, the sodium-calcium exchanger; SERCA, the sarco-/endoplasmic reticulum calcium ATPase. (Grienberger, C et al, 2012)

1.6 Endophthalmitis

Bacterial endophthalmitis is an infection of internal part of eye, which is associated with bad visual outcomes[121]. It is diagnosed by clinical symptoms (pain, decrease of vision, hypopyon, opaque vitreous, retinal reaction), combined with biological analysis such as culture of samples from vitreous and aqueous humor[122]. But there is about 20% of clinical endophthalmitis which are negative in culture of samples obtained from aqueous humor and vitreous. This might be due to viral infection or technique limitation[123]. Thereby, the diagnosis of endophthalmitis is based on clinical symptoms and systemic risk factors together with multiple biological analyses[122]. The visual outcomes vary from recovery to loss of vision, depending on many factors such as the virulence of the pathogen and the delay of treatment[124].

Bacterial endophthalmitis often results in poor prognosis. Only 43%–53% of patients can achieve 20/40 or better visual acuity (VA), and about 20% have 20/100 or worse even after

appropriate treatment management[125, 126]. Enucleation or evisceration are still common options in severe cases of endophthalmitis[127]. Recently, treatments such as vitrectomy and intravitreal injections of antibiotics have been introduced. However, visual outcomes are not significantly improved[126].

1.6.1 The classification of endophthalmitis

Endophthalmitis is divided into post-operative, post-traumatic and endogenous endophthalmitis according to the initial condition. The post-operative endophthalmitis occurs after ocular intervention surgery, post-traumatic endophthalmitis occurs after the bleach of eyeball in accident. Endogenous endophthalmitis is resulted from metastasis of pathogen from other organs through ocular barrier. Those three kinds of endophthalmitis present different pathogenic characteristics and different difficulties in treatment[121].

1.6.1.1 Post-operative endophthalmitis

The rate of endophthalmitis after ocular surgical intervention is very low, between 0.05% to 0.37%, depending on the types of intraocular surgery[121]. But post-operative endophthalmitis remains great prudence for surgeons considering the great number of ocular surgery and bad visual outcomes. The factors contributing to bad outcomes include intracapsular cataract surgery, poor presenting visual acuity, presence of vitreous cells, inability to visualize the optic disc on indirect ophthalmoscopy, presence of vitreous membranes on ultrasonography, and a culture-positive vitreous biopsy[128]. One important factor is the virulence of the organism isolated from intraocular samples. Intraocular infections caused by virulent strains such as *S. aureus*, *enterococci, Bacillus,* or Gram-negative strains are often difficult to treat and result in bad vision[129].

In post-operative endophthalmitis, the most common pathogens detected are $Gram^+$ bacteria, occupying 94%. The Endophthalmitis Vitrectomy Study (EVS) reported that 84% of $Gram^+$ endophthalmitis cases resulted in at least 20/100 VA and 50% of these cases resulted in at least 20/40 VA, while only 30% of endophthalmitis cases caused by virulent organism attained 20/100 VA[129].

Among these $Gram^+$ bacteria, the coagulase-negative staphylococci (CoNS) is the most frequent, occupying 47 to 70% of all the cases. *S. aureus* is the second, occupying about 10%[130]. Most endophthalmitis caused by CoNS result in good visual outcomes, but some present delayed-onset, chronic and often painless inflammation, even severe ocular damages such as retinal detachments[131].

1.6.1.2 Post-traumatic endophthalmitis

The rate of endophthalmitis after penetrating ocular trauma ranges from 3.3% to 17%, which is about 100 times greater than that of post-operative endophtalmitis[121]. The setting place of accident influences greatly the incidence of endophthalmitis. In rural places, the

penetrated eyes have 30% incidence of endophthalmitis. While in urban place, the penetrated eyes have 11% possibility to develop endophthalmitis[132]. Also, the delayed removal of intraocular foreign body (IOFB) and the type of IOFB increase significantly the incidence of endophthalmitis after accident[133]. Other factors associated with poor visual outcomes include trauma by needle (hypodermic or sewing), poor presenting visual acuity, inability to visualize the optic disc on indirect ophthalmoscopy, presence of vitreous membranes on ultrasonography, breach of lens capsule, and delayed primary repair and culture-positive vitreous biopsy[128, 134].

S. aureus is the most common virulent organism isolated from post-traumatic endophthalmitis. The second frequent virulent bacterium is *B. cereus*, which is ten times more likely to be isolated from post-traumatic endophthalmitis than from post-operative endophthalmitis[128]. The CoNS, such as *Corynebacterium*, and *Propionibacterium acnes,* are considered as nonvirulent microorganisms, but they can also result in bad visual outcomes[135].

1.6.1.3 Endogenous endophthalmitis

The endogenous endophthalmitis occurs when organisms migrate from other infectious organ via the bloodstream and enter the internal eye by overcoming the blood–ocular barrier[136]. The rate of endogenous endophthalmitis is low, 2-8% of total endophthalmitis. But they have very poor visual outcomes[137]. The patients have usually immunocompromised condition, and it is easy to misdiagnose and delay the treatment. Blood sample culture (74%-94%) is more often positive than interocular sample culture (56%)[138]. The causative bacteria to endogenous endophthalmitis include the $Gram^+$ microorganisms (*S. aureus*, *Bacillus spp*, CoNS, group *B streptococci*, *Streptococcus pneumoniae*, and *Listeria* monocytogenes) and $Gram^-$ microorganisms (*Escherichia coli, Neisseria meningitidis, Pseudomonas aeruginosa,* and *Klebsiella spp*). The rates of causative organisms vary geographically. The opportunistic fungus *Candida albicans* represents particularly more than 50% of the cases of endogenous endophthalmitis in Europe[139]. $Gram^-$ organisms are reported as the most common causative organisms from East Asian hospitals, while $Gram^+$ organisms are more common in North America[138].

1.6.2 Inflammatory changes in retina during endophthalmitis

During endophthalmitis, retina undergoes rapidly inflammatory changes to react the invading pathogens, such as cytokines and chemokines release, neutrophils infiltration. Those inflammation could modify retinal architecture, resulting in function loss.

1.6.2.1 Cytokines and chemokines release

Cytokines, chemokines, and adhesion molecules are released in bacterial endophthalmitis. TNF-α, IL-1β, and CINC (rat homologue of IL-8) are detected in the vitreous within 6 h and

elevated significantly 24 h after intravitreal injection of *S. aureus*[140]. In experimental *B. cereus* endophthalmitis, the significant increase of TNF-α occurs at 4 to 6 h postinfection[141]. IL-1β, IL-6, and MIP-3α increase in the aqueous humor and vitreous humor from eyes with endophthalmitis[142].

1.6.2.2 Inflammatory cells infiltrate into retinal tissue

Severe infection is often accompanied by infiltration of neutrophils. In *B. cereus* and *S. aureus* induced endophthalmitis, the recruitment and activation of neutrophils within the eye are noticed within several hours[141, 143]. Neutrophils infiltrate into the retina 24 h after PVL injection[57]. The neutrophils infiltration is essential for eliminating the invaded pathogens. The depletion of neutrophils delays the onset of severe ocular inflammation, but also prevents adequate clearance of bacteria[143]. But the generation of toxic reactive oxygen and other inflammatory mediators by neutrophils cause irreversible tissue damage in the eye and impair the visual functions[144].

1.6.2.3 Retinal architectural changes and function loss

Retinal structural changes during endophthalmitis include photoreceptor layer folding, retinal detachment, and complete dissolution of retinal cell layers[121, 130]. Retinal Müller cells expand vertically the whole retina and play a role in maintaining the retinal integrity and participating in many physiological processes[145]. Müller cell dysfunction is tightly related to retinal structural alterations[146, 147]. The upregulation of GFAP is a hallmark of gliosis[62]. So, GFAP increase in Müller cells is considered as a signal of retinal architecture deformation. *B. cereus* (100 CFU) is intravitreally injected in mice and toxins are intraocularly produced and herein interact with Müller cell. The increase of GFAP immunostaining is detected as early as 4 h post-infection, which is paralleled with the decline of retinal function[141].
Blood-retina barrier (BRB) is constituted of inner and outer blood-retinal barriers. These barriers protect retina from toxic cells and molecules and maintain ocular physiology and function[148, 149]. The zonula occludens between endothelial cells in retinal vessels are impaired by ocular inflammation, resulting in damage of BRB[150]. The BRB permeability is hallmark of retinal structure integrity. Leakage from BRB appears early during endophthalmitis and restores after 1 month[151]. *B. cereus* infects retinal pigment epithelium (RPE) cell monolayer, leading to the decrease of the expression of occludin and zonula occludens-1, and cytotoxicity to RPE[152]. Retinal Müller cell processes connect closely to retinal vessels. Bacteria or bacterial toxins activate retinal Müller cells and cause high permeability of BRB [153].

1.6.3 Treatment: vitrectomy and intravitreal antibiotic

From 1995, the diagnosis and treatment have improved. For diagnosis, culture and PCR analysis are routinely used to analyze the samples form anterior chamber and vitreous. For management, the vitrectomy and intravitreal antibiotic increase, while subconjunctival and intravenous injection of antibiotic decrease[154]. Vitrectomy surgery debrides infecting organisms, the toxins and inflammatory cells from vitreous cavity, which is valuable in the treatment of endophthalmitis[155]. The rate of vitrectomy is about 45% in United States[126].

The vitrectomy is an effective adjunct to anti-microbial therapy in suspected endophthalmitis cases following intraocular surgery. The immediate vitrectomy (within 6 h) is especially of significant benefit to patient who have only light perception[129]. The vitrectomy could somehow improve final ocular condition for patients with only light perception[126]. The vitrectomy could maintain ocular formation and structure and prevent the globe shrinkage and chronic inflammation[154]. Many reports agree that vitrectomy should be performed without delay in severe cases of endophthalmitis, especially those presenting IOFBs[126, 156, 157].

The intravitreal injection of antibiotic is an important treatment. The systemic antibiotic administration of vancomycin and aminoglycosides could partially penetrate blood-ocular fluid barrier due to the increase of BRB permeability caused by intraocular inflammation[158]. But the systemic antibiotic does not demonstrate additional benefits in combination with intravitreal antibiotic administration[159]. The intravitreal antibiotic should cover most possible and multidrug resistance strains[160]. The appropriate antibiotics include gentamicin with vancomycin or clindamycin, the fourth-generation fluoroquinolones such as gatifloxacin and moxifloxacin which penetrate BRB and have broad-spectrum of antibacterial activity[160]. Considering the possible toxicity of fluoroquinolones and aminoglycosides, the routine intravitreal administration consists of 1.0 mg of vancomycin and 2.0 mg of ceftazidime[161, 162].

The vitrectomy and intravitreal antibiotic contribute to eliminate pathogens from ocular cavity to control the evolution of endophthalmitis. But retinal function is disturbed even at the very early stage of infection. Although great improvement in diagnosis and management is achieved, the visual outcomes are not always significantly improved.

1.7 Animal model

1.7.1 Intravitreal injection

1.7.1.1 The employment of intravitreal injection

Posteriors ocular diseases, such as age-related macular degeneration (AMD), diabetic retinopathy (DR), diabetic macular edema (DME), infection, occlusion of retinal vein, often cause severe visual acuity loss. The prognosis of posterior ocular diseases depends on the efficiency and safety of delivery drugs to posterior segment of eye. Delivery of drug to posterior segment of eye is always challenging, due to anatomical and physiological barriers of the eye. The methods include systemic administration of medicament, periocular and intravitreal injection, and local eyedrop.

Systemic administration is a traditional way to treat severe intra-ocular disease. But many drugs cannot freely pass BRB. If drugs can pass through BRB because of specific structure of drugs or the pathogenic BRB break-down, it requires also a great bolus to achieve sufficient intraocular concentration and could cause systemic unwanted side-effects. Eye drop can infiltrate into ocular surface tissue such as cornea and conjunctiva. But it

penetrates slowly in intra-ocular space and cannot be used to treat posterior diseases. Periocular injection, including sub-conjunctive and posterior ocular injection, can improve the concentration and duration of drug in periocular tissue. But it cannot efficiently deliver drug to intraocular posterior segment.

Intravitreal injection of medication has many advantages. It can immediately deliver medication to vitreous and retinal tissue and maintain the concentration of medication in vitreous for long time even when small quantity of medicament is injected. Since 1940s, intravitreal application of antibiotic was studied to treat endophthalmitis. Triamcinolone acetonide is the first widespread drug administrated by intravitreal injection. Since then, many novel medications, such as anti-vascular endothelial growth factor (VEGF), dexamethasone, fluoquinolone and ocriplasmin, have been developed to be administrated by intravitreal injection. Medications are intravitreally injected to treat different posterior ocular diseases: triamcinolone to treat macular edema; anti-VEGF agents to treat retinal neovascular disease; antibiotics, antivirals and antifungals to treat endophthalmitis.

Intravitreal injection presents some disadvantages including elevation of intraocular pressure or glaucoma, endophthalmitis and retinal decollement. For intravitreal injection of corticosteroid, the most frequent complication is the elevated intraocular pressure and glaucoma. Intravitreal anti-VEGF and anti-microbials injections have relatively a low complication rate. The incidence of lens injury is 0.006% (2/32,318) and retinal detachment is 0.013% (5/35,942). The rate of suspected endophthalmitis is 0.018% after bevacizumab and 0.027% after ranibizumab injections. Sterile inflammation is observed after Avastin injections. Increased intraocular pression is observed after repeated injection of anti-VEGF[163].

1.7.1.2 Intravitreal injection in experiment

Intravitreal injection is also used in experiment. Adeno-associated viral (AAV) gene therapy has potential of treating retinal disorders such as retinitis pigmentosa and age-related macular degeneration. Intravitreal administration of gene vectors can provide safe and efficient gene delivery[164].

Intravitreal injection of bacteria, bacterial products and other medications is a common method to analyze their effects on retina. In this way, products can immediately be delivered to retina with little disturbance of physical ocular functions and anatomy.

1.7.1.3 The mechanism of passage

Diffusion in vitreous

Vitreous gel is bloodless and contains more than 98-99% water. In addition to water, an extensive and delicate meshwork of collagen fibrils with glycosaminoglycan and hyaluronan is filled in vitreous. Owing to those solid components, vitreous humor is viscous and has a gelatinous consistency. The diffusion of drugs depends on microstructure and microrheology of vitreous. The pore size of meshwork and electrocharged characteristics

are two key factors to influence the diffusion in vitreous of intravitreal medication.
The composition and microstructure of bovine vitreous are similar to those of human vitreous. The mesh pores of bovine vitreous are estimated as large as 2 micrometers. Recently, it was shown that the pore size is 550 ± 50 nm, with some pores as large as 1000 nm. Large particles (> 500 nm) cannot easily pass through meshwork and diffuse slowly[165]. If particles exhibit adhesive interactions with meshwork, they diffuse slowly. In vitreous, glycosaminoglycans are negatively charged. Positive charged particles are trapped by negative meshwork and diffuse slowly. Negative charged particles are repelled by the same charge of meshwork. If anionic particles are in small size and at low concentration, they can fluently diffuse in vitreous. At high concentration, anionic particles cumulate and generate enough strong adhesive interactions to collapse collagen fibrils, resulting in immobilized particles in vitreous[165].
In conclusion, the size, surface charge and concentration influence the diffusion of intravitreal injection medications in vitreous[165]. The vitreous gel is not homogeneous and the diffusion of medication in vitreous could be heterogeneous. PVL is positive charged in physiological pH.

Diffusion in retina

After penetrating the vitreous gel, drugs reach to retina. The retina is semipermeable membrane. It is reported that molecule larger than 100 kDa could not easily pass the retinal layer to the subretinal space, due to barriers formed by inner limiting membrane (ILM), outer limiting membrane (OLM) and Müller cells. The inner and outer plexiform layers are also the sites of highest resistance to diffusion[166]. ILM is a basal membrane between the endfeet of Müller cells and vitreous. The pore size of human ILM is estimated to be 10 nm. ILM acts as a biological and electrostatic barrier with a net negative charge, preventing macromolecular drug to penetrate into the retina. ILM is a barrier to gene vector delivery to specific retinal cells. After digestion of ILM, the efficiency of delivering gene vector to retina is improved[164]. Müller cells could uptake the diffused molecules, which is mediated by receptors. OLM is formed by tight junctions between the apical processes of Müller cells and inner segments of the photoreceptors. Albumin and gamma-globulin cannot pass through an intact OLM. However, the limit of particle size to penetrate OLM is not quite clear[167].
In total, the maximum size of molecule capable of diffusing freely across retina is 76.5 +/- 1.5 kDa (6.11 +/- 0.04 nm) in human, 86 +/- 30 kDa (6.38 +/- 0.88 nm) in rabbit[166]. The molecular mass of PVL is around 60 kDa.

Drug clearance

The intravitreal drugs could be cleared by metabolism in vitreous or elimination by blood circulation. Vitreous contains minor amounts of metabolic enzymes, the principal elimination is through blood circulation, then by metabolic clearance in liver and renal excretion to the urine[167].
Ocular clearance mechanisms limit the duration of drugs delivered by intravitreal injection. Pharmacokinetic of intravitreal drugs is dependent on their molecular characteristics and ocular factors such as ocular volume, vitreous liquefaction, lens status and prior vitrectomy.

1.7.2 Retinal explant culture

1.7.2.1 The advantage of explant model

The primary cells culture from dissociated retina is useful to elucidate the direct effect of one type of cells. But it is time-consuming, expensive and has limits in reproducing conditions *in vivo* for absence of intercellular interaction[168]. Retinal explant is an important alternative between dissociated primary cell culture and animal model *in vivo*. First, retinal explant maintains the neurons *in situ* and in contact with other cells and extracellular matrix au maximum. For this reason, explant culture provides more predictive results for experiments *in vivo*. Second, retinal explant provides an easily controlled environment. The medicament can be directly applied on the surface of explant in a more manageable and direct manner. The serum-free medium has accurate and defined ingredients, ensuring the reproducibility of experiments. Third, retinal explant undergoes rapid regression of the blood vasculature, resulting in lack of retinal and choroidal blood supply. It can eliminate the possible potential disturbance of myeloid cells in blood circulation and the effects of BRB break-down[169].

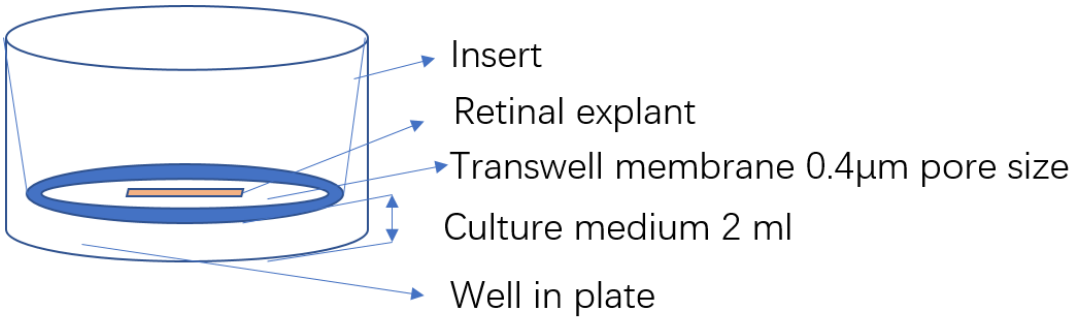

Figure 10: Simple illustration of explant system
The fresh retinal explant is deposited on polycarbonate membrane of an insert. This insert is placed in a well of a plate. The well is filled with 2 ml culture medium, just in contact to the membrane.

1.7.2.2 Introduction of this method

The retina is dissected from fresh eye and placed immediately on semipermeable polycarbonate membrane inserted in a well containing culture medium. The photoreceptor layer is facing downward on membrane which is kept just in contact to culture medium. This culture system keeps retinal explant in fluid-air condition, which is essential for explant culture and allows adding supplement in culture medium and on the surface of retinal explant (Figure 10).
This technique begun around 1976 with *Xenopus laevis* retina and adult golden fish retina

to study the effect of prior optic nerve crush[170]. In 1981, the mouse retina was used as retinal explant to study ganglion development after optic nerve cut[171]. Since then, organotypic retinal culture was wildly used in various researches mainly for retinal neurons. The animal species does not influence the explant culture and many species have successfully been used in retinal explant culture, such as fish, mice, rats, rabbits, chickens, monkeys, pigs, bovines, and postmortem humans[169].

1.7.2.3 Retinal explant morphology and genetic changes

Retinal explant decreases their thickness but preserve their cell layers. For adult mouse retinal explant, the retinal thickness decreases by half even though the retinal layers are preserved 4 days after culture[172]. Human retina culture demonstrates progressive retinal degeneration with decrease of plexiform layer thickness, reduction in the number of nuclei[173]. The retinal explant lacks choroid and retinal blood supply. This decrease of retina thickness might be due to the degeneration of retinal vasculature.

The mean RNA yield of retinal explant decreases. Mean RNA yield per microgram of adult mouse retina is decreased by almost 75% at 1-day culture[172]. RNA yield of pig colonic explant dropped from 505.0 ± 48.64 μg/mg to 227.6 ± 25.52 μg/mg at 6 h and 159.3 ± 24.19 μg/mg at 12 h of incubation. After 3 h incubation, RNA integrity was also decreased[174]. This decrease might be due to the decrease of rhodopsin RNA expression and RNA instability because of the dramatic changes of condition after isolation.

Retinal photoreceptors undergo apoptosis 4-day after culture, while ganglion cells undergo physically apoptosis in neonatal retinal explant in the first hours after culture[175]. In neonatal rat retinal explant, retinal ganglion cells underwent physiologically apoptosis 6 h and peaked at 48 h after culture. Photoreceptor underwent apoptosis 6-day after culture[176]. Another study showed that apoptosis of photoreceptor appeared and increased greatly after 4-day culture[172]. This apoptosis of photoreceptor results from ER stress and is related to damages of inner retina[173, 177].

The activation of Müller and microglia cells occurs in retinal explant. In rat retinal organotypic explant, microglial cells present features of activation: amoeboid form and retraction of processes. After 6 days culture, microglial cells regain their ramified morphology[178]. One day after culture, TNF-α, IL-6 and MCP-1 are detected in the culture supernatant, microglial cells undergo proliferation as revealed by Ki67, a cell proliferation-associated marker[179]. In neonatal rabbit retinal explants, Müller cells upregulate GFAP and decrease glutamine synthetase[180].

Retinal explant is better to culture with serum free medium in addition of appropriate neurotrophic factors. Retinal explant in medium containing serum is more often associated with tissue degradation, cell death than in serum free medium[181]. Glial cell line-derived neurotrophic factor added into medium can improve preservation of photoreceptors and horizontal cells[182].

In conclusion, retinal explant undergoes some changes in the first few days culture. In different studies of retinal explant, the culture method might be very different, such as rat or rabbit, postnatal or embryo retina, in defined serum-free media or serum-containing medium.

1.7.2.4 The employment of retinal explant

In the first two decades, retinal explant was used to study degeneration of retinal neurons induced by axotomy. In recent years, retinal explant culture enriches its functions by combining with other experimental technologies and is proved to be a good model to study pathogenic mechanism and possible treatment.

1.) Organic retinal explant is wildly used to study retinal development, CNS regeneration and neurodegeneration from the beginning of this technique. Embryo retinal explant combining with gene transfer is used to study retinal cell differentiation and retinal developement[183, 184]. Adult retinal explant is also employed to study the neuronal survival and axon regeneration, the endothelial cells angiogenic responses[169, 185, 186]. Retinal explant is employed to search the retinal survival mechanisms and to test potential novel neuroprotective agents in the treatment of retinal vascular and neurodegenerative diseases.

2). Combining retinal explant with cell labelling technologies, such as gene transfection cell labelling, calcium labelling and retrograde labelling, can facilitate the use of time-lapse imaging or screening system in research[187]. Animal is genetically transformed to have fluorescence-expressing retinal cells, such as Thy1-YFP mouse. Combining time-lapse imaging to fluorescent retinal explant can view ganglion cells dendritic arbors and evaluate the neuroprotective effects of neurotrophic agents over a course of several days[188]. The ganglion cells can also be labeled by retrograde injection of FluoroGold before eye isolation. This screening system provides fast, reproductive and sensitive method to detect neurotoxicity[189].

3). In a more controlled environment, retinal explant can be developed as pathology model to study retinal disease mechanisms and to test potential treatments with less animal suffering. The serum-free culture medium ensures metabolic quantitation and pharmacological interfering[190]. Culture in hypoxic conditions, retinal explant can establish retinal ischemic model to investigate hypoxic retinal neuropathies and possible treatment[191].

4). Retinal explant can help the developments of gene therapy and stem cell therapy to treat retinal diseases. The gene therapy is delivery of DNA to retina to cure hereditary retinal diseases. It needs vector tropism to target specific type of cell, which ensures the efficiency of gene transduction. It is currently performed by intravitreal injection of vector and genes in animal model. But the difference of receptors among species could influence the results in human. To better evaluate the transduction efficiency of vector, organic explant culture with human postmortem retina is a good model[192, 193]. Adding progenitor cells to retinal explant culture can imitate the intravitreal retinal stem cell therapy. Progenitor cells are added on the surface of retinal explant. They migrate and differentiate in retina, which can improve some function and reduce retinal cell loss[181, 194].

1.8 Objectives

Bacterial virulence is related to bad visual prognosis of bacterial endophthalmitis. PVL is a well characterized virulent toxin of *S. aureus*, which is related to severe infections. Instead of intravitreal injection of bacteria, we injected intravitreally PVL in rabbit eyes to analyze directly the effects of toxin on retina. We wanted to study early PVL effects on retina and know if PVL could induce inflammation in neural tissue after targeting neurons. Namely, we looked at identifying PVL retinal cell targets and analyzing the eventual inflammatory retinal response. Understanding PVL effects on retina could help to better understand the mechanisms of toxin leading to bad visual prognosis. This might provide some evidences for new therapeutic strategy to treat bacterial endophthalmitis.

In the first article, we employed intravitreal injection of PVL in an *in vivo* rabbit model. Whereas, in the second article, we tried to figure out if it was possible to obtain similar results in an *ex vivo* model, using retinal explants. Indeed, we developed retinal explant, which seemed to be a less expensive and more manageable model to study the effects of PVL on retinal cells and the possible cellular relationship after infection.

One of the main results, somehow surprising, was that PVL targeted retinal neurons, which seemed to induce glial cell activation and retinal inflammation. We were then interested in searching in the literature if neurogenic inflammation was already reported in retina and by which mechanism inflammation was enhanced. Even if neurogenic inflammation has not been studied in retinal infections, it has been described that bacterial toxins induce neurogenic inflammation during cerebellar and skin infections.

2. Materials and Methods

2.1 PVL

2.1.1 PVL purification

PVL is composed by two components, LukS-PV and LukF-PV. Their genes are located in a bacteriophage. The genes of LukS-PV and LukF-PV, from *S. aureus* strain V8 (ATCC 49775), were fused to Glutathion-S-Transferase (GST) in the plasmid pGEX6P-1. This fusion was carried by GST fusion protein System™ (Pharmacia), which allowed the overexpression, purification and detection of inserted protein in *Escherichia coli* BL21. The inserted plasmids were transferred to *E. coli* BL21. When *E. coli* BL21 containing recombined plasmid Pgex6p-1 was cultured to DO_{600nm} 0.4-0.6, 0.2 mM IPTG was added to the overnight culture to induce the expression of inserted plasmids. The bacteria were then centrifuged and grinded by French Pressure Cell Press (SLM AMINO). The lysate was centrifuged, and the supernatant was collected. The concentration of supernatant protein was measured by quantifying GST. The combined protein was purified by affinity chromatography on Glutathion Sepharose 4B™ (Amersham-Bioscience). The elution containing GST activity was collected and treated by PreScission Protease® (GE Healthcare, Villacoublay, France) to cleave GST from the combined protein. The cleaved protein solution was passed cation-exchange fast-performance liquid chromatography to purify LukS-PV and LukF-PV, separately. The purity and identification of protein was assessed by SDS-polyacrylamide gel electrophoresis and radial gel immunoprecipitation before storage at −80 ◦C. This method can obtain 99% purity of LukS-PV and LukF-PV.

2.1.2 Evaluation PVL effects by PMNs

2.1.2.1 Purification of human PMNs

PMNs were prepared from buffy coats of healthy donors of either sex, provided by the Etablissement Régional de Transfusion Sanguine de Strasbourg, France. The white-cell-enriched blood was diluted by 0.9 % NaCl (1/3, v/v). 5 ml perfusion solution (Plasmion; Lab. Roger Bellon, Neuilly sur Seine, France) was added to 20 ml of blood cell dilution. Blood cells were left to sedimentate for 30 min, and then centrifuged. The sediment was washed in HEPES buffer (140 mM NaCl, 5 mM KCl, 10 mM glucose, 0.1 mM EGTA, 10 mM HEPES, 3 mM Tris base, pH 7.3). Blood cells were collected and diluted to 40 ml by 0.9% NaCl (1/3, v/v), and then was layered on 12 ml of J Prep (Techgen International, Voisins le Bretonneux, France). After 20 min centrifugation (800 × g), the pellet was suspended in 30 ml of 0.9% NaCl and added to 10 ml of 6% (w/v) dextran, which was left

to sedimentate for 30 min and was centrifuged for 10 min at 800 × g. The pellet was suspended in HEPES buffer and the contaminating erythrocytes were removed by hypotonic lysis (45 s). The dilution was centrifuged and washed in HEPES buffer. The final suspension was adjusted to 6 × 10^6 PMNs / ml.

2.1.2.2 Evaluation of PVL effects by optic microscope

PMNs concentration was adjusted to 1 × 10^6/ml. A series of PVL concentrations (0.25 mM, 2.5 mM, 25 mM, 250 mM) were added to PMNs dilution in different tubes. At 5 min and 10 min, 6.6 µL PMNs dilution was added to Glassitc Slide and viewed under optic microscope. Results: PMNs were lysis at 5 min treated by 2.5 mM PVL. PVL was in good quality.

2.1.3 Evaluation of PVL effect in different culture media using cytometry

Purpose: Different culture media contained different calcium and zinc concentrations, which could influence PVL effects in calcium mobilization. Some media did not provide their ingredients. The purpose was to ensure that culture medium did not cause bad influence on PVL effects during explant culture.
It was proved that PVL could cause increase of cytoplasmic calcium concentration in PMNs during several minutes. The variation of calcium concentration in PMNs was recorded by measuring intensity of Fluro3 fluorescence with flow cytometry. In order to evaluate PVL effect in different culture medium, we measured the intensity of Fluo3 fluorescence of PMNs diluted in different culture medium and treated by 25 nM PVL suing cytometry.

Flow cytometry
Flow cytometry data were obtained using a FACSort cytometer (Becton Dickinson, Le Pont de Claix, France) equipped with a 15-mW argon laser tuned to 488 nm. PMNs were diluted to 1*10^6 / ml in different media (Table 4). PVL and Fluo3AM (2 mM, DMSO) were added into it. PMNs were classically distinguished by forward and side light scatter, and then their fluorescence was recorded during 10 min. Fluorescein and Fluo3 fluorescence intensities were recorded in the FL1 channel (emission wavelength, 530 nm). The FACSort cytometer was set in such a way that calibrated fluorescent microbeads (Immuno-Brite; Coulter Corporation, Hialeah, FL) displayed the same fluorescence intensity for each experiment. Thus, mean fluorescein fluorescence intensity was expressed in standardized fluorescence units. Variations of the intracellular Ca^{2+} levels were determined by measuring the intensity of Fluo3-AM fluorescence (Table 5).

Table 4. The components of tested tubes

Numbers	1	2	3	4	5	6	7	8
Culture Medium	Neurobasal A	i-CO2	HBSS	RPMI	Neurobasal A	i-CO2	HBSS	RPMI
PVL 25nM	0	0	0	0	10 µL	10 µL	10 µL	10 µL
Fluo-3AM 2mM	4 µL	4 µL	4 µL	4 µL	4 µL	4 µL	4 µL	4 µL
Total 1 ml PMN 1 x 10^6/ml								

Table 5. Intensity of Fluo3 fluorescence measured by cytometry

Numbers	0 min	2 min	4 min	6 min	8 min	10 min
1	171.46	191.48	191.03	204.62	220.16	197.08
2	127.67	132.81	124.41	127.42	133.33	135.54
3	155.31	151.8	151.1	161.51	165.7	168.67
4	114	123.1	117.26	125.83	124.6	125.83
5	255.53	331.01	359.86	447.45	543.17	627.68
6	132.66	136.1	136.17	169.87	214.26	262.44
7	149.28	188.34	189.74	247.15	285.42	297.01
8	115.12	114.62	122.41	147.7	210.64	309.1

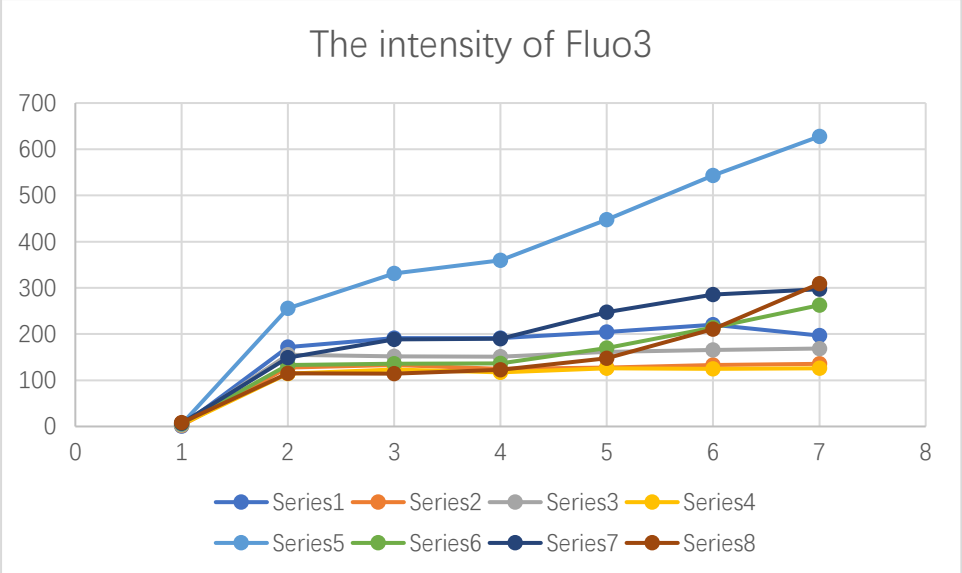

Conclusion: The four media (Neurobasal A, i-CO2, HBSS, RPMI) do not influence PVL effect in mobilizing calcium.

2.2 Animal and surgical procedure

2.2.1 Ethics of the protocol

The animal experiments were approved by the Ministère de l'Education nationale, de l'Enseignement Supérieur et de la Recherche, France (APAFiS no. 4986). The surgical procedure was performed in accordance with the guidelines in the laboratory of the Association for Research in Vision and Ophthalmology within the accredited A67-482-34 and B67-482-34 animal facilities.
For retinal explants, the rabbits were euthanized before the enuclearation of eyes. No special protocle was required.

2.2.2 Anesthesia, PVL intravitreal injection and euthanasia

Anesthesia
Pigmented rabbits (Bleu de Champagne) were aged one year and weighted 3.5–4 kg. They were anesthetized by intramuscular injection of combined ketamine (20 mg/kg Virbac, Carros, France) and xylazine (3 mg/kg Bayer Healthcare, Puteaux, France). After 3-5 min, the rabbit began to lose conscience. The anesthetic state of rabbit was evaluated by touching the eyes: if there was no palpebral reflex, the anesthesia was fine.

PVL intravitreal injection
Two drops of oxybuprocaine chlorhydrate (Théa, Clermont-Ferrand, France) were added to conjunctiva as local anesthesia. PVL was diluted in phosphate-buffered saline (PBS) (3 µg/50 µL) and intravitreally injected with a 30-Gauge needle. The inserted point was 4 mm behind the corneal limbus.
In *in vivo* PVL-injection endophthalmitis model, there was three control eyes which was injected with 50-µL PBS using the same technique. After PVL injection, animals were sacrificed at pointed times (30 min, 1, 2, 4 and 8 h). There was three different eyes for each time point.

Euthanasia
After intramuscular anesthesia with combined ketamine-xylazine (as mentioned above), 22-Gauge catheter was inserted in the marginal auricular vein and a lethal dosage of 2-mL Pentobarbital Dolethal® (Vetoquinol, Lure, France) was injected through this catheter.

2.2.3 Retinal explant preparation and organotypic culture

Retinal explant requires a swift extraction of retina from intact eye and the retinal flat mounting on a hydrophilic membrane with minimum disturbance of the tissue. Briefly, pigmented rabbits were sacrificed, and eyes were enucleated as mentioned above. Eyes were immerged in cold i-CO2 medium and transported on ice to the laboratory.

In aseptic condition, each eyeball was immersed in disinfection medium (Pursept A, xpress Germany) and washed with cold i-CO2 medium. Under a stereomicroscope equipped with an internal light source, the eye was held in place with a paire of blunt-ended forceps and 18-gauge needle was inserted into the eye at the ora serrata to make a hole. A pair of fine spring scissor was inserted into the hole and made a circumferential incision around the limbus, dividing the ocular globe into anterior and posterior eyecups. The vitreous was removed, and the posterior eyecup was placed into another dish containing fresh i-CO2 medium and was cut into 4 pieces 7×7 mm, avoiding the visible blood vessels and myeline. The peripherial sclera was held with fine forceps, choroid was teared away from the sclera and the optic nerve was cut with fine scissor. The neuroretina was detached gently from the pigment epithelium by tearing the choroid.

The retina was transferred using a micropipette (3.5 ml), the tip of which as cut a few millimeters to widen the opening. Once the retina was within the transfer pipette, it can be oriented to vessel side facing up by drawing the medium up and down. The retina was dropped with photoreceptor layer facing up on membrane which was inserted into Transwell® culture dishes (Corning Inc., Corning, NY). After flat-mounting was complete, all the remaining dissection medium around the retina was aspirated away. During mounting the retina on membrane, retina should not be touched. Then, 2 ml culture medium, neurobasal-A (Gibco, Life technologies, Carlsbad, USA) supplemented with Penicillin-Streptomycin (100 U/mL) mixture, was added into culture well. The culture medium level was maintained in contact with the support membrane beneath the explant. The retinal explants were incubated at 37 °C with 5% CO_2 in a humidified atmosphere.

A series of PVL concentrations were prepared: 0.176, 0.352, 1.76 and 12.48 µM. Our previous study used PVL (3 ug/50 ml), equal to 1.76 µM. So, 1.76 µM PVL was used as the reference concentration. A 10-µL droplet of PVL diluted in culture medium was deposited on the surface of nerve fiber layer in each explant after retina flat-mounting. An equivalent volume of culture medium was deposited onto the surface of control explants. Retina explants were collected at different time points (30 min, 2, 4, 8 and 24 h), and fixed immediately with 4% paraformaldehyde or stored at -80 °C according to the design (Table 8).

Table 6. The numbers of explants at different time points and with different PVL concentrations

Time points	control	0.176 µM PVL	0.352 µM PVL	1.76 µM PVL	12.48 µM PVL
30 min	3 fixed	3 fixed	3 fixed	3 fixed	3 fixed
2 h	3 fixed	3 fixed	3 fixed	3 fixed	3 fixed
4 h	3 fixed; 4 frozen	3 fixed	3 fixed	3 fixed; 4 frozen	3 fixed
8 h	3 fixed; 4 frozen	3 fixed	3 fixed	3 fixed; 4 frozen	3 fixed
24 h	3 fixed; 4 frozen	3 fixed	3 fixed	3 fixed; 4 frozen	2 fixed

2.3 Immunohistochemistry

2.3.1 Preparation of paraformaldehyde 16%

Added 16 g paraformaldehyde in powder in 100 ml PBS.
Heated them to 60~70 °C with stirring until the powder was dissolved.
Added 1-2 drops of NaOH (1 M) to clarify the dilution.
Adjusted dilution PH to 6.9 with HCl.
Filtered dilution through 0.45 µm membrane and stored it at -20 °C

2.3.2 Tissue for immunohistochemistry

The eyes were intravitreally injected with 100 µL of 4% (wt/vol) paraformaldehyde (Thermo Fisher Scientific, Rockford, IL, USA) immediately after rabbit sacrifice, and were then oriented and enucleated. The cornea, iris, and crystalline lens were immediately removed. The eye globe was fixed for 3 h in 4% paraformaldehyde. The dissected eyes were successively immersed in 10% (wt/vol) and 20% (wt/vol) sucrose and stored in 30% (wt/vol) sucrose overnight at 4 °C.

2.3.3 Vertical section

For a better cryosection, the retina was separated from the pigmented epithelium. The temporal zone of 1–5 mm near the optic disc was isolated and then immersed in optimal cutting temperature compound (Sakura Finetek, Torrance, CA, USA). Vertical cryostat 8-µm-thick sections were mounted on a Super Frost™ Plus microscope slides (Thermo Fisher Scientific, Rockford, IL, USA) and stored at −20 °C.

2.3.4 Tissue for whole mount

The fixed retina was identified and stored at −80 °C.

2.3.5 Immunohistochemistry for retinal sections

Immunohistochemistry was performed to analyze the retinal cells targeted by PVL. Retinal sections were permeabilized in 0.05% (v/v) TritonX-100 for 1 h and then were blocked with 10% (v/v) donkey or goat serum (Sigma-Aldrich, St. Louis, MO, USA) for 1 h. Retinal sections were incubated with primary antibody or lectin (see Table 7 for details) at 4°C overnight in a humidity chamber. Retinal sections were then incubated for 1 h at room temperature with fluorescent secondary antibodies or TUNEL (except when lectin was used) (see Table 7 for details). The sections were counter-stained with Hoechst 33258 and mounted in 10% (v/v) Mowiol® solution (Polysciences, Eppelheim, Germany). Images of fluorescent sections were obtained using an epifluorescence Olympus BX60 microscope connected to a Hamamatsu C11440 digital camera.

2.3.6 Immunohistochemistry for retinal whole mounts

The retinal whole mounts were incubated in conical small wells and transferred with 3 ml pippet. Retinal whole mounts were permeabilized 0.2% (v/v) TritonX-100 for 30 min. The staining steps were the same as those of section immunoistochemistry. At last, the retinal whole mounts were mounted on slides and covered with thinner and smaller cover slides in 10% (v/v) Mowiol® solution.

2.3.7 Cell counting

Different microscope fields (266 µm × 266 µm) of vertical retinal immunofluorescent images were randomly captured by the camera.

For PVL-endophtalmitis *in vivo* model

The proportions of PVL-positive RGCs and DACs were measured in the RGC layer. PVL-positive cells were double-labeled by PVL and cell-specific markers for RGCs and DACs.

The percentages of PVL-positive RGCs and DACs in each time point were established by mean mounts of 3 different eyes (five different study fields for each eye). TUNEL positive cell counts for each time point and control were established by mean number of TUNEL positive cells from 3 eyes (5 different study fields for each eye).

For retinal explant *ex vivo* model

PVL-positive retinal cells were evaluated by double immunohistochemistry: PVL-positive cells were double-labeled by PVL and retinal cell-specific markers. The percentages of PVL-positive RGCs at each time point (30 min, 2, 4, 8 and 24 h with 1.76 μM PVL) were established by mean mounts of 3 explants (each explant had five study fields randomly captured by camera). The mount of TUNEL positive cells in each time point and concentration was established by mean mounts per study field (3 explants, 5 study fields for each explant).

2.3.8 Statistical analysis

Statistical analysis was performed with GraphPad InStat version 3.10. Statistical significance was calculated with one-way ANOVA using the Tukey-Kramer multiple comparisons test and paired t-tests. Statistical significance was assumed at $p < 0.05$.

Table 7. List of specific markers used in this study

Primary antibodies or lectin

Target	Antiserum	Source	Concentration
PVL	Rabbit anti-LukS-PV polyclonal	EA-7290, Strasbourg, France	2 µg/mL
C5aR	Rabbit anti-C5aR polyclonal	Abcam, Cambridge, UK	2 µg/mL
Ganglion cells	Guinea pig anti-RBPMS polyclonal	UCLA Neurobiology, Los Angeles, CA, USA	2 µg/mL
Starburst amacrine cells	Goat anti-ChAT polyclonal	Chemicon Merck-Millipore, Temecula, CA, USA	20 µg/mL
Müller cells	Mouse anti-GFAP polyclonal	Bio-Rad AbD Serotec, Oxfordshire, UK	2 µg/mL
Microglial cells	FITC-tagged GSAI-B4	Sigma Aldrich, Saint Louis, MO, USA	2 µg/mL
amacrine cells	Rabbit anti-Pax 6 polyclonal	Abcam	2 µg/mL
All Amacrine cells	Mouse anti-calretinin monoclonal	Santa Cruz Biotechnology, Heidelberg, Germany	2 µg/mL
Horizontal cells	Mouse anti-calbindin monoclonal	Santa Cruz Biotechnology	2 µg/mL
Nitrotyrosine	Mouse anti-nitrotyrosine monoclonal	Santa Cruz Biotechnology, Heidelberg, Germany	2 µg/mL
C5L2	Rabbit anti-C5L2 polyclonal	GeneTex, San Antonio, TX, USA	2 µg/mL
β-actin	Rabbit anti-β-actin polyclonal	Santa Cruz Biotechnology, Heidelberg, Germany	1:2000
IL-6	Mouse anti-IL-6 monoclonal	Abbexa Ltd, Cambridge, UK	1:2000
IL-8	Mouse anti IL-8 monoclonal	Abbexa Ltd, Cambridge, UK	1:2000
IL-1β	Rabbit anti-IL-1β polyclonal	Abbexa Ltd, Cambridge, UK	1:2000
TNF-α	Mouse anti-TNFα monoclonal	Abbexa Ltd, Cambridge, UK	1:2000
	Secondary antibodies		
Anti-rabbit	Goat and donkey polyclonal Alexa 555nm-conjugated	Life Technologies, Carlsbad, CA, USA	2 µg/mL
Anti-goat	Donkey polyclonal Alexa 488-conjugated	Molecular Probes, Eugene, OR, USA	2 µg/mL
Anti-mouse	Donkey polyclonal Alexa 488-conjugated	Abcam	2 µg/mL
Anti-guinea pig	Goat polyclonal Alexa 488-conjugated	Abcam	2 µg/mL
TUNEL	DNA strand breaks	Roche Life Science, Indianapolis, IN, USA	---
Nuclei	Hoechst 33258	Molecular Probes™, Eugene, OR, USA	0.1µg/mL
Anti-rabbit	Anti-Rabbit IgG (whole molecule)–Peroxidase	Sigma Aldrich	1:10000
Anti-mouse	Goat anti-mouse IgG-Peroxidase	Santa Cruz Biotechnology	1:10000

Abbreviations: RBPM, RNA-binding protein with multiple splicing; CHAT, choline acetyl transferase; GFAP, glial fibrillary acidic protein; GSAI, *Griffonia simplicifolia* agglutinin isolectin. TUNEL, terminal deoxynucleotidyl transferase dUTP nick-end labeling.

2.4. Western blotting

2.4.1 Tissue preparation for western blot

The eyes were enucleated without any injection. Briefly, the conjunctiva was open then the ocular muscles were cut. Finally, the optical nerf was cut and the eye was immersed into cold i-CO2 medium. Eighteen-Gauge needle was inserted at 4 mm behind the corneal limbus and then removed. A micro-scissor was inserted into this pore and cut circumferentially the ocular globe. The cornea, iris, crystalline lens and vitreous were removed. The retina was gently peeled and removed to a tube with transfer pipette. The retina in tube was immediately stored at -80 °C. Retinal dissection was undertaken in cold i-CO2 medium within 10 min.

2.4.2 Extraction protein from retina for western blotting

RIPA buffer: 1% (v/v) NP-40, 0.1% SDS, 1% (w/v) sodium deoxycholate, 50 mM sodium chloride, 25 mM Tris-HCl pH 8.0

One half of whole frozen retinas were placed in microfuge tubes of Eppendorf tuves. The tissue was immersed with 500 µL RIPA buffer containing an inhibitor protease cocktail (Roche). The tissue was homogenized by passing through a 22-Gauge needle and then 26-Gauge needle several times in RIPA buffer. The tubes were sonicated for 20 s and then agitated for 2 h at 4 °C.

The tubes were centrifuged for 20 min at 12,000 rpm at 4 °C in a microcentrifuge. The tubes were gently removed from the centrifuge and placed on ice. The supernatant was aspirated and identified, and then was immediately stored at -80 °C. The pellets were discarded.

2.4.3 Quantify protein using BCA kit

Prepared bovine serum albumin (BSA) 2.5 mg/mL in H_2O.

Prepared a series of BSA concentrations (Table 8)

Table 8. The preparation of a series of BSA concentrations

Numbers	1	2	3	4	5	6	7
[BSA] µg/mL	0	200	500	800	1200	1600	2000
BSA 2.5mg/ml (µL)	0	4	10	16	24	32	40
H2O (µL)	50	46	40	34	26	18	10

The samples were diluted 1/10^{e}, a volume of 50 µL. One control was prepared with the same buffer.
The necessary volume of reagent 660-nm Protein Assay (660-nm Protein Assay Reagent, Pierce Biotechnology) was prepared: 0.5 g detergent (IDCR; 2263) + 10 ml Pierce 660. Mix well the reagent.
Added 750 µL reagent to all the BSA dilutions (50 µL, Table 8), sample dilutions (50 µL), and controls (50 µL). Mixed well and waited for 5 min.
Read all samples and control at 660 nm by spectrometry.
Noted the figures and developed equator using the figures of the series of BSA concentrations.
Calculated the concentration of samples with this equator.

2.4.4 Migration

The SDS-PAGE gels were from commercial laboratory (Bio-Rad Laboratories, Hercules, CA, USA). Considering the weight of target proteins (10-50 kDa) to be revealed, we chose 4-15% Tris-HCl gel. The samples (30 µg) were diluted to 20 µL in loading buffer and water. The sample mixtures were heated at +95 °C for 5 min and loaded in each lane. The gels were submerged in migration buffer and electrophoresed for 30 min at 200 V.

2.4.5 Transfer

After migration, proteins were transferred to a nitrocellulose membrane by wet transfer. The gel and membrane were sandwiched between sponges and paper (2 spongs / 3 papers / gel / membrane / 3 papers / 3 sponges) and all were clamped tightly together. When the membrane was deposited on the gel, it needed ensure that no air bubbles have formed and all the papers, sponges and menbrane were wet in transfer buffer. Then, the sandwich was submerged in transfer buffer to which an electrical field was applied. The negatively-changed proteins travelled towards to positively-charged electrode. But the membrane (0.2 µm pore) stopped and bound them. The transfer was carried on for 1.5 h at 40 V.

2.4.6 Staining of the membrane

To prevent non-specific background binding of primary and/or secondary antibodies to the membrane, the membrane was blocked in 5% (w/v) skimmed milk diluted in PBS at room temperature for 1 h.
The primary antibodies (see Table 7) were diluted in phosphate-buffered saline with 0.05% Tween® (PBST) to suggested dilution (1:500-1: 2000). One membrane can be stripped into two or three parts according to the design. The stripped membranes were incubated into primary antibodies dilution overnight at 4 °C. The membranes were washed three times in PBST while agitating. The membranes were incubated in Peroxidase-conjugated

secondary antibodies dilution (see Table 7) for 1 h at room temperature with agitation, then were washed three times in PBST while agitating.
The membranes were developed using ECL Western blotting detection reagent (Bio-Rad Laboratories, Hercules, CA, USA). The digital images were captured by a chemiluminescence camera (ChemiDoc™ XRS, Bio-Rad). The protein expressions were quantified by densitometry analysis of Western Blots bands using BIO-1D software.

2.5 Real-time RT-qPCR

In PVL-endophthalmitis *in vivo* model, we analyzed tested retinas (PVL 4 h and PVL 8 h, 3 eyes for each group) and control retinas (PBS 4 h, 6 eyes) using RT-qPCR to see the elevation of cytokines, the sign of retinal inflammation.
In retinal explant *ex vivo* model, we analyzed PVL-treated explants (4 and 8 h, 4 explants for each time point) and control explants (4 and 8 h, 4 explants for each time point).

2.5.1 Tissue preparation for RT-qPCR

This is the same preparation as for western blot.

2.5.2 RNA extraction

Retina stored in 1.5 ml Eppendorf tube was removed from -80 °C and 600 µL TRIzol (Sigma, Saint-Louis, USA) was immediately added into it. Retina was passed several times 23-Gauge then 26-Gauge needle to be homogenized. The homogenized retina was incubated for 10 min at room temperature (RT). Sixty µL of chloroform was added into tube and mixed well. The mixture was incubated for 5 min at RT. Then the tube was centrifuged at 10,000 x *g* at 4 °C for 15 min. The supernatant was carefully aspirated and put into a new tube. Then, 400 µL isopropanol was added into it and mixed well. The mixture was incubated for 10 min at RT. The tube was centrifuged at 10,000 x *g* at 4 °C for 10 min and all the liquid was poured. The pellet was kept and washed with 75% EtOH. The tube was centrifuged 10,000 x *g* at 4 °C for 5 min. The liquid was poured, and the pellet was kept. Another wash was repeated with 75% EtOH. The pellet was dried for 5 min at 65 °C and dissolved the pellet in 50 µL of water at 55 °C for 15 min.

2.5.3 RNA quantification and integrity

The final RNA solutions were quantified with spectrophotometry (NanoDrop; Thermo Scientific, Waltham, USA). Spectrophotometer showed absorbance measurements at 230 nm, 260 nm and 280 nm, and concentration of nucleotides. The ratio of absorbance at 260 nm and 280 nm was used to assess the purity of DNA and RNA. The ratio $\geqslant$1.8 was generally accepted as “pure” for RNA using for RT-qPCR; the ratio< 1.8 was unacceptable for RT-qPCR: too many DNA was mixed with RNA and needed to be treated with DAN-free

kit DNase. The ratio 260 nm/230 nm was used as the indicator of nucleic acid purity. Expected the ratio 260 nm/230 nm was commonly in the range of 2.0-2.2. If the ratio was appreciably lower than the expected, it may indicate the presence of contaminants which absorbed at 230 nm, such as EDTA carbohydrates and phenol. The sample needed to be washed again with 75% EtOH.

2.5.4 DNase treatment with DNA-free kit DNase

RNA (10 µg), 10 x DNase buffer 5 µL, TURBO DNase (Ambion, Life technologies), sterile water brought the volume up to 50 µL total. The components were added in this order: water, RNA, buffer, DNase. Mixed gently and centrifuged briefly the mixture, which was then incubated at 37 °C for 30 min. Add 5 µL DNase inactivation reagent and mixed well. Incubated 2 min at RT and centrifuged at 10,000 x *g* for 1.5 min and transferred the RNA to a fresh tube.

2.5.5 Primers design

The primer design was undertaken using Primer 3 website software. The results showed several choices of primers. The most adaptable primers were chosen by the general primer design rules, such as primer length 18-24 bps, annealing temperature around 60 °C, avoid repeats of nucleotide sequence at 3' end. The successful primer design was verified by evaluating the purity of PCR product, which showed one sharp pick at melting curve and one band at agarose gel.

Table 9. The sequences of primers used in this thesis

Nom	left primers	right primers
VEGF	cgagaccttggtggacatctt	tgcattcacatttgttgtgct
SP	acagcgaccagatcaaggag	cccattagtccaacaaaggaa
CGRP	ggcgtaaacaaagtgggaag	tggatctcaacagcagtcatag
iNOS	ccaagccctcacctacttcc	aactcctccagcacctcca
Actin-β	gcgggacatcaaggagaag	aggaaggagggctggaaga
IL-1	ttgtcagtcgttgtggctct	ggatttctgttgtgcatcct
IL-8	tggctgtggctctcttgg	atttgggatggaaaggtgtg
IL-6	tcaggccaagttcaggagtg	atgaagtggatcgtggtcgt
TNF-α	cgtagtagcaaacccgcaag	tgagtgaggagcacgtagga
MCP-1	aacgcttctgtgcctgct	ggacccacttctgcttgg

2.5.6 RT

Total RNA was immediately reverse transcribed (RT) using Superscript First-Strand Synthesis for RT-qPCR (Invitrogen, Life technologies). Briefly, Diethyl decarbonate (DEPC) (Sigma) treated H_2O was added to RT mixture (0.5 µL random hexamers (200 ng/ml), 500 ng total RNA, 1 µL NTP) to achieve a 12 µL volume. The mixture was gently centrifuged and then incubated at +65 °C for 5 min and placed in glass for 2 min.
Then 0.5 µL of 0.1 M DDT, 0.5 µL of transcriptase, 4 µL of First Strand buffer, 3 µL of DEPC treated H_2O were added to the mixture. Then, the total mixture was gently centrifuged and put into ThermoCycler, which was programmed at +42 °C for 50 min and at +70 °C for 15 min. The cDNA was diluted in 3 times with DEPC treated H_2O.

2.5.7 PCR to check cDNA

To ensure the cDNA was well produced, PCR was employed to reproduce β-actin using this cDNA. The mixture contained 2 µL cDNA, 0.125 µL Taq DNA Polymerase, 2.5 µL 10 x standard buffer, 0.5µL dNTPs, 2 µL forward and reverse primers (100µm), DEPC treated H_2O which brought to 25 µL total. ThermoCycler was programmed as initial denaturation step at +95 °C for 5 min, 40 cycles of amplification (denaturation at +95 °C for 25 s, annealing at +58 °C for 20 s, extension at + 68 °C for 25 s), final extension at +68 °C for 5 min, hold at +4 °C. The PCR products was verified by agarose gel electrophoresis (see below).

2.5.8 Real-time qPCR

5 µL of diluted cDNA, 10 µL SYBR mix (LightCycler 480 SYBR Green I Master, Roche, Basel, Switzerland), 2 µL of forward and reverse primers (100 µm), and 3 µL DEPC treated H_2O were mixed and put into 96 wells plate. The plate was placed into Real-Time PCR System (Light Cycler 480, Roche). The primers were designed to have Tm around 60°C. PCR was programmed as initial denaturation step at + 95 °C for 10 min, 45 cycles of amplification (denaturation at + 95 °C for 15 s, annealing at + 60 °C for 20 s, extension at + 72 °C for 15 s), and melting curve analysis (+ 60 °C to + 95 °C increment at + 0.3 °C). Products of RTs without reverse transcriptase were used as controls to assure no significant DNA contamination

2.5.9 Production specificity verification

The specificity of PCR products was verified according to one melting curve peak and one band in agarose gel electrophoresis.

2.5.9.1 Melting curve analysis

SYBR Green I is fluorescence which bind double-stranded DNA. Both heterozygous and homozygous single-base variants could contribute to the fluorescence. DNA melting curves were acquired by measuring the fluorescence of SYBR Green I during a linear temperature transition. Melting curves could distinguish well between specific PCR product and non-specific PCR product such as "primer-dimers" that often had a considerably lower Tm.

2.5.9.2 Analysis on non-denaturing agarose gel electrophoresis

Prepare agarose was diluted in concentration of 2% and 0.5 μg/ml ethidium bromide: 60 ml 0.5 X TBE +1.2 g agarose in powder + 3 μL 10 mg/ml ethidium bromide;
Mix well and heat to boiling with microwave oven, then pour the hot mixture to tank with comb, which is a mould for gel. Cool the mixture to form gel.
Take away the comb and pour down enough TBE buffer to immerge the gel.
Load 20 μL RNA or DNA samples with loading buffer into each lane. Set running voltage up to 10 V/cm and run electrophoresis.
View the gel under chemiluminescence and take image with camera.
The good PCR product showed one clear band at the appropriate site corresponding to its length. The good RNA sample showed two clear bands (28s rRNA and 18s rRNA from up to down separately), the intensity of 28s rRNA was almost two times of that of 18s rRNA.

2.5.10 Statistical analysis

The β-actin was used as reference gene and target genes were normalized using this reference gene. The method ∆Ct was used to calculate relative quantification between control retina and tested retina. The fold changes were calculated using $2^{-\Delta\Delta Ct}$. The tests were achieved in triplicates. The significant changes of every target gene were statistically analyzed with ∆Ct paired t-tests using GraphPad InStat version 3.10. Statistical significance was assumed at $p < 0.05$.

3. Results

3.1 Article 1: Panton–Valentine Leukocidin Colocalizes with Retinal Ganglion and Amacrine Cells and Activates Glial Reactions and Microglial Apoptosis

Preface

The virulence of infecting bacteria is an important factor to influence the visual prognosis of bacterial endophthalmitis. PVL, one virulent leukotoxins of S. aureus, can cause severe necrotic tissue infection. Intravitreal injection of bacteria or bacterial products is an experimental model employed for a longtime. It imitates the natural pathway of pathogens invading to the interior of eyes. As PVL recognizes only human and rabbit C5aR, not murine C5aR, so rabbit model is the only available animal model for PVL study. Previous studies revealed that intravitreal injection of PVL could cause severe endophthalmitis in rabbit, producing retinal inflammation, breakdown of the blood–retinal barrier and neutrophils infiltration. Exploring the initial retinal cell target and the features of early inflammation can help understand the mechanism of PVL infection to retina, the development of following fulminant inflammation. This could well explain the role of bacterial virulence in bad visual prognosis of bacterial endophthalmitis. The objectives of this part are to identify PVL cell target and analyze the early inflammatory changes in rabbit retina, using PVL intravitreal injection in vivo model.

In this PVL-endophthalmitis in vivo model, we found that PVL was always fixed specifically in retinal ganglion cell layer from 30 min to 8 h after injection. Using double-immunohistochemistry, we showed that PVL increasingly colocalized with retinal ganglion cells (RGCs) within 2 h, while PVL transiently colocalized with displaced amacrine cells (DACs) within 4 h. The C5aR immunoactivity colocalized with RGCs, not with other retinal cells. Müller and microglial cells were increasingly activated after PVL injection from 30 min to 8 h. IL-6 mRNA and protein expression in retina increased and some microglial cells underwent apoptosis 4 h and 8 h after PVL infection, which might be associated with abnormal nitrotyrosine production in the retina.

In a previous study, PVL reacted on cerebellar neuronal cells. This study showed that PVL could colocalize rapidly with RGCs and transiently with DACs, following inflammatory reaction in retina. In retina, only RGCs colocalized with C5aR immunoactivity, the specific receptor of PVL. PVL probably incited RGCs reaction through C5aR and initiated retinal inflammation. This study also showed the early inflammatory changes in retina, which could modify retinal structure, and furtherly recruit leukocytes to retinal tissue, interrupt the visual function, resulting in major consequences to the visual outcomes. Other animal

models, such as retinal explant and *in situ* sophisticated approaches, are needed to confirm those results, which could bring more insights about the sequential activity of retinal cells, the relation between PVL binding on neuronal cell and glial cell activation.

SCIENTIFIC REPORTS

OPEN

Panton–Valentine Leukocidin Colocalizes with Retinal Ganglion and Amacrine Cells and Activates Glial Reactions and Microglial Apoptosis

Received: 20 April 2017
Accepted: 11 January 2018
Published online: 13 February 2018

XuanLi Liu[1], Pauline Heitz[2], Michel Roux[3], Daniel Keller[1], Tristan Bourcier[1,2], Arnaud Sauer[2], Gilles Prévost[1] & David Gaucher[1,2]

Experimental models have established Panton–Valentine leukocidin (PVL) as a potential critical virulence factor during *Staphylococcus aureus* endophthalmitis. In the present study, we aimed to identify retinal cell targets for PVL and to analyze early retinal changes during infection. After the intravitreous injection of PVL, adult rabbits were euthanized at different time points (30 min, 1, 2, 4 and 8 h). PVL location in the retina, expression of its binding receptor C5a receptor (C5aR), and changes in Müller and microglial cells were analyzed using immunohistochemistry, Western blotting and RT-qPCR. In this model of PVL eye intoxication, only retinal ganglion cells (RGCs) expressed C5aR, and PVL was identified on the surface of two kinds of retinal neural cells. PVL-linked fluorescence increased in RGCs over time, reaching 98% of all RGCs 2 h after PVL injection. However, displaced amacrine cells (DACs) transiently colocalized with PVL. Müller and microglial cells were increasingly activated after injection over time. IL-6 expression in retina increased and some microglial cells underwent apoptosis 4 h and 8 h after PVL infection, probably because of abnormal nitrotyrosine production in the retina.

Bacterial endophthalmitis is a common but severe infection of the eye, which is often caused by ocular surgery or trauma[1]. The visual prognosis of endophthalmitis depends on many factors, one of the most important being the virulence of the infecting bacteria, as reported in a recent study[2]. Though *Staphylococcus aureus* is rarely involved in ocular endophthalmitis, it secretes an extensive repertoire of cytotoxins that represent a significant threat to visual outcomes.

Methicillin-resistant *S. aureus* (MRSA) places a significant burden on healthcare resources due to its resistance to antimicrobial treatment. Community-associated (CA)-MRSA, which emerged in 1990s, can be distinguished from hospital-acquired (HC)-MRSA, primarily because it bears the gene encoding Panton–Valentine leukocidin (PVL)[3,4]. Recent studies have reported that the percentage of CA-MRSA has significantly increased in MRSA infection isolates and may continue to rise in the future due to the horizontal transfer of genes and inter-human transmission[5]. PVL is composed of two distinct proteins, a class S (31–32 kDa) and a class F component (33–34 kDa), which organize as alternate octamers, called prepores, and are internalized into polymorphonuclear cells where they initiate intracellular relapsing of Ca^{2+} storages. The class S component binds to the C5a membrane receptor (C5aR), allowing the secondary interaction of the F component. Unaccompanied class S or F proteins never seem to produce any effect on targeted cells[6]. PVL may result in tissue necrosis during *S. aureus* infection, especially necrotizing infections, such as furuncles, acute necrotizing pneumonia, and osteomyelitis[7,8].

[1]Université de Strasbourg, Hôpitaux Universitaires de Strasbourg, Fédération de Médecine Translationnelle de Strasbourg, EA7290 Virulence Bactérienne Précoce, Institut de Bactériologie, Strasbourg, France. [2]Hôpitaux Universitaires de Strasbourg, Service d'Ophtalmologie du Nouvel Hôpital Civil, Strasbourg BP426, 67091 cedex, France. [3]Department of Translational Medicine and Neurogenetics, Institut de Génétique et de Biologie Moléculaire et Cellulaire, CNRS UMR_7104, Inserm U 964, Université de Strasbourg, Illkirch, France. Correspondence and requests for materials should be addressed to D.G. (email: david.gaucher@chru-strasbourg.fr)

Recent studies have reported that PVL binds to human complement C5a receptor. This binding largely decreases in rodents but is conserved in rabbits[9]. Recent studies on humanized mice with C5aR showed the critical role played by PVL in the determination of necrotizing pneumonia and its severity[10,11]. Other staphylococcal leukotoxins have been characterized, but only LukS-PV and HlgC were shown to bind C5aR[10,11]. There has been evidence of PVL targeting myeloid cells such as monocytes (M), macrophages (Mϕ), and polymorphonuclear cells (PMNs), but not lymphocytes[12]. Another recent study showed that *in vitro*, PVL could target dorsal root neurons and cerebellum granular neurons[13]. In the rabbit eye, previous studies revealed that PVL and other staphylococcal leukotoxins injected into the rabbit vitreous could cause retinal inflammation and breakdown of the blood–retinal barrier (BRB)[14,15]. However, the mechanism leading to such inflammation remains to be determined albeit vitreous is mainly devoid of cells.

IL-6 has been shown to have effective angiogenic activities and inflammatory role in models of choroidal neovascularization, ocular inflammation and tumor angiogenesis[16]. In this study, our purpose was to identify retinal cell targets for PVL and to analyze initial mechanisms that might support or indicate inflammation and inter-cellular communication. In particular, we studied the potential consequences of retinal cell infection, such as glial reaction, neuronal cell damage, and the presence of inflammatory markers. The results reported herein strongly suggest that PVL colocalized with two types of retinal neurons: displaced amacrine cells (DACs) very early in the translocation process, and retinal ganglion cells (RGCs), which triggered a glial reaction and an increase of IL-6 expression in the retina.

Results

PVL was located in RGCs and DACs. An anti-LukS-PV antibody (Table 1) was used to identify PVL translocation from the rabbit vitreous into the retina. Results indicated that PVL was concentrated in the ganglion cell layer. Since this cell layer is composed of RGCs and DACs, we investigated the exact target of PVL using specific labeling for RGCs (anti-RBPMS antibody) and DACs (anti-CHAT antibody) (Table 1).

RGCs were PVL-positive. The rate of positive RGCs significantly increased from 47% to 76% from 30 min to 1 h ($p < 0.05$) after PVL injection. This rate reached 98% after 2 h ($p < 0.05$ compared with the rate of 1 h) and 99% 4 h after PVL injection (Fig. 1). The majority of DACs were PVL-positive at 30 min after PVL injection. However, the rate of PVL-positive DACs significantly decreased from 68% to 32% between 30 min and 1 h ($p < 0.01$) after PVL injection, respectively. This rate continued to significantly decrease and was 27% at 2 h and 5% at 4 h following PVL injection ($p < 0.01$) (Fig. 2). Eight hours after PVL injection, all RGCs colocalized with PVL, while 4% of DACs still colocalized with PVL (see Supplementary Fig. S1).

To further investigate whether PVL was specifically colocalized with the RGCs and DACs, we examined the rabbit retina for C5aR and C5L2 expression using specific antibodies, since PVL binds with human neutrophils through the C5a receptor[9,17]. The anti-C5L2 antibody did not detect any specific staining in rabbit retina (Fig. 3G). C5aR was consistently expressed in RGCs suggesting that PVL might colocalize with RGCs through C5aR. C5aR did not colocalize with DACs (Fig. 3 and Table 1). Therefore, another mechanism for PVL colocalization (possibly with a decreased affinity) and possible penetration in DACs cannot be excluded.

The Müller and microglial cells were activated after PVL injection. Müller cells can transform into an activated state, characterized by the rapid upregulation of glial fibrillary acidic protein (GFAP). This upregulation occurs after acute retinal injuries or inflammation states[18]. Anti-GFAP antibody was used to label Müller cells (Table 1). As early as 30 min after PVL injection, Müller cells abnormally expressed GFAP in the outer retina (Fig. 4 and Table 1). This abnormal GFAP expression was not observed in the controls. Only a few Müller cell processes stained with GFAP were visible in the outer retina at 30 min, whereas the number and extension of processes increased from 1 to 2 h after PVL injection. At these time points, the outer plexiform layer (OPL) was well defined with GFAP staining. At 4 h, it seemed that the architecture of the retina had changed as numerous disruptions of GFAP staining within outer processes and the OPL were noticed (Fig. 4). These disruptions were not detected at earlier time points (Fig. 4).

Morphological changes of Cy3-tagged GSAI-B4 labeled microglial cells (Table 1) were observed 2 h following PVL injection. The cell bodies and dendrites were enlarged, and the number of dendritic processes clearly decreased, which may correspond to an early activation state[19]. After 4 h, the microglial dendritic processes disappeared. However, no apparent microglial cell migration across the retina was observed on vertical sections (Fig. 5).

Some retinal microglial cells underwent apoptosis. Terminal deoxynucleotidyl transferase dUTP nick-end labeling (TUNEL)-positive cells were located in the inner plexiform layer and ganglion cell layer 4 h and 8 h after PVL injection (Fig. 6A,B), while TUNEL were negative in control retinas and PVL injected retinas at 30 min, 1 h, 2 h time points retinas (see Supplementary Fig. S2). TUNEL-positive cells did not colocalize with either RBPMS-immunoreactive RGCs or CHAT-immunoreactive DACs (see Supplementary Fig. S3 and Table 1). Only microglial cells colocalized with TUNEL-positive cells, as shown in Fig. 6. At 4 h, the mean number of TUNEL-positive cells/field was 1.06. At 8 h, the number of apoptotic cells increased: mean number of TUNEL-positive cells/field was 1.86.

IL-6 and nitrotyrosine inflammation markers increased 4 h and 8 h after PVL injection. The immunohistochemistry staining of nitrotyrosine 4 h and 8 h after PVL injection showed increased nitrotyrosine accumulation in the retina compared with the controls (Fig. 6F,G,H). The nitrotyrosine-modified proteins increased by almost two times in PVL-treated retinas after 4 h compared with the controls, as demonstrated by Western blotting (Fig. 6I,J). Nitrotyrosine is a stable marker of peroxynitrite-mediated oxidative damage, which is indicative of nitric oxide (NO) production in the retina after PVL injection.

Primary antibodies or lectin			
Target	**Antiserum**	**Source**	**Concentration**
PVL	Rabbit anti-LukS-PV polyclonal	EA-7290, Strasbourg, France	2 µg/mL
C5aR	Rabbit anti-C5aR polyclonal	Abcam, Cambridge, UK	2 µg/mL
Ganglion cells	Guinea pig anti-RBPMS polyclonal	UCLA Neurobiology, Los Angeles, CA, USA	2 µg/mL
Displaced amacrine cells	Goat anti-CHAT polyclonal	Chemicon Merck-Millipore, Temecula, CA, USA	20 µg/mL
Müller cells	Mouse anti-GFAP polyclonal	Bio-Rad AbD Serotec, Oxfordshire, UK	2 µg/mL
Microglial cells	Cy3-tagged GSAI-B4	Sigma Aldrich, Saint Louis, MO, USA	2 µg/mL
Nitrotyrosine	Mouse anti-nitrotyrosine monoclonal	Santa Cruz Biotechnology, Heidelberg, Germany	2 µg/mL
C5L2	Rabbit anti-C5L2 polyclonal	GeneTex, San Antonio, TX, USA	2 µg/mL
β-actin	Rabbit anti-β-actin polyclonal	Santa Cruz Biotechnology, Heidelberg, Germany	1:2000
IL-6	Mouse anti-IL-6 monoclonal	Abbexa Ltd, Cambridge, UK	1:2000
IL-8	Mouse anti IL-8 monoclonal	Abbexa Ltd, Cambridge, UK	1:2000
IL-1β	Rabbit anti-IL-1β polyclonal	Abbexa Ltd, Cambridge, UK	1:2000
TNF-α	Mouse anti-TNFα monoclonal	Abbexa Ltd, Cambridge, UK	1:2000
Secondary antibodies			
Anti-rabbit	Goat and donkey polyclonal Alexa 555 nm-conjugated	Life Technologies, Carlsbad, CA, USA	2 µg/mL
Anti-goat	Donkey polyclonal Alexa 488-conjugated	Molecular Probes, Eugene, OR, USA	2 µg/mL
Anti-mouse	Donkey polyclonal Alexa 488-conjugated	Abcam	2 µg/mL
Anti-guinea pig	Goat polyclonal Alexa 488-conjugated	Abcam	2 µg/mL
TUNEL	DNA strand breaks	Roche Life Science, Indianapolis, IN, USA	—
Nuclei	Hoechst 33258	Molecular Probes™, Eugene, OR, USA	0.1 µg/mL
Anti-rabbit	Anti-Rabbit IgG (whole molecule)–Peroxidase	Sigma Aldrich, Saint Louis, MO, USA	1:10000
Anti-mouse	Goat anti-mouse IgG-Peroxidase	Santa Cruz Biotechnology, Heidelberg, Germany	1:10000

Table 1. list of Specific markers used in the current study. RBPM, RNA-binding protein with multiple splicing; CHAT, choline acetyl transferase; GFAP, glial fibrillary acidic protein; GSAI, *Griffonia simplicifolia* agglutinin isolectin. TUNEL, terminal deoxynucleotidyl transferase dUTP nick-end labelling.

RT-qPCR test revealed that IL-6 mRNA significantly increased in retinal tissue by 11.24 folds and 13.74 folds at 4 and 8 h respectively after PVL injection compared to controls (Fig. 7A). Semi-quantitative analysis of western blot results showed that IL-6 proteins expression in retinal tissue was also increased by 1.85 folds at 4 h and 2.87 folds at 8 h after PVL injection compared to controls (Fig. 7B). mRNA and protein expression of other inflammatory factors such as IL-8, TNFα, IL-1β, VEGF MCP-1 were also measured by RT-qPCR and western blot. But no significant difference, albeit variations, were noted between controls and PVL infected retinas (Fig. 7A and Supplementary Fig. S4).

Discussion

PVL colocalizes with RGCs through C5aR and transiently colocalizes with DACs through an unknown mechanism in the rabbit retina. Müller and microglial cells are activated after that PVL colocalizes with both RGC and DAC neural cells.

The exact mechanism by which neural cells are activated remains unknown. A recent report established that LukS-PV can bind C5aR and C5L2, the two complement C5a receptors, to mediate the toxin binding and toxicity in rabbit and human blood cells[9]. C5a receptors are abundantly expressed in myeloid cells, but they are less expressed in non-myeloid cells. Neural cells have been identified to express functional complement C5a receptors[20]. In general, we consider that C5aR is the major receptor and C5L2 is the minor receptor for C5a, and possibly for PVL. C5L2 is an intracytoplasmic G-protein-coupled receptor, never present at the cell membrane. C5L2 does not couple with G proteins, is not found to have a direct signaling function[21], and is not identified in any neurons. In addition, the quantity of mRNA and protein of C5L2 are significantly lower than those of C5aR in leukocytes, although C5L2 has nearly similar affinity to LukS-PV as C5aR in U937 C5aR-transfected cells[22]. The findings of the present study confirm the presence of C5aR but not of C5L2 in the rabbit retina. C5aR expression in the retina is demonstrated before: one report detected the presence of C5aR in the inner plexiform layer and occasionally in the ganglion cell layer in human retina[23], and another report showed that C5aR was expressed in the ganglion cell layer of mouse retina[24]. There are two kinds of cells in the ganglion cell layers: RGCs and DACs. Neither of the two reports could distinguish whether only one of them expresses C5aR. Finally, another report showed that retinal Müller cells could also express C5aR (*in vitro*)[25]. In the present study, only RGCs expressed C5aR. As PVL concentrates in RGCs and RGCs express C5aR (Fig. 3), we believe that PVL colocalizes with RGCs through C5aR.

DACs did not express C5aR, but they were transiently colocalized with PVL. Although it was shown that LukS-PV is unable to bind any blood cells without C5aR, all these studies investigated myeloid cells only[9]. The

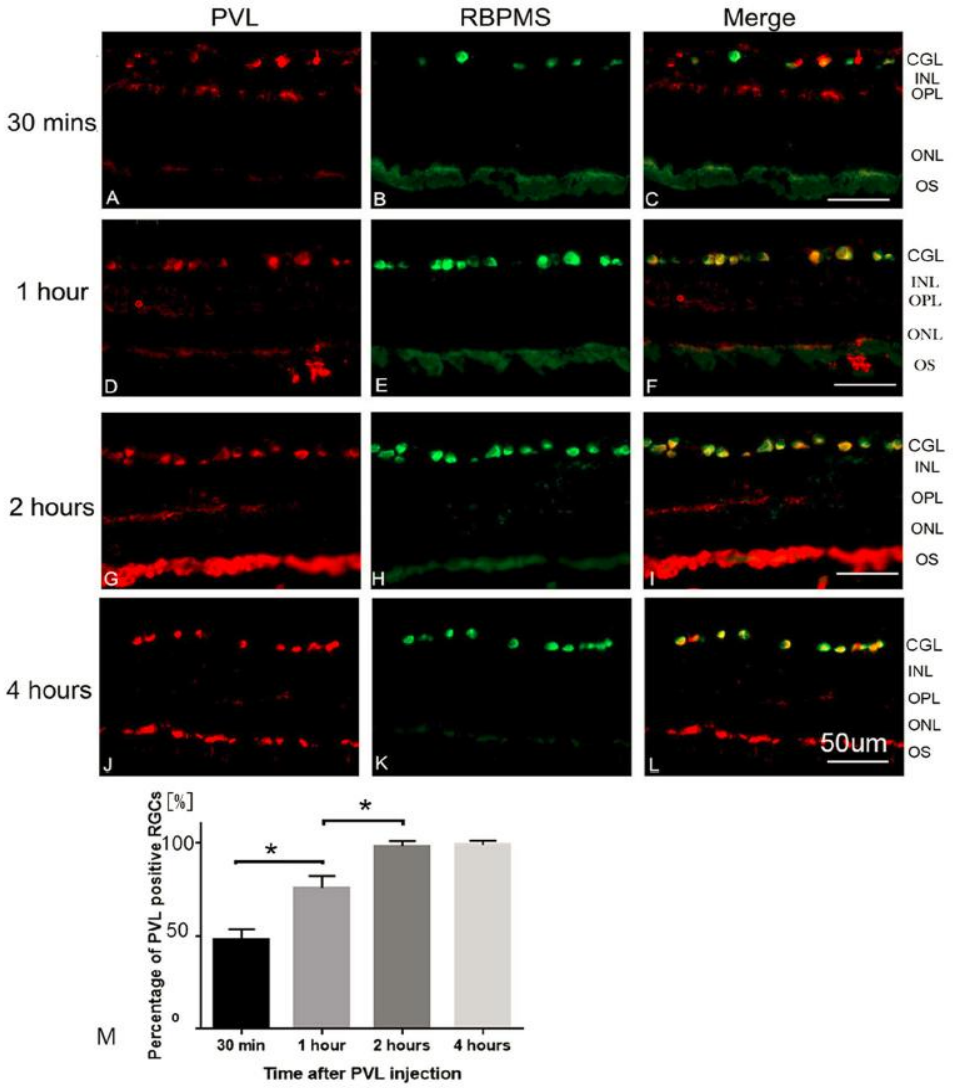

Figure 1. PVL expression in RGCs. PVL (red fluorescence **A**,**D**,**G**,**J**) colocalized with RGCs labeled with anti-RBPMS antibody (green fluorescence **B**,**E**,**H**,**K**) in the retinal vertical sections 30 min (**A**–**C**), 1 h (**D**–**F**), 2 h (**G**–**I**), and 4 h (**J**–**L**) after PVL injection. The number of PVL-positive RGCs increased with time (**C**,**F**,**I**,**L** yellow fluorescence), the rate of PVL-positive RGCs were 47%, 76%, 98%, 99% for 30 min and 1, 2, and 4 h (M, $***p < 0.001$, $*p < 0.05$ $n = 3$ eyes at each time point). Abbreviated symbols: PVL, Panton–Valentine leukocidin; RGCs, retinal ganglion cells; RBPMS, RNA-binding protein with multiple splicing; GCL, ganglion cell layer; INL, inner nuclear layer; OPL, outer plexiform layer; ONL, outer nuclear layer; OS, photoreceptor outer segments.

sensitivity of neurons to PVL was first addressed by Jover *et al.*, who demonstrated the neurotoxic activity of HlgC/B and PVL[13]. Given that DACs are neurons, we cannot exclude the possibility of another PVL-binding mechanism

PVL concentration increased in RGCs with time, while PVL expression decreased in DACs within a few hours. The diverse kinetics of PVL association with RGCs and DACs is difficult to explain apart from another specificity for an eventual second receptor. RGCs are long-projection neurons and may establish links with other cells such as DACS and microglia or other glial cells. They send visual information through their long axons from the retina to the brain[26]. DACs are integrated interneurons without axons. Because they are located at the second synaptic level of light pathways, consisting of the photoreceptor-bipolar-ganglion cell chain, DACs play the role of modulating and interposing the signal transmitter[27]. Compared to RGCs, DACs are more resistant

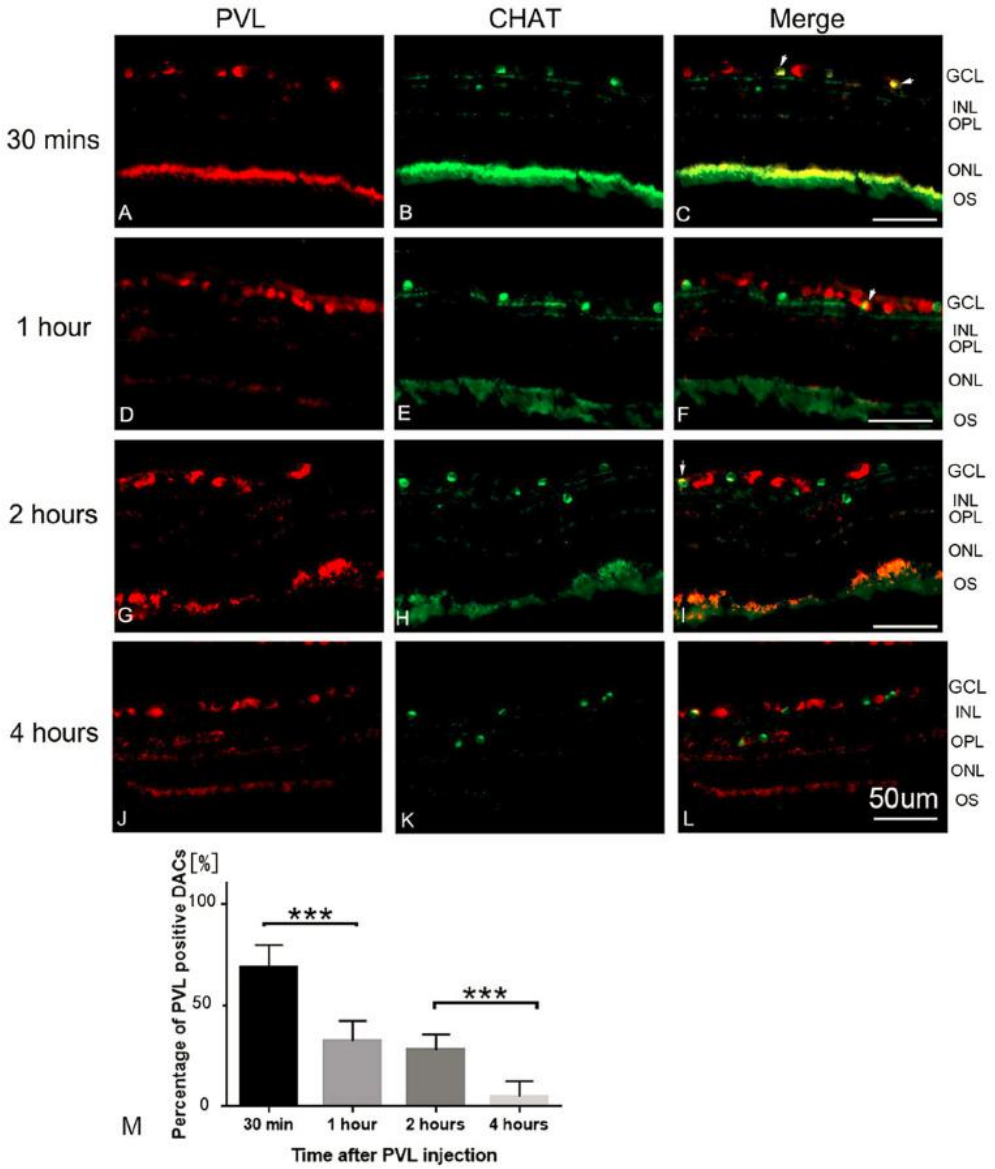

Figure 2. PVL expression was transient in DACs. Thirty minutes after PVL injection, the majority of DACs labeled with anti-CHAT antibody (green fluorescence **B**,**C**) colocalized with PVL (red fluorescence **A**,**C**). After 1 h, the PVL-positive DACs decreased (**D**–**L**). The percentage of PVL-positive DACs were 68%, 32%, 27%, 5% for 30 min and 1, 2, and 4 h (M, $***p < 0.001$, $*p < 0.05$, $n = 3$ eyes at each time point). Abbreviated symbols: PVL, Panton–Valentine leukocidin; DACs, displaced amacrine cells; CHAT, choline acetyl transferase; GCL, ganglion cell layer; INL, inner nuclear layer; OPL, outer plexiform layer; ONL, outer nuclear layer; OS, photoreceptor outer segments.

to neurodegeneration than RGCs after glaucoma and complete optic nerve transection[28]. Some selective RGCs may be postsynaptic to DACs[29]. However, little is known about the other relationships between RGCs and DACs.

Laventie *et al.* injected PVL and antibodies against S or/and F component in rabbit vitreous for 24 h[29]. The animal groups with humanised antibodies against either S or F component along PVL injection did not show a significant ocular inflammation, while the group injected with only PVL showed a great ocular inflammation. In this work, it was demonstrated that both the S and F components of leukotoxins were necessary to cause a physiological response[29]. Through the possible C5aR binding, PVL could initiate the rise of intracellular Ca^{2+} concentration and the release of glutamate, as was recently shown in newborn rat cerebellar granular neurons[13]. The rise of Ca^{2+} concentration can activate some signal pathways to produce pro-inflammatory cytokines, chemotaxis or neurotransmitters in neurons and initiate inflammation[30–32]. Chiu *et al.* showed that bacteria secrete

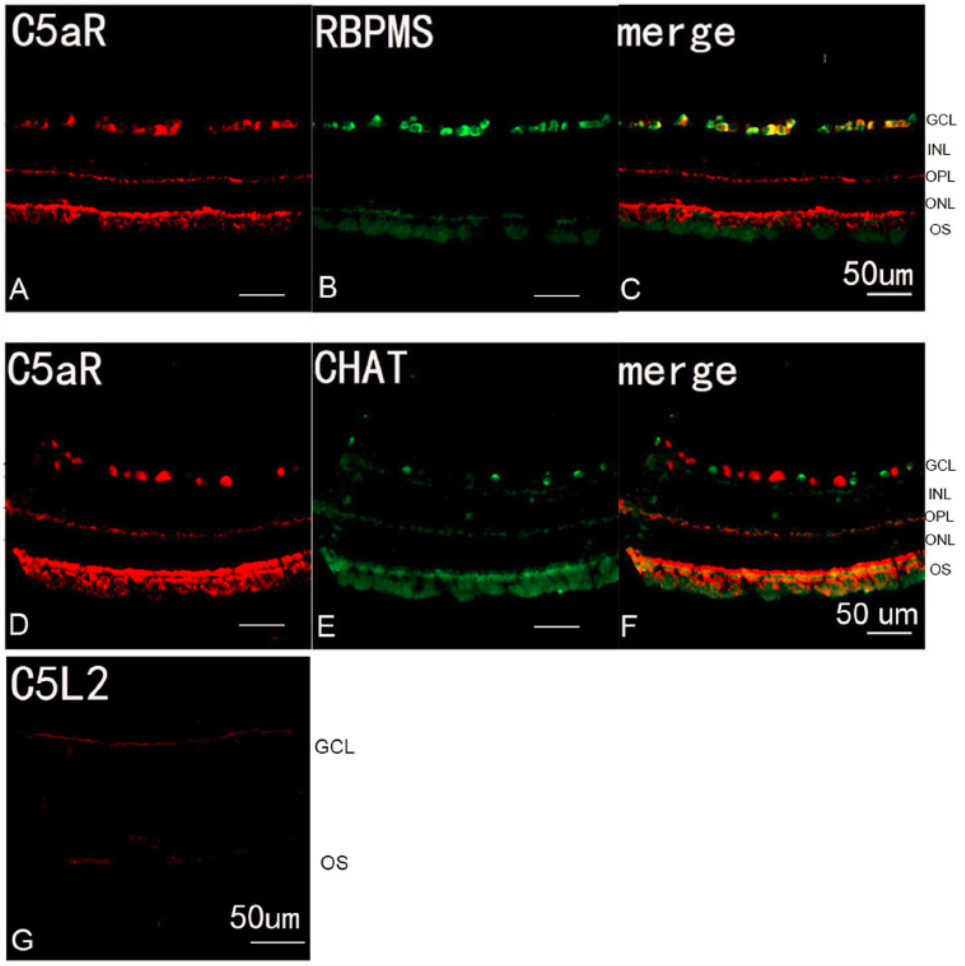

Figure 3. C5aR was expressed by RGCs. Double-labeling immunohistochemistry in the control eyes showed that RGCs labeled with anti-RBPMS antibody (green fluorescence **A**,**C**) colocalized with anti-C5aR staining (red fluorescence **B**,**C**), and the DACs labeled with anti-CHAT antibody (green fluorescence **E**,**F**) did not colocalize with anti-C5aR staining (red fluorescence **D**,**F**). The anti-C5L2 labeling did not show specific staining in retina (red fluorescence **G**). Abbreviated symbols: RGCs, retinal ganglion cells; RBPMS, RNA-binding protein with multiple splicing; DACs, displaced amacrine cells; CHAT, choline acetyl transferase; GCL, ganglion cell layer; INL, inner nuclear layer; OPL, outer plexiform layer; ONL, outer nuclear layer; OS, photoreceptor outer segments.

N-formylated peptides and α-hemolysin, which directly induce calcium flux and action potentials through nociceptors at the end of sensory neurons[33], resulting in the release of neuropeptides and neurogenic inflammation[34].

The morphological changes in Müller and microglial cells were observed in this study at 30 min and 2 h respective after PVL injection. We found elevated inflammatory markers at 4 h post-PVL injection. It is difficult to deduce whether the activated glial cells are a consequence or a cause of neural dysfunction. Indeed, when the neuron system is subjected to injury due to inflammation or trauma the glial cells are activated and exhibit gliosis[18]. Activated Müller cells can disturb the structural support or metabolic function of neurons, resulting in their dysfunction and loss. The activated microglia can also modulate the expression of trophic factors by Müller cells, which indirectly affects photoreceptors[35,36]. However, in this study, we could not detect any neuronal damage at least until 8 h after PVL injection.

Nitrotyrosine represents reactive oxygen species and reactive nitrogen species, which have diffused in the retinal tissue[37]. Increased nitrotyrosine concentration reflects an underlying inflammatory process with significant NO production, and this was observed in the retinal tissue as early as 4 h after PVL injection. It has established that NO can downregulate the tight junction proteins occludin and ZO-1, resulting in the breakdown of the BRB[38]. The state of microglial cell activation is conversely correlated with cell viability. In a recent study, apoptosis of *in vitro* activated microglial cells was promoted by NO production. Indeed, microglial cells can produce NO and undergo apoptotic death when they are significantly activated[39]. As our study showed that some microglial

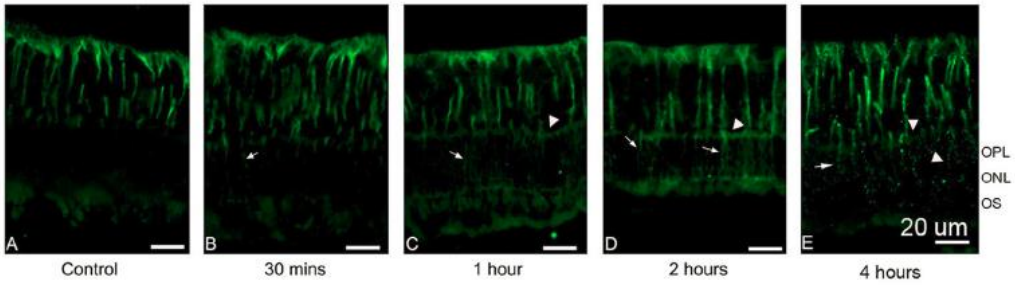

Figure 4. Müller cell reactivity was observed as early as 30 min after PVL injection. Compared with control eyes (green fluorescence **A**), anti-GFAP labeling was abnormally present in outer retina in PVL-injected eyes (green fluorescence **B**–**E**). More anti-GFAP-stained Müller processes (arrows) were noted at 1 h (**C**), 2 h (**D**), and 4 h (**E**) than at 30 min after PVL injection. At 1 h and 2 h, OPL was well defined with GFAP staining (arrowheads). At 4 h, disruptions of GFAP staining within outer processes and the OPL were noticed (arrowheads). ($n = 3$ eyes at each time point). Abbreviated symbols: GFAP, glial fibrillary acidic protein; OPL, outer plexiform layer; ONL, outer nuclear layer; OS, photoreceptor outer segments.

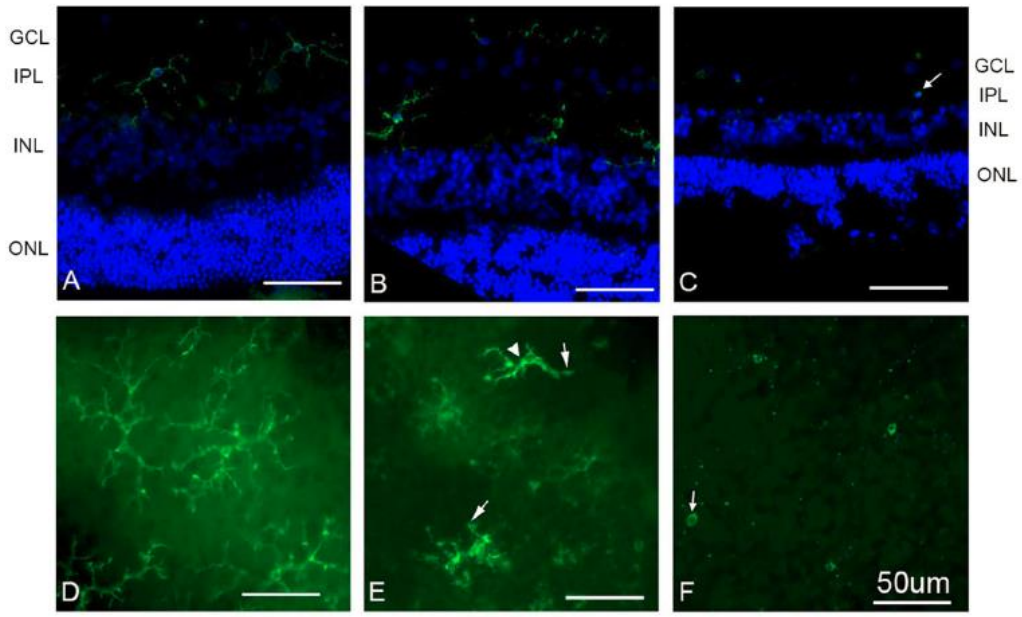

Figure 5. The microglial cells underwent morphological changes 2 h after PVL injection. (**A**–**C**) were vertical retinal sections, while (**D**–**F**) were whole retinal mounts. Cy3-tagged GSAI-B4 labeled microglial cell. Hoechst stained nuclei (blue fluorescence **A**-**C**). No microglial cell migration was observed (green fluorescence **A**–**C**). However, microglial cells showed retracted dendrites (arrow) and enlarged proximal parts of processes (arrowhead) (green fluorescence **B**,**E**) compared to controls (green fluorescence **A**,**D**). After 4 h, the microglial processes disappeared (arrow) (green fluorescence **C**,**F**). ($n = 3$ eyes at each time point). Abbreviated symbols: GCL, ganglion cell layer; IPL, inner plexiform layer; INL, inner nuclear layer; ONL, outer nuclear layer.

cells underwent apoptotic death and nitrotyrosine concentration increased 4 h after PVL injection, there might be a significant correlation between NO production, microglial cell apoptosis, and retinal inflammation during PVL infection.

IL-6 interacts with its receptor and then elicits JAK/STAT (Janus kinase/signal transducer and activator of transcription) and MAPK (mitogen-activated protein kinase) pathways which enhance numerous biological activities[40]. IL-6 was proved to be associated to many ocular pathologies related to inflammations, such as uveitis, glaucoma, ocular neovascularization and autoimmune disease[16]. The humanized anti-human IL-6R mAb, Tocilizumab, is effective to treat refractory uveitis and potent new therapeutic for other ocular diseases[41]. Rojas *et al*. proved that intravitreal injection of angiotensin II caused increases of IL-6 mRNA and protein. IL-6 was localized to retinal microglia and/or macrophages[42]. The present study showed that IL-6 mRNA and protein in retina increased after 4 h and 8 h PVL injection. The increased IL-6 expression might be due to activated microglial cells and may play a great role in nitrotyrosine production and retinal inflammation.

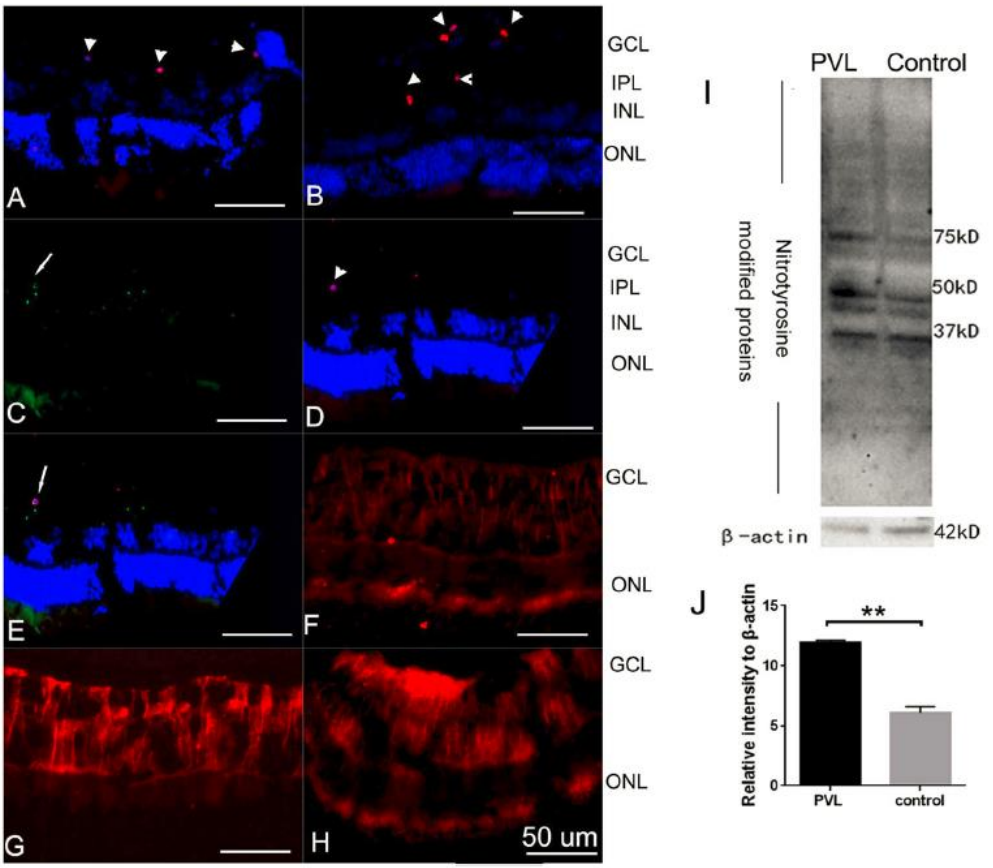

Figure 6. Some microglial cells underwent apoptosis, nitrotyrosine accumulated in the retina 4 h and 8 h after PVL injection. Apoptotic cells were situated in inner retina at 4 h (arrow head, red fluorescence **A**) and 8 h (arrow head, red fluorescence **B**) after PVL injection. The TUNEL-positive cells (arrow head, red fluorescence **D**,**E**) colocalized with microglial cells (arrow, green fluorescence **C**,**E**). Hoechst stained nuclei (blue fluorescence **A**,**B**,**D**,**E**). RGCs and DACs did not colocalize with TUNEL-positive cells (Supplementary Fig. S3). The immune activity of nitrotyrosine increased in the retina 4 h (red fluorescence **G**) and 8 h (red fluorescence **H**) after PVL injection compared with controls (red fluorescence **F**). Western blotting experiments showed that nitrotyrosine-modified proteins were expressed (migration of bands between 37 to 75 kDa) in both PVL-treated 4 h retinas and controls. The full-length blots are presented in Supplementary Fig. S5. Nitrotyrosine and β-acitin blot were from the same samples in the same gel (**I**). However, the total intensity of bands quantified by densitometry was increased almost two times in PVL-treated 4 h retinas compared to controls. (**I**,**J**). (**$p < 0.01$, $n = 3$ eyes). Abbreviated symbols: TUNEL, terminal deoxynucleotidyl transferase dUTP nick-end labeling; RGCs, retinal ganglion cells; DACs, displaced amacrine cells. GCL, ganglion cell layer; IPL, inner plexiform layer; INL, inner nuclear layer; ONL, outer nuclear layer; OS, photoreceptor outer segments. ns: no significant difference.

Nevertheless, early activation of Müller and microglial cells may cause major consequences to the visual outcomes in this PVL-mediated endophthalmitis model[14]. Further investigations of the effects of PVL binding on neural activity and the relation between neurogenic inflammation and glial cell activation should be performed. Retinal explants and *in situ* sophisticated approaches might bring more insights about the sequential activity of retinal cells.

Materials and Methods

Animal and surgical procedure. The animal experiments were approved by the Ministère de l'Education nationale, de l'Enseignement supérieur et de la Recherche, France (APAFiS no. 4986). The surgical procedure was performed in accordance with the guidelines in the laboratory of the Association for Research in Vision and Ophthalmology within the accredited A67-482-34 and B67-482-34 animal facilities. Nine pigmented rabbits (Bleu de Champagne) aged one year and weighing 3.5–4 kg were anesthetized by a lumbar intramuscular injection of ketamine, 20 mg/kg (Virbac, Carros, France) and xylazine, 3 mg/kg (Bayer Healthcare, Puteaux, France). After local anesthesia of the eyeball with 2–3 drops of oxybuprocaine chlorhydrate (Théa, Clermont-Ferrand, France), PVL in phosphate-buffered saline (PBS) (3 µg/50 µL), purified from ATCC49775 *S. aureus*[43], was intravitreally injected with a 30-Gauge needle inserted 4 mm behind the corneal limbus. For controls, three eyes were injected with 50-µL PBS using the same technique. After PVL injection, animals were sacrificed at 30 min, 1, 2

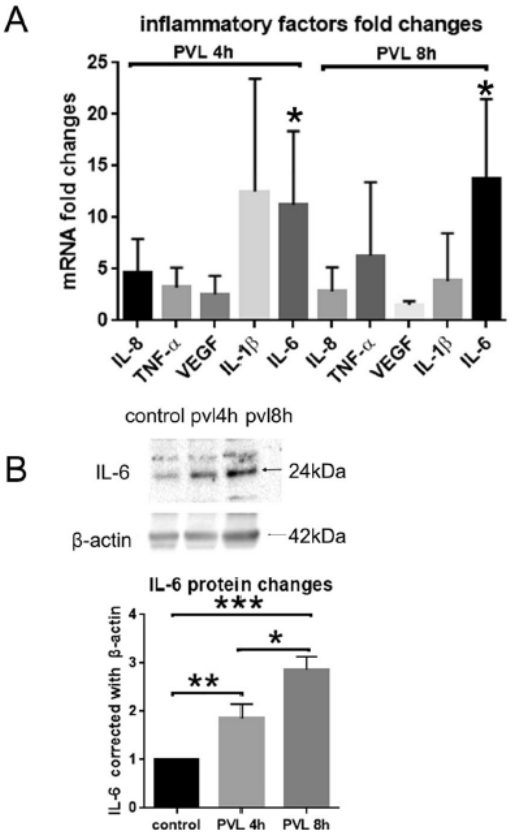

Figure 7. IL-6 mRNA and protein expression were increased 4 h and 8 h after PVL injection. The mRNA extracted from retinal tissue were analyzed by RT-qPCR. The mRNA (IL-8, TNF-α, VEGF, IL-1β, IL-6) levels were normalized by those of β-actin and presented as fold changes relative to control groups. The results ΔCt were analyzed statistically by the paired t-test. Only IL-6 showed significant difference, increasing 11.24 ± 4.123 folds at 4 h and 13.74 ± 4.457 folds at 8 h after PVL injection (**A**, $*p < 0.05$, n = 3 eyes for each group). The proteins expression of IL-8, TNF-α, IL-1β, IL-6 were also semi-quantitatively measured by Western blotting. The full-length blots are presented in Supplementary Figs S4, 6, 7. Only IL-6 expression significantly increased by 1.85 ± 0.3 folds at 4 h and 2.87 ± 0.26 folds at 8 h after PVL injection. The blots of IL-6 and β-actin were from the same samples in the same gels with different exposure time (**B**, $*p < 0.05$, $**p < 0.01$, $***p < 0.005$ n = 3 eyes for each group).

and 4 h (two animals: three eyes with PVL and one control eye in each group) first using anesthesia with ketamine-xylazine (as mentioned above), followed by a lethal intravenous injection of 2-mL Pentobarbital Dolethal® (Vetoquinol, Lure, France) through a 22-Gauge catheter inserted in the marginal auricular vein.

Eye preparation. The eyes were intravitreally injected with 100 µL of 4% (wt/vol) paraformaldehyde (Thermo Fisher Scientific, Rockford, IL, USA) immediately after sacrifice, and were then oriented and enucleated. The cornea, iris, and crystalline lens were immediately removed. Half of the eye globe was fixed for 3 h in 4% paraformaldehyde, and the remainder was immediately frozen. The dissected eyes were successively immersed in 10% (wt/vol) and 20% (wt/vol) sucrose and stored in 30% (wt/vol) sucrose overnight at 4 °C. For a better cryosection, the retina was separated from the pigmented epithelium. The temporal zone of 1–5 mm near the optic disc was isolated and then immersed in optimal cutting temperature compound (Sakura Finetek, Torrance, CA, USA). Vertical cryostat 8-µm-thick sections were mounted on a Super Frost™ Plus microscope slides (Thermo Fisher Scientific, Rockford, IL, USA) and stored at −20 °C.

Immunohistochemistry. Immunohistochemistry was performed to analyze the retinal cells targeted by PVL. PVL protein was stained using anti-LukS-PV-specific antibody. Retinal sections and whole mounts were permeabilized in 0.05% (v/v) and 0.1% (v/v) TritonX-100, respectively, for 1 h and then were blocked with 10% (v/v) donkey or goat serum (Sigma-Aldrich, St. Louis, MO, USA) for 1 h. Retinal sections were incubated with primary antibody (see Table 1 for details) at 4 °C overnight in a humidity chamber. Retinal sections were then incubated for 1 h at room temperature with fluorescent secondary antibodies or TUNEL (except when lectin was used) (see Table 1 for details). The sections were counter-stained with Hoechst 33258 and mounted in 10% (v/v) Mowiol® solution (Polysciences, Eppelheim, Germany). Images of fluorescent sections and whole mounts were obtained using an epifluorescence Olympus BX60 microscope connected to a Hamamatsu C11440 digital camera.

Cell counting. Five different microscope fields (266 µm × 266 µm) of vertical retinal sections were captured by the camera. The proportions of PVL-positive RGCs and DACs were measured in the RGC layer. PVL-positive cells were double-labeled by PVL and cell-specific markers for RGCs and DACs (Figs 1 and 2). The percentages of PVL-positive RGCs and DACs in each eye were established after triplicate experiments. For TUNEL positive cells count, five different microscope fields were analyzed for each retina.

Western blotting. One half of whole frozen retinas were homogenized by passing through a 26-Gauge needle several times in RIPA buffer [1% (v/v) NP-40, 0.1% SDS, 1% (w/v) sodium deoxycholate, 50 mM sodium chloride, 25 mM Tris-HCl pH 8.0] containing an inhibitor protease cocktail. The concentration of proteins in the supernatant was quantified using the BCA kit (660-nm Protein Assay Reagent, Pierce Biotechnology). The same amount of protein was loaded in each lane of SDS-PAGE gel (Bio-Rad Laboratories, Hercules, CA, USA). After migration, proteins were transferred to a nitrocellulose membrane, which was blocked in 5% (w/v) skimmed milk in PBS and probed in primary antibody anti-nitrotyrosine, anti-IL-6, anti-IL-8, anti-TNFα, anti-IL-1β (see Table 1) overnight at 4 °C. The membranes were washed three times in phosphate-buffered saline with Tween® (PBST) and incubated in Peroxidase-conjugated anti-mouse or anti-rabbit secondary antibodies (see Table 1) for 1 h at room temperature. The digital images were developed using ECL Western blotting detection reagent (Bio-Rad Laboratories, Hercules, CA, USA) and a chemiluminescence camera (ChemiDoc™ XRS, Bio-Rad). The protein expressions were quantified by densitometry analysis of Western Blots bands using BIO-1D software. The tests were triplicate.

Real-time RT-qPCR. We analyzed tested retinas (PVL 4 h and PVL 8 h, 3 eyes for each group) and control retinas (PBS 4 h, 6 eyes) using RT-qPCR to see the elevation of cytokines as sign of retinal inflammation. The eyes were immediately dissected after the death of rabbit at the end of times course and put into CO_2-independent medium (Gibco, Life technologies, Carlsbad, USA). The retinas were immediately isolated in CO2-independent medium and stocked immediately at −80 °C. Trizol reagent (Sigma, Saint-Louis, USA) was added into tube contained frozen retina, the retinas were passed through 23-Gauge needle then 26-Gauge needle several times to homogenize the retina. Total RNA was isolated using Trizol reagent according to the manufacturer's instructions. The final RNA solutions were quantified with spectrophotometry (NanoDrop; Thermo Scientific, Waltham, USA). Then, 10 µg RNA aliquotes were treated with DNA-free kit DNase treatment (Ambion, Life technologies) at 37 °C for 30 min and removal reagents according to manufacturer's instructions. RNA integrity was analyzed using non-denaturing agarose gel electrophoresis. Total RNA was immediately reverse transcribed(RT) using Superscript First-Strand Synthesis for RT-PCR (Invitrogen, Life technologies). Diethyl pyrocarbonatedecarbonate (DEPC) (Sigma) treated H_2O was added to RT mixture (0.5 µl random hexamers (200 ng/ml), 500ng total RNA, 1 µl NTP) to achieve a 12 µl volume, then incubated at +65 °C for 5 min and placed in glass for 2 min. Then 0.5 µl of 0.1 M DDT, 0.5 µl of transcriptase, 4 µl of First Strand buffer, 3 ul of sterile H_2O were added to the mixture. Then, the total mixture was put into ThermoCycler programmed at +42 °C for 50 min and at +70 °C for 15 min. The cDNA was diluted in 3 times with DEPC treated H_2O. 5 µl of diluted DNA, 10 µl SYBR mix (LightCycler 480 SYBR Green I Master, Roche, Basel, Switzerland), 2 µl of forward and reverse primers, and 3ul H_2O were mixed and put into 96 wells plate. The plate was placed into Real-Time PCR System (Light Cycler 480, Roche). The primers were designed to have Tm around 60 °C by using Primer3 software. PCR was programmed as initial denaturation step at +95 °C for 10 min, 45 cycles of amplification (denaturation at +95 °C for 15 s, annealing at +60 °C for 20 s, extension at +72 °C for 15 s), and melting curve analysis (+60 °C to +95 °C increment at +0.3 °C). The specificity of PCR products was verified according to one melting curve peak and one band in agarose gel electrophoresis. RTs without reverse transcriptase were used as controls to assure no significant DNA contamination. The sequences of primers: β-actin forward primer 5′-gcgggacatcaaggagaag-3′, afterward primer 5′-aggaaggagggctggaaga-3′; IL-6 forward primer 5′-tcaggccaagttcaggagtg-3′, afterward primer 5′-atgaagtggatcgtggtcgt-3′; IL-8 forward primer 5′-tggctgtggctctcttgg-3′, afterward primer 5′-atttgggatggaaaggtgtg-3′; TNFα forward primer 5′-cgtagtagca aacccgcaag-3′, afterward primer 5′-tgagtgaggagcacgtagga-3′; IL-1β forward primer 5′-ttgtcagtcgttgtggctct-3′, afterward primer 5′-ggatttctgttgtgcatcct-3′; VEGF forward primer 5′-cgagaccttggtggacatctt-3′, afterward primer 5′-tgcattcacatttgttgtgct-3′; MCP-1 forward primer 5′-aacgcttctgtgcctgct-3′, afterward primer 5′-ggacccacttctgcttgg-3′. The β-actin was used as reference gene and target genes were normalized using this reference gene. The method ΔCt was used to calculate relative quantification between control retina and tested retina. The fold changes were calculated using $2^{-\Delta\Delta Ct}$. The tests were triplicate. The significant changes of every target gene were statistically analyzed using ΔCt paired t-tests.

Statistical analysis. Statistical analysis was performed with GraphPad InStat version 3.10. Statistical significance was calculated with one-way ANOVA using the Tukey-Kramer multiple comparisons test and paired t-tests. Statistical significance was assumed at $p < 0.05$.

Data availability. All data sets generated, including those that were analyzed during the current study, are available with the corresponding author on request.

References

1. Callegan, M. C. *et al.* Bacterial endophthalmitis: therapeutic challenges and host-pathogen interactions. *Progress in Retinal and Eye Research* **26**, 189–203 (2007).
2. Combey de Lambert, A. *et al.* Baseline factors predictive of visual prognosis in acute postoperative bacterial endophthalmitis in patients undergoing cataract surgery. *JAMA Ophthalmology* **131**, 1159–1166 (2013).
3. David, M. Z. & Daum, R. S. Community-associated methicillin-resistant *Staphylococcus aureus*: epidemiology and clinical consequences of an emerging epidemic. *Clinical Microbiology Reviews* **23**, 616–687 (2010).

4. Hidron, A. I., Low, C. E., Honig, E. G. & Blumberg, H. M. Emergence of community-acquired meticillin-resistant *Staphylococcus aureus* strain USA300 as a cause of necrotising community-onset pneumonia. *The Lancet. Infectious Diseases* **9**, 384–392 (2009).
5. Diep, B. A. *et al*. Complete genome sequence of USA300, an epidemic clone of community-acquired meticillin-resistant *Staphylococcus aureus*. *Lancet* **367**, 731–739 (2006).
6. Alonzo, F. 3rd & Torres, V. J. The bicomponent pore-forming leucocidins of *Staphylococcus aureus*. *Microbiology and Molecular Biology Reviews: MMBR* **78**, 199–230 (2014).
7. Diep, B. A. *et al*. Polymorphonuclear leukocytes mediate *Staphylococcus aureus* Panton-Valentine leukocidin-induced lung inflammation and injury. *Proceedings of the National Academy of Sciences of the United States of America* **107**, 5587–5592 (2010).
8. Sina, H. *et al*. Variability of antibiotic susceptibility and toxin production of *Staphylococcus aureus* strains isolated from skin, soft tissue, and bone related infections. *BMC Microbiology* **13**, 188 (2013).
9. Spaan, A. N. *et al*. *The staphylococcal toxin* Panton-Valentine Leukocidin targets human C5a receptors. *Cell Host & Microbe* **13**, 584–594 (2013).
10. Prince, A., Wang, H., Kitur, K. & Parker, D. Humanized mice exhibit increased susceptibility to *Staphylococcus aureus* pneumonia. *The Journal of Infectious Diseases* **215**, 1386–1395 (2016).
11. Tseng, C. W. *et al*. Increased susceptibility of humanized NSG mice to Panton-Valentine Leukocidin and *Staphylococcus aureus* skin infection. *PLoS Pathogens* **11**, e1005292 (2015).
12. Prévost, G. *et al*. Panton-Valentine leucocidin and gamma-hemolysin from *Staphylococcus aureus* ATCC 49775 are encoded by distinct genetic loci and have different biological activities. *Infection and Immunity* **63**, 4121–4129 (1995).
13. Jover, E., Tawk, M. Y., Laventie, B. J., Poulain, B. & Prévost, G. Staphylococcal leukotoxins trigger free intracellular Ca(2+) rise in neurones, signalling through acidic stores and activation of store-operated channels. *Cellular Microbiology* **15**, 742–758 (2013).
14. Siqueira, J. A. *et al*. Channel-forming leucotoxins from *Staphylococcus aureus* cause severe inflammatory reactions in a rabbit eye model. *Journal of Medical Microbiology* **46**, 486–494 (1997).
15. Laventie, B. J. *et al*. p-Sulfonato-calix[n]arenes inhibit staphylococcal bicomponent leukotoxins by supramolecular interactions. *The Biochemical Journal* **450**, 559–571 (2013).
16. Ghasemi, H. Roles of IL-6 in Ocular Inflammation: A Review. *Ocul Immunol Inflamm*, 1–14(2017).
17. Spaan, A. N. *et al*. Differential interaction of the staphylococcal toxins Panton-Valentine Leukocidin and gamma-hemolysin CB with human C5a receptors. *Journal of Immunology* **195**, 1034–1043 (2015).
18. Dyer, M. A. & Cepko, C. L. Control of Muller glial cell proliferation and activation following retinal injury. *Nature Neuroscience* **3**, 873–880 (2000).
19. Stence, N., Waite, M. & Dailey, M. E. Dynamics of microglial activation: a confocal time-lapse analysis in hippocampal slices. *Glia* **33**, 256–266 (2001).
20. O'Barr, S. A. *et al*. Neuronal expression of a functional receptor for the C5a complement activation fragment. *The Journal of Immunology* **166**, 4154–4162 (2001).
21. Okinaga, S. *et al*. C5L2, a nonsignaling C5A binding protein. *Biochemistry* **42**, 9406–9415 (2003).
22. Ohno, M. *et al*. A putative chemoattractant receptor, C5L2, is expressed in granulocyte and immature dendritic cells, but not in mature dendritic cells. *Molecular Immunology* **37**, 407–412 (2000).
23. Vogt, S. D., Barnum, S. R., Curcio, C. A. & Read, R. W. Distribution of complement anaphylatoxin receptors and membrane-bound regulators in normal human retina. *Experimental Eye Research* **83**, 834–840 (2006).
24. Yu, M., Zou, W., Peachey, N. S., McIntyre, T. M. & Liu, J. A novel role of complement in retinal degeneration. *Investigative Ophthalmology & Visual Science* **53**, 7684–7692 (2012).
25. Cheng, L. *et al*. Modulation of retinal Muller cells by complement receptor C5aR. *Investigative Ophthalmology & Visual Science* **54**, 8191–8198 (2013).
26. Sanes, J. R. & Masland, R. H. The types of retinal ganglion cells: current status and implications for neuronal classification. *Annual Review of Neuroscience* **38**, 221–246 (2015).
27. Kunzevitzky, N. J., Almeida, M. V. & Goldberg, J. L. Amacrine cell gene expression and survival signaling: differences from neighboring retinal ganglion cells. *Investigative Ophthalmology & Visual Science* **51**, 3800–3812 (2010).
28. Kielczewski, J. L., Pease, M. E. & Quigley, H. A. The effect of experimental glaucoma and optic nerve transection on amacrine cells in the rat retina. *Investigative Ophthalmology & Visual Science* **46**, 3188–3196 (2005).
29. Briggman, K. L., Helmstaedter, M. & Denk, W. Wiring specificity in the direction-selectivity circuit of the retina. *Nature* **471**, 183–188 (2011).
30. Uceyler, N., Tscharke, A. & Sommer, C. Early cytokine expression in mouse sciatic nerve after chronic constriction nerve injury depends on calpain. *Brain, Behavior, and Immunity* **21**, 553–560 (2007).
31. Zhang, D. *et al*. Two chromogranin a-derived peptides induce calcium entry in human neutrophils by calmodulin-regulated calcium independent phospholipase A2. *PloS One* **4**, e4501 (2009).
32. Hensler, T., Koller, M., Prévost, G., Piemont, Y. & Konig, W. GTP-binding proteins are involved in the modulated activity of human neutrophils treated with the Panton-Valentine leukocidin from *Staphylococcus aureus*. *Infection and Immunity* **62**, 5281–5289 (1994).
33. Chiu, I. M. *et al*. Bacteria activate sensory neurons that modulate pain and inflammation. *Nature* **501**, 52–57 (2013).
34. Chiu, I. M., von Hehn, C. A. & Woolf, C. J. Neurogenic inflammation and the peripheral nervous system in host defense and immunopathology. *Nature Neuroscience* **15**, 1063–1067 (2012).
35. Wang, M., Ma, W., Zhao, L., Fariss, R. N. & Wong, W. T. Adaptive Muller cell responses to microglial activation mediate neuroprotection and coordinate inflammation in the retina. *Journal of Neuroinflammation* **8**, 173 (2011).
36. Harada, T. *et al*. Microglia-Muller glia cell interactions control neurotrophic factor production during light-induced retinal degeneration. *The Journal of Neuroscience: the Official Journal of the Society for Neuroscience* **22**, 9228–9236 (2002).
37. Liu, J. S., Zhao, M. L., Brosnan, C. F. & Lee, S. C. Expression of inducible nitric oxide synthase and nitrotyrosine in multiple sclerosis lesions. *Am J Pathol* **158**, 2057–2066 (2001).
38. Leal, E. C. *et al*. Inducible nitric oxide synthase isoform is a key mediator of leukostasis and blood-retinal barrier breakdown in diabetic retinopathy. *Investigative Ophthalmology & Visual Science* **48**, 5257–5265 (2007).
39. Lee, P. *et al*. NO as an autocrine mediator in the apoptosis of activated microglial cells: correlation between activation and apoptosis of microglial cells. *Brain Res* **892**, 380–385 (2001).
40. Peter C. Heinrich, I., Serge, H., Heike, M., Hermanns, G. M. & Schaper, U.-N. A. F. Principles of interleukin (IL)-6-type cytokine signalling and its regulation. pdf. *Biochem. J.* **15**, 1–20 (2003).
41. Zahir-Jouzdani, F., Atyabi, F. & Mojtabavi, N. Interleukin-6 participation in pathology of ocular diseases. *Pathophysiology: the official journal of the International Society for Pathophysiology* **24**, 123–131 (2017).
42. Rojas, M. *et al*. *Role of IL-6 in angiotensin II-induced retinal* vascular inflammation. *Investigative Ophthalmology & Visual Science* **51**, 1709–1718 (2010).
43. Gravet, A. *et al*. Characterization of a novel structural member, LukE-LukD, of the bi-component staphylococcal leucotoxins family. *FEBS Letters* **436**, 202–208 (1998).

Acknowledgements
LIU Xuanli was awarded by the Chinese Scholarship Council. We thank Gaëlle Zimmermann-Meisse for her assistance. This work was supported by a recurrent research EA7290 award from the University of Strasbourg and a grant from Novartis. The Dermatology service of Strasbourg University Hospital is thanks for access to vertical cryostat.

Author Contributions
Liu X.L., Heitz P. and Keller D. conducted the experiments and acquired data. Gaucher D., Roux M., Bourcier T., Sauer A. and Prévost G. conceived and designed the study. Liu X.L., Gaucher D. and Prévost G. analyzed and interpreted the data, drafted the article. Prévost G. gave final approval of the version to be submitted. All authors reviewed the manuscript.

Additional Information
Supplementary information accompanies this paper at https://doi.org/10.1038/s41598-018-20590-z.

Competing Interests: The authors declare no competing interests.

Publisher's note: Springer Nature remains neutral with regard to jurisdictional claims in published maps and institutional affiliations.

Supplementary Figures S1-S7

Title: Panton–Valentine Leukocidin Colocalizes with Retinal Ganglion and Amacrine Cells and Activates Glial Reactions and Microglial Apoptosis

XuanLi LIU [1], Pauline HEITZ [2], Michel J[3]ROUX, Daniel KELLER [1], Arnaud SAUER [2], Gilles PREVOST [1], David GAUCHER [1,2#]

1. Université de Strasbourg, Hôpitaux Universitaires de Strasbourg, Fédération de Médecine Translationnelle de Strasbourg, EA7290 Virulence Bactérienne Précoce, Institut de Bactériologie, Strasbourg, France.

2. Hôpitaux Universitaires de Strasbourg, Service d'Ophtalmologie du Nouvel Hôpital Civil, Strasbourg Cedex - France.

3. Department of Translational Medicine and Neurogenetics, Institut de Génétique et de Biologie Moléculaire et Cellulaire, CNRS UMR_7104, Inserm U 964, Université de Strasbourg, Illkirch, France

The fax, telephone number, and e-mail address of the corresponding author:

Tel: +33 (0)3 69 55 11 15; +33 (0)6 63 12 75 98. Fax: +33 (0)3 69 55 18 49. Email: david.gaucher@chru-strasbourg.fr

Supplementary Figure S1.

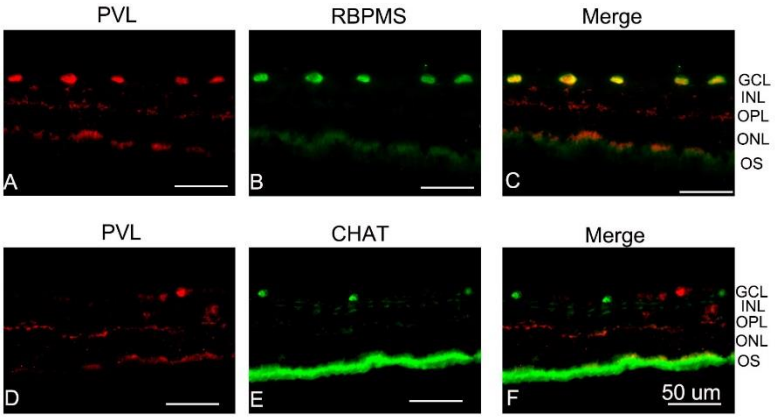

Supplementary Figure S1. PVL colocalized with RGCs and few DACs 8 h after PVL injection. PVL (red fluorescence A, C) colocalized with RGCs labeled with anti-RBPMS antibody (green fluorescence B, C) in the retinal vertical sections. DACs labeled with anti-CHAT antibody (green fluorescence E, F) did not colocalize with PVL (red fluorescence D, F).

Abbreviated symbols: RGCs, retinal ganglion cells; DACs, displaced amacrine cells; CHAT, choline acetyl transferase; RBPM, RNA-binding protein with multiple splicing; GCL, ganglion cell layer; OPL, outer plexiform layer; INL, inner nuclear layer; ONL, outer nuclear layer. OS, photoreceptor outer segments.

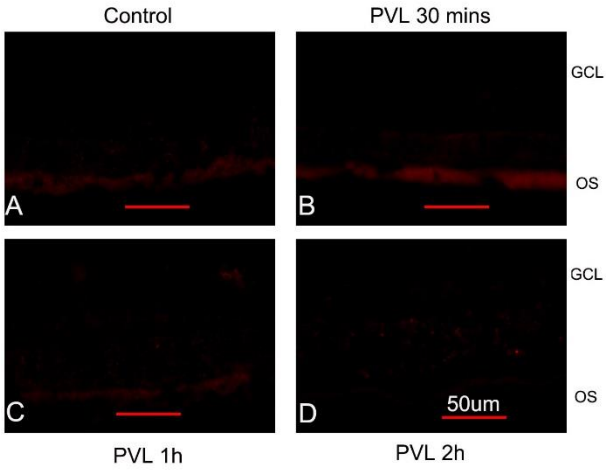

Supplementary Figure S2. TUNEL test were negative in controls and retinas 30 mins, 1 h, 2 h after PVL injection. The TUNEL test did not show any specific positive fluorescence in retina control(A), in retina 30 mins after PVL injection (B), in retina 1 h after PVL injection (C) and in retina 2 h after PVL injection (D).

Abbreviated symbols: TUNEL, terminal deoxynucleotidyl transferase dUTP nick-end labeling; GCL, ganglion cell layer; OS, photoreceptor outer segments.

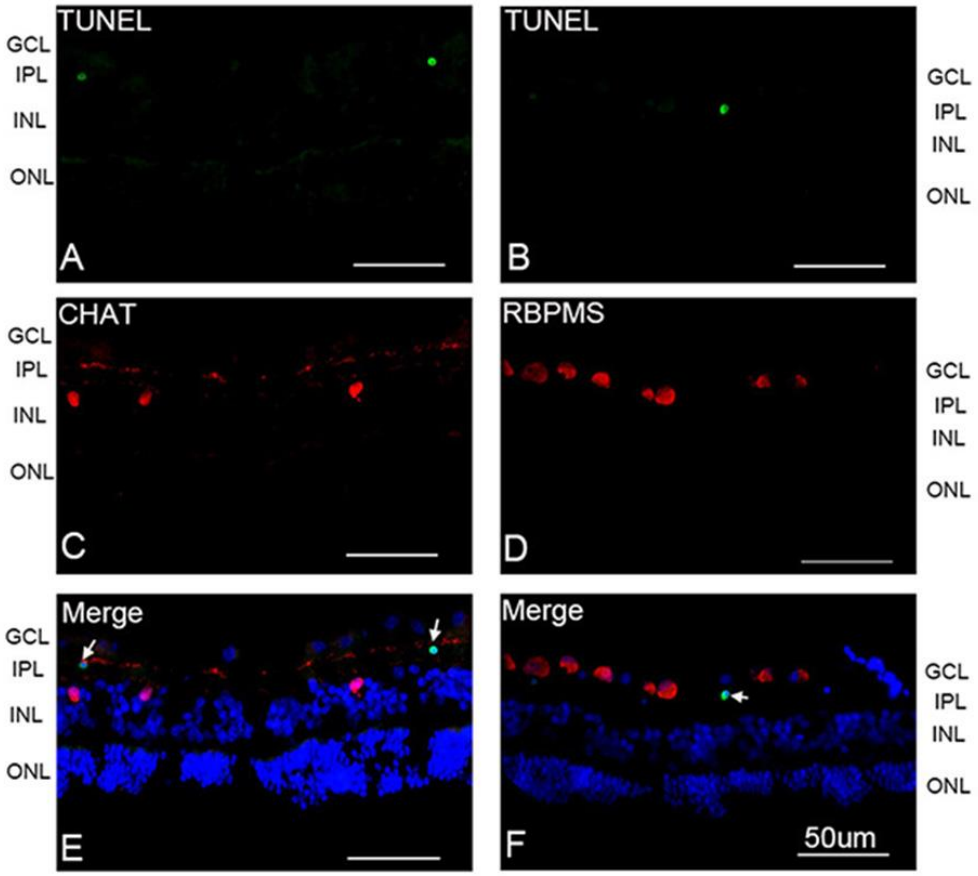

Supplementary Figure S3. RGCs and DACs did not colocalize with TUNEL-positive cells. The TUNEL-Positive cells (green fluorescence A, B, E, F) did not colocalize with anti-CHAT labeled DACs (red fluorescence C, E), nor with anti-RBPMS labeled RGCs (red fluorescence D, F). Hoechst stained nuclei (blue fluorescence E, F).

Abbreviated symbols: RGCs, retinal ganglion cells; DACs, displaced amacrine cells; TUNEL, terminal deoxynucleotidyl transferase dUTP nick-end labeling; CHAT, choline acetyl transferase; RBPM, RNA-binding protein with multiple splicing; GCL, ganglion cell layer; IPL, inner plexiform layer; INL, inner nuclear layer; ONL, outer nuclear layer.

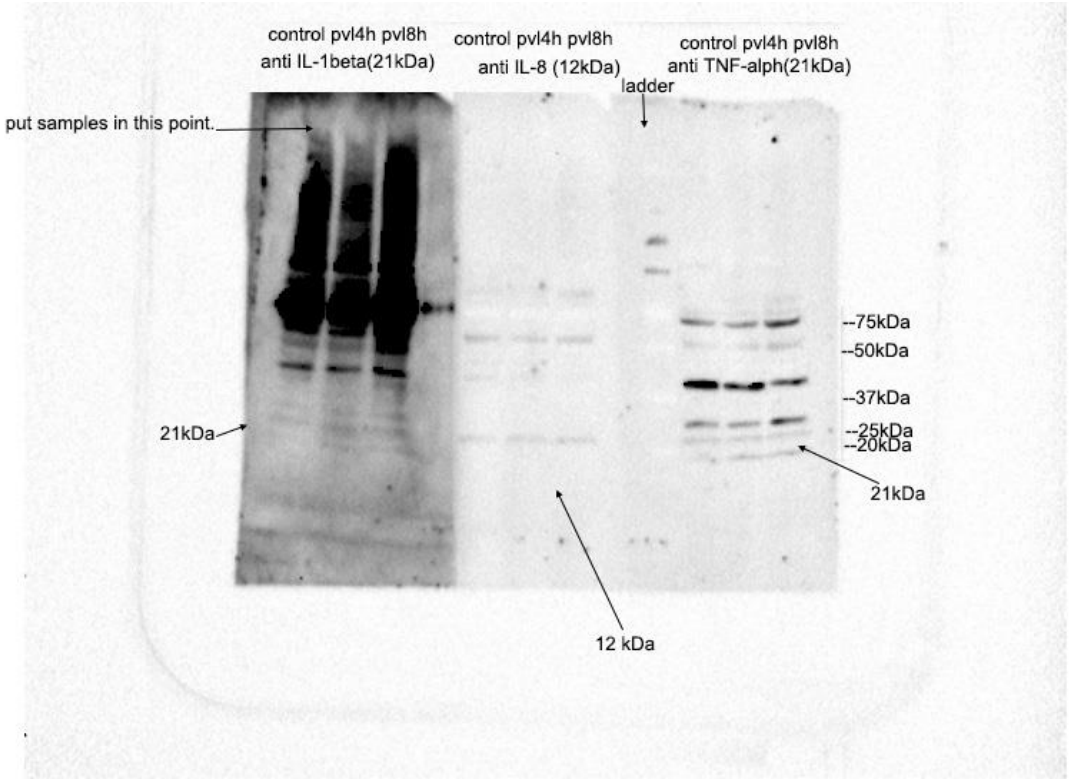

Supplementary Figure S4. The full-length blots for IL-1β, IL-8 and TNF-α. The primary antibodies were rabbit anti human IL-1β, mouse anti rabbit IL-8 and mouse anti-rabbit TNF-α from left to right. The lanes were put the same quantity proteins (40 ug/ lane) extracted form retina control, PVL 4 h, PVL 8 h from left to right according to the results of BCA kit. The specific bands for IL-1β were around the 21kDa, those for IL-8 were around 12kDa and those for TNF-α were around 21kDa. We could see that thses three factors have no sepecific bands in lanes of all samples (control, PVL 4 h, PVL 8 h) using western blotting method.

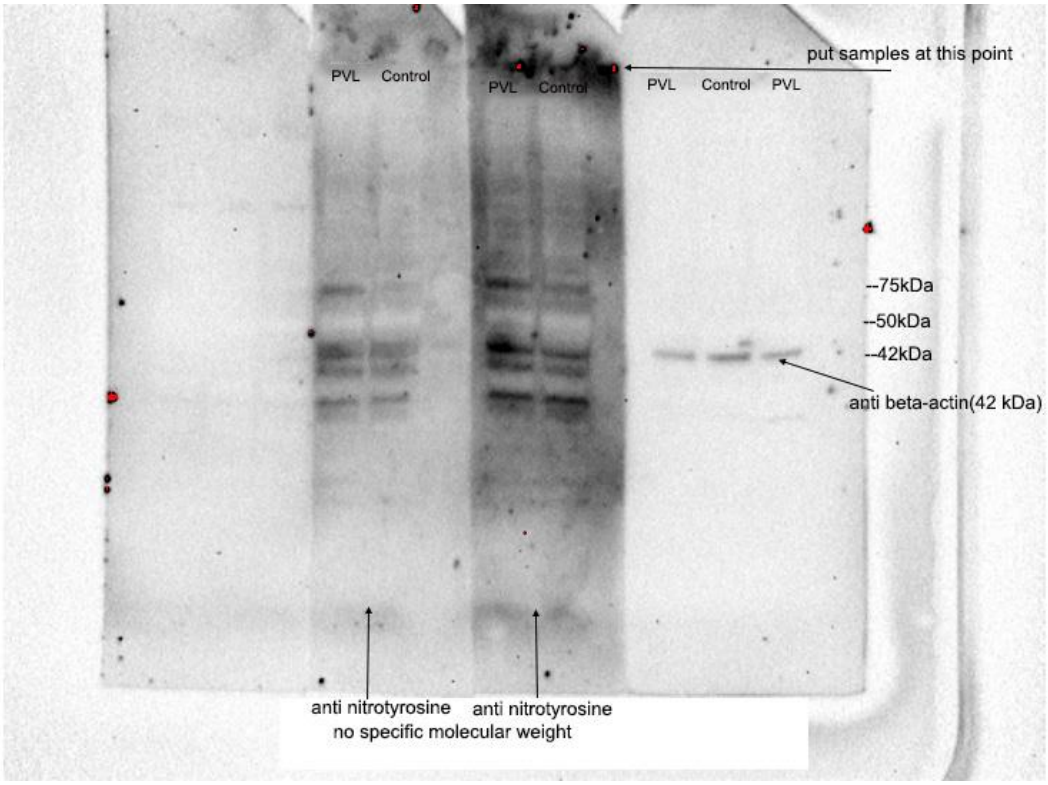

Supplementary Figure S5. The full-length blots for nitrotyrosine and β-actin. The first anti nitrotyrosine was treated with more detergents than the second anti nitrotyrosine. In this gel, all the lanes were loaded with the same quantity of test proteins (pvl 4h) and the same quantity of control proteins (40ug/lane) calculated with BCA kits. The anti-nitrotyrosine antibody recognizes free/protein-bound 3-NT which has no relation with molecular weight. The different bands correspond to different nitrotyrosine bound proteins that have between 37 kDa and 75 kDa molecular weight. The specific β-actin bands were showed around 42 kDa. The bots for nitrotyrosine and β-actin were from the same samples.

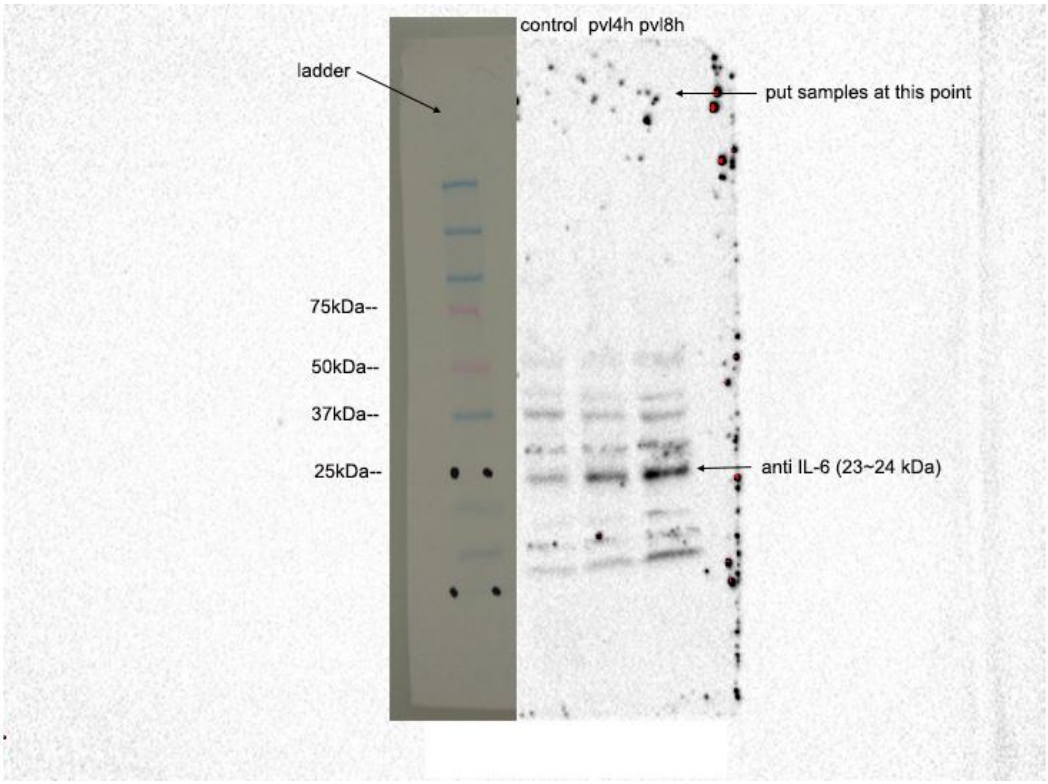

Supplementary Figure S6. The full-length blots for IL-6. The primary antibody was mouse anti human IL-6. The lanes were put the same quantity proteins (40 ug/ lane) extracted form retinas (control, PVL 4 h, PVL 8 h from left to right) according to the results of BCA kit. The specific bands were around the 24kDa. We could see clear bands in lanes around 24kDa of PVL 4 h and PVL 8 h, weak band around 24kDa in lane of control.

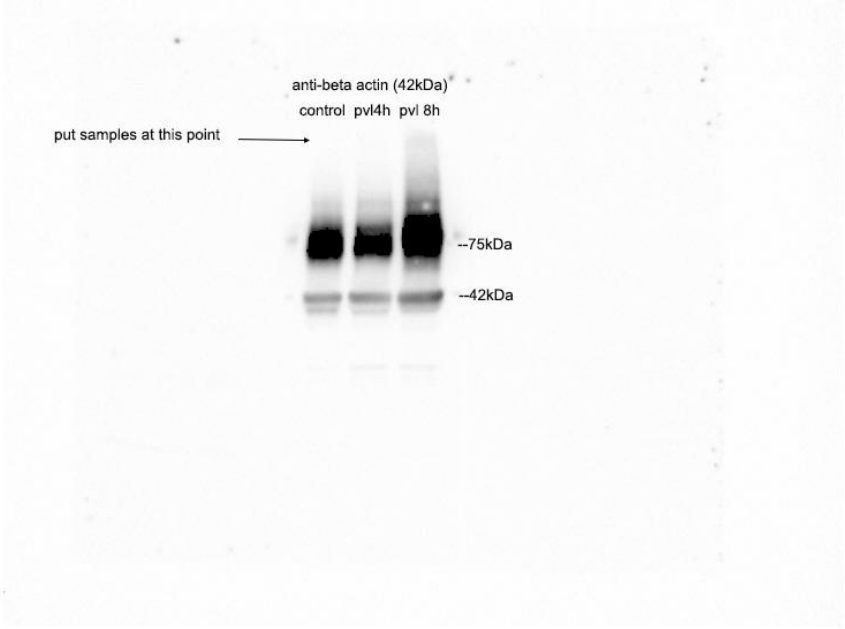

Supplementary Figure S7. The full-length blots for β-actin with IL-6 The primary antibody was rabbit anti human β-actin, the lanes were put the same quantity proteins (40 ug/ lane) extracted form retinas (control, PVL 4 h, PVL 8 h from left to right) according to the results of BCA kit. The specific bands were around the 42kDa.

3.2 Article 2: Panton–Valentine Leukocidin Induces Neuronal and Microglial Apoptosis together with Müller and Microglial Cell Activation in a Rabbit Retinal Explant Model

Preface

In the first part of this study, we employed the intravitreal injection method, injecting intravitreally PVL and analyzing retinal structure and PVL location at different time points. We have identified RGCs as PVL target in retina and showed early inflammatory changes of retina, including glial cell activation, microglial cell apoptosis, increase of IL-6 and nitrotyrosine production. Other animal model is needed to confirm these results. PVL colocalized with retinal neuronal cells. Did this colocalization really significate PVL targeting those retinal cells? After targeting those retinal cells, what cellular reaction and mechanism did PVL induce? Could the inhibitors of the mechanism block PVL toxicity to retina? Those questions are difficult to study using *in vivo* model. Developing cell- and tissue-based in vitro models are important for the following studies to understand the mechanism of PVL infecting retina and testing of potential therapeutics.

Intravitreal injection was constraint to test more different time point and different concentration of PVL for the reason of limited number of rabbit usages. Testing PVL with high concentration and longer time points might bring some more evident results to have more concrete conclusion. The retinal explant lacks choroid and retinal blood supply, it can exclude the possible interferences from break-down of blood-ocular barrier and infiltrated myeloid cells. PVL could be directly applied on the retinal surface without diffusion in vitreous. Compared to the animal model *in vivo*, retinal explant provides a more applicable and more easily controlled environment, which might show direct PVL effects in retina. In this second part, the objectives were to furtherly analyze PVL effects by testing different PVL concentrations and different PVL-treated time points in rabbit retinal explants, an *ex vivo* model which was important for the following studies to know the molecular mechanism of PVL-endophthalmitis.

In retinal explants, PVL fixation was more rapid and the spectrum of colocalized cells was larger than *in vivo* model. PVL colocalized rapidly with ganglion cells, and later with some horizontal cells. PVL-positive cells were also observed in INL, which were probably a subpopulation of amacrine cells. Microglial and Müller cells were activated, and apoptotic cells were found in PVL-treated retinal explants, in a concentration and time dependent way. When treated by PVL at high concentration, Müller cells were dissociated, and retinal explant structure was largely destroyed 24 h after PVL treatment. The majority of TUNEL positive cells were a subpopulation of amacrine cells in INL and some microglial cells.

In retinal explants, PVL is applied on the surface of retina in a more manageable and direct way. Retinal explant could be employed in the future studies to explore the mechanism of PVL reacting on retinal cells and the potential therapeutic strategies.

Title: Panton–Valentine Leukocidin Induces Neuronal and Microglial Apoptosis with Müller and Microglial Cell Activation in a Rabbit Retinal Explant Model

Running title: PVL induces glial activation in *ex vivo* retina

XuanLi LIU[1], Michel J ROUX[2], Serge PICAUD[3], Daniel KELLER[1], Arnaud SAUER[4], Pauline HEITZ[4], Gilles PREVOST [1], David GAUCHER [1,4#]

1. Université de Strasbourg, Hôpitaux Universitaires de Strasbourg, Fédération de Médecine Translationnelle de Strasbourg, EA7290 Virulence Bactérienne Précoce, Institut de Bactériologie, Strasbourg, France.

2. Department of Translational Medicine and Neurogenetics, Institut de Génétique et de Biologie Moléculaire et Cellulaire, CNRS UMR_7104, Inserm U 964, Université de Strasbourg, Illkirch, France

3. Sorbonne Université, INSERM, CNRS, Institut de la Vision, 17 rue Moreau, 75012, Paris, France.

4. Hôpitaux Universitaires de Strasbourg, Service d'Ophtalmologie du Nouvel Hôpital Civil, Strasbourg Cedex - France.

The fax, telephone number, and e-mail address of the corresponding author:

Tel: +33 (0)3 69 55 11 15; +33 (0)6 63 12 75 98. Fax: +33 (0)3 69 55 18 49. Email: david.gaucher@chru-strasbourg.fr

Total count of Words

Abstract: 222

Introduction: 597

Methods: 1443

Results: 1238

Discussion: 1110

Conclusion: 161

References: 1153

Number of figures: 8

Number of supplementary figures: 3

Number of tables:2

Abstract

Purpose: Panton–Valentine leukocidin (PVL) is a virulent leukotoxin of *Staphylococcus aureus*. A retinal explant was used as an *ex vivo* endophthalmitis model to identify PVL-targeted retinal cells and to analyze the early retinal inflammatory response following PVL treatment.

Method: Rabbit retinal explants were treated with PVL at different concentrations. PVL location and Müller and microglial cell activation were examined using immunohistochemistry at different time points following PVL treatment. Inflammatory factors were analyzed using RT-qPCR at 4 and 8 h following PVL treatment. These results were compared with those of untreated control explants.

Results: PVL co-localized rapidly with retinal ganglion cells and with horizontal cells. PVL induced Müller and microglial cell activation, which resulted in structure alteration in the retina. Some amacrine and microglial cells underwent apoptosis. All the results increased in a PVL concentration- and time-dependent manner. In PVL-treated explants, inflammatory factor expression was lower than that in control explants, and the RNA yield significantly decreased.

Conclusion: PVL co-localized with neuronal cells and incited Müller and microglial cell activation. Glial activation was associated with neuronal and microglial apoptosis together with retinal structural damage. These results demonstrated that PVL is an aggravating factor of *S. aureus* endophthalmitis. Retinal explant is a feasible and reproducible *ex vivo* model, which can be employed to explore the molecular effects of PVL on the retinal tissue.

Key words: Panton–Valentine Leukocidin; apoptosis; Müller cell activation; microglial cell activation; retinal explant

Main Points: In an *ex vivo* model of retinal infection, Panton–Valentine leucocidin, a toxin of *S. aureus*, colocalized with retinal neurons, and induced glial and microglial activation, and amacrine and microglial cells apoptosis in a concentration- and time-dependent manner.

Introduction

Bacterial endophthalmitis is an acute ocular infection and often results in poor visual outcomes [1]. The severity of bacterial endophthalmitis is related to virulence factors from infectious strains [2]. *Staphylococcus aureus* is a common bacterium found in the human body and is often a virulent strain found in endophthalmitis cases. Genomic studies of *S. aureus* have failed to demonstrate the relationship between bacteria and their virulence [3]. Conversely, it has been shown that the toxins secreted by *S. aureus* are related to its virulence [4]. Analyzing the effects of toxins on the retina could reveal the mechanism by which virulent factors aggravate bacterial endophthalmitis and provide a new target for therapeutic strategies.

S. aureus strains can produce five leukotoxins: two gamma-hemolysins (HlgA/HlgB and HlgC/HlgB), Panton–Valentine leukocidin (PVL), LukED, and LukAB [5]. Leukotoxin is composed of two distinct proteins: class S (31–32 kDa) and class F components (33–34 kDa). The class S component binds membrane receptors, which allow secondary interaction of the F component. Unaccompanied class S or F protein do not produce any effect on targeted cells [6]. The PVL gene is present in most community-associated methicillin-resistant *S. aureus*, which is known for its virulence[7]. Horizontal transfer of this gene has been observed, and the percentage of PVL-carrying strains has been continuously increasing [8]. PVL-encoding *S. aureus* strains are associated with necrotic lesions [9], and in some rare cases, could cause septic shock after furuncles and severe pneumonia [10]. We previously demonstrated that PVL can also cause severe ocular inflammation [11-13].

PVL employs human and rabbit C5a complement receptors (C5aR) to bind target cells and exert cytotoxicity. PVL has a species-specific preference and does not recognize mice C5aR, as the latter exhibits different sequences of amino acids in its second extracellular loop [5]. Therefore, we used PVL-induced endophthalmitis in a rabbit model to investigate the early retinal damage caused by PVL. In this study, PVL co-localized with retinal ganglion cells (RGCs) and caused glial cell activation, as well as some microglial apoptosis. Inflammation was also triggered following a PVL infection, as IL-6 and nitrotyrosine increased after intravitreal PVL injection [14].

Primary neuron culture from the dissociated retina is time-consuming and expensive and has a limited reproducibility under *in vivo* conditions. Retinal explants are an alternative between dissociated primary cell culture and animal models. It maintains the neurons *in situ* and in contact with other cells and the extracellular matrix physiologically, provides an easily controlled environment, and lacks a retinal and choroidal blood supply. It can eliminate the possible potential disturbance of myeloid cells in the blood circulation and the effects of blood–ocular barrier breakdown [15].

We used retinal explants to analyze PVL effects at different concentrations and time points to further confirm PVL toxicity for the retina. We found that retinal explants are an excellent model to examine PVL toxicity for the retina, as the majority of our *in vivo* findings were confirmed in the retinal explant model. Indeed, PVL co-localized rapidly with RGCs, later

with some horizontal cells, and possibly with a subpopulation of amacrine cells. PVL induced Müller and microglial cell activation, which resulted in retinal structural changes. Some amacrine and microglial cells underwent apoptosis. All of these results increased in a PVL concentration- and time-dependent manner.

Materials and methods

PVL purification

PVL (LukS-PV/LukF-PV) was purified as described in a previous study [16] by affinity chromatography on glutathione-Sepharose 4B followed by cation-exchange fast-performance liquid chromatography after removal of glutathione S-transferase tag with Precision Protease (GE Healthcare, Villacoublay, France). Preparation homogeneity was assessed by radial gel immunoprecipitation and SDS-polyacrylamide gel electrophoresis before storage at −80 ◦C.

Retinal explant preparation and organotypic culture

The animal experiments were approved by the Ministère de l'Education nationale, de l'Enseignement supérieur et de la Recherche, France. The surgical procedure was performed in accordance with the guidelines in the laboratory of the Association for Research in Vision and Ophthalmology, in adherence to the ARVO Animal Statement.

Retinal explant requires swift extraction of the retina and retinal flat mounting on a hydrophilic membrane with minimum disturbance of the tissue. Briefly, pigmented rabbits (Bleu de Champagne) aged 6 months and weighing 2.5–3 kg were anesthetized by a lumbar intramuscular injection of ketamine, 20 mg/kg (Virbac, Carros, France) and xylazine, 3 mg/kg (Bayer Healthcare, Puteaux, France), followed by a lethal intravenous injection of 2-mL Pentobarbital Dolethal® (Vetoquinol, Lure, France) through a 22-Gauge catheter inserted in the marginal auricular vein. The eyes were immediately enucleated after euthanasia and immersed in ice-cold CO_2-independent medium (Gibco, Life technologies, Carlsbad, USA). Eyes were transported to aseptic condition. Each eyeball was immersed in disinfection medium (Pursept A, xpress Germany) and washed with cold i-CO_2 medium. Under a stereomicroscope, the eye globes were diessected and the posterior segment was cut into four 7×7 mm pieces avoiding to cut out visible blood vessels and myelinilised retinal parts. The choroid was teared away from the sclera and the optic nerve was cut with fine scissor. The neuroretina was gently detached from the pigment epithelium by tearing the choroid off.

The retina was dropped with photoreceptor layer facing down on membrane which was inserted into Transwell® culture dishes (Corning Inc, Corning, NY). After the retinal flat-mounting, 2 ml culture medium, neurobasal-A (Gibco, Life technologies, Carlsbad, USA) supplemented with 1% antibiotic–antimycotic mixture, was added into the culture well. The culture medium level was maintained in contact with the support membrane beneath the explant. The retinal explants were incubated at 37 °C with 5% CO_2 in a humidified atmosphere.

PVL-treated explants and contrl explants

A series of PVL concentrations (0.176, 0.352, 1.76 and 12.48 μM) were prepared and applied to 3 or 7 (for 1.76 μM PVL) different explants at each time point (30 min, 2, 4, 8 and 24 h). Our previous study used PVL (3 μg/50 ml), equal to 1.76 μM. So PVL 1.76 μM was used as reference concentration. A 10-μL droplet of PVL diluted in culture medium was deposited on the surface of nerve fiber layer in each tested explant after retina flat-mounting. An equivalent volume of culture medium was deposited onto the surface of control explants. Retina explants were collected and immediately fixed by 4% (wt/vol) paraformaldehyde. Four explants treated by 1.76 μM PVL were immediately frozen at -80°C for RT-qPCR at each time point (4, 8 and 24 h).

Tissue processing

The explants were fixed for 1 h in 4% (wt/vol) paraformaldehyde and then embedded successively in 10% (wt/vol) and 20% (wt/vol) sucrose and stored in 30% (wt/vol) sucrose overnight at 4°C. The fixed retinal explants were divided and immersed in optimal cutting temperature compound (Sakura Finetek, Torrance, CA, USA) for cryosections, or stored in plastic tube (0.5ml) directly at -80 °C for retinal whole-mounts. Retinal cryosections of 8 μm were cut and mounted on a Super Frost™ Plus microscope slides (Thermo Fisher Scientific, Rockford, IL, USA) and stored at -20 °C.

Fluorescent immunostaining

Retinal sections were permeabilized in 0.05% (v/v) TritonX-100 for 1 h and then were blocked with 10% (v/v) donkey serum (Sigma-Aldrich, St. Louis, MO, USA) for 1 h. Retinal sections were incubated with primary antibodies (Table 1) at 4°C overnight in a humidity chamber. Washing with PBS x 1 for 3 times, retinal sections were then incubated for 1 h at room temperature with fluorescent secondary antibodies (Table 1). Some sections were continually incubated in terminal deoxynucleotidyl transferase dUTP nick end labeling (TUNEL) mixed solution for another 1 h. Washing with PBS x 1 for 3 times, sections were counter-stained with Hoechst 33258 and mounted in 10% (v/v) Mowiol® solution (Polysciences, Eppelheim, Germany).

Retina whole mounts were permeabilized 0.2% (v/v) TritonX-100 for 30 min. The retina whole mounts were incubated in conical small wells and transferred with 3 ml pipette. The staining steps were the same as those of immunoistochemistry section. At last, the retinal whole mounts were mounted on microscope slides and covered with thinner and smaller cover slides in 10% (v/v) Mowiol® solution. Images of fluorescent sections and whole mounts were obtained using an epifluorescence Olympus BX60 microscope connected to a Hamamatsu C11440 digital camera.

Cell counting

Different microscope fields (266 μm × 266 μm) of retinal immunofluorescent images were captured by the camera. PVL-positive retinal cells were evaluated by double immunohistochemistry: PVL-positive cells were double-labeled by PVL and retinal cell-

specific markers. The percentages of PVL-positive RGCs at each time point (30 min, 2, 4, 8 and 24 h with 1.76 μM PVL) were established by mean mounts of 3 explants (each explant has five study fields randomly captured by camera). For TUNEL positive cells count, five different microscope fields were analyzed for each explant, three different explants for each time point and PVL concentration. The mounts of TUNEL positive cells in each time points and concentration were established by mean mounts of all study fields.

RNA extraction

TRIzol reagent (Sigma, Saint-Louis, USA) was added into tubes contained frozen retina. The retinas were passed through 23-Gauge needle then 26-Gauge needle several times to be homogenized. Total RNA was isolated using TRIzol reagent according to the manufacturer's instructions. The total RNA concentration was quantified with spectrophotometry (NanoDrop; Thermo Scientific, Waltham, USA). The RNA yield of each explant was calculated as a total weight of extracted RNA versus explant weight. RNA yield of control explants and 1.76 μM PVL-treated explants were quadruple at each time point.

Real-time RT-qPCR

10 μg RNA aliquots were treated with DNA-free kit DNase treatment (Ambion, Life technologies) at 37 °C for 30 min according to manufacturer's instructions. 5 μL of RNA solution after DNase treatment was immediately reverse transcribed (RT) using Superscript First-Strand Synthesis for RT-PCR (Invitrogen, Life technologies). Diethyl decarbonate (DEPC) (Sigma) treated H_2O was added to RT mixture (0.5 μL random hexamers (200 ng/ml), 5 μL total RNA, 1 μL NTP) to achieve a 12 μL volume, then incubated at +65 °C for 5 min and placed in glass for 2 min. Then, 0.5 μL of 0.1 M DDT, 0.5 μL of transcriptase, 4 μL of First Strand buffer, 3 μL of sterile H_2O were added to the mixture. Then, the total mixture was put into a ThermoCycler programmed at +42 °C for 50 min and at + 70 °C for 15 min. The cDNA was diluted 3 times with DEPC treated H_2O. Then, 5 μL of diluted cDNA, 10 μL SYBR Green mix (LightCycler 480 SYBR Green I Master, Roche, Basel, Switzerland), 2 μL of forward and reverse primers (100 μm), and 3μL H_2O were mixed and put into 96 wells plate. The plate was placed into Real-Time PCR System (Light Cycler 480, Roche). PCR was programmed as initial denaturation step at +95 °C for 10 min, 45 cycles of amplification (denaturation at + 95 °C for 15 s, annealing at +60 °C for 20 s, extension at + 72 °C for 15 s), and melting curve analysis (+60 °C to +95 °C increment at +0.3 °C). The specificity of PCR products was verified according to one melting curve peak and one band in agarose gel electrophoresis. Products of RTs without reverse transcriptase were used as controls to ascertain no significant DNA contamination.

The primers were designed to have Tm around 60°C by using Primer3 software. The sequences of primers: β-actin forward primer 5'-gcgggacatcaaggagaag-3', afterward primer 5'-aggaaggagggctggaaga-3'; IL-6 forward primer 5'-tcaggccaagttcaggagtg-3', afterward primer 5'-atgaagtggatcgtggtcgt-3'; IL-8 forward primer 5'-tggctgtggctctcttgg-3', afterward primer 5'-atttgggatggaaaggtgtg-3'; TNF-α forward primer 5'-cgtagtagcaaacccgcaag-3', afterward primer 5'-tgagtgaggagcacgtagga-3'; VEGF forward primer 5'-cgagaccttggtggacatctt-3', afterward primer 5'-tgcattcacatttgttgtgct-3'; iNOS

forward primer 5'-ccaagccctcacctacttcc-3', afterward primer 5'-aactcctccagcacctcca-3'. The β-actin was used as reference gene and target gens were normalized using this reference gene. The method ∆Ct was used to calculate relative quantification between control explants and PVL-treated explants. The fold changes were calculated using $2^{-\Delta\Delta Ct}$. The tests were triplicate. The significant changes of every target gene were statistically analyzed using ∆Ct paired t-tests.

Statistical analysis

Statistical analysis was performed with GraphPad InStat version 3.10. Statistical significance was calculated paired t-tests, unpaired t-tests or ANOVA test. Statistical significance was assumed at $p < 0.05$.

Results

PVL co-localized with RGCs and horizontal cells

An anti-LukS-PV antibody (Table 1) was used to identify the PVL fixation after being deposited on the retinal explant. PVL co-localized with RGCs labeled with an anti-RBPMS antibody in the retinal section (Figure 1 A–C). In the retina, RGCs co-localized with C5aR immunoactivity (Figure 1 D–F). PVL co-localized with some horizontal cells labeled with an anti-calbindin antibody at 8 and 24 h after PVL treatment (Figure 1 G–L). The mean (± SEM) percentage of PVL-positive RGCs were 33.7% ± 5.5%, 44.3% ± 4.7%, 47.0% ± 6.2%, 42.0% ± 4.0%, and 45% ± 3.1% for 30 min, 2, 4, 8, and 24 h after PVL treatment, respectively (Figure 2 A–P). The rate of PVL-positive RGCs did not significantly change between 30 min and 24 h after culture ($p > 0.05$, Figure 2 P).

PVL immunoreactivity was also observed in some cells in the inner part of the inner nuclear layer (INL; Figures 1 A–C and 2 A–I). However, we could not identify the cell type. The immunolabeling showed that they were not cholinergic amacrine cells labeled with the anti-ChAT antibody, AII amacrine cells labeled with an anti-calretinin antibody, or calbindin-positive bipolar cells (Supplementary Figure S1). Using a polyclonal anti-Pax6 antibody, other subpopulations of amacrine cells corresponded to the PVL-positive cells in the INL (Supplementary Figure S1 J, K). Unfortunately, we could not find a commercially available anti-Pax6 antibody that recognized rabbit Pax6 and was developed from a species other than rabbit. Consequently, we could not perform double immunolabeling for anti-Pax6 or anti-PVL antibodies (developed from rabbit).

Müller and microglial cells were dramatically activated early by PVL in a concentration- and time-dependent manner.

Müller cells extended their processes through the whole retina to provide architectural support to retinal neurons. The hallmark of retinal Müller cell activation is a shape change resulting from rapid upregulation of glial fibrillary acidic protein (GFAP) following acute retinal injury [17]. In control explants, Müller cells were regularly arranged on the inner side of the retina from 2 to 24 h after culture (Figure 3 A–D). Müller cells showed an abnormal extension in the outer nuclear layer in 1.76 µM PVL-treated explants, which increased from

2 to 24 h after PVL treatment (Figure 3 E–H) and from low (0.176 μM) to high (12.48 μM) PVL concentrations (Figure 4 A–H). Dissociation of Müller cell organization was observed 24 h after culture in retinal explants treated with 1.76 μM PVL (Figure 3 H and Figure 4 G). At 24 h, a complete destruction of Müller cells was noted in the retinal explants treated with 12.48 μM PVL (Figure 4 H and Supplementary Figure S2). The retinal architecture was damaged when treated with 12.48 μM PVL at 8 and 24 h (Supplementary Figure S2). This retinal disfigurement may be related to Müller cell dysfunction.

Microglial cells could demonstrate a broad range of morphological changes at different activated stages, including an enlargement of the soma, retraction and shortening of processes, and transformation into an amoeboid form, a round cell soma without processes [18]. In control explants, microglial cells began to retract their processes 8 h after culture, enlarged their soma and retracted their processes 24 h after culture (Figure 5 G, H). While in PVL-treated explants, microglial cells were transformed into the amoeboid form, losing all of their processes 2 h after PVL treatment (Figure 5 E, F, I, J). Microglial cells were sensitive to PVL treatment and were dramatically activated 2 h after culture from 0.176 to 12.48 μM PVL (Figure 4 I–L).

A subpopulation of amacrine cells underwent apoptosis in PVL-treated explants

In control explants (n = 3 for each time point with five study fields for each explant), TUNEL-positive cells were found 24 h after culture, and the mean number was 0.81 per study field (Figure 6 A–C and Table 2). In PVL-treated explants (n = 3 for each time point and PVL concentration with five study fields for each explant), several TUNEL-positive cells were found 4 h after treatment with 1.76 and 12.48 μM PVL. The mean numbers of TUNEL-positive cells were 2.25 and 2.00 per study field, respectively (Figure 6 D, G and Table 2). TUNEL-positive cells significantly increased, and the mean numbers were 2.00 and 5.00 per study field 8 and 24 h after 1.76 μM PVL treatment, respectively, and the mean numbers were 6.00 and 11.67 per study field 8 and 24 h after 12.48 μM PVL treatment, respectively (Figure 6 E, F, H, I and Table 2). In 12.48 μM PVL-treated explants, more TUNEL-positive cells were found than in 1.76 μM PVL-treated explants (**** $p < 0.0001$, Figure 6 J).

In PVL-treated explants, the TUNEL cells were mostly situated in the inner part of the INL and several positive cells were in the ganglion cell layer. In control explants, a few TUNEL-positive cells could be found in the whole retina 24 h after culture. In total, PVL-treated explants exhibited significantly more TUNEL-positive cells than control explants (****$p <$ 0.0001, Figure 6 K).

Double immunohistochemistry with TUNEL and specific antibodies of retinal cell types demonstrated that some microglial cells (labeled with FITC-tagged GSAI-B4) were TUNEL-positive in the whole retinal mount (Figure 7 A–C, a–c), TUNEL-positive cells also co-localized with amacrine cells (labeled with an anti-Pax6 antibody) in the INL (Figure 7 D–G, d–f). To further distinguish which subpopulation of amacrine cells were apoptotic, two specific antibodies were used and showed that starburst amacrine (labeled with an anti-ChAT antibody) and AII amacrine (labeled with an anti-calretinin antibody) did not co-

localize with TUNEL-positive cells (Supplementary Figure S3). TUNEL-positive cells did not co-localize with RGCs nor with calbindin-positive bipolar or horizontal cells (Supplementary Figure S3).

Although RNA yield decreased in all explants, inflammatory factor expression was lower in PVL-treated explants than in controls.

The total RNA was extracted from retinal explants by using a TRIzol reagent and quantified with spectrophotometry. The RNA yield was expressed by RNA production per microgram. Twenty-four hours after culture, the mean RNA yield significantly decreased by 81.2% (*p < 0.05) in control explants, the mean RNA yield was significantly reduced by 97.2% (***p < 0.001) in PVL-treated explants, and the mean RNA yield in PVL-treated explants decreased significantly more than in control explants (*p < 0.05) (Figure 8 A).

RT-qPCR was used to analyze inflammatory factor expression in explants 4 and 8 h after culture. At these time points, control explants expressed more inflammatory factor mRNA than PVL-treated explants (Figure 8 B, C). Four hours after culture, control explants had increased the IL-6 and IL-8 mRNA expression (IL-6: 12.42 ± 6.40-fold change, IL-8: 19.13 ± 11.43-fold change). Conversely, IL-6 and IL-8 mRNA expression did not increase in PVL-treated explants (Figure 8 B).

Eight hours after culture, control explants had significantly increased IL-6 and IL-8 mRNA expression (IL-6: 7.63 ± 2.25-fold change, IL-8: 19.66 ± 1.0-fold change), together with PVL-treated explants (IL-6: 3.70 ± 0.98-fold change, IL-8: 6.36 ± 1.16-fold change). PVL-treated explants expressed lower inflammatory factors (IL-6 and IL-8) than control explants (*p < 0.05, Figure 8 C). For control explants, IL-6 and IL-8 mRNA expression did not significantly change from 4 to 8 h after culture. Although IL-6 and IL-8 mRNA expression increased in PVL-treated explants, TNF-α expression significantly decreased (0.15 ± 0.02-fold change). This was not the case for control explants.

Discussion

In retinal explants, PVL co-localized rapidly with RGCs, then with horizontal cells, and possibly with a subpopulation of amacrine cells in the INL. PVL incited Müller and microglial cell activation together with amacrine and microglial cell apoptosis in a PVL concentration- and time-dependent manner.

We recently showed that PVL increasingly co-localized with RGCs from 30 min to 2 h after PVL infection and transiently with displaced amacrine cells in an *in vivo* rabbit model [14]. In the present *ex vivo* study, PVL also rapidly co-localized with RGCs and later with horizontal cells. It is also possible that PVL targeted a subpopulation of amacrine cells: Some cells in the INL were PVL-positive and had the form and location of amacrine cells (Supplementary Figure S1 J, K). However, we could not precisely demonstrate this fact as antibodies for double immunolabeling were not commercially available for rabbit. Nevertheless, those cells were not bipolar, horizontal, starburst, or AII amacrine cells. They seemed to

correspond to amacrine cells labeled with an anti-Pax 6 antibody. Interestingly, the amacrine cells underwent apoptosis a few hours after PVL treatment. The differences in cell targeting between *in vivo* and *ex vivo* retinas might be because of different mechanisms of PVL diffusion in the retina. The retina is a semipermeable membrane. Even if the inner limiting membrane of the retina is considered a significant barrier for molecular diffusion, the inner and outer plexiform layers are likely the sites of highest resistance to molecular diffusion [19]. During intravitreal injection, PVL diffuses into the retina but might be constrained in the ganglion cell layer by the diffusion resistance of the inner plexiform layer. In retinal explants, PVL diffused more profoundly in the retina and reached the INL (i.e., horizontal cells). The retinal explant lacks a blood supply and the retinal vasculature rapidly shrinks. This might modify the retinal homeostasis and decrease the capacity of diffusion resistance from the inner plexiform layer. Consequently, PVL could diffuse more efficiently through the retina.

PVL caused apoptosis of a subpopulation of amacrine cells in PVL-treated explants. PVL could incite intracellular calcium increase and glutamate release from neuronal cells [20]. The amacrine cells express ionotropic glutamate receptors. Excessive activation of ionotropic glutamate receptors could lead to amacrine cell death [21]. The PVL-positive cells were RGCs and some neuronal cells in the INL, which might release excessive glutamate and incite apoptosis in amacrine cells.

We showed that Müller cells were activated in a and PVL concentration- and time-dependent manner. The Müller cell reaction was also associated with some retinal structural damage. Significant destruction of the retinal structure occurred 8 h after PVL treatment and might be due to retinal edema. Müller cells are the primary cells responsible for K^+ and fluid influx regulation in the retina [22]. In retinal inflammation, Müller cells are activated and transformed into gliosis, which results in a significant decrease in potassium and water channel protein expression [23]. Müller cells swell and the retinal fluid absorption function decreases, leading to retinal edema and degeneration [24].

Microglial cell activation is a typical early phenomenon in response to retinal injuries and inflammation before retinal cell death [25]. Activated microglial cells demonstrate various phenotypes with a different degree of stimuli and could undergo apoptosis by overactivation [26]. In control explants, microglial cells were slightly activated at 8 and 24 h after culture. Microglial cells were significantly activated 2 h after PVL treatment, some of them were apoptotic, which might be because of the overaction incited by PVL. The activation and gene expression of microglial cells are influenced by the balance of excitatory and inhibitory stimuli from the microenvironment around the microglial cells, especially neurons which might incite a microglial inflammatory response [27-29].
The mechanism of cell reaction incited by PVL is not well known. LukS-PV binds C5aR, which provokes calcium mobilization in neutrophils and neuronal cells (Jover et al., 2013). LukS-PV alone does not incite cell reaction. It needs the presence of LukF-PV for PVL cytotoxicity[6, 20]. Recently, it was identified that CD45 is one receptor for LukF-PV [30]. In retina, it is clear that ganglion cells express C5aR and that some microglial cells express

CD45 [31]. However, we do not know if LukF-PV and CD45 have role in the activation/cytotoxicity of microglial cells.

Our study shows that the inflammatory factor expression increased and microglial cells are slightly activated in control explants. Another study has shown the same inflammatory state of retinal explants. In rat retinal explants, microglial cells show features of activation. Some microglial cells became amoeboid and others retracted their processes. TNF-a, IL-6, and MCP-1 were detected in the culture supernatant using an ELISA test 1 day after culture [32]. In PVL-treated explants, the increase of IL-6 and IL-8 expression was lower than in control explants and the TNF-α expression decreased, whereas Müller and microglial cells were dramatically activated earlier than expected. This discrepancy between morphological results and inflammatory factor expression is difficult to explain. Our previous results using an *in vivo* model demonstrated that PVL injection incited both morphological changes and inflammatory factor release. On the one hand, in PVL-treated explants, it is possible that Müller and microglial cells were too disturbed (Figure 4) to express inflammatory factors. On the other hand, in retinal explants, inflammatory factor release from cells other than Müller and microglial cells (neutrophils, macrophages, and mast cells) that infiltrate the retina from the blood circulation is not possible. However, in contrast to the *in vivo* model, there is no blood supply in retinal explants, which explains the discrepancy between the *in vivo* and *ex vivo* results.

Our results showed that the RNA yield decreased more in the PVL-treated explants (by 97.2%) than in the control explants (by 81.2%) 1 day after culture. One study showed that the RNA yield of nontreated retinal explants decreased by 75% 1 day after culture [33], which is in accordance with our results. The decreased RNA yield might be mainly because of a decrease in RNA expression and the instability of mRNA during dramatic changes of retinal homeostasis conditions [33, 34]. These results demonstrate that PVL deteriorates the capacity of the retina to produce proteins. This effect might explain the decrease in inflammatory factor release in the PVL-treated explants.

Conclusion

Developing cell- and tissue-based *in vitro* models is essential to understand the mechanism of PVL infecting the retina and to perform tests for potential therapeutics. In this study using a retinal explant *ex vivo* model, we confirmed previous results from an *in vivo* model. PVL co-localized with retinal neurons and incited retinal inflammation, probably via Müller and microglial cell activation. In retinal explants, there was substantial evidence that PVL led to glial activation and later destruction; however, inflammatory markers usually associated with glial activation were not markedly increased. It is likely that glial destruction following PVL infection has limited the possibility of glial cells to secrete inflammatory factors. The lack of blood supply due to the retinal explants condition might also have played a role in the weak inflammatory response. Nevertheless, retinal explants are a useful and more manageable model to study PVL effects on the retina. PVL, or other

bacterial toxins, could aggravate bacterial endophthalmitis through neuronal and glial interaction.

Acknowledgments: This work was supported by a recurrent research EA7290 award from the University of Strasbourg and a grant from Novartis. LIU Xuanli was awarded by the Chinese Scholarship Council. Thank Enago (www.enago.com) for the English language review.
Potential conflicts of interest: None

Reference

1. Callegan MC, Engelbert M, Parke DW, 2nd, Jett BD, Gilmore MS. Bacterial endophthalmitis: epidemiology, therapeutics, and bacterium-host interactions. *Clinical Microbiology Reviews* 2002;15:111-124.
2. Callegan MC, Gilmore MS, Gregory M, et al. Bacterial endophthalmitis: therapeutic challenges and host-pathogen interactions. *Progress in Retinal and Eye Research* 2007;26:189-203.
3. Laabei M, Uhlemann AC, Lowy FD, et al. Evolutionary Trade-Offs Underlie the Multi-faceted Virulence of *Staphylococcus aureus*. *PLoS Biology* 2015;13:e1002229.
4. Fanny Vincenota MS, GillesPrévost. Les facteurs de virulence de *Staphylococcus aureus*. *Revue Francophone des Laboratoires* 2008;2008:61-69.
5. Spaan AN, Schiepers A, de Haas CJ, et al. Differential Interaction of the Staphylococcal Toxins Panton-Valentine Leukocidin and gamma-Hemolysin CB with Human C5a Receptors. *Journal of Immunology* 2015;195:1034-1043.
6. Alonzo F, 3rd, Torres VJ. The bicomponent pore-forming leucocidins of *Staphylococcus aureus*. *Microbiology and Molecular Biology Reviews : MMBR* 2014;78:199-230.
7. Vandenesch F, Naimi T, Enright MC, et al. Community-acquired methicillin-resistant *Staphylococcus aureus* carrying Panton-Valentine leukocidin genes: worldwide emergence. *Emerging Infectious Diseases* 2003;9:978-984.
8. Diep BA, Gill SR, Chang RF, et al. Complete genome sequence of USA300, an epidemic clone of community-acquired meticillin-resistant *Staphylococcus aureus*. *Lancet (London, England)* 2006;367:731-739.
9. Lina G, Piemont Y, Godail-Gamot F, et al. Involvement of Panton-Valentine leukocidin-producing *Staphylococcus aureus* in primary skin infections and pneumonia. *Clinical Infectious Diseases* 1999;29:1128-1132.
10. Gillet Y, Issartel B, Vanhems P, et al. Association between *Staphylococcus aureus* strains carrying gene for Panton-Valentine leukocidin and highly lethal necrotising pneumonia in young immunocompetent patients. *Lancet (London, England)* 2002;359:753-759.
11. Laventie BJ, Potrich C, Atmanene C, et al. p-Sulfonato-calix[n]arenes inhibit staphylococcal bicomponent leukotoxins by supramolecular interactions. *The Biochemical Journal* 2013;450:559-571.
12. Laventie BJ, Rademaker HJ, Saleh M, et al. Heavy chain-only antibodies and tetravalent bispecific antibody neutralizing *Staphylococcus aureus* leukotoxins. *Proceedings of the National Academy of Sciences of the United States of America* 2011;108:16404-16409.

13. Siqueira JA, Speeg-Schatz C, Freitas FI, Sahel J, Monteil H, Prevost G. Channel-forming leucotoxins from *Staphylococcus aureus* cause severe inflammatory reactions in a rabbit eye model. *Journal of Medical Microbiology* 1997;46:486-494.
14. Liu X, Heitz P, Roux M, et al. Panton-Valentine Leukocidin Colocalizes with Retinal Ganglion and Amacrine Cells and Activates Glial Reactions and Microglial Apoptosis. *Scientific Reports* 2018;8:2953.
15. Sawamiphak S, Ritter M, Acker-Palmer A. Preparation of retinal explant cultures to study ex vivo tip endothelial cell responses. *Nature Protocols* 2010;5:1659-1665.
16. Werner S, Colin DA, Coraiola M, Menestrina G, Monteil H, Prevost G. Retrieving biological activity from LukF-PV mutants combined with different S components implies compatibility between the stem domains of these staphylococcal bicomponent leucotoxins. *Infection and Immunity* 2002;70:1310-1318.
17. Dyer MA, Cepko CL. Control of Muller glial cell proliferation and activation following retinal injury. *Nature Neuroscience* 2000;3:873-880.
18. Ransohoff RM, Cardona AE. The myeloid cells of the central nervous system parenchyma. *Nature* 2010;468:253-262.
19. Jackson TL, Antcliff RJ, Hillenkamp J, Marshall J. Human retinal molecular weight exclusion limit and estimate of species variation. *Investigative Ophthalmology & Visual Science* 2003;44:2141-2146.
20. Jover E, Tawk MY, Laventie BJ, Poulain B, Prevost G. Staphylococcal leukotoxins trigger free intracellular Ca(2+) rise in neurones, signalling through acidic stores and activation of store-operated channels. *Cellular Microbiology* 2013;15:742-758.
21. Duarte CB, Ferreira IL, Santos PF, Carvalho AL, Agostinho PM, Carvalho AP. Glutamate in life and death of retinal amacrine cells. *Gen Pharmacol* 1998;30:289-295.
22. Eberhardt C, Amann B, Feuchtinger A, Hauck SM, Deeg CA. Differential expression of inwardly rectifying K+ channels and aquaporins 4 and 5 in autoimmune uveitis indicates misbalance in Muller glial cell-dependent ion and water homeostasis. *Glia* 2011;59:697-707.
23. Deeg CA, Amann B, Lutz K, et al. Aquaporin 11, a regulator of water efflux at retinal Muller glial cell surface decreases concomitant with immune-mediated gliosis. *Journal of Neuroinflammation* 2016;13:12.
24. Reichenbach A, Wurm A, Pannicke T, Iandiev I, Wiedemann P, Bringmann A. Muller cells as players in retinal degeneration and edema. *Graefes Arch Clin Exp Ophthalmol* 2007;245:627-636.
25. Karlstetter M, Scholz R, Rutar M, Wong WT, Provis JM, Langmann T. Retinal microglia: Just bystander or target for therapy? *Progress in Retinal and Eye Research* 2015;45:30-57.
26. Hanisch UK, Kettenmann H. Microglia: active sensor and versatile effector cells in the normal and pathologic brain. *Nature Neuroscience* 2007;10:1387-1394.
27. Broderick C, Hoek RM, Forrester JV, Liversidge J, Sedgwick JD, Dick AD. Constitutive retinal CD200 expression regulates resident microglia and activation state of inflammatory cells during experimental autoimmune uveoretinitis. *Am J Pathol* 2002;161:1669-1677.
28. Zhang YK, Zhao L, Wang X, et al. Repopulating retinal microglia restore endogenous organization and function under CX3CL1-CX3CR1 regulation. *Sci Adv* 2018;4:14.
29. D'Orazio TJ, Niederkorn JY. A novel role for TGF-beta and IL-10 in the induction of immune privilege. *Journal of Immunology* 1998;160:2089-2098.

30. Tromp AT, Van Gent M, Abrial P, et al. Human CD45 is an F-component-specific receptor for the staphylococcal toxin Panton-Valentine leukocidin. *Nature Microbiology* 2018.
31. Gregerson DS, Yang J. CD45-Positive Cells of the Retina and Their Responsiveness to In Vivo and In Vitro Treatment with IFN-γ or Anti-CD40. *Investigative Ophthalmology & Visual Science* 2003;44:3083-3093.
32. Mertsch K, Hanisch UK, Kettenmann H, Schnitzer J. Characterization of microglial cells and their response to stimulation in an organotypic retinal culture system. *J Comp Neurol* 2001;431:217-227.
33. Muller B, Wagner F, Lorenz B, Stieger K. Organotypic Cultures of Adult Mouse Retina: Morphologic Changes and Gene Expression. *Investigative Ophthalmology & Visual Science* 2017;58:1930-1940.
34. Bahar B, O'Doherty JV, Sweeney T. Assessment of RNA integrity in the postmortem pig colonic tissue ex vivo. *Journal of Animal Science* 2012;90 Suppl 4:22-24.

Table 1. List of specific markers used in the current study

Target	Antiserum	Source	Concentration
Primary antibodies or lectin			
PVL	Rabbit anti-LukS-PV polyclonal	EA-7290, Strasbourg, France	2 µg/mL
C5aR	Rabbit anti-C5aR polyclonal	Abcam, Cambridge, UK	2 µg/mL
Ganglion cells	Guinea pig anti-RBPMS polyclonal	UCLA Neurobiology, Los Angeles, CA, USA	2 µg/mL
Starburst amacrine cells	Goat anti-ChAT polyclonal	Chemicon Merck-Millipore, Temecula, CA, USA	20 µg/mL
Müller cells	Mouse anti-GFAP polyclonal	Bio-Rad AbD Serotec, Oxfordshire, UK	2 µg/mL
Microglial cells	FITC-tagged GSAI-B4	Sigma Aldrich, Saint Louis, MO, USA	2 µg/mL
amacrine cells	Rabbit anti-Pax 6 polyclonal	Abcam	2 µg/mL
All Amacrine cells	Mouse anti-calretinin monoclonal	Santa Cruz Biotechnology, Heidelberg, Germany	2 µg/mL
Horizontal cells	Mouse anti-calbindin monoclonal	Santa Cruz Biotechnology	2 µg/mL
Secondary antibodies			
Anti-rabbit	Goat and donkey polyclonal Alexa 555nm-conjugated	Life Technologies, Carlsbad, CA, USA	2 µg/mL
Anti-goat	Donkey polyclonal Alexa 488-conjugated	Molecular Probes, Eugene, OR, USA	2 µg/mL
Anti-mouse	Donkey polyclonal Alexa 488-conjugated	Abcam	2 µg/mL
Anti-guinea pig	Goat polyclonal Alexa 488-conjugated	Abcam	2 µg/mL
TUNEL	DNA strand breaks	Roche Life Science, Indianapolis, IN, USA	---
Nuclei	Hoechst 33258	Molecular Probes™, Eugene, OR, USA	0.1µg/mL

Abbreviations: RBPM, RNA-binding protein with multiple splicing; CHAT, choline acetyl transferase; GFAP, glial fibrillary acidic protein; FITC, Fluorescein isothiocyanate; GSAI, *Griffonia simplicifolia* agglutinin isolectin. TUNEL, terminal deoxynucleotidyl transferase dUTP nick-end labeling.

Table 2. **The mean number of apoptotic cells per study field**

PVL concentration	4 h	8 h	24 h
0 (control)	0	0	0.81
0.176 μM	0	0.22	2.50
0.352 μM	0	1.36	3.67
1.76 μM	2.25	2.00	5.00
12.48 μM	2.00	6.00	11.67

The table shows the mean number of apoptotic cells per study field of different explants 4, 8 and 24 h after treatment of different PVL concentrations. The mean number of apoptotic cells was calculated from 3 different explants and 5 study fields of each explant (****p <0.0001).

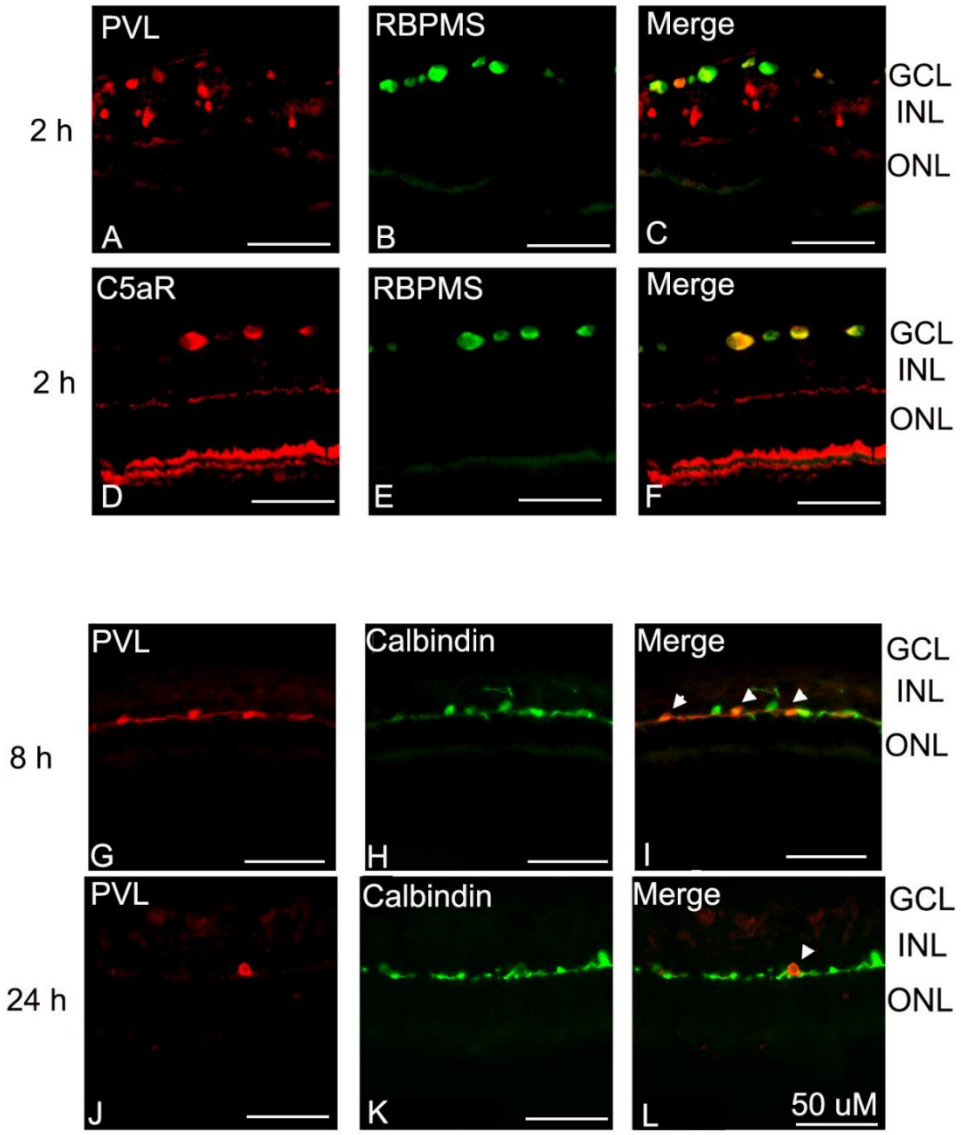

Figure 1: Panton–Valentine leukocidin (PVL) co-localized with retinal ganglion cells (RGCs) and then with horizontal cells. RGCs co-localized with C5aR immunoactivity. PVL (red fluorescence) co-localized with RGCs labeled with an anti-RBPMS antibody (green fluorescence) (A–C), and C5aR immunoactivity co-localized with RGCs (D–F) in the retinal explants 2 h after PVL treatment. PVL also co-localized with some horizontal cells labeled with an anti-calbindin antibody (green fluorescence) in the outer limit of the INL 8 (G–I) and 24 h (J–L) after PVL treatment.

Abbreviations: PVL, Panton–Valentine leukocidin; RGCs, retinal ganglion cells; RBPMS, RNA-binding protein with multiple splicing; C5aR, C5a receptor; GCL, ganglion cell layer; INL, inner nuclear layer; ONL, outer nuclear layer.

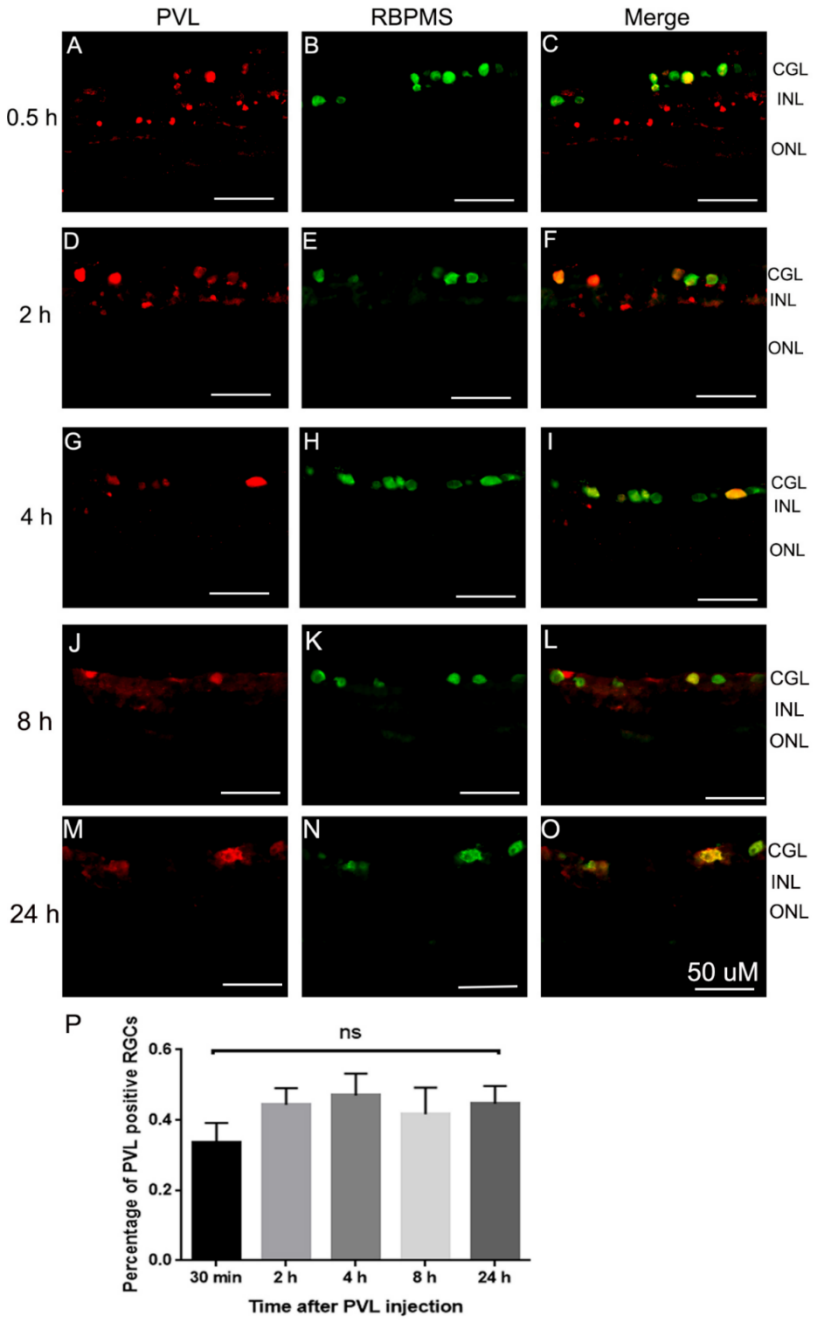

Figure 2: The rate of PVL-positive RGCs did not change from 30 min to 24 h. PVL (red fluorescence) co-localized with RGCs labeled with an anti-RBPMS antibody (green fluorescence) in the vertical retinal sections. The rate of PVL-positive RGCs was 33.7% ± 5.5%, 44.3% ± 4.7%, 47.0% ± 6.2%, 42.0% ± 4.0%, and 45% ± 3.1% for 30 min (A–C, P), 2 (D–F, P), 4 (G–I, P), 8 (J–L, P), and 24 h (M–O, P) after PVL treatment, respectively. No significant difference was observed for the rate of PVL-positive RGCs from 30 min to 24 h. The PVL immunoreactivity was also observed in some cells in the inner part of the INL before 4 h after PVL treatment (A–I).

Abbreviations: PVL, Panton–Valentine leukocidin; RGCs, retinal ganglion cells; RBPMS, RNA-binding protein with multiple splicing; GCL, ganglion cell layer; INL, inner nuclear layer; ONL, outer nuclear layer, ns, no significant.

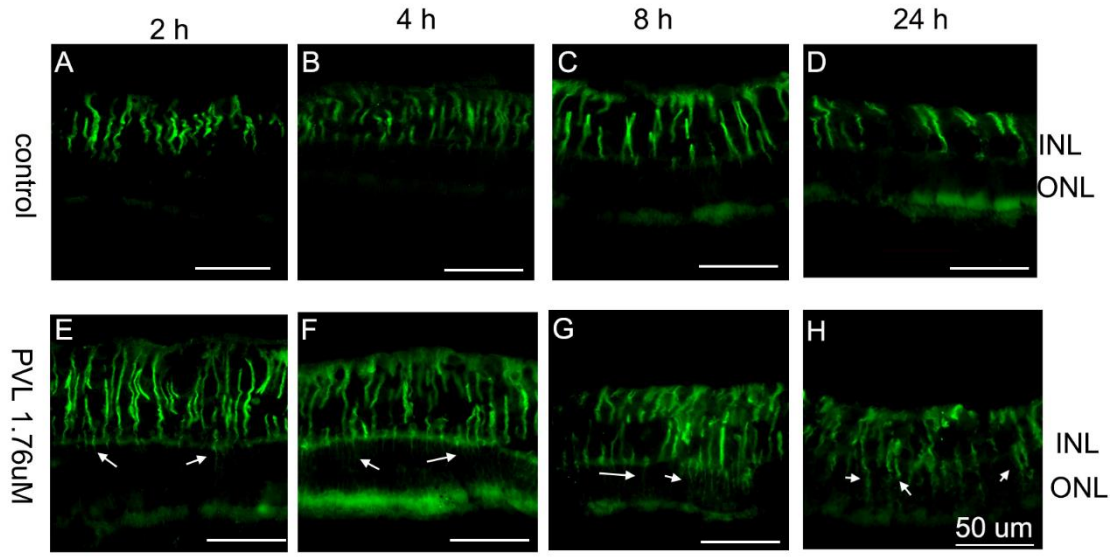

Figure 3: Müller cells were activated in PVL-treated explants. In control explants (A–D), Müller cell processes labeled with an anti-GFAP antibody were regularly arranged in the inner part of the retina. In PVL-treated explants, Müller cells labeled with an anti-GFAP antibody showed an abnormal extension in the outer nuclear layer (ONL), which increased from 2 to 24 h after PVL treatment (arrow, E–H). At 24 h, the anti-GFAP labeling was visible in the whole retina, from the inner to the outer part, demonstrating the abnormal glial reactivity (H).

Abbreviations: PVL, Panton–Valentine leukocidin; GFAP, glial fibrillary acidic protein; ONL, outer nuclear layer; INL, inner nuclear layer.

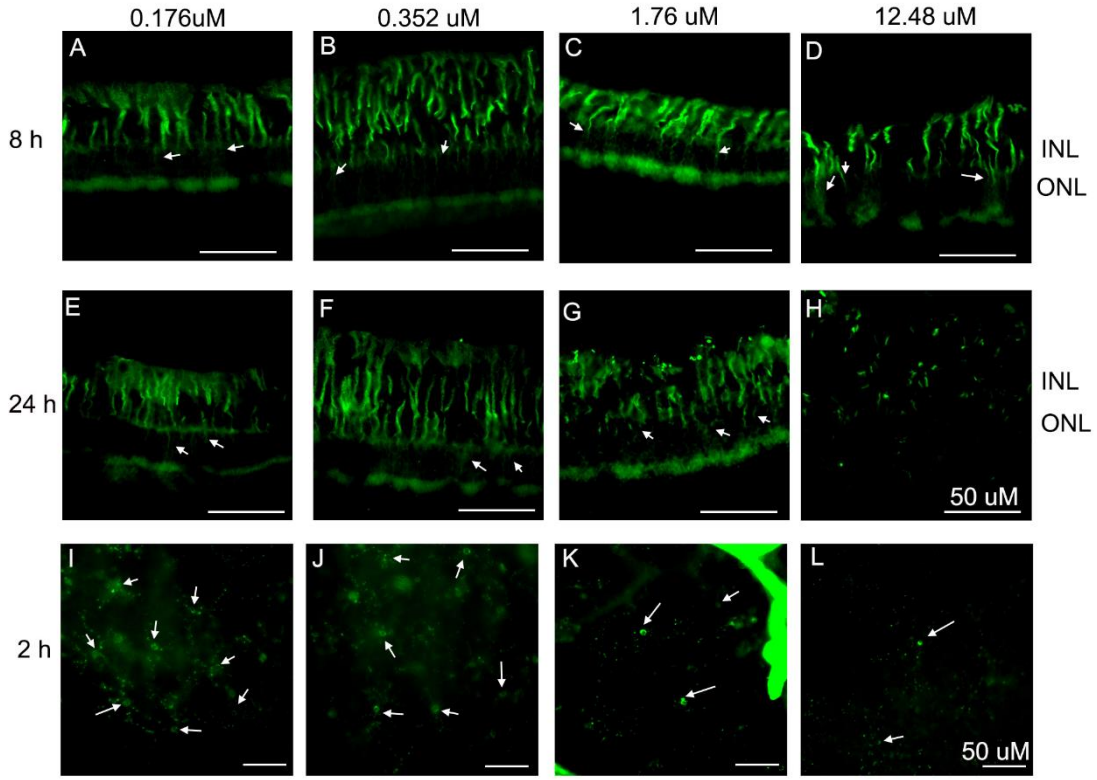

Figure 4: In PVL-treated explants, Müller and microglial cells were activated in a concentration- and time-dependent manner. A–H represent vertical retinal sections. I–L represent whole retinal mounts. Müller cells labeled with anti-GFAP showed an abnormal extension in the ONL 8 h after PVL treatment, which increased from 0.176 to 1.76 μM PVL (arrow, A–C). Müller cells showed a dissociated arrangement when treated with 12.48 μM PVL (arrow, D). Müller cells showed an abnormal extension in the ONL 24 h after treatment with 0.176 and 0.352 μM PVL (arrow, E, F). Müller cells appeared damaged, and the retinal structure was dissociated when treated with 1.76 (arrow, G) and 12.48 μM (arrow, H) PVL. Two hours after culture, microglial cells labeled with FITC-tagged GSAI-B4 began to lose their processes with 0.176 μM PVL (arrow, I), their processes were dissolved with 0.352 μM PVL (arrow, J), their processes disappeared with 1.76 (arrow, K), and their soma became smaller when treated with 12.48 μM PVL (arrow, L).

Abbreviations: PVL, Panton–Valentine leukocidin; GFAP, glial fibrillary acidic protein; ONL, outer nuclear layer; INL, inner nuclear layer.

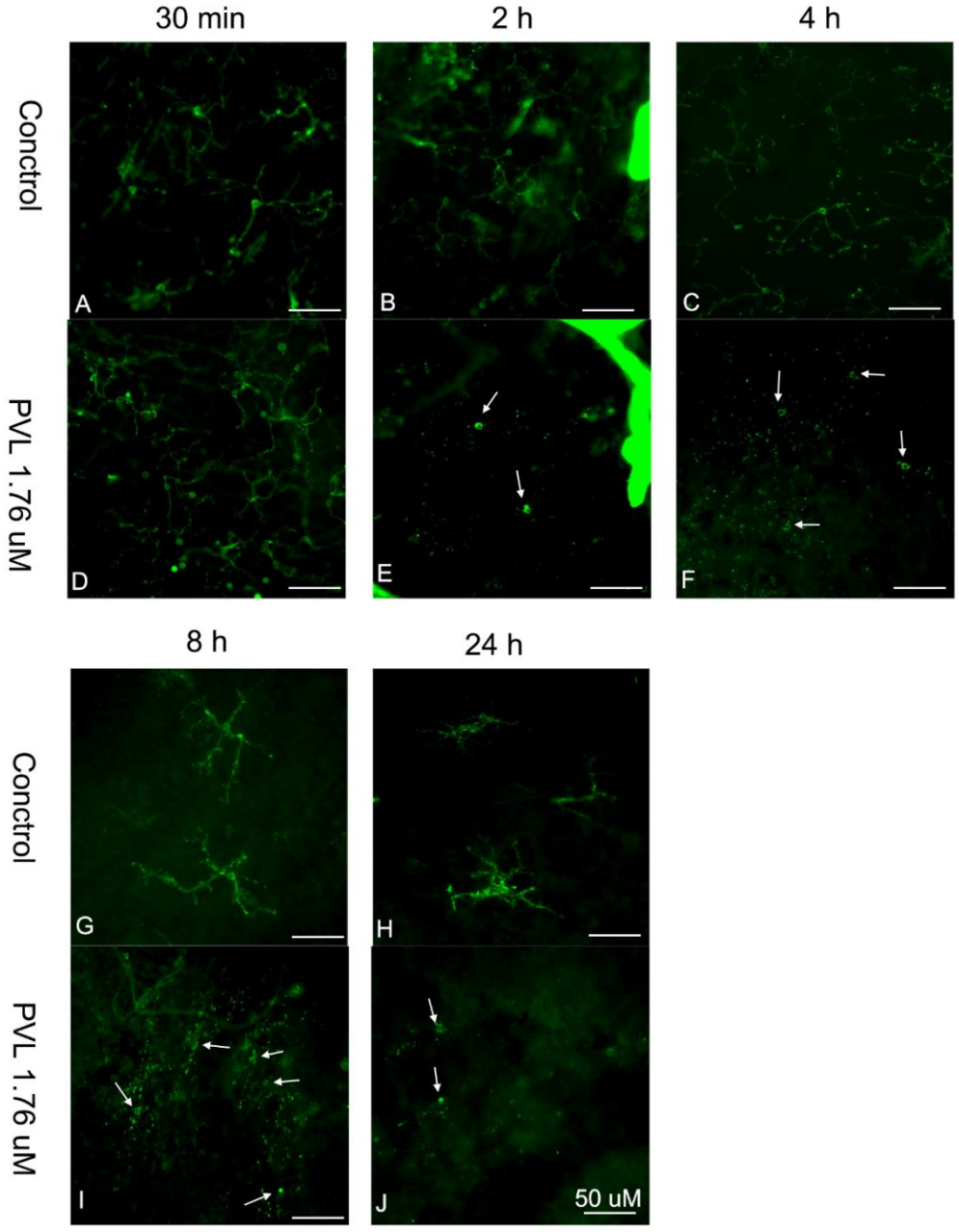

Figure 5: Microglial cells were activated 2 h after PVL treatment. A–J represents images of the whole retinal mount. Microglial cells were labeled with FITC-tagged GSAI-B4. In control explants, microglial cells were normal before 4 h (A–C) and began to retract their processes 8 h after culture (arrow, G). At 24 h, mild enlargement of the soma and a retraction of processes of microglial cells were observed in control explants (H). In contrast, microglial cells were normal at 30 min (D) in PVL-treated explants (1.76 μM) but were drastically transformed into amoeboid forms and lost all their processes from 2 to 24 h after PVL treatment (arrow, E, F, I, J).

Abbreviations: PVL, Panton–Valentine leukocidin; FITC, Fluorescein isothiocyanate; GSAI-B4, Griffonia Simplicifolia I Isolectin B4.

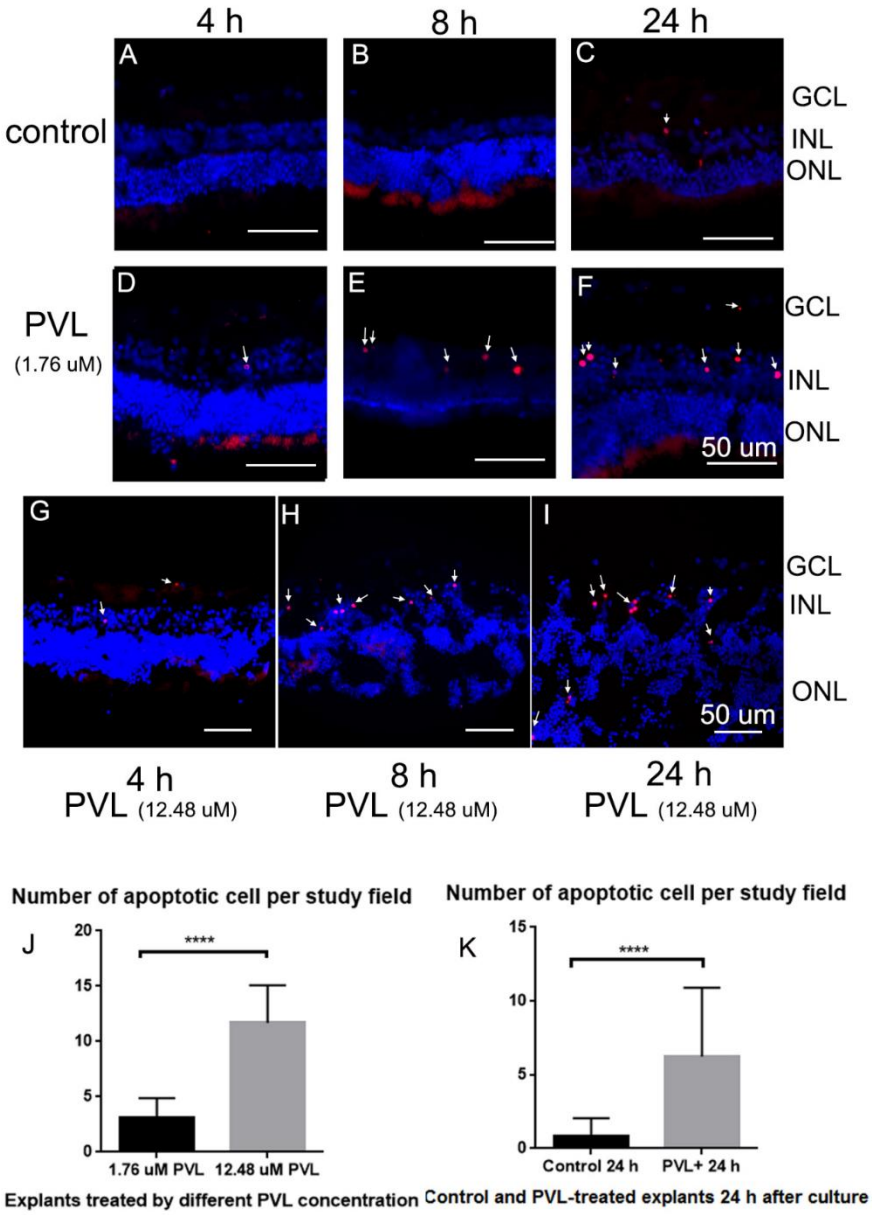

Figure 6: In PVL-treated explants, TUNEL-positive cells were found and increased in a concentration- and time-dependent manner. In control explants, no TUNEL-positive cells were detected 4 (A) or 8 h (B) after culture. However, a few TUNEL-positive cells were detected 24 h after culture (arrow, C). In PVL-treated explants (1.76 and 12.48 μM), TUNEL-positive cells were found and greatly increased from 4 to 24 h after treatment (arrow, D–I). The number of TUNEL-positive cells significantly increased between 1.76 (E, F) and 12.48 μM (H, I) PVL (J, ****$p < 0.0001$) and between PVL-treated explants to control explants (K, ****$p < 0.0001$). In 12.48 μM PVL-treated explants, the retinal structure was damaged 8 (H) and 24 h (I) after treatment. Retinal cell layers labeled with Hoechst dye were not distinguishable.

Abbreviations: PVL, Panton–Valentine leukocidin; TUNEL, terminal deoxynucleotidyl transferase dUTP nick end labeling; GCL, ganglion cell layer; ONL, outer nuclear layer; INL, inner nuclear layer.

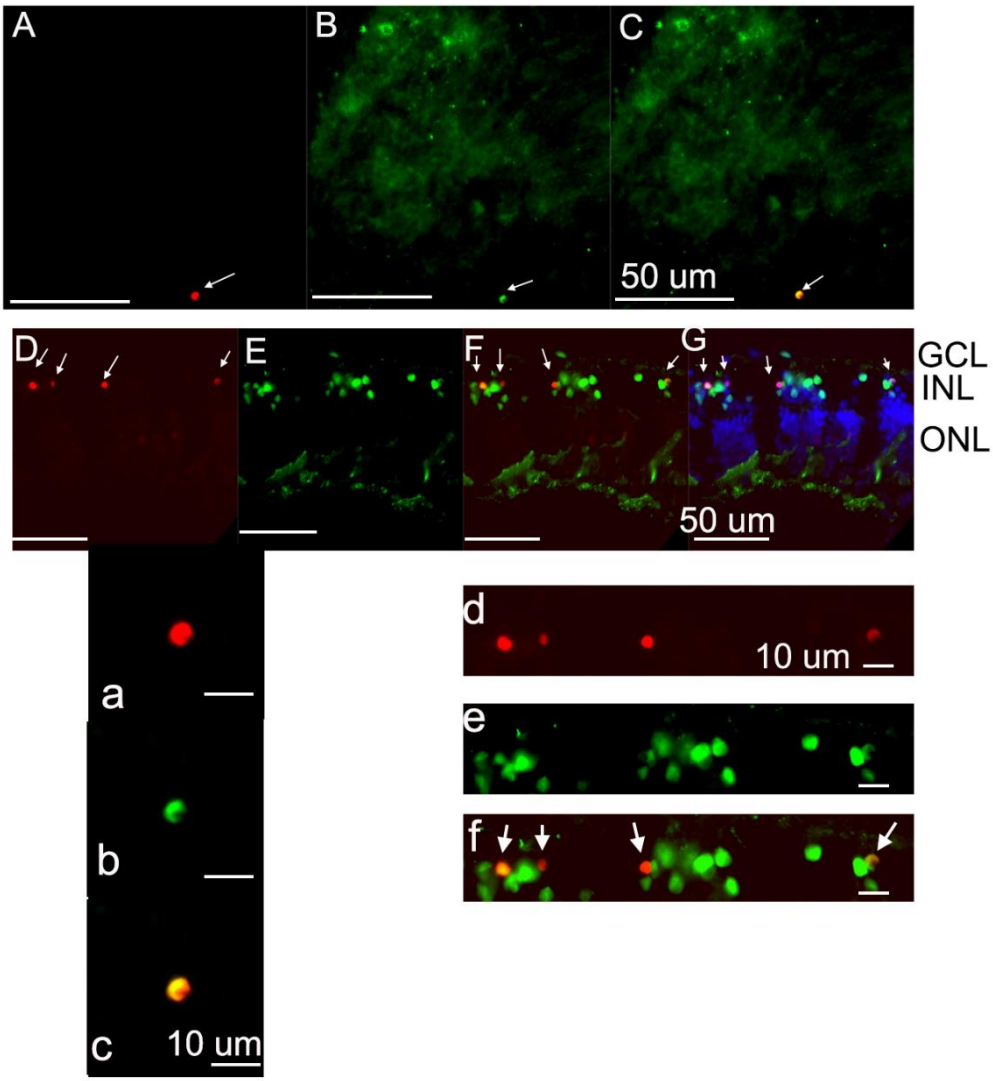

Figure 7: TUNEL-positive cells co-localized with microglial and amacrine cells in the INL. One microglial cell (labeled with FITC-tagged GSAI-B4) co-localized with TUNEL-positive cell in the whole retinal mount (A–C, enlarged images a–c). The majority of TUNEL-positive cells were localized in the INL and co-localized with amacrine cells (labeled with an anti-Pax 6 antibody) in vertical retinal sections (D–G, enlarged images d–f).

Abbreviations: PVL, Panton–Valentine leukocidin; TUNEL, terminal deoxynucleotidyl transferase dUTP nick end labeling; GCL, ganglion cell layer; ONL, outer nuclear layer; INL, inner nuclear layer.

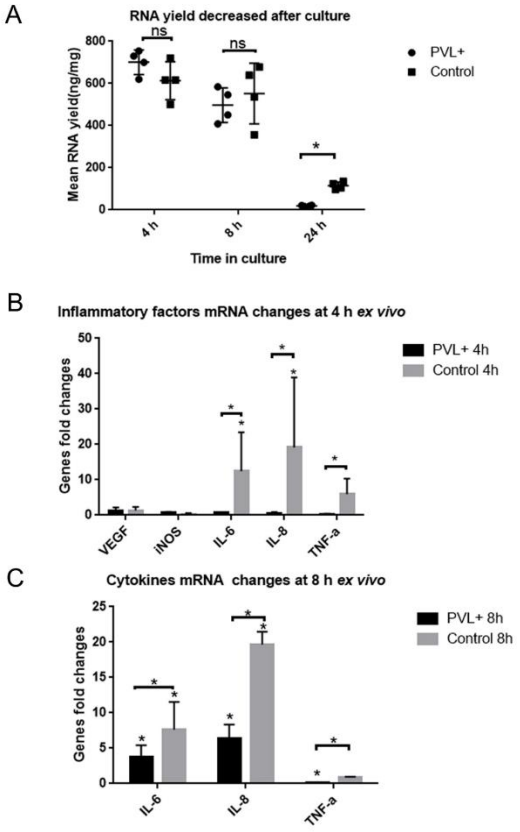

Figure 8: Although RNA yield decreased in all explants, the inflammatory factor expression was lower in PVL-treated explants than in controls. In control explants, the mean RNA yield per microgram was 613.0 ± 89.9 ng/ml at 4 h, 552.3 ± 143.9 ng/ml at 8 h, and 115.3 ± 17.4 ng/ml at 24 h. The mean RNA yield per microgram was reduced by 81.2% (*$p < 0.05$) 24 h after culture. In the PVL-treated group, the mean RNA yields per microgram were 701.0 ± 58.3 ng/ml at 4 h, 497.3 ± 81.7 ng/ml at 8 h, and 19.6 ± 2.4 ng/ml at 24 h. The mean RNA yield per microgram was significantly reduced by 97.2% (***$p < 0.001$) after 24 h treatment. There was a significant difference in RNA yield between control explants and PVL-tested explants 24 h after culture (A, *$p < 0.05$). Control explants had significantly increased IL-6 and IL-8 mRNA expression 4 h after culture, whereas PVL-tested explants did not show significantly increased inflammatory factor mRNA. Control explants expressed more inflammatory factor mRNA than PVL-treated explants 4 h after culture: IL-6, 12.42 ± 6.40 vs. 0.64 ± 0.05 (B, *$p < 0.05$); IL-8, 19.13 ± 11.43 vs. 0.51 ± 0.22 (B, *$p < 0.05$); and TNF-α, 6.00 ± 2.50 vs. 0.28 ± 0.09 (B, *$p < 0.05$). At 8 h after culture, control and PVL-tested explants had significantly increased IL-6 and IL-8 mRNA expressions, whereas PVL-tested explants had a significantly decreased TNF-α mRNA expression. Control explants expressed more inflammatory factors mRNA than PVL-treated explants after culture: IL-6, 7.63 ± 2.25 vs. 3.70 ± 0.98 (C, *$p < 0.05$); IL-8, 19.66 ± 1.05 vs. 6.36 ± 1.16 (C, *$p < 0.05$); TNF-α, 0.89 ± 0.04 vs. 0.15 ± 0.02 (C, *$p < 0.05$). The control explants did not significantly change the mRNA expression of IL-6, IL-8, or TNF-α from 4 to 8 h after culture.

Abbreviations: PVL, Panton–Valentine leucocidin.

Supplementary Figures S1-S3

Title: Panton–Valentine Leukocidin Induces Neuronal and Microglial Apoptosis together with Müller and Microglial Cell Activation in a Rabbit Retinal Explant Model
Running title: PVL induces glial activation in *ex vivo* retina

XuanLi LIU[1], Michel J ROUX[2], Serge PICAUD[3], Daniel KELLER[1], Arnaud SAUER[4], Pauline HEITZ[4], Gilles PREVOST [1], David GAUCHER [1,4#]

1. Université de Strasbourg, Hôpitaux Universitaires de Strasbourg, Fédération de Médecine Translationnelle de Strasbourg, EA7290 Virulence Bactérienne Précoce, Institut de Bactériologie, Strasbourg, France.

2. Department of Translational Medicine and Neurogenetics, Institut de Génétique et de Biologie Moléculaire et Cellulaire, CNRS UMR_7104, Inserm U 964, Université de Strasbourg, Illkirch, France

3. Sorbonne Université, INSERM, CNRS, Institut de la Vision, 17 rue Moreau, 75012, Paris, France.

4. Hôpitaux Universitaires de Strasbourg, Service d'Ophtalmologie du Nouvel Hôpital Civil, Strasbourg Cedex - France.

The fax, telephone number, and e-mail address of the corresponding author:

Tel: +33 (0)3 69 55 11 15; +33 (0)6 63 12 75 98. Fax: +33 (0)3 69 55 18 49. Email: david.gaucher@chru-strasbourg.fr

Supplementary Figure S1.

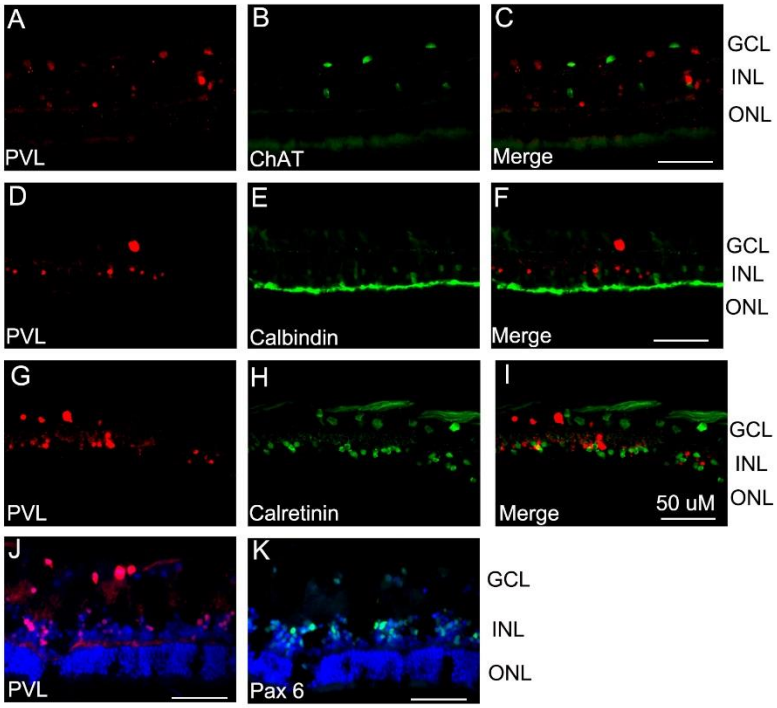

Supplementary Figure S1: PVL did not colocalize with cholinergic amacrine cells, nor AII amacrine cells; nor calbindin-positive bipolar cells, nor horizontal cells before 4 h after PVL treatment. PVL (red fluorescence) did not colocalize with cholinergic amacrine cells labeled with an anti-ChAT antibody, nor AII amacrine cells labeled with an anti-Calretinin antibody. PVL did not colocalize with calbindin-positive bipolar cells, nor horizontal cells before 4 h after PVL treatment. It seemed that amacrine cells labeled by anti-Pax6 antibody (K) correspond to the PVL-positive cells in INL (J).

Abbreviations: PVL, Panton–Valentine leukocidin; ChAT, Anti-Choline Acetyltransferase; GCL, ganglion cell layer; INL, inner nuclear layer; ONL, outer nuclear layer.

Supplementary Figure S2.

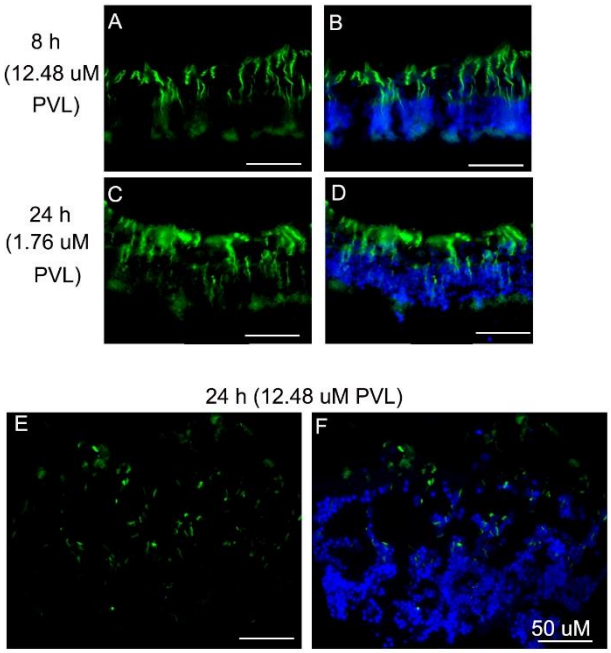

Supplementary Figure S2: Müller cells were activated and retinal structure was destroyed in PVL-treated explants. Müller cells labeled with an anti-GFAP antibody showed abnormal extension in ONL, and nuclei labeled with Hoechst began to show disordered organization 8 h after PVL treatment (1.76 μM PVL) (A, B). At 24 h, Müller cell processes were visible in the whole retina, nuclei could not show normal retinal structure in 1.76 μM PVL-treated explants (C, D). The Müller cells and nuclei were dissolved, retinal structure was destroyed 24 h after PVL treatment (12.48 μM PVL) (E, F).

Abbreviations: PVL, Panton-Valentine leukocidin; GFAP, glial fibrillary acidic protein; ONL, outer nuclear layer.

Supplementary Figure S3.

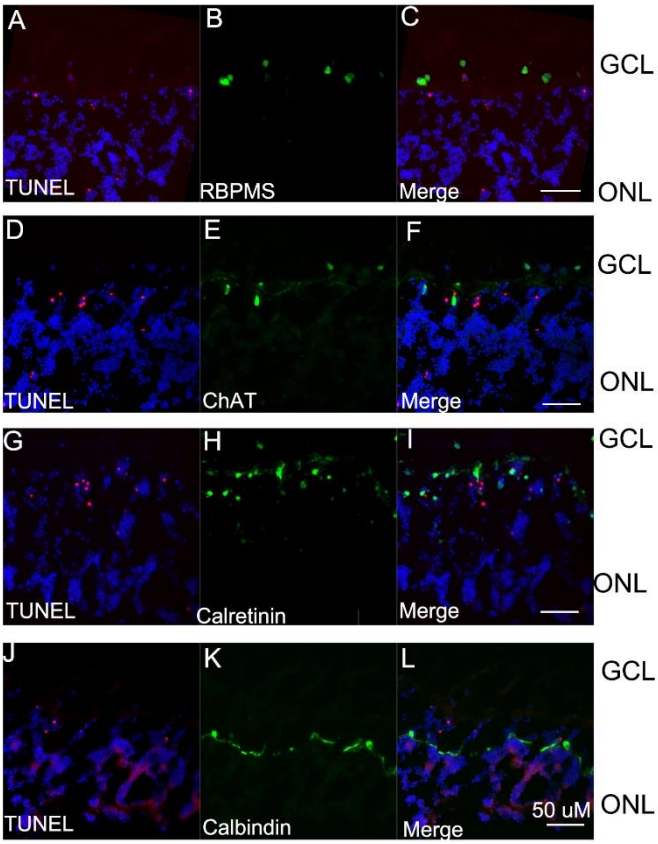

Supplementary Figure S3: TUNEL positive cells did not colocalized with RGCs, nor cholinergic amacrine cells, nor AII amacrine cells, nor calretinin-positive cells (bipolar and horizontal cells) in PVL-treated explants. The TUNEL positive cells did not colocalized with RGCs labeled with an anti-RBPMS antibody (A-C), nor with cholinergic amacrine cells labeled with an anti-ChAT antibody (D-F), nor with AII amacrine cells labeled with an anti-calretinin antibody (G-I), nor with calbindin-positive bipolar or horizontal cells labeled with an anti-calbindin antibody (J-L).

Abbreviation: PVL, Panton-Valentine leukocidin; TUNEL, terminal deoxynucleotidyl transferase dUTP nick end labeling; RGCs, retinal ganglion cells; RBPMS, RNA-binding protein with multiple splicing; ChAT, Anti-Choline Acetyltransferase; GCL, ganglion cell layer; ONL, outer nuclear layer.

3.3 Article 3: Bacterial toxins aggravate bacterial endophthalmitis by interacting directly with neurons

Preface

Our studies showed that PVL colocalized with retinal neurons and induced early retinal inflammation, including glial cell activation and inflammatory factors production. Other previous study showed that PVL could incite intracellular calcium mobilization in primary neuronal cells, which was associated with glutamate release from these neuronal cells without any membrane damages. The mechanism by which PVL initiates retinal inflammation by firstly targeting retinal neurons is unknown. By looking for the mechanism by with bacterial toxins incited inflammation in other neuronal system, the retinal molecular basis and the clinical symptoms of bacterial retinal inflammation in literature, we tried to find the most possible mechanism by which PVL initiating retinal inflammation by firstly targeting neuronal cells in bacterial endophthalmitis.

This review firstly supported the virulent role of bacterial toxins in aggravating bacterial endophthalmitis, and then examined how toxins induce inflammation in other neural systems. Bacterial components can directly act on neurons to produce neurogenic inflammation or stimulate neural circuits, both of which can modulate the innate immune response. This complex process is known as neuron-mediated inflammation. The retina has the molecular basis for innate immune response and neurogenic inflammation. It also discussed that the neuroretinitis, an infectious symptom induced by many kinds of bacterial and viral pathogens, is a disease probably resulting from retinal neuron-mediated inflammation by pathogens interacting directly on neuronal cells.

We hypothesize that bacterial toxins are able to trigger neurogenic inflammation in the very early phase of endophthalmitis. Neurogenic inflammation may then evolve, interact, and/or modulate the innate immune response to bacterial infection. When the retinal structure is modified by inflammation, irreversible damage to the retinal tissue occurs, leading to a decrease of visual functions. Further studies are required to confirm this neuron-mediated inflammation induced by toxins initially targeting neuronal cells during bacterial endophthalmitis and, if confirmed, whether toxins could represent a new therapeutic target.

Title: Bacterial toxins aggravate bacterial endophthalmitis by interacting directly with neurons.

XuanLi LIU [1] MD, Gilles PREVOST [1] PhD, David GAUCHER [1,2#] MD, PhD

1. Université de Strasbourg, Hôpitaux Universitaires de Strasbourg, Fédération de Médecine Translationnelle de Strasbourg, EA7290 Virulence Bactérienne Précoce, Institut de Bactériologie, Strasbourg, France.

2. Hôpitaux Universitaires de Strasbourg, Service d'Ophtalmologie du Nouvel Hôpital Civil, Strasbourg Cedex - France.

The fax, telephone number, and e-mail address of the corresponding author:

Tel: +33 (0)3 69 55 11 15; +33 (0)6 63 12 75 98. Fax: +33 (0)3 69 55 18 49. Email: david.gaucher@chru-strasbourg.fr

Key words: 1. Bacterial endophthalmitis 2. Bacterial toxin 3. neuron-mediated inflammation 4. neurogenic inflammation 5. Substance P (SP) 6. calcitonin gene-related peptide (CGRP)

Abstract

Bacterial endophthalmitis threatens the vision. The severity of bacterial endophthalmitis is related to the bacterial virulence. Bacterial toxins are evident virulence factors of bacteria. This study reviewed the proves in the literature that bacterial toxins might interact directly with neurons and induce neuron-mediated inflammation in retina.

In the neural system, there are two types of inflammation that may be involved when bacterial toxins interact with neuronal cells: one type is related to innate immune recognition system through pathogen-associated molecular patterns and pattern recognition receptors (PRRs), whereas the other is related to neurogenic response, principally mediated by substance P (SP), calcitonin gene-related peptide (CGRP) and probably glutamate, which are released from neuron terminals following induction by noxious stimuli. In neural system, bacterial components can act directly on neurons to produce neurogenic inflammation or stimulate neural circuits, both of which can modulate the subsequent innate immune response. This complex process is called neuron-mediated inflammation. Retina presents biologic potential to undergo neuron-mediated inflammation: the retina expresses PRRs, SP, and CGRP, and has the molecular basis for innate immune response and neurogenic inflammation. The steroid is controversial for bacterial endophthalmitis and useless for toxin inducing endophthalmitis. We hypothesized that bacterial toxins can trigger neuron-mediated inflammation in the very early phase of endophthalmitis. This may interact, and/or modulate the innate immune response to bacterial infection, and finally aggravate retinal lesions. Further studies are required to confirm the exact role of toxins during bacterial endophthalmitis.

Introduction

Bacterial endophthalmitis is an acute ocular inflammation that occurs because of postoperative, posttraumatic, or, in rare cases, endogenous bacterial infection. The bacterial infection causes the breakdown of the blood–ocular fluid barriers and infiltration of polymorphonuclear leucocytes into the retina, choroid, and other ocular tissues, resulting in enhanced release of complement and proinflammatory cytokines and modification of the retinal structure[1]. Bacterial endophthalmitis is often associated with a poor prognosis. Only 43%–53% of patients achieve 20/40 or better visual acuity (VA), and about 20% have 20/100 or worse even after appropriate therapeutic management[2-3]. Enucleation or evisceration are still common options in severe cases of endophthalmitis[4]. Recently, treatments such as vitrectomy and intravitreal injections of antibiotics have been introduced; however, visual outcome was not significantly improved[3].

The visual outcomes vary from visual recovery to loss of eye depending on many factors such as the types of infectious bacteria and the delay of treatment[5]. It is well demonstrated that virulent bacteria often cause severe endophthalmitis. Endophthalmitis caused by coagulase-negative *staphylococci* (CNS) result usually in good visual outcomes, causing generally less damage to retina than *Staphylococcus aureus*, *Enterococci*, *Bacillus*, and Gram-negative bacteria[6]. However, some endophthalmitis caused by CNS present delayed-onset, chronic and often painless inflammation, even severe ocular damages such as late retinal detachments[7]. Other factors than bacterial strains may explain the various severity of bacterial endophthalmitis.

S. aureus produces a large variety of toxins[8]. CNS serve as gene reservoirs for promoting *S. aureu*s colonization and virulence, possibly via toxin gene transfer among the strains[9]. The toxin expression in *Staphylococci* is related to bacterial virulence[8, 10], while the other virulence genes expressions, such as adhesin genes, fail to determine disease pathogenesis of *Staphylococci* strains[11-12]. Bacterial toxins might be the key factors which aggravate endophthalmitis, leading to a poor prognosis.

This review examined the virulent role of bacterial toxins in endophthalmitis. We reviewed briefly the innate immune response to infections, and neurogenic inflammation initiated by bacterial toxins in the central neural system. The retina has the potential to undergo innate immune response and neurogenic inflammation. The steroid is useless for toxin inducing endophthalmitis. Therefore, it is likely that bacterial toxins initiate rapidly neurogenic inflammation by interacting directly on neuronal cells then trigger innate immune response, which may lead to retinal damage and aggravation of bacterial endophthalmitis.

1. Bacterial toxins are related to severe bacterial endophthalmitis

CNS occupy 38%–80% of bacterial endophthalmitis cases, among which *Staphylococcus epidermidis* represents 30%–82%[13-16]. Approximately 9% of *S. epidermidis* endophthalmitis have poor visual outcomes[17]. *S. epidermidis* is a common colonizer at the ocular surface. One explanation for the pathogeny of *S. epidermidis* in endophthalmitis is due to its multidrug resistance and formation of biofilm[18]. However, it remains controversial whether antibiotic resistance and biofilm formation could differ between infectious and noninfectious strains. It is also unclear whether these two factors play a key role in poor visual outcomes in endophthalmitis[14, 19-20]. There are a variety of genotypic and phenotypic differences in *S. epidermidis* strains from endophthalmitis cases and healthy ocular surfaces, and the infectious and healthy strains shared only a few genetic characteristics[18, 21-22].

S. epidermidis may contain virulence factors, such as proteases, esterases, phenol-soluble modulins, and enterotoxin C, which are related to the severity of its infection[9-10, 23]. Enterotoxin C, a toxin of *S. aureus,* is found in some *S. epidermidis* strains (9%) that are related to severe clinical syndromes[10]. The expression of toxins in severe endophthalmitis caused by *S. epidermidis* remains to be elucidated.

Whereas, the role of toxins in *S. epidermidis* infections is not well studied, the aggravating effect of toxins in *S. aureus* infection is well demonstrated. *S. aureus* accounts for 7.2% of bacterial endophthalmitis cases with positive culture and is associated with a poor visual prognosis: 50% of patients achieve a VA of 20/100 or less[2]. The pathogenesis of *S. aureus* depends on the production of a myriad of virulent factors, among which toxins are frequently expressed. Toxin production can differentiate virulent from nonvirulent strains[24]. *S. aureus* secretes a variety of pore-forming toxins, such as α-toxin and bicomponent leukotoxins, proteolytic toxins, and superantigens[8]. Among these, leukotoxins, particularly Panton–Valentine leukocidin (PVL), can cause severe ocular inflammation[25-27]. In a PVL-induced endophthalmitis rabbit model, PVL is colocalized with retinal ganglion cells, which express PVL-specific receptor, C5aR, resulting in glial cell activation, apoptosis of microglial cells, and IL-6 release 4 h after intravitreal PVL injection[28]. The breakdown of hemo–retinal barrier leads to inflammation and PMNs infiltration in retina 24 h after PVL intravitreal injection. These results demonstrate that PVL toxin can alter retinal tissue *per se.* Moreover, antibodies against PVL can attenuate PVL-induced endophthalmitis[26].
Treatments for endophthalmitis include intravitreal antibiotic injection and vitrectomy to eliminate the pathogen from the eye[1]. However, irreversible structural damages to retina could occur during the first several hours[29]. The toxin-induced retinal inflammation might explain the early modifications to retina in endophthalmitis, which may help to identify a new treatment strategy or prophylaxis to block retinal modifications and improve visual outcomes.

2. The innate immune response to infections

Microorganism infection is detected by innate pattern recognition receptors (PRRs), which include transmembrane proteins such as Toll-like receptors (TLRs) and C-type lectin receptors (CLRs), cytoplasmic proteins such as retinoic acid-inducible gene (RIG-I)-like receptors (RLRs), and nucleotide oligomerization domain (NOD)-like receptors (NLRs). PRRs in different zones have different functions: transmembrane PRRs are responsible for detecting extracellular pathogen-associated molecular patterns (PAMPs), PRRs in the cytoplasm are usually specific for hydrophobic lipids and proteins, whereas PRRs in endosomes detect nucleic acids, especially viral genomes.[30]
PRRs recognize PAMPs, which are conserved microbial structures or damage-associated molecular patterns released from host cells after injury. PAMPs include the classic molecular patterns such as lipopolysaccharide (LPS) and nucleic acids. Indeed, many microorganisms are sensed by PRRs detecting their genomes or nucleic acids, especially for viral detection[30]. PRRs trigger intracellular signaling, generally myeloid differentiation primary response gene 88 (MyD88)/nuclear factor-κB (NF-κB), or Toll/interleukin-1 receptor (TIR)-domain-containing adapter-inducing interferon-β (TRIF)-dependent signaling, and mitogen-activated protein kinase (MAPK)-p38/Jun signaling pathways, leading to transcriptional expression of inflammatory factors such as proinflammatory cytokines, interferons (IFNs), chemokines, antimicrobial proteins[31].
TLRs recognize bacterial components and induce NF-κB and IFN signaling to produce

proinflammatory cytokines

TLRs are the most prevalent and studied PRRs. TLRs share a common extracellular leucine-rich repeat and a cytoplasmic TIR domain[32]. TLRs 1, 2, 4, 5, and 6 are located on the plasma membrane, whereas TLRs 3, 7, 8, and 9 are endosomal receptors. TLRs are responsible for detecting extracellular and endosomal PAMPs. Activated by PAMPs, TLRs elicit MyD88-dependent NF-κB or TRIF-dependent IFN signaling to produce cytokines or chemokines and IFNs[32] (Figure 1).

RLRs recognize intracellular viral RNA and induce NF-κB and IFN signaling

RLRs recognize 5′-triphosphorylated, uncapped ssRNA, which is a common feature in many viral genomes. However, it is unable to recognize the capped 5′-triphosphorylated ssRNA from the host cell. RIRs include three RNA helicases: retinoic acid-inducible gene I (RIG-I), melanoma differentiation-associated gene 5 (MDA-5), and laboratory of genetics and physiology-2 (LGP-2)[30]. LGP-2 is considered a regulator. After recognizing viral RNA, RIG-I or MDA-5 are activated then interact with adaptor proteins such as mitochondrial antiviral signaling protein (MAVS). MAVS activates the IκB kinase-related kinase and then triggers the TRIF-dependent IFN signaling pathway and the NF-κB signaling pathway[31] (Figure 1).

NLRs recognize intracellular bacterial components and induce NF-κB and MAPK signaling

NLRs are intracellular receptors comprising NOD1 and NOD2, which induce transcriptional upregulation of proinflammatory cytokine genes through the NF-κB and MAPK signaling pathways. NOD1 recognizes the structures of bacterial peptidoglycans; NOD2 recognizes ɣ-D-glutamyl-meso-diaminopimelic acid and muramyl dipeptide. More often, NOD1 and NOD2 crosstalk with other PRRs and regulate the innate immune response[33] (Figure 1).

CLRs recognize microbiological carbohydrates and induce NF-κB and nuclear factor of activated T-cells (NFAT) signaling

CLRs are transmembrane receptors that detect carbohydrates on microorganisms such as viruses, bacteria, and especially fungi. They activate MAPK, NFAT, and NF-κB pathways to produce proinflammatory cytokines[31] (Figure 1).

The expression of PPRs on different cell types and subcellular structures is related to different immune responses[34]. TLR9 ligands, such as dsDNA, are retained in the endosomal vesicles of plasmacytoid dendritic cells (pDCs), while they are rapidly transferred to lysosomal vesicles in conventional dendritic cells. The ability to retain TLR9 ligands in endosomes makes pDCs have a more robust IFN production than conventional dendritic cells[35]. High level of TLRs 2, 4 expressions is observed on macrophages, which produce mainly cytokines. Whereas TLRs7, 9 are mainly expressed on pDCs, which are responsible to produce cytokines and type I IFNs (IFN-α and IFN-β)[32].

3. Neurogenic inflammation

Neurogenic inflammation occurs after the activation of peripheral sensory neuron terminals by various physical or molecular stimuli, characterized by releasing substance P (SP) and calcitonin gene-related peptide (CGRP) or other biological substances (e.g., glutamate), which interact with neural, immune, and endothelial cells[36]. SP and CGRP are released from small-diameter sensory neurons, which is ultimately dependent on intracellular Ca^{2+} mobilization[37]. The receptors of CGRP and SP are expressed on endothelial and myeloid cells, and in the peripheral and central nervous systems[38]. CGRP and SP are potent vasodilators that act synergistically. SP acts on postcapillary

venules[39], and CGRP acts on arterioles to produce plasma extravasation and vascular permeability[38]. CGRP is a 37-amino-acid peptide[37]. Many receptors and ion channels can be activated to release CGRP from sensory nerves in response to various factors or conditions such as bradykinin (BK), low pH, capsaicin, nicotine, ouabain, and ischemia[40]. CGRP binds to CGRP1 receptor and incites production of cAMP in endothelial cells[41], resulting in arteriolar vasodilation and increase of blood flow to inflamed tissues[42]. CGRP has diverse immunomodulatory actions when it targets myeloid cells, such as potential anti-inflammatory effect[43]. CGRP colocalizes often with SP in C-fiber nerves in dorsal ganglion neurons and skin. CGRP can be cleaved by protease released from infiltrated mast cells, which is induced by SP[44] (Figure 2).

SP is an 11-amino-acid polypeptide. SP and its receptors are expressed in the peripheral and central nervous system as well as the immune system[45]. During neurogenic inflammation, SP induces cyclooxygenase-2 (Cox-2) expression and stimulates adhesion and infiltration of neutrophils to vein endothelial cells[46-47], resulting in vein gap formation and plasma extravasation. After binding to its receptors, SP stimulates the NF-κB signaling pathway, which produces IL-8 in human astrocytoma cells[48] and modulates maturation and responsiveness of immune cells[49]. CGRP and SP release into tissue may cause edema and neutrophil infiltration. Antagonists of the CGRP1 receptor ($CGRP_{8–37}$) and SP receptors (RP67580) attenuate this edema[50]. SP binds to neurokinin1 (NK1) receptor on the cytoplasmic membrane and is internalized with the NK1 receptor and transported to endosomes. This internalization reduces the number of NK1 receptors on the cell surface, and SP is intracellularly degraded. This desensitization of SP is effective in limiting SP action[39]. SP can also be degraded by extracellular enzymes. The extracellular proteolysis of SP limits the concentration and effect of SP[51] (Figure 2).

Glutamate is a possible direct factor of neurogenic inflammation. Glutamate is a classical excitatory neurotransmitter and can be toxic when released in excess. Glutamate binds the *N*-methyl-D-aspartate receptor (NMDAR) and induces calcium influx, triggering calcium-dependent proteins and signaling cascades that could promote neural death or survival. This dual effect is due to distinct NMDAR subpopulations, which are mediated by the concentration of glutamate. Some NMDARs bind to death signaling proteins, which could be activated by high concentration of glutamate to produce noxious substance such as the nitric oxide[52].

During neurogenic inflammation, the direct factors (SP, CGRP, and possible glutamate), exert the principal effects, namely, vasoactive action and immunomodulation[36]. Other neuropeptides, such as BK and neurotrophic factors, act as transmitters to enhance the release and the action of direct neurogenic factors. They initiate the transduction cascades and increase the influx of calcium and protein phosphorylation, resulting in neural hypersensitivity and release of direct neurogenic factors [53-54].

Peripheral neurons, especially nociceptor neurons, could detect numerous noxious stimuli (serotonin, endothelin, histamine, BK, ATP, TNF-α, and interleukin) through various receptors (G protein–coupled receptors (GPCR), receptor tyrosine kinases, and TNFR family) or ion (Na^+, K^+, and Ca^{2+}) channels[36]. The cAMP and PKC signaling pathways are the main cellular mechanisms that regulate neuronal inflammatory reactions. The MAPK pathway can also participate in regulating neuronal inflammation[36]. Cytokines, prostaglandins, nitric oxide, opioids, and adrenergic substances are produced by primary afferent nociceptors after being triggered by neuropeptides[55] (Figures 2 and 3).

4. The interaction between the innate immune response and

neurogenic inflammation

The innate immune response and neurogenic inflammation interact tightly. Immune cells and neurons share many pathogen recognition receptors, such as transient receptor potential ion channels[56] and TLRs 3, 4, 7, and 9[57-58]. The neurotransmitters released from neurons not only activate vasculature but also initiate immune cells[59]. Neuropeptides can activate immune cells to secrete cytokines and chemokines. For example, SP stimulates mast cells to release TNF-α[60]. Anatomically, CGRP is closely associated with Langerhans cells; CGRP could inhibit the antigen presentation of Langerhans cells[61]. CGRP influences immune responses through mediating Th1 and Th2 cells, and upregulates IL-4 production from T cells[62]. Cytokines play an important role in communication between neurons and innate immune cells. IL-1β induces Cox-2 and prostanoid release in neurons[63]. The disturbance of neuron–immune mediation could cause autoimmune and allergic diseases[58].

5. Pathogen components can directly interact with neurons

Nociceptor neurons possess some PPRs as immune cells, and also present other stimulus receptor-related detection systems such as GPCRs and ligand-gated ions channels[64-65], through which bacterial pathogens can bind to neuronal cells and incite neuronal depolarization, leading to rapid calcium mobilization and CGRP release[66].

Bacterial formyl peptides and α-hemolysin, substances of *S. aureus*, bind to their receptors, formyl peptide receptors and a disintegrin and metalloprotease 10, respectively, leading to calcium mobilization and depolarization of isolated nociceptors. Neuropeptides (CGRP, galanin, and somatostatin) are released from purified nociceptors following heat-killed *S. aureus* stimulation[67]. Neuropeptides induce the vasodilation and capillary permeability in neurogenic inflammation. They can modulate directly innate immune response. CGRP decreases TNF-α production from macrophages and suppresses the lymphadenopathy during *S. aureus* infection. This immune modulation of neuropeptides occurs later than the acute vascular action of neuropeptides[67]. T2R38, a test receptor expressed in bitter sensory neurons, can be directly stimulated by *Pseudomonas aeruginosa* and undergo calcium-dependent nitric oxide production, contributing to antimicrobial effects[68]. Leukotoxins secreted by *S. aureus*, HlgC/HlgB and PVL, activate calcium mobilization and glutamate release from primary sensory neurons and cerebellar granular neurons[69]. In PVL-injection endophthalmitis, PVL colocalizes with retinal ganglion cells which express PVL-specific receptor, C5aR, resulting in glial cell activation and increase of IL-6 expression[28] (Table 1).

The neural circuits could maintain immune system homeostasis during bacterial infection through modulating the system of acetylcholine-α7 nicotinic acetylcholine receptor (α7 nAChR). The sensory neurons detect injury or infection and send information to central neurons. The central neurons produce and send neural circuits through the vagus nerve to the spleen or other immune organs in which acetylcholine-producing T cells are incited to release acetylcholine[70,27]. Acetylcholine binds to α7 nAChR on immune cells and triggers anti-inflammatory pathway and regulation of cytokine release from innate immune cells (Figure 3)[71]. In nematodes, neural circuits regulate the innate immune system to maintain homeostasis and promote the survival after being infected by pathogens[72]. The neural circuits and neuropeptides can also modulate the immune reactions of lymph nodes[73,74,67](Figure 3).

Bacteria or their components can directly activate peripheral sensory neurons and induce neuron-

mediated inflammation. Indeed, in the first phase of neural inflammation, bacteria trigger neural circuits and/or neurogenic inflammation, resulting in vasodilation and vascular permeability; then, during the second phase, immune cells infiltrate and produce cytokines to eliminate the pathogens. On one hand, the neurotransmitters promote the infiltration of immune cells. On the other hand, they modulate the amplitude of innate immune response in the second phase (Figure 3).

6. Bacterial toxin might aggravate endophthalmitis by neuron-mediated inflammation

The retina expresses neuropeptides and PPRs

The retina expresses neuropeptides and their receptors, the molecular bases for neurogenic inflammation. Neuropeptides (CGRP, neuropeptide Y, vasoactive intestinal peptide, and SP) are present in the adventitia and perivascular space within the optical nerve in monkey and rat, where the CGRP and SP immunoreactivities are fully colocalized[75]. SP immunoreactivity is evidently expressed in displaced amacrine and ganglion cells in rabbit and rat retina[76-78]. CGRP and its receptors immunoreactivities are detected on the nerve fiber layer, ganglion cell layer, and inner nuclear cell layer[79].

Retinal ganglion cells and amacrine cells are the main cells that express SP, CGRP, and other neuropeptides. Their nerve processes are localized in the inner plexiform layer, where the retinal vasculature is dense[78]. This anatomical colocalization of vessels and neuropeptides may contribute to regulation of the retinal circulation[75].

The retina also expresses PRRs. Müller cells express TLRs 1–10 and NLRs, which recognize pathogens. TLRs agonists or pathogens (*S. aureus*, *P. aeruginosa*, and *Candida albicans*) activate Müller cells to produce proinflammatory cytokines (TNF-α, IL-1β, IL-6, and IL-8) and nitric oxide[80]. Mouse cone photoreceptor lines express functional TLRs 1–9 and respond to pathogen stimuli. Primary photoreceptor is identified to express TLR4[81-82]. Microglial cells express TLRs 2–4 that play an important role in recognizing pathogens and neural inflammatory reaction[83].

The steroid is controversial for bacterial endophthalmitis and useless for toxin inducing endophthalmitis

The efficient treatment for bacterial endophthalmitis is consisted by anti-infection and anti-inflammation. However, the usage of steroid as anti-inflammation in bacterial endophthalmitis is controversial[84]. The bacterial endophthalmitis treated by steroid adjunct to antibiotic has good outcomes than those treated by antibiotic alone, but it is uncertain the effects of steroid on the resolution of endophthalmitis and harms to eye[85]. The major concern to use steroid is that steroid could suppress the immune response to eliminate bacteria, resulting in aggravating the infection[84, 86].

The effects of steroid on bacterial endophthalmitis is dependent on the early timing of administration, varying according to the virulence of bacteria[84]. Some studies showed that early (less than 24 h) intravitreal injection of antibiotic concomitant steroid results in good outcomes, even for the virulent bacterial strains, such as *S. aureus, B. cereus*[87-89]. The intravitreal injection of steroid concomitant with antibiotic before 5 h incidence of infection is efficient to control experimentally induced *Pseudomonas* endophthalmitis. While the same treatment is given after 10 h incidence of infection, the retina is destroyed even though the infection is controlled[90]. When the intravitreal dexamethasone with antibiotic is administrated 24 h after intravitreal injection of *S. epidermidis*,

the treatment could decrease the intraocular inflammation[91-92]. When dexamethasone with antibiotic is given at 48 h after intravitreal injection of *S. epidermidis*, the treatment does not reduce the intraocular inflammation even though the infection is controlled[91].

Steroid is not useful for endophthalmitis caused by toxin expressing stains[84]. The antibiotic and steroid administrated 1 day after the infection do not improve endophthalmitis caused by *enterococcus faecalis* toxin expressing strains, while the endophthalmitis caused by *E. faecalis* non-toxin expression strains responded well to those treatment[86]. In *B. cereus* exotoxins inducing endophthalmitis, the concomitant injections of dexamethasone with antibiotic could not attenuate the retinal necrosis and inflammation[93]. Steroid bind to its receptor, which could suppress multiple inflammatory transductions, such as MAPK, NF-κB and activator protein-1[94]. Bacterial toxin induces retinal inflammation as early as 4 h[28, 93], probably by the mechanism of neuron mediated-inflammation, which is dependent on the rapid calcium mobilization and might not be influenced by steroid anti-inflammatory effects.

The retina expresses TLRs, SP, and CGRP proteins in the optical nerve and inner layers of the retina. We deduce that bacterial toxins could rapidly interact with neurons through their specific receptor(s) to release neurotransmitters, resulting in vascular excavation and breakdown of the blood–retinal barrier during the early stages of bacterial endophthalmitis. Retinal inflammation is amplified by innate immune cell infiltration and the retinal glial cell activation. Irreversible retinal damage result in poor visual prognosis, despite efficient antibiotic treatment.

Conclusions

Bacterial pathogens may interact directly with neurons to produce neuropeptides, neural circuits and innate immune response. Neuropeptides and neural circuits modulate the following innate immune response. The retina expresses a variety of receptors and neuropeptides, presenting the possibility for neuron-mediated inflammation. We deduce that bacterial toxins induce neurogenic inflammation and subsequently innate immune response during bacterial endophthalmitis. To improve the prognosis of bacterial endophthalmitis, the bacteria must be eliminated and, additionally, the bacterial toxins must also be blocked to cause the early inflammatory processes.

Acknowledgments: This work was supported by a recurrent research EA7290 award from the University of Strasbourg and a grant from Novartis. LIU Xuanli was awarded by the Chinese Scholarship Council.

Potential conflicts of interest: None

References

1. Callegan, M. C.; Engelbert, M.; Parke, D. W., 2nd; Jett, B. D.; Gilmore, M. S., Bacterial endophthalmitis: epidemiology, therapeutics, and bacterium-host interactions. *Clinical Microbiology Reviews* **2002,** *15* (1), 111-24.

2. GROUP, T. E. V. S., Microbiologic factors and visual outcome in the endophthalmitis vitrectomy study. *Am J Ophthalmol* **1996,** *122* (6), 830-46.

3. Gower, E. W.; Keay, L. J.; Stare, D. E.; Arora, P.; Cassard, S. D.; Behrens, A.; Tielsch, J. M.; Schein, O. D., Characteristics of Endophthalmitis after Cataract Surgery in the United States Medicare Population. *Ophthalmology* **2015,** *122* (8), 1625-32.

4. Lu, X.; Ng, D. S.-C.; Zheng, K.; Peng, K.; Jin, C.; Xia, H.; Chen, W.; Chen, H., Risk factors for

endophthalmitis requiring evisceration or enucleation. *Scientific Reports* **2016,** *6*, 28100.
5. Durand, M. L., Bacterial endophthalmitis. *Current Infectious Disease Reports* **2009,** *11* (4), 283-8.
6. Callegan, M. C.; Gilmore, M. S.; Gregory, M.; Ramadan, R. T.; Wiskur, B. J.; Moyer, A. L.; Hunt, J. J.; Novosad, B. D., Bacterial endophthalmitis: therapeutic challenges and host-pathogen interactions. *Progress in Retinal and Eye Research* **2007,** *26* (2), 189-203.
7. Ormerod, L. D.; Ho, D. D.; Becker, L. E.; Cruise, R. J.; Grohar, H. I.; Paton, B. G.; Frederick, A. R., Jr.; Topping, T. M.; Weiter, J. J.; Buzney, S. M.; et al., Endophthalmitis caused by the coagulase-negative *staphylococci*. 1. Disease spectrum and outcome. *Ophthalmology* **1993,** *100* (5), 715-23.
8. Fanny Vincenota, M. S., GillesPrévost, Les facteurs de virulence de *Staphylococcus aureus*. *Revue Francophone des Laboratoires* **2008,** *2008* (407), 61-69.
9. Otto, M., Coagulase-negative *staphylococci* as reservoirs of genes facilitating MRSA infection: Staphylococcal commensal species such as *Staphylococcus epidermidis* are being recognized as important sources of genes promoting MRSA colonization and virulence. *BioEssays : News and Reviews in Molecular, Cellular and Developmental Biology* **2013,** *35* (1), 4-11.
10. Nanoukon, C.; Argemi, X.; Sogbo, F.; Orekan, J.; Keller, D.; Affolabi, D.; Schramm, F.; Riegel, P.; Baba-Moussa, L.; Prevost, G., Pathogenic features of clinically significant coagulase-negative *staphylococci* in hospital and community infections in Benin. *International Journal of Medical Microbiology : IJMM* **2017,** *307* (1), 75-82.
11. Laabei, M.; Uhlemann, A. C.; Lowy, F. D.; Austin, E. D.; Yokoyama, M.; Ouadi, K.; Feil, E.; Thorpe, H. A.; Williams, B.; Perkins, M.; Peacock, S. J.; Clarke, S. R.; Dordel, J.; Holden, M.; Votintseva, A. A.; Bowden, R.; Crook, D. W.; Young, B. C.; Wilson, D. J.; Recker, M.; Massey, R. C., Evolutionary Trade-Offs Underlie the Multi-faceted Virulence of *Staphylococcus aureus*. *PLoS Biology* **2015,** *13* (9), e1002229.
12. Peacock, S. J.; Moore, C. E.; Justice, A.; Kantzanou, M.; Story, L.; Mackie, K.; O'Neill, G.; Day, N. P., Virulent combinations of adhesin and toxin genes in natural populations of *Staphylococcus aureus*. *Infection and Immunity* **2002,** *70* (9), 4987-96.
13. Lin, M.; Zhang, W.; Liu, Y.; Wang, L.; Ding, Y.; Wu, X.; Shi, Y.; Sun, L.; Li, Y., Nosocomial acute-onset postoperative endophthalmitis at a university teaching hospital in China. *J. Hosp. Infect.* **2011,** *79* (4), 323-327.
14. Chiquet, C.; Maurin, M.; Altayrac, J.; Aptel, F.; Boisset, S.; Vandenesch, F.; Cornut, P. L.; Romanet, J. P.; Gain, P.; Carricajo, A., Correlation between clinical data and antibiotic resistance in coagulase-negative *Staphylococcus* species isolated from 68 patients with acute post-cataract endophthalmitis. *Clin Microbiol Infect* **2015,** *21* (6), 592 e1-8.
15. Fernandez, M. D.; Villegas, V. M.; Oliver, A. L., Vitreous Cultures and Antibiotic Analysis in Puerto Rican Endophthalmitis Patients. *P. R. Health Sci. J.* **2011,** *30* (4), 198-202.
16. Bannerman, T. L.; Rhoden, D. L.; McAllister, S. K.; Miller, J. M.; Wilson, L. A., The source of coagulase-negative *staphylococci* in the Endophthalmitis Vitrectomy Study. A comparison of eyelid and intraocular isolates using pulsed-field gel electrophoresis. *Archives of Ophthalmology (Chicago, Ill. : 1960)* **1997,** *115* (3), 357-61.
17. Combey de Lambert, A.; Campolmi, N.; Cornut, P. L.; Aptel, F.; Creuzot-Garcher, C.; Chiquet, C., Baseline factors predictive of visual prognosis in acute postoperative bacterial endophthalmitis in patients undergoing cataract surgery. *JAMA Ophthalmology* **2013,** *131* (9), 1159-66.
18. Jena, S.; Panda, S.; Nayak, K. C.; Singh, D. V., Identification of Major Sequence Types among

Multidrug-Resistant *Staphylococcus epidermidis* Strains Isolated from Infected Eyes and Healthy Conjunctiva. *Frontiers in Microbiology* **2017,** *8*, 1430.
19. Shirodkar, A. R.; Flynn, H. W.; Alliman, K.; Lalwani, G. A.; Alabiad, C.; Moshfeghi, A. A.; Miller, D., The comparison of clinical outcomes of endophthalmitis from fluoroquinolone-resistant and susceptible bacteria. *Clinical Ophthalmology (Auckland, N.Z.)* **2010,** *4*, 211-4.
20. Nayak, N., Biofilm: The Haven for *Staphylococcus epidermidis* in Post-operative Endophthalmitis. *Journal of Clinical & Experimental Ophthalmology* **2014,** *05* (04).
21. Flores-Paez, L. A.; Zenteno, J. C.; Alcantar-Curiel, M. D.; Vargas-Mendoza, C. F.; Rodriguez-Martinez, S.; Cancino-Diaz, M. E.; Jan-Roblero, J.; Cancino-Diaz, J. C., Molecular and Phenotypic Characterization of *Staphylococcus epidermidis* Isolates from Healthy Conjunctiva and a Comparative Analysis with Isolates from Ocular Infection. *PloS One* **2015,** *10* (8), e0135964.
22. Duggirala, A.; Kenchappa, P.; Sharma, S.; Peeters, J. K.; Ahmed, N.; Garg, P.; Das, T.; Hasnain, S. E., High-resolution genome profiling differentiated *Staphylococcus epidermidis* isolated from patients with ocular infections and normal individuals. *Investigative Ophthalmology & Visual Science* **2007,** *48* (7), 3239-3245.
23. Mehlin, C.; Headley, C. M.; Klebanoff, S. J., An inflammatory polypeptide complex from *Staphylococcus epidermidis*: isolation and characterization. *The Journal of Experimental Medicine* **1999,** *189* (6), 907-18.
24. Prévost, G., Toxins in *Staphylococcus aureus* Pathogenesis. *Microbial Toxins: Molecular and Cellular Biology* (Chapter 10), 243-283.
25. Laventie, B. J.; Potrich, C.; Atmanene, C.; Saleh, M.; Joubert, O.; Viero, G.; Bachmeyer, C.; Antonini, V.; Mancini, I.; Cianferani-Sanglier, S.; Keller, D.; Colin, D. A.; Bourcier, T.; Anderluh, G.; van Dorsselaer, A.; Dalla Serra, M.; Prevost, G., p-Sulfonato-calix[n]arenes inhibit staphylococcal bicomponent leukotoxins by supramolecular interactions. *The Biochemical Journal* **2013,** *450* (3), 559-71.
26. Laventie, B. J.; Rademaker, H. J.; Saleh, M.; de Boer, E.; Janssens, R.; Bourcier, T.; Subilia, A.; Marcellin, L.; van Haperen, R.; Lebbink, J. H.; Chen, T.; Prevost, G.; Grosveld, F.; Drabek, D., Heavy chain-only antibodies and tetravalent bispecific antibody neutralizing *Staphylococcus aureus* leukotoxins. *Proceedings of the National Academy of Sciences of the United States of America* **2011,** *108* (39), 16404-9.
27. Siqueira, J. A.; Speeg-Schatz, C.; Freitas, F. I.; Sahel, J.; Monteil, H.; Prevost, G., Channel-forming leucotoxins from *Staphylococcus aureus* cause severe inflammatory reactions in a rabbit eye model. *Journal of Medical Microbiology* **1997,** *46* (6), 486-94.
28. Liu, X.; Heitz, P.; Roux, M.; Keller, D.; Bourcier, T.; Sauer, A.; Prevost, G.; Gaucher, D., Panton-Valentine Leukocidin Colocalizes with Retinal Ganglion and Amacrine Cells and Activates Glial Reactions and Microglial Apoptosis. *Scientific Reports* **2018,** *8* (1), 2953.
29. Francke, M.; Faude, F.; Pannicke, T.; Bringmann, A.; Eckstein, P.; Reichelt, W.; Wiedemann, P.; Reichenbach, A., Electrophysiology of rabbit Muller (glial) cells in experimental retinal detachment and PVR. *Investigative Ophthalmology & Visual Science* **2001,** *42* (5), 1072-9.
30. Thompson, M. R.; Kaminski, J. J. Kurt-Jones, E. A.; Fitzgerald, K. A., Pattern recognition receptors and the innate immune response to viral infection. *Viruses* **2011,** *3* (6), 920-40.
31. Takeuchi, O.; Akira, S., Pattern recognition receptors and inflammation. *Cell* **2010,** *140* (6), 805-20.
32. Kaisho, T.; Akira, S., Toll-like receptor function and signaling. *J Allergy Clin Immunol* **2006,**

117 (5), 979-87; quiz 988.
33. Franchi, L.; Warner, N.; Viani, K.; Nunez, G., Function of Nod-like receptors in microbial recognition and host defense. *Immunological Reviews* **2009,** *227* (1), 106-28.
34. Begon, E.; Michel, L.; Flageul, B.; Beaudoin, I.; Jean-Louis, F.; Bachelez, H.; Dubertret, L.; Musette, P., Expression, subcellular localization and cytokinic modulation of Toll-like receptors (TLRs) in normal human keratinocytes: TLR2 up-regulation in psoriatic skin. *European Journal of Dermatology : EJD* **2007,** *17* (6), 497-506.
35. Honda, K.; Ohba, Y.; Yanai, H.; Negishi, H.; Mizutani, T.; Takaoka, A.; Taya, C.; Taniguchi, T., Spatiotemporal regulation of MyD88-IRF-7 signalling for robust type-I interferon induction. *Nature* **2005,** *434* (7036), 1035-40.
36. Richardson, J. D.; Vasko, M. R., Cellular mechanisms of neurogenic inflammation. *The Journal of Pharmacology and Experimental Therapeutics* **2002,** *302* (3), 839-45.
37. Meng, J.; Wang, J.; Lawrence, G.; Dolly, J. O., Synaptobrevin I mediates exocytosis of CGRP from sensory neurons and inhibition by botulinum toxins reflects their anti-nociceptive potential. *Journal of Cell Science* **2007,** *120* (Pt 16), 2864-74.
38. Supowit, S. C.; Ethridge, R. T.; Zhao, H.; Katki, K. A.; Dipette, D. J., Calcitonin gene-related peptide and substance P contribute to reduced blood pressure in sympathectomized rats. *Am J Physiol Heart Circ Physiol* **2005,** *289* (3), H1169-75.
39. Bowden, J. J.; Garland, A. M.; Baluk, P.; Lefevre, P.; Grady, E. F.; Vigna, S. R.; Bunnett, N. W.; McDonald, D. M., Direct observation of substance P-induced internalization of neurokinin 1 (NK1) receptors at sites of inflammation. *Proceedings of the National Academy of Sciences of the United States of America* **1994,** *91* (19), 8964-8.
40. Russell, F. A.; King, R.; Smillie, S. J.; Kodji, X.; Brain, S. D., Calcitonin gene-related peptide: physiology and pathophysiology. *Physiological Reviews* **2014,** *94* (4), 1099-142.
41. Hong, K. W.; Yoo, S. E.; Yu, S. S.; Lee, J. Y.; Rhim, B. Y., Pharmacological coupling and functional role for CGRP receptors in the vasodilation of rat pial arterioles. *The American Journal of Physiology* **1996,** *270* (1 Pt 2), H317-23.
42. Brain, S. D.; Williams, T. J.; Tippins, J. R.; Morris, H. R.; MacIntyre, I., Calcitonin gene-related peptide is a potent vasodilator. *Nature* **1985,** *313* (5997), 54-6.
43. Springer, J.; Geppetti, P.; Fischer, A.; Groneberg, D. A., Calcitonin gene-related peptide as inflammatory mediator. *Pulmonary Pharmacology & Therapeutics* **2003,** *16* (3), 121-30.
44. Brain, S. D.; Williams, T. J., Substance P regulates the vasodilator activity of calcitonin gene-related peptide. *Nature* **1988,** *335*, 73.
45. Douglas, S. D.; Leeman, S. E., Neurokinin-1 receptor: functional significance in the immune system in reference to selected infections and inflammation. *Annals of the New York Academy of Sciences* **2011,** *1217*, 83-95.
46. Dianzani, C.; Collino, M.; Lombardi, G.; Garbarino, G.; Fantozzi, R., Substance P increases neutrophil adhesion to human umbilical vein endothelial cells. *British Journal of Pharmacology* **2003,** *139* (6), 1103-10.
47. Gallicchio, M.; Rosa, A. C.; Benetti, E.; Collino, M.; Dianzani, C.; Fantozzi, R., Substance P-induced cyclooxygenase-2 expression in human umbilical vein endothelial cells. *British Journal of Pharmacology* **2006,** *147* (6), 681-9.
48. Lieb, K.; Fiebich, B. L.; Berger, M.; Bauer, J.; Schulze-Osthoff, K., The neuropeptide substance P activates transcription factor NF-kappa B and kappa B-dependent gene expression in human

astrocytoma cells. *Journal of Immunology* **1997,** *159* (10), 4952-8.
49. Bost, K. L., Tachykinin-mediated modulation of the immune response. *Frontiers in Bioscience : a Journal and Virtual Library* **2004,** *9*, 3331-2.
50. Steinhoff M, V. N., Young SH, Tognetto M, Amadesi S, Ennes HS, Trevisani M, Hollenberg MD, Wallace JL, Caughey GH, Mitchell SE, Williams LM, Geppetti P, Mayer EA, Bunnett NW, Agonists of proteinase-activated receptor 2 induce inflammation by a neurogenic mechanism. *Nature Medicine* **2000,** *6(2)*, 151-8.
51. Mitchell, A. J.; Lone, A. M.; Tinoco, A. D.; Saghatelian, A., Proteolysis controls endogenous substance P levels. *PloS One* **2013,** *8* (7), e68638.
52. Lai, T. W.; Zhang, S.; Wang, Y. T., Excitotoxicity and stroke: identifying novel targets for neuroprotection. *Progress in Neurobiology* **2014,** *115*, 157-88.
53. Vasko, M. R.; Campbell, W. B.; Waite, K. J., Prostaglandin E2 enhances bradykinin-stimulated release of neuropeptides from rat sensory neurons in culture. *The Journal of Neuroscience : the Official Journal of the Society for Neuroscience* **1994,** *14* (8), 4987-97.
54. Delafoy, L.; Gelot, A.; Ardid, D.; Eschalier, A.; Bertrand, C.; Doherty, A. M.; Diop, L., Interactive involvement of brain derived neurotrophic factor, nerve growth factor, and calcitonin gene related peptide in colonic hypersensitivity in the rat. *Gut* **2006,** *55* (7), 940-5.
55. Levine, J. D.; Fields, H. L.; Basbaum, A. I., Peptides and the primary afferent nociceptor. *The Journal of neuroscience : the official journal of the Society for Neuroscience* **1993,** *13* (6), 2273-86.
56. Link, T. M.; Park, U.; Vonakis, B. M.; Raben, D. M.; Soloski, M. J.; Caterina, M. J., TRPV2 has a pivotal role in macrophage particle binding and phagocytosis. *Nature Immunology* **2010,** *11* (3), 232-9.
57. Liu, T.; Xu, Z. Z.; Park, C. K.; Berta, T.; Ji, R. R., Toll-like receptor 7 mediates pruritus. *Nature Neuroscience* **2010,** *13* (12), 1460-2.
58. Chiu, I. M.; von Hehn, C. A.; Woolf, C. J., Neurogenic inflammation and the peripheral nervous system in host defense and immunopathology. *Nature Neuroscience* **2012,** *15* (8), 1063-7.
59. Levite, M., Neurotransmitters activate T-cells and elicit crucial functions via neurotransmitter receptors. *Current Opinion in Pharmacology* **2008,** *8* (4), 460-71.
60. Ansel, J. C.; Brown, J. R.; Payan, D. G.; Brown, M. A., Substance P selectively activates TNF-alpha gene expression in murine mast cells. *Journal of Immunology* **1993,** *150* (10), 4478-85.
61. Hosoi, J.; Murphy, G. F.; Egan, C. L.; Lerner, E. A.; Grabbe, S.; Asahina, A.; Granstein, R. D., Regulation of Langerhans cell function by nerves containing calcitonin gene-related peptide. *Nature* **1993,** *363* (6425), 159-63.
62. Mikami, N.; Matsushita, H.; Kato, T.; Kawasaki, R.; Sawazaki, T.; Kishimoto, T.; Ogitani, Y.; Watanabe, K.; Miyagi, Y.; Sueda, K.; Fukada, S.; Yamamoto, H.; Tsujikawa, K., Calcitonin gene-related peptide is an important regulator of cutaneous immunity: effect on dendritic cell and T cell functions. *Journal of Immunology* **2011,** *186* (12), 6886-93.
63. Samad, T. A.; Moore, K. A.; Sapirstein, A.; Billet, S.; Allchorne, A.; Poole, S.; Bonventre, J. V.; Woolf, C. J., Interleukin-1beta-mediated induction of Cox-2 in the CNS contributes to inflammatory pain hypersensitivity. *Nature* **2001,** *410* (6827), 471-5.
64. Geppetti, P.; Veldhuis, N. A.; Lieu, T.; Bunnett, N. W., G Protein-Coupled Receptors: Dynamic Machines for Signaling Pain and Itch. *Neuron* **2015,** *88* (4), 635-49.
65. Sheng, M.; Pak, D. T. S., Ligand-Gated Ion Channel Interactions with Cytoskeletal and

Signaling Proteins. *Annual Review of Physiology* **2000,** *62* (1), 755-778.
66. Wang, L. H. a. X., PKC and PKA, But Not PKG Mediate LPS Induced CGRP Release and [Ca2+]i elevation in DRG neurons of neonatal rats. *Journal of Neuroscience Research* **2001,** *66* (415 November 2001), 592-600.
67. Chiu, I. M.; Heesters, B. A.; Ghasemlou, N.; Von Hehn, C. A.; Zhao, F.; Tran, J.; Wainger, B.; Strominger, A.; Muralidharan, S.; Horswill, A. R.; Bubeck Wardenburg, J.; Hwang, S. W.; Carroll, M. C.; Woolf, C. J., Bacteria activate sensory neurons that modulate pain and inflammation. *Nature* **2013,** *501* (7465), 52-7.
68. Lee, R. J.; Xiong, G.; Kofonow, J. M.; Chen, B.; Lysenko, A.; Jiang, P.; Abraham, V.; Doghramji, L.; Adappa, N. D.; Palmer, J. N.; Kennedy, D. W.; Beauchamp, G. K.; Doulias, P. T.; Ischiropoulos, H.; Kreindler, J. L.; Reed, D. R.; Cohen, N. A., T2R38 taste receptor polymorphisms underlie susceptibility to upper respiratory infection. *The Journal of Clinical Investigation* **2012,** *122* (11), 4145-59.
69. Jover, E.; Tawk, M. Y.; Laventie, B. J.; Poulain, B.; Prevost, G., Staphylococcal leukotoxins trigger free intracellular Ca(2+) rise in neurones, signalling through acidic stores and activation of store-operated channels. *Cellular Microbiology* **2013,** *15* (5), 742-58.
70. Rosas-Ballina, M.; Olofsson, P. S.; Ochani, M.; Valdes-Ferrer, S. I.; Levine, Y. A.; Reardon, C.; Tusche, M. W.; Pavlov, V. A.; Andersson, U.; Chavan, S.; Mak, T. W.; Tracey, K. J., Acetylcholine-synthesizing T cells relay neural signals in a vagus nerve circuit. *Science* **2011,** *334* (6052), 98-101.
71. Andersson, U.; Tracey, K. J., Reflex principles of immunological homeostasis. *Annual Review of Immunology* **2012,** *30*, 313-35.
72. Sun, J.; Singh, V.; Kajino-Sakamoto, R.; Aballay, A., Neuronal GPCR controls innate immunity by regulating noncanonical unfolded protein response genes. *Science* **2011,** *332* (6030), 729-32.
73. Weihe, E.; Nohr, D.; Michel, S.; Muller, S.; Zentel, H. J.; Fink, T.; Krekel, J., Molecular anatomy of the neuro-immune connection. *The International Journal of Neuroscience* **1991,** *59* (1-3), 1-23.
74. Mignini, F.; Streccioni, V.; Amenta, F., Autonomic innervation of immune organs and neuroimmune modulation. *Autonomic & Autacoid Pharmacology* **2003,** *23* (1), 1-25.
75. Ye, X. D.; Laties, A. M.; Stone, R. A., Peptidergic innervation of the retinal vasculature and optic nerve head. *Investigative Ophthalmology & Visual Science* **1990,** *31* (9), 1731-7.
76. Brecha, N.; Johnson, D.; Bolz, J.; Sharma, S.; Parnavelas, J. G.; Lieberman, A. R., Substance P-immunoreactive retinal ganglion cells and their central axon terminals in the rabbit. *Nature* **1987,** *327* (6118), 155-8.
77. Fukuda, M.; Kuwayama, Y.; Shiosaka, S.; Ishimoto, I.; Shimizu, Y.; Takagi, H.; Inagaki, S.; Sakanaka, M.; Semba, E.; Takatsuki, K.; Tohyama, M., Demonstration of a substance P-like immunoreactivity in retinal cells of the rat. *Neurosci Lett* **1981,** *23* (3), 239-42.
78. Campbell, J. P.; Zhang, M.; Hwang, T. S.; Bailey, S. T.; Wilson, D. J.; Jia, Y.; Huang, D., Detailed Vascular Anatomy of the Human Retina by Projection-Resolved Optical Coherence Tomography Angiography. *Scientific Reports* **2017,** *7*, 42201.
79. Blixt, F. W.; Radziwon-Balicka, A.; Edvinsson, L.; Warfvinge, K., Distribution of CGRP and its receptor components CLR and RAMP1 in the rat retina. *Experimental Eye Research* **2017,** *161*, 124-131.
80. Kumar, A.; Shamsuddin, N., Retinal Muller glia initiate innate response to infectious stimuli via toll-like receptor signaling. *PloS One* **2012,** *7* (1), e29830.
81. Yi, H.; Patel, A. K.; Sodhi, C. P.; Hackam, D. J.; Hackam, A. S., Novel role for the innate immune

receptor Toll-like receptor 4 (TLR4) in the regulation of the Wnt signaling pathway and photoreceptor apoptosis. *PloS One* **2012,** *7* (5), e36560.
82. Tu, Z.; Portillo, J. A.; Howell, S.; Bu, H.; Subauste, C. S.; Al-Ubaidi, M. R.; Pearlman, E.; Lin, F., Photoreceptor cells constitutively express functional TLR4. *J Neuroimmunol* **2011,** *230* (1-2), 183-7.
83. Facci, L.; Barbierato, M.; Marinelli, C.; Argentini, C.; Skaper, S. D.; Giusti, P., Toll-Like Receptors 2, -3 and -4 Prime Microglia but not Astrocytes Across Central Nervous System Regions for ATP-Dependent Interleukin-1β Release. *Scientific Reports* **2014,** *4*, 6824.
84. Ching Wen Ho, D.; Agarwal, A.; Lee, C. S.; Chhablani, J.; Gupta, V.; Khatri, M.; Nirmal, J.; Pavesio, C.; Agrawal, R., A Review of the Role of Intravitreal Corticosteroids as an Adjuvant to Antibiotics in Infectious Endophthalmitis. *Ocul Immunol Inflamm* **2018,** *26* (3), 461-468.
85. Kim, C. H.; Chen, M. F.; Coleman, A. L., Adjunctive steroid therapy versus antibiotics alone for acute endophthalmitis after intraocular procedure. *The Cochrane Database of Systematic Reviews* **2017,** *2*, Cd012131.
86. Jett, B. D.; Jensen, H. G.; Atkuri, R. V.; Gilmore, M. S., Evaluation of therapeutic measures for treating endophthalmitis caused by isogenic toxin-producing and toxin-nonproducing *Enterococcus faecalis* strains. *Investigative Ophthalmology & Visual Science* **1995,** *36* (1), 9-15.
87. Liu, F.; Kwok, A. K.; Cheung, B. M., The efficacy of intravitreal vancomycin and dexamethasone in the treatment of experimental *bacillus cereus* endophthalmitis. *Curr Eye Res* **2008,** *33* (9), 761-8.
88. Yoshizumi, M. O.; Lee, G. C.; Equi, R. A.; Kim, I. T.; Pitchekian-Halabi, H.; Adamu, S. A.; Mondino, B. J., Timing of dexamethasone treatment in experimental *Staphylococcus aureus* endophthalmitis. *Retina (Philadelphia, Pa.)* **1998,** *18* (2), 130-5.
89. Falk, N. S.; Beer, P. M.; Peters, G. B., 3rd, Role of intravitreal triamcinolone acetonide in the treatment of postoperative endophthalmitis. *Retina (Philadelphia, Pa.)* **2006,** *26* (5), 545-8.
90. Graham, R. O.; Peyman, G. A., Intravitreal injection of dexamethasone. Treatment of experimentally induced endophthalmitis. *Archives of Ophthalmology (Chicago, Ill. : 1960)* **1974,** *92* (2), 149-54.
91. Yildirim, O.; Oz, O.; Aslan, G.; Cinel, L.; Delialioglu, N.; Kanik, A., The efficacy of intravitreal levofloxacin and intravitreal dexamethasone in experimental *Staphylococcus epidermidis* endophthalmitis. *Ophthalmic Res* **2002,** *34* (6), 349-56.
92. Smith, M. A.; Sorenson, J. A.; D'Aversa, G.; Mandelbaum, S.; Udell, I.; Harrison, W., Treatment of experimental methicillin-resistant *Staphylococcus epidermidis* endophthalmitis with intravitreal vancomycin and intravitreal dexamethasone. *The Journal of Infectious Diseases* **1997,** *175* (2), 462-6.
93. Pollack, J. S.; Beecher, D. J.; Pulido, J. S.; Lee Wong, A. C., Failure of intravitreal dexamethasone to diminish inflammation or retinal toxicity in an experimental model of *Bacillus cereus* endophthalmitis. *Curr Eye Res* **2004,** *29* (4-5), 253-9.
94. Barnes, P. J., Corticosteroid effects on cell signalling. *The European Respiratory Journal* **2006,** *27* (2), 413-26.

Table 1. Bacterial pathogens directly act on neurons to cause effects

Pathogen molecules	Receptors	neurons	effects
LPS	TLR4/ CD14	primary dorsal root ganglia neurons	Intracellular Ca^{2+} increase, CGRP release
Formyl peptides	FPRs	isolated nociceptors	Ca^{2+} influx and depolarization of neurons,
α-haemolysin	ADAM10	isolated nociceptors	Ca^{2+} influx and depolarization of neurons,
Heat-killed *S. aureus*		purified nociceptors	Neuropeptides (CGRP, galanin, somastatin) were highly expressed
P. aeruginosa	T2R38	bitter sensory neurons	Calcium-dependent NO production
PVL, HlgC/HlgB		primary sensory nerves from dorsal root ganglia,	Ca^{2+} mobilization, glutamate release
PVL	C5aR	retinal ganglion cells	Retinal glial cells activation, IL-6 expression increase, NO production increase, retinal microglial apoptosis

Abbreviation: LPS, Lipopolysaccharides; TLR4, toll-like receptor 4; CD14, cluster of differentiation 14; FPRs, formyl peptide receptors; ADAM10, a disintegrin and metalloprotease 10; T2R38, taste 2 receptor member 38; NO, nitric oxide; PVL, Panton–Valentine leukocidin; C5aR, C5a receptor.

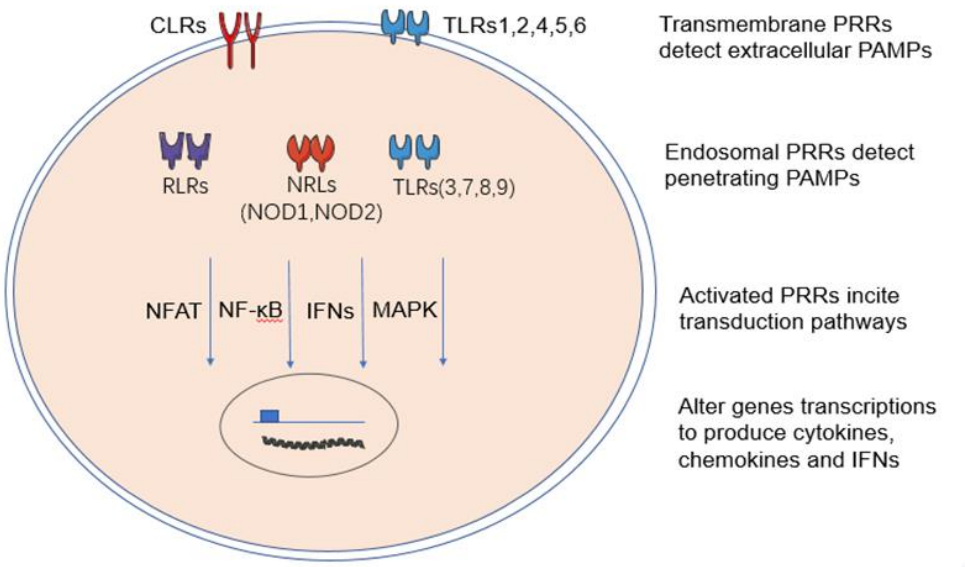

Figure 1: The innate immune system response to infection. The transmembrane PRRs, CLRs and TLR-1, 2, 4 and 5 detect extracellular PAMPs. The endosomal PRRs detect intracellular penetrating PAMPs. After PAMPs interacting PRRs, the transduction pathways are activated, including NF-κB, IFNs, NFAT and MAPK, which could modulate genes transcription and produce inflammatory cytokines, chemokines and IFNs.

Abbreviations: PAMPs, pathogen-associated molecular patterns; PRRs, pattern recognition receptors(PRRs); TLRs, Toll-like receptors (TLRs); CLRs, C-type lectin receptors (CLRs); RLRs, cytoplasmic proteins RIG-I-like receptors (RLRs); NLRs, nucleotide oligomerization domain(NOD)-like receptors(NLRs). NF-κB, nuclear factor kappa-B kinase; IFNs, type I interferons; NFAT, nuclear factor of activated T-cells; MAPK, mitogen-activated protein kinase.

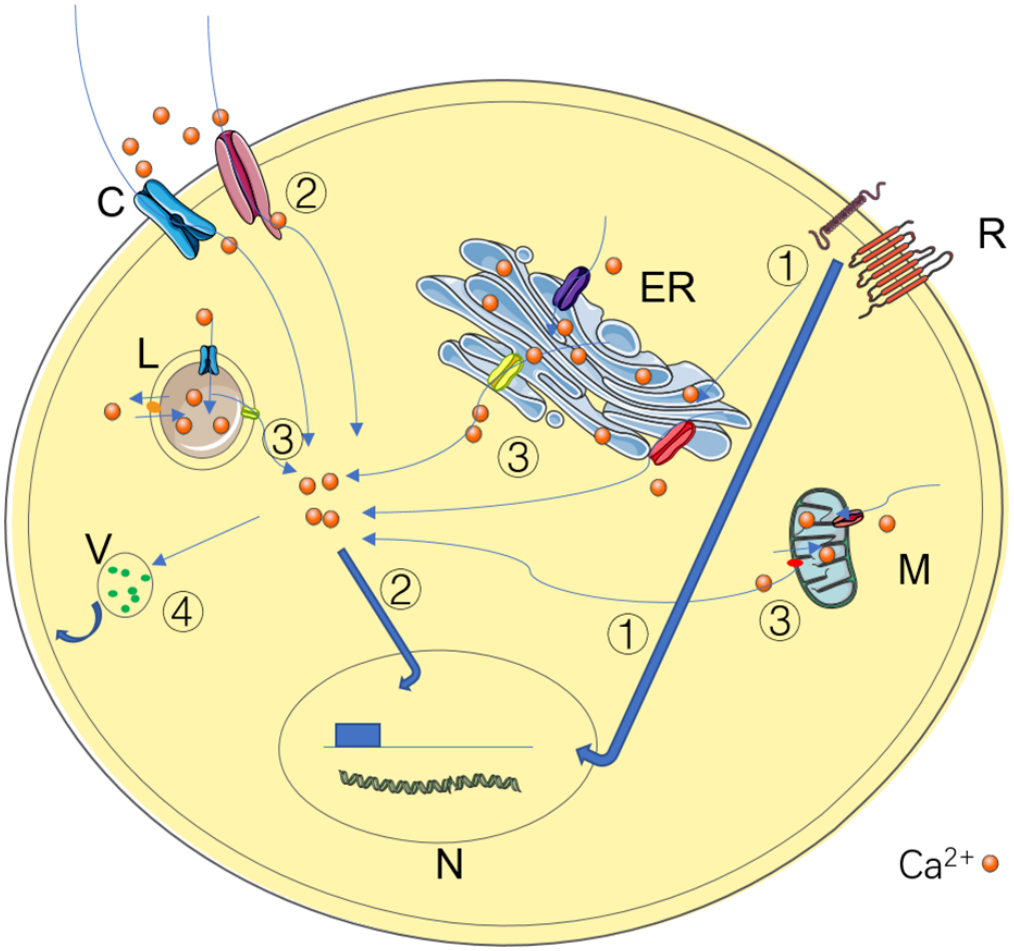

Figure 2: The inflammatory signaling pathways in neurons. The noxious stimuli act through various receptors or ions channels on neurons. 1)The neural transmembrane receptors (CPGR, RTKs, TNFR family) detect noxious stimulus and substances. The cAMP, PKC and MAPK signaling pathways incite intracellular calcium mobilization and alter genes transcriptions to produce endogenous mediators. 2) Other stimulus and substances react directly on neural ions channels, which initiate calcium influx and incite intracellular calcium mobilization. Calcium binding proteins can alter genes transcriptions. 3) Lysosome, endoplasmic reticulum and mitochondria play also great role in mobilizing intracellular calcium. 4) The increase of intracellular calcium could lead to SP and CGRP release from neuronal vesicles.

Abbreviations: R, receptors; RTKs, receptor tyrosine kinases; TNFR, tumor necrosis factor receptors; cAMP, cyclic adenosine monophosphate; PKC, protein kinase C; MAPK, mitogen-activated protein kinase; C, channels; L, lysosome; M, mitochondria; ER, endoplasmic eeticulum; V, vesicle; N, nuclear; SP, substance P; CPGR, G-protein-coupled receptors.

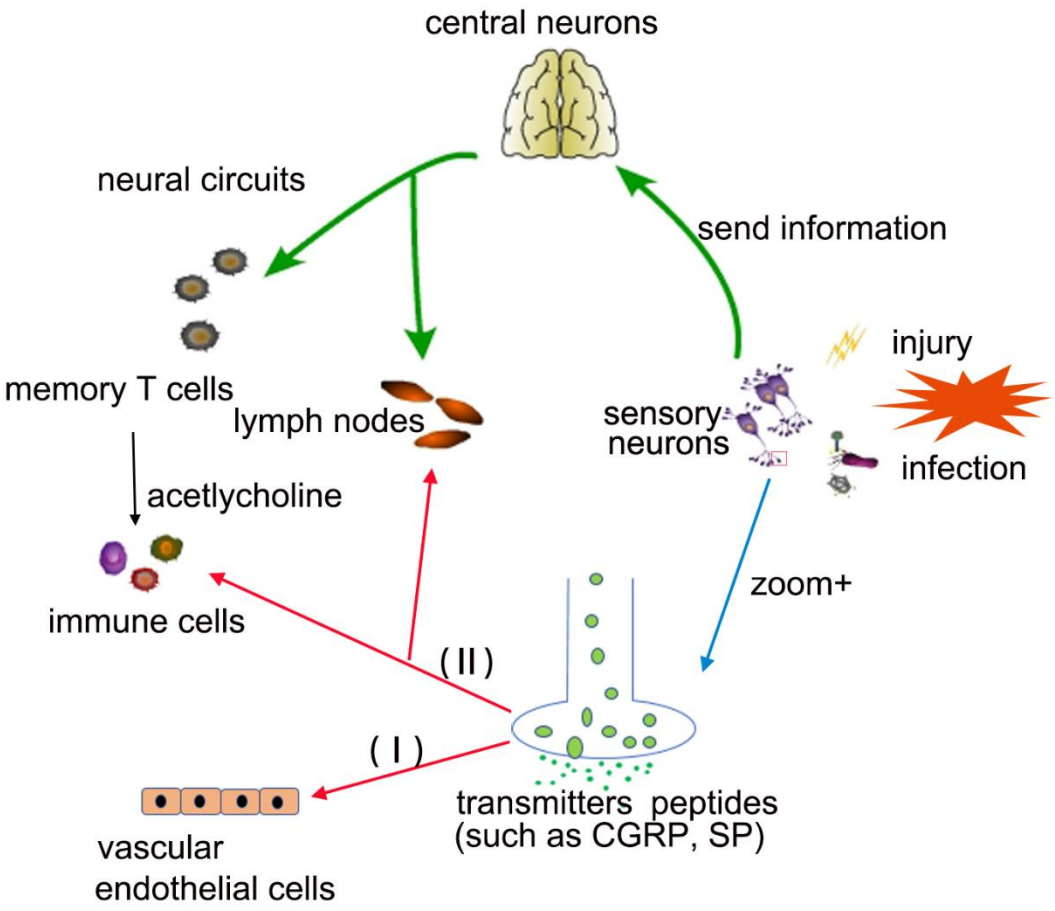

Figure 3: The neural circuits and neuropeptides modulate innate immune response. After detecting infections or injury, the sensory neurons release neuropeptides and send information to central neurons. The central neurons produce neural circuits sending to spleen or other immune organs through vague nerve. The neural circuits incite acetylcholine-producing memory T cells to produce choline, which binds to α 7 nAChR expressed on immune cells and lymphoid nodes to modulate innate immune response. The released neuropeptides, such as SP and CGRP, could cause two phases of neural inflammation: the first phase (Ⅰ), SP and CGRP act on arteriole and venules to cause plasma extravasation and permeability; the second phase (Ⅱ), they act on immune cells and lymphoid nodes to modulate the innate immune response.

Abbreviations: α 7 nAChR, α 7 nicotinic acetylcholine receptors. SP, substance P; CGRP, calcitonin gene-related peptide.

4. Discussion

In this study, we showed that PVL alone without *S. aureus* could induce severe retinal inflammation, due to PVL active effects towards neuronal cells and glial cells. One phenomena demonstrated *in vitro* on PMNs is that PVL binds to C5aR before being internalized into cytoplasm[56]. In retina, we did not demonstrate whether or not PVL bound to C5aR on retinal ganglion cells. Because C5aR was present on retinal ganglion cells, we hypothesized that PVL bound to the receptors and was internalized into neuronal cells. It could also diffuse across gap junctions to neighboring neurons. It is interesting to note that PVL also colocalized with amacrine cells and horizontal cells which do not express C5aR. Further study should try to figure out whether PVL was really internalized into neuronal cells, and if yes, by which mechanism. Is C5aR involved in this process? Does another receptor play a role in the process especially on amacrine and horizontal cells? Those points are crucial to understand and better characterize the infection process.
This characterization of the role of C5aR is a complex task. Indeed, PVL and its S component recognize only human and rabbit C5aR, and not the murine C5aR. This preference of animal species makes the research on PVL effects more complicated. First, the research on rabbit is more limited than mouse or rat. There are much less commercial antibodies available for rabbit species, which limits our researches. Second, there is no transgenic rabbit, especially it is impossible to get C5aR knock-out rabbit. Third, it is better to test PVL cellular reaction on isolated retinal neuronal cells or retinal neuronal cell lines. However, there is no reliable cell line for rabbit or human retinal neurons. Retina is small and contains many kinds of neurons and glial cells. The possible technique to isolate one type of retinal neurons is immunopanning, which requires enough rabbit retina and special antibodies which recognize the rabbit cells. It needs time to establish this technique to isolate retinal neuronal cells.

In this study, we obtained some controversial results concerning the neuronal apoptosis and cytokine production between the *in vivo* model and the *ex vivo* model.
In the *in vivo* model, PVL induced apoptosis of some microglial cells, no neuronal apoptosis was observed. But in the *ex vivo* model, there was some amacrine cells which underwent apoptosis 8 h after PVL treatment. As we already discussed that this difference might be due to different diffusion of PVL in retina between two models, we could extend the time to 24 h after intravitreal PVL injection and see if some amacrine cells underwent apoptosis. In general, the glial cell activation is associated with neuronal cell death during infection process. It is somehow astonishing that PVL induced *in vivo* glial cell activation and no neuronal cell apoptosis, even if in *ex vivo* model amacrine cell apoptosis was observed. In both models, no ganglion cells underwent apoptosis, whereas it seemed to be the most PVL-targeted cell type.
More conflicting results were observed concerning cytokines production. PVL induced IL-6 increase in *in vivo* model, whereas IL-6 expression decreased in PVL-treated explants compared to controls. Beyond the differences between the two models and the possible reasons why apoptosis and cytokines production were different, those conflicting results

raise questions about the reliability of retinal explant model. We believe that retinal explant can be used to study PVL effects and eventual treatments by evaluating glial cell activation and amacrine cell apoptosis. Concerning cytokine and inflammation pathways, it should be interesting to look for other cytokines and/or neurotransmitters than IL-6. The results in *ex vivo* model may indicate that IL-6 is not main factor to trigger glial cell reaction. As reported in our review, bacterial toxins could induce neurogenic inflammation. Recently, it has been shown that HlgAB directly induced calcium influx through transient receptor potential ion channels in dorsal root ganglion neurons[195]. It is highly possible that PVL initiate neurogenic inflammation after binding to retinal neuronal cells. The principal neurotransmitters for neurogenic inflammation are CGRP, SP and glutamate. We tried to reveal the change of CGRP immunoactivity on retinal tissue in *ex vivo* model. Unfortunately, we did not find specific CGRP immunoreactivity in rabbit retinal tissue. This might be due to unspecific antibody which recognizes human CGRP. Indeed, no commercial antibody for rabbit CGRP was available. Another explanation is that PVL-positive neuronal cells released other neurotransmitters, such as glutamate or SP, to induce neurogenic inflammation. Larger spectrum of neurotransmitters could be researched, such as SP, CGRP and glutamate in *in vivo* or *ex vivo* models.

Perspectives of research

Murine model for testing PVL effects on retina

Human C5aR knock-in mouse was used to tested PVL effects. The neutrophils of this C5aR humanized mouse showed a reduced sensitivity to PVL. The humanized mouse is only partly humanized, the proteins in the subsequent signaling pathway could influence the effects. Recently, it was found that CD45 was the receptor of F component of PVL and influenced the sensitivity of neutrophils of C5aR humanized mouse to PVL[31]. Maybe, we could test PVL effect on retina using human C5aR and CD45 knock-in mouse in future studies.

Neurotransmitters and retinal explant

We hypothesize that amacrine cell apoptosis might be due to excessive glutamate release induced by PVL. We could previously treat retinal explant with inhibitors of glutamate receptors for a short time and evaluate amacrine cell apoptosis induced by PVL. If the apoptosis induced by PVL decreased significantly in retinal explants treated by inhibitors of glutamate receptors compared to non-treated retinal explants, it could prove that amacrine cell apoptosis is due to excessive glutamate release.

Research for other receptors for PVL

We could add antibodies against S or F components of PVL in PVL solution and to see if those antibodies could effectively block PVL effects on retinal explants by evaluating the glial cell activation and amacrine cell apoptosis. We hypothesize that there might be another mechanism, possible another receptor except for C5aR, for PVL targeting

neuronal cells in retina. We could test this hypothesis by adding antagonism of C5aR to retinal explant and evaluate PVL effects on retina.

Calcium imaging

The calcium mobilization is the mechanism to release neurotransmitters and initiate neurogenic inflammation. Ganglion cells are in the surface of retinal explant, which is easy to be visualized for calcium imaging. To further confirm calcium mobilization after PVL infection, Fura-2 and PVL could be applied on the surface of retinal explants and intracellular calcium mobilization could be visualized through Fura-2 fluorescence with microscope equipped with filter (340 nm/380 nm) and camera. This calcium imaging could prove that PVL interacting with retinal ganglion cells through calcium mobilization.

The antagonisms of neurotransmitters and calcium channels could be added to retinal explants and evaluate the changes of PVL effects on retina. This could further explore the molecular mechanism of PVL effects on neuronal cells.

Clinical study

PVL positive *S. aureus* strain is rare in France, but much more frequent in developing countries. The prevalence of PVL positive *S. aureus* was 12.5% of all the *S. aureus* isolates from hospitalized patients in east China[196], 35.6% among the hospital isolates in Nepal[197], 57% of *S. aureus* infections isolates in western and central Africa[198], 73.91% of all *S. aureus* isolates from pediatric patients in Colombia[199]. A clinical study showed that the prevalence of PVL positive *S. aureus* was 10% among the *S. aureus* isolates from endophthalmitis in United Sates[200]. We could furtherly evaluate the impact of PVL on endophthalmitis by clinical study in the developing countries in which the prevalence of PVL positive *S. aureus* is much higher. The endophthalmitis caused by *S. aureus* will be included. We collect *S. aureus* strains and analyze the prevalence of PVL positive *S. aureus* in endophthalmitis. We will compare the symptoms and prognostic of PVL positive *S. aureus* endophthalmitis with those of PVL negative *S. aureus* endophthalmitis. We could also analyze IL-6 level in the aqueous humor or vitreous from patients of those *S. aureus* endophthalmitis. Moreover, some antibiotics inhibit PVL release, such as clindamycin, linezolid, fusidic acid and rifampicin. We could do clinical study to test the combination of those inhibitory antibiotics in antibiotic treatment to see if there will be difference in prognosis of *S. aureus* infection.

5. Conclusion

PVL is a virulent leukotoxin of *S. aureus*, associated with CA-MRSA infections. It presents active effects towards leukocytes and neuronal cells. We explored PVL effects on retina, a neuronal tissue, and tried to find the processes of bacterial toxins aggravating bacterial endophthalmitis.

We employed two different rabbit models to study the PVL effects on retina: intravitreal injection of PVL *in vivo* animal model and retina explant *ex vivo* model. We showed that RGCs were the major cell targets of PVL through the presence of C5aR. PVL induced early retinal inflammation such as Müller and microglial cell activation and some microglial cell apoptosis. Those two models showed some different results: In *in vivo* animal model, PVL transiently colocalized with displaced amacrine cells, nitrotyrosine and IL-6 expression increased in retina. In *ex vivo* explant, PVL colocalized later with some horizontal cells and also possibly with a subpopulation of amacrine cells. Some amacrine cells in INL underwent apoptosis after PVL treatment. Those results clearly demonstrated that PVL alone without *S. aureus* bacteria could induce great inflammation in retina after targeting neurons.

The two models we developed, *in vivo* and *ex vivo*, help to understand the aggravating role of PVL in retinal staphylococcal infection. They also allow to further explore the biologic mechanisms leading to PVL effects on retinal neurons and to test potential new therapeutic strategies.

6. Publications and posters

Publications:

1. Liu X, Heitz P, Roux M, Keller D, Bourcier T, Sauer A, Prévost G, Gaucher D. Panton–Valentine Leukocidin Colocalizes with Retinal Ganglion and Amacrine Cells and Activates Glial Reactions and Microglial Apoptosis. Sci Rep. 2018 Feb 13;8(1):2953. doi: 10.1038/s41598-018-20590-z.

2. Liu X, Prévost G, Gaucher D. Bacterial toxins aggravate bacterial endophthalmitis by interacting directly with neurons. Submitted to *Toxins*

3. XuanLi LIU, Michel J ROUX, Serge PICAUD, Daniel KELLER, Arnaud SAUER, Pauline HEITZ, Gilles PREVOST, David GAUCHER. Panton–Valentine Leukocidin Induces Neuronal and Microglial Apoptosis together with Müller and Microglial Cell Activation in a Rabbit Retinal Explant Model. Submitted to *Investigative Ophthalmology & Visual Science*

Posters:

1. Congress 18 ETOX, a label for a well-established series “European Workshop on Bacterial Protein Toxins” 27-30 Jun 2017 at Paris. Poster title: Panton-Valentine leukocidin enhances glial reaction and microglial apoptosis through retinal ganglion and amacrine cell binding
2. Congress “European Association for Vision and Eye Research (EVER) 2017” 27-30 September 2017 at Nice. Poster title: Panton-Valentine leukocidin enhances glial reaction and microglial apoptosis through retinal ganglion and amacrine cell binding

7. Bibliography

1. Peacock SJ, de Silva I, Lowy FD. What determines nasal carriage of *Staphylococcus aureus*? *Trends in Microbiology* 2001;9:605-610.
2. Fanny Vincenota MS, GillesPrévost. Les facteurs de virulence de *Staphylococcus aureus*. *Revue Francophone des Laboratoires* 2008;2008:61-69.
3. Liu J, Chen D, Peters BM, et al. Staphylococcal chromosomal cassettes mec (SCCmec): A mobile genetic element in methicillin-resistant *Staphylococcus aureus*. *Microbial Pathogenesis* 2016;101:56-67.
4. David MZ, Daum RS. Community-associated methicillin-resistant *Staphylococcus aureus*: epidemiology and clinical consequences of an emerging epidemic. *Clinical Microbiology Reviews* 2010;23:616-687.
5. Valsesia G, Rossi M, Bertschy S, Pfyffer GE. Emergence of SCCmec Type IV and SCCmec Type V Methicillin-Resistant *Staphylococcus aureus* Containing the Panton-Valentine Leukocidin Genes in a Large Academic Teaching Hospital in Central Switzerland: External Invaders or Persisting Circulators? *J Clin Microbiol* 2010;48:720-727.
6. Dufour P, Gillet Y, Bes M, et al. Community-acquired methicillin-resistant *Staphylococcus aureus* infections in France: emergence of a single clone that produces Panton-Valentine leukocidin. *Clinical Infectious Diseases : an Official Publication of the Infectious Diseases Society of America* 2002;35:819-824.
7. Vandenesch F, Naimi T, Enright MC, et al. Community-acquired methicillin-resistant *Staphylococcus aureus* carrying Panton-Valentine leukocidin genes: worldwide emergence. *Emerging Infectious Diseases* 2003;9:978-984.
8. Lodise TP, Graves J, Evans A, et al. Relationship between Vancomycin MIC and Failure among Patients with Methicillin-Resistant *Staphylococcus aureus* Bacteremia Treated with Vancomycin. *Antimicrobial Agents and Chemotherapy* 2008;52:3315-3320.
9. Courvalin P. Vancomycin resistance in gram-positive cocci. *Clinical infectious diseases : an official publication of the Infectious Diseases Society of America* 2006;42 Suppl 1:S25-34.
10. Micek ST. Alternatives to Vancomycin for the Treatment of Methicillin-Resistant *Staphylococcus aureus* Infections. *Clinical Infectious Diseases* 2007;45:S184-S190.
11. Thomas CM, Nielsen KM. Mechanisms of, and barriers to, horizontal gene transfer between bacteria. *Nat Rev Microbiol* 2005;3:711-721.
12. McCarthy AJ, Witney AA, Lindsay JA. *Staphylococcus aureus* temperate bacteriophage: carriage and horizontal gene transfer is lineage associated. *Frontiers in Cellular and Infection Microbiology* 2012;2:6.
13. Foster TJ, Hook M. Surface protein adhesins of *Staphylococcus aureus*. *Trends in Microbiology* 1998;6:484-488.
14. Feng Y, Chen C-J, Su L-H, Hu S, Yu J, Chiu C-H. Evolution and pathogenesis of *Staphylococcus aureus* : lessons learned from genotyping and comparative genomics. *FEMS Microbiology Reviews* 2008;32:23-37.
15. Rooijakkers SH, Ruyken M, van Roon J, van Kessel KP, van Strijp JA, van Wamel WJ. Early expression of SCIN and CHIPS drives instant immune evasion by *Staphylococcus aureus*. *Cellular Microbiology* 2006;8:1282-1293.

16. Postma B, Poppelier MJ, van Galen JC, et al. Chemotaxis inhibitory protein of *Staphylococcus aureus* binds specifically to the C5a and formylated peptide receptor. *Journal of Immunology* 2004;172:6994-7001.
17. McCormick JK, Tripp TJ, Llera AS, et al. Functional analysis of the TCR binding domain of toxic shock syndrome toxin-1 predicts further diversity in MHC class II/superantigen/TCR ternary complexes. *Journal of Immunology* 2003;171:1385-1392.
18. Pinchuk IV, Beswick EJ, Reyes VE. Staphylococcal enterotoxins. *Toxins* 2010;2:2177-2197.
19. Bukowski M, Wladyka B, Dubin G. Exfoliative toxins of *Staphylococcus aureus*. *Toxins* 2010;2:1148-1165.
20. Vandenesch F, Lina G, Henry T. *Staphylococcus aureus* hemolysins, bi-component leukocidins, and cytolytic peptides: a redundant arsenal of membrane-damaging virulence factors? *Frontiers in Cellular and Infection Microbiology* 2012;2:12.
21. Spaan AN, Schiepers A, de Haas CJ, et al. Differential Interaction of the Staphylococcal Toxins Panton-Valentine Leukocidin and gamma-Hemolysin CB with Human C5a Receptors. *Journal of Immunology* 2015;195:1034-1043.
22. Spaan AN, van Strijp JAG, Torres VJ. Leukocidins: staphylococcal bi-component pore-forming toxins find their receptors. *Nat Rev Microbiol* 2017.
23. Cooney J, Kienle Z, Foster TJ, O'Toole PW. The gamma-hemolysin locus of *Staphylococcus aureus* comprises three linked genes, two of which are identical to the genes for the F and S components of leukocidin. *Infection and Immunity* 1993;61:768-771.
24. Prevost G, Cribier B, Couppie P, et al. Panton-Valentine leucocidin and gamma-hemolysin from *Staphylococcus aureus* ATCC 49775 are encoded by distinct genetic loci and have different biological activities. *Infection and Immunity* 1995;63:4121-4129.
25. Jover E, Tawk MY, Laventie BJ, Poulain B, Prevost G. Staphylococcal leukotoxins trigger free intracellular Ca(2+) rise in neurones, signalling through acidic stores and activation of store-operated channels. *Cellular Microbiology* 2013;15:742-758.
26. Alonzo F, 3rd, Kozhaya L, Rawlings SA, et al. CCR5 is a receptor for *Staphylococcus aureus* leukotoxin ED. *Nature* 2013;493:51-55.
27. DuMont AL, Yoong P, Liu X, et al. Identification of a crucial residue required for *Staphylococcus aureus* LukAB cytotoxicity and receptor recognition. *Infection and Immunity* 2014;82:1268-1276.
28. Barrio MB, Rainard P, Prevost G. LukM/LukF'-PV is the most active *Staphylococcus aureus* leukotoxin on bovine neutrophils. *Microbes and Infection / Institut Pasteur* 2006;8:2068-2074.
29. Koop G, Vrieling M, Storisteanu DM, et al. Identification of LukPQ, a novel, equid-adapted leukocidin of *Staphylococcus aureus*. *Scientific Reports* 2017;7:40660.
30. Spaan András N, Henry T, van Rooijen Willemien JM, et al. The Staphylococcal Toxin Panton-Valentine Leukocidin Targets Human C5a Receptors. *Cell Host & Microbe* 2013;13:584-594.
31. Tromp AT, Van Gent M, Abrial P, et al. Human CD45 is an F-component-specific receptor for the staphylococcal toxin Panton-Valentine leukocidin. *Nature Microbiology* 2018.
32. Metcalf D. On hematopoietic stem cell fate. *Immunity* 2007;26:669-673.
33. Junger WG. Purinergic regulation of neutrophil chemotaxis. *Cellular and Molecular Life Sciences : CMLS* 2008;65:2528-2540.
34. Lacy P. Mechanisms of degranulation in neutrophils. *Allergy, asthma, and clinical immunology : official journal of the Canadian Society of Allergy and Clinical Immunology*

2006;2:98-108.
35. Stone KD, Prussin C, Metcalfe DD. IgE, mast cells, basophils, and eosinophils. *J Allergy Clin Immunol* 2010;125:S73-80.
36. Guilliams M, Ginhoux F, Jakubzick C, et al. Dendritic cells, monocytes and macrophages: a unified nomenclature based on ontogeny. *Nature Reviews Immunology* 2014;14:571-578.
37. Kusunoki Y, Kyoizumi S, Hirai Y, et al. Flow Cytometry Measurements of Subsets of T, B and NK Cells in Peripheral Blood Lymphocytes of Atomic Bomb Survivors. *Radiation Research* 1998;150:227-236.
38. Badiou C, Dumitrescu O, Croze M, et al. Panton-Valentine leukocidin is expressed at toxic levels in human skin abscesses. *Clin Microbiol Infect* 2008;14:1180-1183.
39. Cribier B, Prevost G, Couppie P, Finck-Barbancon V, Grosshans E, Piemont Y. *Staphylococcus aureus* leukocidin: a new virulence factor in cutaneous infections? An epidemiological and experimental study. *Dermatology (Basel, Switzerland)* 1992;185:175-180.
40. Gillet Y, Issartel B, Vanhems P, et al. Association between *Staphylococcus aureus* strains carrying gene for Panton-Valentine leukocidin and highly lethal necrotising pneumonia in young immunocompetent patients. *Lancet (London, England)* 2002;359:753-759.
41. Diep BA, Chan L, Tattevin P, et al. Polymorphonuclear leukocytes mediate *Staphylococcus aureus* Panton-Valentine leukocidin-induced lung inflammation and injury. *Proceedings of the National Academy of Sciences of the United States of America* 2010;107:5587-5592.
42. Gillet Y, Dohin B, Dumitrescu O, et al. [Osteoarticular infections with staphylococcus aureus secreting Panton-Valentine leucocidin]. *Archives de Pediatrie : Organe Officiel de la Societe Francaise de Pediatrie* 2007;14 Suppl 2:S102-107.
43. Cremieux AC, Dumitrescu O, Lina G, et al. Panton-valentine leukocidin enhances the severity of community-associated methicillin-resistant *Staphylococcus aureus* rabbit osteomyelitis. *PloS One* 2009;4:e7204.
44. Staali L, Monteil H, Colin DA. The staphylococcal pore-forming leukotoxins open Ca2+ channels in the membrane of human polymorphonuclear neutrophils. *The Journal of Membrane Biology* 1998;162:209-216.
45. Tawk MY, Zimmermann-Meisse G, Bossu JL, et al. Internalization of staphylococcal leukotoxins that bind and divert the C5a receptor is required for intracellular Ca(2+) mobilization by human neutrophils. *Cellular Microbiology* 2015;17:1241-1257.
46. Werner S, Colin DA, Coraiola M, Menestrina G, Monteil H, Prevost G. Retrieving biological activity from LukF-PV mutants combined with different S components implies compatibility between the stem domains of these staphylococcal bicomponent leucotoxins. *Infection and Immunity* 2002;70:1310-1318.
47. Finck-Barbancon V, Duportail G, Meunier O, Colin DA. Pore formation by a two-component leukocidin from *Staphylococcus aureus* within the membrane of human polymorphonuclear leukocytes. *Biochimica et Biophysica Acta* 1993;1182:275-282.
48. Genestier AL, Michallet MC, Prevost G, et al. *Staphylococcus aureus* Panton-Valentine leukocidin directly targets mitochondria and induces Bax-independent apoptosis of human neutrophils. *The Journal of Clinical Investigation* 2005;115:3117-3127.
49. Pilsczek FH, Salina D, Poon KK, et al. A novel mechanism of rapid nuclear neutrophil extracellular trap formation in response to *Staphylococcus aureus*. *Journal of Immunology* 2010;185:7413-7425.

50. Chi CY, Lin CC, Liao IC, et al. Panton-Valentine leukocidin facilitates the escape of *Staphylococcus aureus* from human keratinocyte endosomes and induces apoptosis. *The Journal of Infectious Diseases* 2014;209:224-235.
51. Hensler T, Koller M, Prevost G, Piemont Y, Konig W. GTP-binding proteins are involved in the modulated activity of human neutrophils treated with the Panton-Valentine leukocidin from *Staphylococcus aureus*. *Infection and Immunity* 1994;62:5281-5289.
52. Konig B, Prevost G, Piemont Y, Konig W. Effects of *Staphylococcus aureus* leukocidins on inflammatory mediator release from human granulocytes. *The Journal of Infectious Diseases* 1995;171:607-613.
53. Colin DA, Monteil H. Control of the oxidative burst of human neutrophils by staphylococcal leukotoxins. *Infection and Immunity* 2003;71:3724-3729.
54. Holzinger D, Gieldon L, Mysore V, et al. *Staphylococcus aureus* Panton-Valentine leukocidin induces an inflammatory response in human phagocytes via the NLRP3 inflammasome. *Journal of Leukocyte Biology* 2012;92:1069-1081.
55. Perret M, Badiou C, Lina G, et al. Cross-talk between *Staphylococcus aureus* leukocidins-intoxicated macrophages and lung epithelial cells triggers chemokine secretion in an inflammasome-dependent manner. *Cellular Microbiology* 2012;14:1019-1036.
56. Zimmermann-Meisse G, Prevost G, Jover E. Above and beyond C5a Receptor Targeting by Staphylococcal Leucotoxins: Retrograde Transport of Panton-Valentine Leucocidin and gamma-Hemolysin. *Toxins* 2017;9.
57. Laventie BJ, Rademaker HJ, Saleh M, et al. Heavy chain-only antibodies and tetravalent bispecific antibody neutralizing *Staphylococcus aureus* leukotoxins. *Proceedings of the National Academy of Sciences of the United States of America* 2011;108:16404-16409.
58. Laventie BJ, Potrich C, Atmanene C, et al. p-Sulfonato-calix[n]arenes inhibit staphylococcal bicomponent leukotoxins by supramolecular interactions. *The Biochemical Journal* 2013;450:559-571.
59. Bringmann A, Pannicke T, Grosche J, et al. Muller cells in the healthy and diseased retina. *Progress in Retinal and Eye Research* 2006;25:397-424.
60. Reis R, Cabral-Da-Silva MEC, de Melloa FG, Taylor JSH. Muller glia factors induce survival and neuritogenesis of peripheral and central neurons. *Brain Research* 2008;1205:1-11.
61. Lahne M, Gorsuch RA, Nelson CM, Hyde DR. Culture of Adult Transgenic Zebrafish Retinal Explants for Live-cell Imaging by Multiphoton Microscopy. *Journal of Visualized Experiments : JoVE* 2017.
62. Dyer MA, Cepko CL. Control of Muller glial cell proliferation and activation following retinal injury. *Nature Neuroscience* 2000;3:873-880.
63. Kim BJ, Braun TA, Wordinger RJ, Clark AF. Progressive morphological changes and impaired retinal function associated with temporal regulation of gene expression after retinal ischemia/reperfusion injury in mice. *Mol Neurodegener* 2013;8:19.
64. Yoshida S, Sotozono C, Ikeda T, Kinoshita S. Interleukin-6 (IL-6) production by cytokine-stimulated human Muller cells. *Current Eye Research* 2001;22:341-347.
65. Lu YB, Iandiev I, Hollborn M, et al. Reactive glial cells: increased stiffness correlates with increased intermediate filament expression. *Faseb Journal* 2011;25:624-631.
66. Lewis GP, Chapin EA, Luna G, Linberg KA, Fisher SK. The fate of Muller's glia following experimental retinal detachment: nuclear migration, cell division, and subretinal glial scar

formation. *Molecular Vision* 2010;16:1361-1372.
67. Kumar A, Pandey RK, Miller LJ, Singh PK, Kanwar M. Muller Glia in Retinal Innate Immunity: A Perspective on Their Roles in Endophthalmitis. *Critical Reviews in Immunology* 2013;33:119-135.
68. Kumar A, Shamsuddin N. Retinal Muller glia initiate innate response to infectious stimuli via toll-like receptor signaling. *PloS One* 2012;7:e29830.
69. Rosenzweig HL, Galster KT, Planck SR, Rosenbaum JT. NOD1 expression in the eye and functional contribution to IL-1beta-dependent ocular inflammation in mice. *Investigative Ophthalmology & Visual Science* 2009;50:1746-1753.
70. Shamsuddin N, Kumar A. TLR2 mediates the innate response of retinal Muller glia to Staphylococcus aureus. *Journal of Immunology* 2011;186:7089-7097.
71. Cotinet A, Goureau O, ThillayeGoldenberg B, Naud MC, deKozak Y. Differential tumor necrosis factor and nitric oxide production in retinal Muller glial cells from C3H/HeN and C3H/HeJ mice. *Ocular Immunology and Inflammation* 1997;5:111-116.
72. Wang JJ, Xu XL, Elliott MH, Zhu ML, Le YZ. Muller Cell-Derived VEGF Is Essential for Diabetes-Induced Retinal Inflammation and Vascular Leakage. *Diabetes* 2010;59:2297-2305.
73. Eberhardt C, Amann B, Feuchtinger A, Hauck SM, Deeg CA. Differential expression of inwardly rectifying K+ channels and aquaporins 4 and 5 in autoimmune uveitis indicates misbalance in Muller glial cell-dependent ion and water homeostasis. *Glia* 2011;59:697-707.
74. Deeg CA, Amann B, Lutz K, et al. Aquaporin 11, a regulator of water efflux at retinal Muller glial cell surface decreases concomitant with immune-mediated gliosis. *Journal of Neuroinflammation* 2016;13:12.
75. Pannicke T, Uckermann O, Iandiev I, Wiedemann P, Reichenbach A, Bringmann A. Ocular inflammation alters swelling and membrane characteristics of rat Muller glial cells. *Journal of Neuroimmunology* 2005;161:145-154.
76. Reichenbach A, Wurm A, Pannicke T, Iandiev I, Wiedemann P, Bringmann A. Muller cells as players in retinal degeneration and edema. *Graefes Arch Clin Exp Ophthalmol* 2007;245:627-636.
77. Bodeutsch N, Thanos S. Migration of phagocytotic cells and development of the murine intraretinal microglial network: An in vivo study using fluorescent dyes. *Glia* 2000;32:91-101.
78. Thomas WE. Brain macrophages: evaluation of microglia and their functions. *Brain Research Reviews* 1992;17:61-74.
79. Penfold PL, Madigan MC, Provis JM. ANTIBODIES TO HUMAN-LEUKOCYTE ANTIGENS INDICATE SUBPOPULATIONS OF MICROGLIA IN HUMAN RETINA. *Visual Neuroscience* 1991;7:383-388.
80. Penfold PL, Provis JM, Liew SCK. HUMAN RETINAL MICROGLIA EXPRESS PHENOTYPIC CHARACTERISTICS IN COMMON WITH DENDRITIC ANTIGEN-PRESENTING CELLS. *Journal of Neuroimmunology* 1993;45:183-191.
81. Lee JE, Liang KJ, Fariss RN, Wong WT. Ex vivo dynamic imaging of retinal microglia using time-lapse confocal microscopy. *Investigative Ophthalmology & Visual Science* 2008;49:4169-4176.
82. Ulbricht E, Pannicke T, Uhlmann S, Wiedemann P, Reichenbach A, Francke M. Activation of retinal microglial cells is not associated with Muller cell reactivity in vitrectomized rabbit eyes. *Acta Ophthalmologica* 2013;91:e48-55.
83. Karlstetter M, Scholz R, Rutar M, Wong WT, Provis JM, Langmann T. Retinal microglia: Just bystander or target for therapy? *Progress in Retinal and Eye Research* 2015;45:30-57.

84. Ransohoff RM, Cardona AE. The myeloid cells of the central nervous system parenchyma. *Nature* 2010;468:253-262.
85. Hanisch UK, Kettenmann H. Microglia: active sensor and versatile effector cells in the normal and pathologic brain. *Nature Neuroscience* 2007;10:1387-1394.
86. Rao NA, Kimoto T, Zamir E, et al. Pathogenic role of retinal microglia in experimental uveoretinitis. *Investigative Ophthalmology & Visual Science* 2003;44:22-31.
87. Sivakumar V, Foulds WS, Luu CD, Ling EA, Kaur C. Retinal ganglion cell death is induced by microglia derived pro-inflammatory cytokines in the hypoxic neonatal retina. *Journal of Pathology* 2011;224:245-260.
88. D'Orazio TJ, Niederkorn JY. A novel role for TGF-beta and IL-10 in the induction of immune privilege. *Journal of Immunology* 1998;160:2089-2098.
89. Broderick C, Hoek RM, Forrester JV, Liversidge J, Sedgwick JD, Dick AD. Constitutive retinal CD200 expression regulates resident microglia and activation state of inflammatory cells during experimental autoimmune uveoretinitis. *Am J Pathol* 2002;161:1669-1677.
90. Liang KJ, Lee JE, Wang YQD, et al. Regulation of Dynamic Behavior of Retinal Microglia by CX3CR1 Signaling. *Investigative Ophthalmology & Visual Science* 2009;50:4444-4451.
91. Zhang YK, Zhao L, Wang X, et al. Repopulating retinal microglia restore endogenous organization and function under CX3CL1-CX3CR1 regulation. *Sci Adv* 2018;4:14.
92. Fontainhas AM, Wang MH, Liang KJ, et al. Microglial Morphology and Dynamic Behavior Is Regulated by Ionotropic Glutamatergic and GABAergic Neurotransmission. *PloS One* 2011;6:14.
93. Fontainhas AM, Wang M, Liang KJ, et al. Microglial morphology and dynamic behavior is regulated by ionotropic glutamatergic and GABAergic neurotransmission. *PloS One* 2011;6:e15973.
94. Harada T, Harada C, Kohsaka S, et al. Microglia-Muller glia cell interactions control neurotrophic factor production during light-induced retinal degeneration. *The Journal of Neuroscience : the Official Journal of the Society for Neuroscience* 2002;22:9228-9236.
95. Wang M, Ma W, Zhao L, Fariss RN, Wong WT. Adaptive Muller cell responses to microglial activation mediate neuroprotection and coordinate inflammation in the retina. *Journal of Neuroinflammation* 2011;8:173.
96. Kunzevitzky NJ, Almeida MV, Goldberg JL. Amacrine cell gene expression and survival signaling: differences from neighboring retinal ganglion cells. *Investigative Ophthalmology & Visual Science* 2010;51:3800-3812.
97. MacNeil MA, Masland RH. Extreme diversity among amacrine cells: Implications for function. *Neuron* 1998;20:971-982.
98. Taylor WR, Smith RG. The role of starburst amacrine cells in visual signal processing. *Visual Neuroscience* 2012;29:73-81.
99. Zhu BS, Straznicky C. Morphology and distribution of serotonin-like immunoreactive amacrine cells in the retina of Bufo marinus. *Visual Neuroscience* 1990;5:371-378.
100. Xin D, Bloomfield SA. Tracer coupling pattern of amacrine and ganglion cells in the rabbit retina. *The Journal of Comparative Neurology* 1997;383:512-528.
101. Massey SC, Mills SL. Gap junctions between All amacrine cells and calbindin-positive bipolar cells in the rabbit retina. *Visual Neuroscience* 1999;16:1181-1189.
102. Sanes JR, Masland RH. The Types of Retinal Ganglion Cells: Current Status and Implications for Neuronal Classification. *Annual Review of Neuroscience* 2015;38:221-246.

103. So KF, Yip HK. Regenerative capacity of retinal ganglion cells in mammals. *Vision Research* 1998;38:1525-1535.
104. Crooks J, Kolb H. Localization of GABA, glycine, glutamate and tyrosine hydroxylase in the human retina. *The Journal of Comparative Neurology* 1992;315:287-302.
105. Wu SM, Maple BR. Amino acid neurotransmitters in the retina: a functional overview. *Vision Research* 1998;38:1371-1384.
106. Skytt DM, Toft-Kehler AK, Braendstrup CT, et al. Glia-Neuron Interactions in the Retina Can Be Studied in Cocultures of Muller Cells and Retinal Ganglion Cells. *Biomed Res Int* 2016;10.
107. Brecha N, Johnson D, Bolz J, Sharma S, Parnavelas JG, Lieberman AR. Substance P-immunoreactive retinal ganglion cells and their central axon terminals in the rabbit. *Nature* 1987;327:155-158.
108. Blixt FW, Radziwon-Balicka A, Edvinsson L, Warfvinge K. Distribution of CGRP and its receptor components CLR and RAMP1 in the rat retina. *Experimental Eye Research* 2017;161:124-131.
109. Catterall WA. Voltage-gated calcium channels. *Cold Spring Harbor Perspectives in Biology* 2011;3:a003947.
110. Simms BA, Zamponi GW. Neuronal voltage-gated calcium channels: structure, function, and dysfunction. *Neuron* 2014;82:24-45.
111. Elke Guenther TR, Holger Taschenberger, Rosemarie Granty. Separation of calcium currents in retinal ganglion cells from postnatal rat. *Brain Res* 1994;223-235.
112. McFadzean I, Gibson A. The developing relationship between receptor-operated and store-operated calcium channels in smooth muscle. *British Journal of Pharmacology* 2002;135:1-13.
113. Grienberger C, Konnerth A. Imaging calcium in neurons. *Neuron* 2012;73:862-885.
114. Nilius B, Owsianik G. The transient receptor potential family of ion channels. *Genome Biology* 2011;12:218.
115. D'Hoedt D, Owsianik G, Prenen J, et al. Stimulus-specific modulation of the cation channel TRPV4 by PACSIN 3. *The Journal of Biological Chemistry* 2008;283:6272-6280.
116. Niswender CM, Conn PJ. Metabotropic glutamate receptors: physiology, pharmacology, and disease. *Annual Review of Pharmacology and Toxicology* 2010;50:295-322.
117. Stammers AN, Susser SE, Hamm NC, et al. The regulation of sarco(endo)plasmic reticulum calcium-ATPases (SERCA). *Canadian Journal of Physiology and Pharmacology* 2015;93:843-854.
118. Duchen MR. Contributions of mitochondria to animal physiology: from homeostatic sensor to calcium signalling and cell death. *The Journal of Physiology* 1999;516 (Pt 1):1-17.
119. Berridge MJ, Bootman MD, Roderick HL. Calcium signalling: dynamics, homeostasis and remodelling. *Nature reviews Molecular cell Biology* 2003;4:517-529.
120. Galione A, Morgan AJ, Arredouani A, et al. NAADP as an intracellular messenger regulating lysosomal calcium-release channels. *Biochemical Society Transactions* 2010;38:1424-1431.
121. Callegan MC, Gilmore MS, Gregory M, et al. Bacterial endophthalmitis: therapeutic challenges and host-pathogen interactions. *Progress in Retinal and eye Research* 2007;26:189-203.
122. Sadiq MA, Hassan M, Agarwal A, et al. Endogenous endophthalmitis: diagnosis, management, and prognosis. *Journal of Ophthalmic Inflammation and Infection* 2015;5:32.
123. Banu A, Sriprakash K, Nagaraj E, Meundi M. Importance of accurate sampling techniques in microbiological diagnosis of endophthalmitis; *Australas Med* J 2011:258-262.
124. Durand ML. Bacterial endophthalmitis. *Current Infectious Disease Reports* 2009;11:283-288.
125. GROUP TEVS. Microbiologic factors and visual outcome in the endophthalmitis vitrectomy

study. *Am J Ophthalmol* 1996;122:830-846.
126. Gower EW, Keay LJ, Stare DE, et al. Characteristics of Endophthalmitis after Cataract Surgery in the United States Medicare Population. *Ophthalmology* 2015;122:1625-1632.
127. Lu X, Ng DS-C, Zheng K, et al. Risk factors for endophthalmitis requiring evisceration or enucleation. *Scientific Reports* 2016;6:28100.
128. Das T, Kunimoto DY, Sharma S, et al. Relationship between clinical presentation and visual outcome in postoperative and posttraumatic endophthalmitis in south central India. *Indian Journal of Ophthalmology* 2005;53:5-16.
129. Josephberg RG. Endophthalmitis: the latest in current management. *Retina (Philadelphia, Pa)* 2006;26:S47-50.
130. Callegan MC, Engelbert M, Parke DW, 2nd, Jett BD, Gilmore MS. Bacterial endophthalmitis: epidemiology, therapeutics, and bacterium-host interactions. *Clinical Microbiology Reviews* 2002;15:111-124.
131. Ormerod LD, Ho DD, Becker LE, et al. Endophthalmitis caused by the coagulase-negative *staphylococci*. 1. Disease spectrum and outcome. *Ophthalmology* 1993;100:715-723.
132. A. Meredith T. *Posttraumatic Endophthalmitis*; 1999:520-521.
133. Jonas JB, Knorr HL, Budde WM. Prognostic factors in ocular injuries caused by intraocular or retrobulbar foreign bodies. *Ophthalmology* 2000;107:823-828.
134. Essex RW, Yi Q, Charles PG, Allen PJ. Post-traumatic endophthalmitis. *Ophthalmology* 2004;111:2015-2022.
135. Lieb DF, Scott IU, Flynn HW, Jr., Miller D, Feuer WJ. Open globe injuries with positive intraocular cultures: factors influencing final visual acuity outcomes. *Ophthalmology* 2003;110:1560-1566.
136. Wong JS, Chan TK, Lee HM, Chee SP. Endogenous bacterial endophthalmitis: an east Asian experience and a reappraisal of a severe ocular affliction. *Ophthalmology* 2000;107:1483-1491.
137. Okada AA, Johnson RP, Liles WC, D'Amico DJ, Baker AS. Endogenous bacterial endophthalmitis. Report of a ten-year retrospective study. *Ophthalmology* 1994;101:832-838.
138. Jackson TL, Eykyn SJ, Graham EM, Stanford MR. Endogenous bacterial endophthalmitis: a 17-year prospective series and review of 267 reported cases. *Survey of Ophthalmology* 2003;48:403-423.
139. Connell PP, O'Neill EC, Fabinyi D, et al. Endogenous endophthalmitis: 10-year experience at a tertiary referral centre. *Eye* 2010;25:66.
140. Giese MJ, Sumner HL, Berliner JA, Mondino BJ. Cytokine expression in a rat model of *Staphylococcus aureus* endophthalmitis. *Investigative Ophthalmology & Visual Science* 1998;39:2785-2790.
141. Ramadan RT, Ramirez R, Novosad BD, Callegan MC. Acute inflammation and loss of retinal architecture and function during experimental Bacillus endophthalmitis. *Curr Eye Res* 2006;31:955-965.
142. Hao X, Changxian Yi, Yuqin Wang, et al. Identification of intraocular inflammatory mediators in patients with endophthalmitis. *Molecular Vision* 2016;22:563-574.
143. Giese MJ, Rayner SA, Fardin B, et al. Mitigation of neutrophil infiltration in a rat model of early *Staphylococcus aureus* endophthalmitis. *Investigative Ophthalmology & Visual Science* 2003;44:3077-3082.
144. Parkunan SM, Randall CB, Astley RA, Furtado GC, Lira SA, Callegan MC. CXCL1, but not IL-6,

significantly impacts intraocular inflammation during infection. *Journal of Leukocyte Biology* 2016;100:1125-1134.
145. Reichenbach A, Bringmann A. New functions of Muller cells. *Glia* 2013;61:651-678.
146. Willbold E, Layer PG. Muller glia cells and their possible roles during retina differentiation in vivo and in vitro. *Histol Histopathol* 1998;13:531-552.
147. Francke M, Faude F, Pannicke T, et al. Electrophysiology of rabbit Muller (glial) cells in experimental retinal detachment and PVR. *Investigative Ophthalmology & Visual Science* 2001;42:1072-1079.
148. Cunha-Vaz J. The blood-ocular barriers. *Survey of Ophthalmology* 1979;23:279-296.
149. Streilein JW. Immunoregulatory mechanisms of the eye. *Progress in Retinal and Eye Research* 1999;18:357-370.
150. Cunha-Vaz JG. The blood-retinal barriers system. Basic concepts and clinical evaluation. *Experimental Eye Research* 2004;78:715-721.
151. Metrikin DC, Wilson CA, Berkowitz BA, Lam MK, Wood GK, Peshock RM. Measurement of blood-retinal barrier breakdown in endotoxin-induced endophthalmitis. *Investigative Ophthalmology & Visual Science* 1995;36:1361-1370.
152. Moyer AL, Ramadan RT, Thurman J, Burroughs A, Callegan MC. *Bacillus cereus* induces permeability of an in vitro blood-retina barrier. *Infection and Immunity* 2008;76:1358-1367.
153. Tretiach M, Madigan MC, Wen L, Gillies MC. Effect of Muller cell co-culture on in vitro permeability of bovine retinal vascular endothelium in normoxic and hypoxic conditions. *Neurosci Lett* 2005;378:160-165.
154. Ng JQ, Morlet N, Pearman JW, et al. Management and outcomes of postoperative endophthalmitis since the endophthalmitis vitrectomy study: the Endophthalmitis Population Study of Western Australia (EPSWA)'s fifth report. *Ophthalmology* 2005;112:1199-1206.
155. Meredith TA. Posttraumatic endophthalmitis. *Archives of Ophthalmology (Chicago, Ill : 1960)* 1999;117:520-521.
156. Mieler WF, Ellis MK, Williams DF, Han DP. Retained intraocular foreign bodies and endophthalmitis. *Ophthalmology* 1990;97:1532-1538.
157. Maguire JI. Postoperative endophthalmitis: optimal management and the role and timing of vitrectomy surgery. *Eye (London, England)* 2008;22:1290-1300.
158. Ferencz JR, Assia EI, Diamantstein L, Rubinstein E. Vancomycin concentration in the vitreous after intravenous and intravitreal administration for postoperative endophthalmitis. *Archives of Ophthalmology (Chicago, Ill : 1960)* 1999;117:1023-1027.
159. Results of the Endophthalmitis Vitrectomy Study. A randomized trial of immediate vitrectomy and of intravenous antibiotics for the treatment of postoperative bacterial endophthalmitis. Endophthalmitis Vitrectomy Study Group. *Archives of Ophthalmology (Chicago, Ill : 1960)* 1995;113:1479-1496.
160. Seal DV, Kirkness CM. Criteria for intravitreal antibiotics during surgical removal of intraocular foreign bodies. *Eye (London, England)* 1992;6 (Pt 5):465-468.
161. Campochiaro PA, Lim JI. Aminoglycoside toxicity in the treatment of endophthalmitis. The Aminoglycoside Toxicity Study Group. *Archives of ophthalmology (Chicago, Ill : 1960)* 1994;112:48-53.
162. Wiechens B, Neumann D, Grammer JB, Pleyer U, Hedderich J, Duncker GIW. Retinal toxicity of liposome-incorporated and free ofloxacin after intravitreal injection in rabbit eyes. *International*

Ophthalmology 1998;22:133.
163. Meyer CH, Krohne TU, Charbel Issa P, Liu Z, Holz FG. Routes for Drug Delivery to the Eye and Retina: Intravitreal Injections. *Developments in Ophthalmology* 2016;55:63-70.
164. Dalkara D, Kolstad KD, Caporale N, et al. Inner limiting membrane barriers to AAV-mediated retinal transduction from the vitreous. *Molecular Therapy : the Journal of the American Society of Gene Therapy* 2009;17:2096-2102.
165. Xu Q, Boylan NJ, Suk JS, et al. Nanoparticle diffusion in, and microrheology of, the bovine vitreous ex vivo. *Journal of Controlled Release : Official Journal of the Controlled Release Society* 2013;167:76-84.
166. Jackson TL, Antcliff RJ, Hillenkamp J, Marshall J. Human retinal molecular weight exclusion limit and estimate of species variation. *Investigative Ophthalmology & Visual Science* 2003;44:2141-2146.
167. Del Amo EM, Rimpela AK, Heikkinen E, et al. Pharmacokinetic aspects of retinal drug delivery. *Progress in Retinal and Eye Research* 2017;57:134-185.
168. Winzeler A, Wang JT. Purification and culture of retinal ganglion cells from rodents. *Cold Spring Harbor protocols* 2013;2013:643-652.
169. Sawamiphak S, Ritter M, Acker-Palmer A. Preparation of retinal explant cultures to study ex vivo tip endothelial cell responses. *Nature Protocols* 2010;5:1659-1665.
170. Landreth GE, Agranoff BW. Explant culture of adult goldfish retina: effect of prior optic nerve crush. *Brain Res* 1976;118:299-303.
171. Smalheiser NR, Crain SM, Bornstein MB. Development of ganglion cells and their axons in organized cultures of fetal mouse retinal explants. *Brain Res* 1981;204:159-178.
172. Muller B, Wagner F, Lorenz B, Stieger K. Organotypic Cultures of Adult Mouse Retina: Morphologic Changes and Gene Expression. *Investigative Ophthalmology & Visual Science* 2017;58:1930-1940.
173. Mohlin C, Liljekvist-Soltic I, Johansson K. Further assessment of neuropathology in retinal explants and neuroprotection by human neural progenitor cells. *J Neural Eng* 2011;8:10.
174. Bahar B, O'Doherty JV, Sweeney T. Assessment of RNA integrity in the postmortem pig colonic tissue ex vivo. *Journal of Animal Science* 2012;90 Suppl 4:22-24.
175. Perry VH, Henderson Z, Linden R. Postnatal changes in retinal ganglion cell and optic axon populations in the pigmented rat. *The Journal of Comparative Neurology* 1983;219:356-368.
176. Engelsberg K, Ehinger B, Wasselius J, Johansson K. Apoptotic cell death and microglial cell responses in cultured rat retina. *Graefe's Archive for Clinical and Experimental Ophthalmology = Albrecht von Graefes Archiv fur klinische und experimentelle Ophthalmologie* 2004;242:229-239.
177. Mohlin C, Johansson K. Death of photoreceptors in organotypic retinal explant cultures: Implication of rhodopsin accumulation and endoplasmic reticulum stress. *J Neurosci Methods* 2011;197:56-64.
178. Iandiev I, Uckermann O, Pannicke T, et al. Glial cell reactivity in a porcine model of retinal detachment. *Investigative Ophthalmology & Visual Science* 2006;47:2161-2171.
179. Mertsch K, Hanisch UK, Kettenmann H, Schnitzer J. Characterization of microglial cells and their response to stimulation in an organotypic retinal culture system. *J Comp Neurol* 2001;431:217-227.
180. Kuhrt H, Walski M, Reichenbach A, Albrecht J. Rabbit retinal organ culture as an in-vitro model of hepatic retinopathy. *Graefe's Archive for Clinical and Experimental Ophthalmology = Albrecht*

von Graefes Archiv fur klinische und experimentelle Ophthalmologie 2004;242:512-522.
181. Johnson TV, Martin KR. Development and characterization of an adult retinal explant organotypic tissue culture system as an in vitro intraocular stem cell transplantation model. *Investigative Ophthalmology & Visual Science* 2008;49:3503-3512.
182. Taylor L, Arner K, Engelsberg K, Ghosh F. Effects of glial cell line-derived neurotrophic factor on the cultured adult full-thickness porcine retina. *Curr Eye Res* 2013;38:503-515.
183. Hatakeyama J, Kageyama R. Retrovirus-mediated gene transfer to retinal explants. *Methods* 2002;28:387-395.
184. Zhang SS, Fu XY, Barnstable CJ. Tissue culture studies of retinal development. *Methods* 2002;28:439-447.
185. Bull ND, Johnson TV, Welsapar G, DeKorver NW, Tomarev SI, Martin KR. Use of an adult rat retinal explant model for screening of potential retinal ganglion cell neuroprotective therapies. *Investigative Ophthalmology & Visual Science* 2011;52:3309-3320.
186. Pattamatta U, McPherson Z, White A. A mouse retinal explant model for use in studying neuroprotection in glaucoma. *Experimental Eye Research* 2016;151:38-44.
187. Nickerson PEB, Ronellenfitch KM, Csuzdi NF, et al. Live imaging and analysis of postnatal mouse retinal development. *BMC Dev Biol* 2013;13:16.
188. Johnson TV, Oglesby EN, Steinhart MR, Cone-Kimball E, Jefferys J, Quigley HA. Time-Lapse Retinal Ganglion Cell Dendritic Field Degeneration Imaged in Organotypic Retinal Explant Culture. *Investigative Ophthalmology & Visual Science* 2016;57:253-264.
189. Smedowski A, Pietrucha-Dutczak M, Maniar R, Ajeleti M, Matuszek I, Lewin-Kowalik J. FluoroGold-Labeled Organotypic Retinal Explant Culture for Neurotoxicity Screening Studies. *Oxidative Med Cell Longev* 2018;11.
190. Valdes J, Trachsel-Moncho L, Sahaboglu A, et al. Organotypic Retinal Explant Cultures as In Vitro Alternative for Diabetic Retinopathy Studies. *ALTEX-Altern Anim Exp* 2016;33:459-464.
191. Hirata M, Shearer TR, Azuma M. Hypoxia Activates Calpains in the Nerve Fiber Layer of Monkey Retinal Explants. *Investigative Ophthalmology & Visual Science* 2015;56:6049-6057.
192. Fradot M, Busskamp V, Forster V, et al. Gene Therapy in Ophthalmology: Validation on Cultured Retinal Cells and Explants from Postmortem Human Eyes. *Hum Gene Ther* 2011;22:587-593.
193. Wiley LA, Burnight ER, Kaalberg EE, et al. Assessment of Adeno-Associated Virus Serotype Tropism in Human Retinal Explants. *Hum Gene Ther* 13.
194. Lamba DA, Karl MO, Ware CB, Reh TA. Efficient generation of retinal progenitor cells from human embryonic stem cells. *Proceedings of the National Academy of Sciences of the United States of America* 2006;103:12769-12774.
195. Blake KJ, Baral P, Voisin T, et al. Staphylococcus aureus produces pain through pore-forming toxins and neuronal TRPV1 that is silenced by QX-314. *Nature Communications* 2018;9:37.
196. Yu F, Chen Z, Liu C, et al. Prevalence of *Staphylococcus aureus* carrying Panton-Valentine leukocidin genes among isolates from hospitalised patients in China. *Clinical Microbiology and Infection* 2008;14:381-384.
197. Shrestha B, Singh W, Raj VS, Pokhrel BM, Mohapatra TM. High Prevalence of Panton-Valentine Leukocidin (PVL) Genes in Nosocomial-Acquired *Staphylococcus aureus* Isolated from Tertiary Care Hospitals in Nepal. *Biomed Res Int* 2014;2014:7.
198. Breurec S, Fall C, Pouillot R, et al. Epidemiology of methicillin-susceptible *Staphylococcus*

aureus lineages in five major African towns: high prevalence of Panton-Valentine leukocidin genes. *Clinical Microbiology and Infection* 2011;17:633-639.
199. Correa-Jiménez O, Pinzón-Redondo H, Reyes N. High frequency of Panton-Valentine leukocidin in *Staphylococcus aureus* causing pediatric infections in the city of Cartagena-Colombia. *Journal of Infection and Public Health* 2016;9:415-420.
200. Rarey KA, Shanks RM, Romanowski EG, Mah FS, Kowalski RP. *Staphylococcus aureus* isolated from endophthalmitis are hospital-acquired based on Panton-Valentine leukocidin and antibiotic susceptibility testing. *J Ocul Pharmacol Ther* 2012;28:12-16.

8. Résume de la thèse en français

Title

Rôle de la leucocidine de Panton-Valentine dans l'infection oculaire staphylococcique : Etude des cibles cellulaires et des conséquences inflammatoires tissulaires rétiniennes sur des modèles d'endophtalmie *in vivo* et *ex vivo* chez le lapin

Introduction

S. aureus est une bactérie Gram positif, la prévalence du portage permanent est d'environ 25%, tandis que la colonisation transitoire est d'au moins 60%. C'est une des espèces les plus couramment isolée en milieu hospitalier, la deuxième bactérie responsable d'infections nosocomiales. Il colonise dans les zones humides, telles que les narines, les aisselles. *S. aureus* cause beaucoup de maladies, de l'infections dermiques a l'infections viscérales et certains syndromes potentiellement mortels. *S. aureus* a une morbidité et une mortalité importantes dans le monde entier, en raison de ses facteurs de virulence et ses multiples résistances aux antibiotiques.

S. aureus résistant à la méthicilline, ou encore appelle SARM, a été découvert en 1961. Ce dernier produit une nouvelle protéine résistante aux antibiotiques β-lactamines. Cette protéine est codée par le gène staphylococcal mec (SCCmec), qui existe en 9 types différents selon leurs tailles, les plus grands codent aussi des résistances a d'autres antibiotiques. Au début, les souches de SARM étaient confinées aux hôpitaux. Depuis les années 1990s, les infections à SARM ont progressé dans la population générale endors de toutes hospitalisation. Elles sont appelées CA-SARM ou bien SARM communitaire. Les SARM communitaire sont différents des SARM hospitalier par leurs caractéristiques génotypiques, épidémiologiques et cliniques. Les SARM hospitalier porte SCCmec de type I, II ou III et sont résistants à de nombreuses classes d'antibiotiques. SARM communitaire qui portent de petits gènes SCCmec de type IV ou V sont sensibles aux antibiotiques non β-lactamines. Le SARM hospitalier sont rarement porteurs du gène de la PVL, tandis que de 60 à 100% des souches de SARM communitaire portent le gène de la PVL.

Les facteurs de virulence de S. aureus comprennent les exoenzymes, les facteurs d'adhésion et les toxines. Les exoenzymes contrôlent la colonisation et la dissémination. Le facteur d'adhésion aide *S. aureus* à adhérer aux cellules, et à la matrice extracellulaire. Les toxines ont une fonction plus offensive en s'attaquant directement au système immunitaire et aux cellules de l'hôte. Le but est de bloquer la réponse adaptative.

Les leucocidines ciblent les leucocytes. Cinq leucocidines à deux composés sont été identifiés chez des *S. aureus* d'origine humaine. Les gènes de HlgA/B, HlgC/B, LukA/B sont dans le génome "core" du chromosome et ils sont exprimés chez 99% des souches. Le gène de LukE/D se trouve dans un îlot de pathogénicité, exprimés par 50 à 75% des *S.*

aureus. Le gène de la PVL se trouve dans 3 bactériophages. Il est exprimé chez 2 à 10% de tous les isolats cliniques de *S. aureus* en Europe, et chez 10 à 60% dans les pays en développement en Afrique ou en Asie. Les composés se fixent par l'intermédiaire de récepteurs, différents selon les toxines et parfois différents en fonction des cibles cellulaires (spécificité / espèces animales).

Les leucocidines sont composés de 2 protéines : une protéine de classe S et une protéine de classe F. Ces deux protéines doivent agir ensemble pour produire un effet sur les cellules ciblées. Le composé de classe S se fixe en premier à la membrane de la cellule ciblée, permettant la fixation du composé de classe F. Il y a ensuite, sois une oligomérisation puis formation du pore octamérique, sois une internalisation. La structure monomérique de la PVL a été résolue. La structure oligomérique du pore créé par la PVL a été décrite du pore de l'α-hémolysine.

LukS-PV se fixe sur les récepteurs C5a. Récemment, CD45 a été identifié comme le récepteur de LukF-PV. Dans le processus de l'internalisation de la PVL, LukS-PV se lie au C5aR, permettant l'interaction secondaire du composé LukF-PV. Ils sont internalisés dans les cellules avec le C5aR phosphorylé. La PVL s'accumule d'abord dans les compartiments lysosomaux et atteint le réseau de Golgi en 3 heures.

La PVL a une préférence pour les monocytes, les macrophages et les PMNs chez l'humains et le lapin, mais pas chez les rongeurs. La PVL peut également induire des réactions sur les neurones cérébraux et radicaux. La PVL peut entraîner une nécrose des tissus au cours de l'infection telles que les furoncles, la pneumonie nécrosante aiguë et l'ostéomyélite. La PVL induit une augmentation du calcium intracellulaire sans dommage pour la membrane.

L'augmentation du calcium intracellulaire commence à 100 s avec une augmentation linéaire pendant 10 min. Cette mobilisation du calcium provient du réticulum endoplasmique, et non des réserves calciques du lysosome. L'influx de calcium est un processus distinct de la formation du pore. Mais le processus initial d'interaction entre la PVL et le récepteur joue un grand rôle dans la mobilisation du calcium.

La PVL induit différentes réactions dans différents types de cellules. Pour les PMNs, la PVL provoque l'apoptose ou une nécrose, une sécrétion d'IL-8, de leucotriène-B4, d'histamine, des enzymes granulaires et des radicaux oxygénés. La PVL active les monocytes et les macrophages pour produire l'inflammasome NLRP3 qui provoque la libération d'IL-1β et d'IL-18. Pour les neurones, la PVL entraîne la mobilisation du calcium et la libération de glutamate. Au total, la PVL entraîne le recrutement et la lyse des leucocytes, favorise la vasodilatation, l'invasion des cellules, et la nécrose des tissus.

La rétine est le tissu neuronal la plus interne du globe oculaire. Elle transforme la lumière en message électrique et envoie cet influx nerveux au système nerveux central pour former une image. Histologiquement, la rétine est constituée de 10 couches. Elle est constituée des cellules neuronales comme les cellules ganglionnaires, l'amacrine, les cellules bipolaires et les photorécepteurs, et des cellules gliales comme les cellules de Müller, les cellules microgliales et les astrocytes. Les cellules de Müller prolongent la rétine. Les cellules microgliales sont dans la partie interne de la rétine. Les cellules ganglionnaires sont dans la couche superficielle du côté interne de la rétine, dont les axons constituent le nerf optique. Du coté interne, la rétine est vascularisée par l'artère de la rétine, qui est

divise en trois couches des vaisseaux. A l'extérieur, les nutriments sont apportés par l'artère choroïde.

L'endophtalmie bactérienne est une infection bactérienne à l'intérieur de l'œil. Les symptômes sont la baisse de l'acuité visuelle, la douleur et la rougeur oculaire, l'hypopion. L'endophtalmie est divisée en endophtalmie postopératoire, post-traumatique et endogène selon l'état initial. Les réactions inflammatoires de la rétine comprennent : la libération de cytokines, l'infiltration des neutrophiles, la perte architecturale et fonctionnelle de la rétine Le pronostic endophtalmie est variable. Des endophtalmies ont de mauvais pronostic, même après une prise en charge appropriée, telle qu'une vitrectomie et une antibiothérapie intravitréenne. Environ 20% des patients ont une acuité visuelle de 20/100 ou moins, même l'énucléation. De nombreux facteurs contribuent au mauvais pronostic, tels que le retard de la mise en place du traitement et le type de bactérie infectieuse. L'endophtalmie causées par des souches virulentes telles que *S. aureus,* sont souvent difficiles à traiter et entraînent une baisse de l'acuité visuelle.

Objectif

La virulence de la bactérie isolée est un facteur important pour le pronostic d'endophtalmie. *S. aureus* est la bactérie virulente la plus fréquente dans l'endophtalmie, la PVL est une toxine qui s'attaque aux cellules de l'hôte. Nous voulons analyser le rôle de la PVL dans l'endophtalmie et rechercher si la PVL pourrait affecter la rétine par des cibles neuronales. À la place de la bactérie, nous avons injecté la LPV dans le vitré du lapin. Donc, nous avons cherché les cellules rétiniennes ciblées par la LPV et analysé la réponse rétinienne inflammatoire éventuelle. Et puis, nous avons employé l'explant rétinien et essayé de développer un modèle *ex vivo*, qui sera utilisable dans le futur.

Résultats

Article 1

Nous avons fait l'injection intravitréenne de la LPV, les lapins ont été sacrifiés à 30 min, 1, 2, 4 et 8 h. Nous trouvons la LPV localisée sur la couche de cellules ganglionnaires. Cette couche est constituée de deux types de cellules, les cellules ganglionnaires et les cellules amacrines déplacées. Nous avons fait deux double-marquages (anti-PVL et anti-RBPMS marquant les cellules ganglionnaires, anti-PVL et anti-CHAT marquant les cellules amacrines déplacées). Ces images montrent que la LPV est co-localisée avec les cellules ganglionnaires et les cellules amacrines déplacées, avec des tendances différentes. Le taux de cellules ganglionnaires positifs à la PVL a augmenté, passant de 47% à 30 min à 98% à 2 h. Alors que le taux des cellules amacrines déplacées positifs pour la PVL a diminué, passant de 68% à 30 min à 5% à 4 h. Ces taux étaient stables de 4 à 8 h. Nous avons identifié l'expression de C5aR et C5L2 dans la rétine. Nous avons trouvé une immunofluorescence spécifique de C5aR dans la couche de cellule ganglionnaire. Nous avons fait deux double-marquages (anti-C5aR et anti-RBPMS, anti-C5aR et anti-CHAT). Il montre que C5aR est colocalisé avec les cellules ganglionnaires, mais pas avec les cellules amacrines déplacée. Alors qu'il n'a aucune immunofluorescence spécifique de C5L2 dans la rétine.

Les cellules ganglionnaires sont colocalisées avec C5aR. La LPV est bien colocalisée avec

les cellules ganglionnaires. Nous pouvons en déduire que la PVL est liée au C5aR sur les cellules ganglionnaires. Les cellules amacrine déplacées n'exprimaient pas le C5aR, mais ils étaient colocalisés de manière transitoire avec la PVL. Nous pensons qu'il y a un autre mécanisme par lequel la PVL se fixe sur les cellules amacrine déplacées, probablement un autre récepteur.

L'activation de la cellule de Müller est caractérisée par l'augmentation de la protéine acide fibrillaire gliale (GFAP). Les cellules de Müller sont marquées par l'anticorps anti-GFAP. Dès 30 min après l'injection de la PVL, les cellules de Müller expriment anormalement la GFAP dans la partie externe de la rétine. Contrairement au témoin, cette anomalie s'accentue de 30 min à 4 h.
Quant aux cellules microgliales, à 2 h, leurs corps sont élargis et leurs dendrites sont atrophiés, c'est un état d'activation précoce. Après 4 h, leurs dendrites ont disparu.

L'apoptose a été observée dans la rétine 4 h après l'injection de la PVL et augmente à 8 h. Pour identifier le type cellulaire en apoptose, nous avons fait trois double-marquages (TUNEL et anti-RBPMS, TUNEL et anti-CHAT, TUNEL et GSAI-B4, une lectine marquant cellules microgliales). Les images montrent que la cellule en apoptose est une cellule microgliale. L'apoptose microgliale pourrait être due à l'activation excessive par la PVL. Alors qu'il n'y pas de double marquage pour les cellules ganglionnaires et les cellules amacrine déplacées.
Les cellules gliales sont activées, qui est en général lié à l'apoptose neuronal dans la rétine. Cependant, dans cette étude, nous n'avons pu détecter aucun dommage neuronal au moins 8 heures après l'injection de la LPV.

Nous avons également montré l'augmentation de l'immunofluorescence de la nitrotyrosine dans la rétine traitée par la PVL par rapport aux témoins. La nitrotyrosine est un métabolite d'oxygène nitrique. Concernant les facteurs inflammatoires, la RT-qPCR a montré que seul IL-6 a significativement augmenté. Le Western blot a également montré l'augmentation de la nitrotyrosine et de l'IL-6. L'augmentation de la nitrotyrosine reflète un processus inflammatoire avec une production de l'oxyde nitrique. L'expression accrue de l'IL-6 pourrait être due l'activation gliales et jouer un rôle important dans l'inflammation de la rétine.

Article 2

Un des facteurs qui limite les recherches de la PVL sur la rétine provient du fait que la PVL ne reconnaisse que des récepteurs d'humain et du lapin. En termes d'éthique animal, l'usage de lapin est très limité pour l'expérimentation. L'explant ne dispose pas d'apport sanguin, dépourvu des leucocytes. On peut analyser directement les effets de la PVL sur les neurones rétiniennes. Dans le deuxième article, nous avons essayé de chercher s'il était possible d'obtenir des résultats similaires dans l'explant rétinien, un modèle *ex vivo,* en utilisant moins des lapins. La rétine est disséquée de l'œil et placée immédiatement sur une membrane semi-perméable insérée dans un puits. La membrane est maintenue juste en contact avec le milieu de culture. Ce système de culture maintient

l'explant rétinien en condition d'air liquide, optimale pour préserver la vitalité des explants.

La PVL est localisée dans la couche de cellule ganglionnaire et la couche nucléaire interne. On a fait cinq double-marquages, anti-PVL et anti-RBPMS, anti-PVL et anti-CHAT, anti-PVL et anti-Calbindin qui marque les cellules AII amacrine, anti-PVL et anti-Calretinin qui marque certaine cellules bipolaires et horizontale, anti-C5aR et anti-RBPMS. La LPV co-localise avec des cellules ganglionnaires. Les cellules ganglionnaires co-localisent avec C5aR (en rouge). Les autre trois double-marquages (anti-PVL et anti-CHAT, anti-PVL et anti-Calbindin, anti-PVL et anti-Calretinin) sont négatifs avant 4 h. Nous n'avons donc pas réussi à identifier le type de ces cellules positives à la PVL dans la couche nucléaire interne. À 8 et 24 h après le traitement à la LPV, la LPV est co-localisé avec certaines cellules horizontales. Le pourcentage moyen des cellules ganglionnaires positives à la PVL était de 34% à 30 min et de 45% à 24 h. Le taux n'a pas changé significativement entre 30 min et 24 h.

Dans les explants témoins, les cellules de Müller ont un aspect normal entre 2 et 24 h. Alors que, dans des explants traités à la PVL (1,76 µM), les cellules de Müller présentent une extension anormale dans la couche nucléaire externe, qui augmentent de 2 à 24 h. Quand les explants sont traités par la PVL à grande concentration, les cellules de Müller sont dissociées, les noyaux nucléaires sont désorganisés, l'architecture rétinienne était endommagée. Cette défiguration de la rétine peut être liée à un dysfonctionnement des cellules de Müller.
Dans les explants témoins, les cellules microgliales ont rétracté leurs dendrites après 24 h de la culture. Alors que dans les explants traités par la LPV, les cellules microgliales ont été transformées en forme amiboïde, perdant tous leurs dendrites à 2 h. Dans des explants traités par la PLV de différentes concentrations à 8 h et 24 h, les cellules de Müller présentent une augmentation de GFAP dans la couche nucléaire externe jusqu'à leur dissociation avec l'augmentation de la concentration de la PVL. À 2 h, les cellules microgliales perdent plus leurs dendrites, et le nombre des cellules microgliales diminue, les noyaux nucléaires sont plus petits avec l'augmentation de la concentration de la PVL. On peut voir que l'activation des cellules de Müller et microgliales augmentent avec la concentration de LPV.

Dans les explants témoins, quelques apoptoses ont été trouvées seulement 24 h après la culture. Dans les explants traités par la PVL, plusieurs apoptoses ont été trouvées des 4 h, et le nombre des cellules en apoptoses augmente à 8 et 24 h. Nous avons effectué les comptages des cellules en apoptose par champ d'étude. Le nombre des cellules en apoptose augment avec la concentration de la PVL et le temps du traitement. Au total, les explants traités à la LPV présentent beaucoup plus de cellules en apoptose que les explants témoins.
Pour identifier quelles cellules sont en apoptose, nous avons fait des double-marquages entre TUNEL et des marquages spécifiques des types de cellules rétiniennes (TUNEL et anti-RBPMS, TUNEL et anti-CHAT, TUNEL et anti-calbindin, TUNEL et anti-Calretinin,

TUNEL et GSAI-B4). Ces images montrent que certaines cellules microgliales et cellules amacrines sont en apoptose. L'apoptose des cellules amacrines pourrait être dues à la libération excessive de glutamate provoquée par la PLV. Mais, les cellules ganglionnaires ne sont pas montrées apoptotiques. Ces trois sub-populations des cellules amacrines ne sont pas les cellules amacrines en apoptose.

On utilise RT-qPCR pour analyser l'expression des facteurs inflammatoires. Quatre heures après la culture, les explants témoins ont augmenté l'expression de l'IL-6 et de l'IL-8. Inversement, l'expression d'IL-6 et d'IL-8 n'a pas augmenté chez les explants traités à la PVL. Après 8 h de la culture, les explants traités à la LPV ont augmenté l'expression d'IL-6 et d'IL-8. Cependant, les taux de l'expression d'IL-6 et d'IL-8 restent en dessous des témoins. Il semble qu'IL-6 et IL-8 ne sont pas les facteurs responsables pour l'activation des cellules gliales, mais ils sont produits par les cellules gliales activées. Dans les explants traites à la LPV, les cellules de Müller et microgliales sont trop perturbées pour exprimer des facteurs inflammatoires. Le facteur causatif pour l'activation des cellules gliales reste à identifier.

Article 3

La PVL ciblait les neurones rétiniens et induit l'activation des cellules gliales et l'inflammation rétinienne. Par quel mécanisme ? Nous avons recherche dans la littérature et nous pensons que c'est probablement l'inflammation neurogène.

L'inflammation neurogène survient après l'activation des terminaisons neuronales, qui libèrent des neurotransmetteurs, entraînant une extravasation plasmatique et une perméabilité vasculaire. Les principaux neurotransmetteurs sont le peptide lié au gène de la calcitonine (CGRP), la substance P et le glutamate, dont leur libération dépende en définitive de la mobilisation du calcium intracellulaire. Dans les littératures, les facteurs de virulence bactériens peuvent activer directement les neurones et provoquer la mobilisation du calcium intracellulaire et des effets inflammatoires. Nous en déduisons que la PVL interagit rapidement avec les neurones pour libérer des neurotransmetteurs, entraînant une extravasation vasculaire et une rupture de la barrière hémato-rétinienne. L'inflammation rétinienne est amplifiée par l'infiltration cellulaire immunitaire et l'activation des cellules gliales rétiniennes.

Discussion

Dans les deux modèles, les cellules ganglionnaires exprimant C5aR sont les cellules principales ciblées par la PVL. Des cellules amacrines sont aussi colocalisées avec la PVL. Mais ils montrent une affinité faible avec la PVL. Il y a peut-être un autre récepteur pour que la PVL se lie sur les cellules amacrines.

Les différences de cibles cellulaires entre les rétines *in vivo* et *ex vivo* pourraient être dues à des mécanismes différents liés à la diffusion de la LPV dans la rétine. L'explant rétinien ne dispose pas d'un apport sanguin et le système vasculaire rétinien se contracte rapidement. La LPV pourrait diffuser plus efficacement à travers la rétine et atteindre les cellules horizontales.

Dans les deux modèles, aucune cellule ganglionnaire n'est entrée en apoptose, alors

qu'elle semblait être le type de cellule privilégiée par la LPV. Ces résultats sont correspondants à la précèdent étude, dans laquelle la PVL provoque la mobilisation du calcium intracellulaire et la libération du glutamate chez neurones cérébraux et radicaux, sans provoquant la mort des neurones.

La LPV induit une augmentation de l'IL-6 dans un modèle *in vivo*, tandis que l'expression de l'IL-6 dans les explants traités à la LPV est plus faible que chez les témoins dans notre modèle d'explant rétinien. Dans les explants rétiniens témoins, l'expression d'IL-6 and d'IL-8 a augmenté à 4 et 8 h, mais les cellules gliales n'étaient pas activées avant 8 h. Etonnamment, sur les explants traite à la PVL, malgré une augmentation moindre de l'expression d'IL-6, les cellules gliales étaient actives des 2 h. IL-6 n'apparait donc pas comme le facteur responsable pour l'activation des cellules gliales. Le facteur causal pour l'activation des cellules gliales reste à identifier.

Nous pensons que l'explant rétinien peut être utilisé pour étudier les effets de la PVL et les traitements éventuels en évaluant l'activation des cellules gliales et l'apoptose des cellules amacrines. En ce qui concerne les cytokines et les voies d'inflammation, il devrait être intéressant de rechercher d'autres facteurs inflammatoires comme les neurotransmetteurs dans l'explant rétinien ou dans le modèle *in vivo*.

Perspectives

L'explant est reproductible et facile à manipuler. Il permet de réduire le nombre de lapin utilise. Il pourrait servir aux recherches futures pour explorer le mécanisme moléculaire de la PVL sur les cellules neuronales.

Les cellules ganglionnaires se trouvent à la surface de l'explant rétinien, ce qui facilite leur visualisation pour l'imagerie du calcium. Cette imagerie du calcium pourrait prouver que la LPV interagit avec les cellules ganglionnaires et provoque la mobilisation du calcium. Les antagonistes des neurotransmetteurs et des canaux calciques pourraient être ajoutés aux explants rétiniens, pour essayer de modifier les effets de la LPV sur la rétine et valider l'inflammation neurogène dans la PVL intoxication rétiniennes. Les inhibiteurs des récepteurs du glutamate pourraient valider l'hypothèse selon laquelle l'apoptose des cellules amacrines serait due à une libération excessive de glutamate. Le blocage de C5aR pourrait mettre en évidence d'autres récepteurs pour la LPV.

S. aureus positive à la LPV est rare en France, 2-5%, mais beaucoup plus fréquente dans les pays en développement. Nous pourrions évaluer l'impact de la LPV sur l'endophtalmie par une étude clinique dans les pays en développement. On peut analyser la prévalence de *S. aureus* positive à la PVL, leur symptôme clinique et leur pronostic, ainsi que l'expression d'IL-6 dans l'humeur aqueuse.

Xuanli LIU

Rôle de la leucocidine de Panton-Valentine dans l'infection oculaire *staphylococcique*

Résumé

Staphylococcus aureus est une bactérie responsable de nombreuses infections chez l'homme. Divers facteurs de virulence sont décrits comme ayant un rôle aggravant dans l'infection staphylococcique. La leucocidine de Panton-Valentine (LPV) en est un. Elle agit par l'intermédiaire du récepteur de C5a (C5aR). Elle interagit avec les leucocytes et les cellules neuronales dans différents tissus, mais son action au niveau rétinien est méconnue. La LPV, pourrait-elle inciter de l'inflammation à partir des cibles neuronales ? Nous avons recherché des cibles rétiniennes cellulaires de l'intoxination à la LPV et étudié ses conséquences cellulaires et inflammatoires précoces dans les tissus rétiniens.

AINSI, deux modèles de lapins ont été créés : l'injection intravitréenne *in vivo* de LPV et les explants rétiniens *ex vivo* traités par la LPV. Dans les deux modèles, les cellules ganglionnaires étaient les principales cibles cellulaires rétiniennes de la LPV et le seul type de neurones rétiniennes qui exprimait C5aR. Les cellules de Müller comme la microglie étaient activées. Certains résultats restaient contradictoires: dans le modèle *in vivo*, la LPV fixait transitoirement des cellules amacrines, la nitrotyrosine et de l'IL-6 étaient hyperexprimés dans les tissus rétiniens. Dans l'explant *ex vivo*, la LPV fixait tardivement des cellules horizontales, elle fixait peut-être aussi des autres cellules amacrines, l'IL-6 était peu exprimée. Une faible apoptose neuronale était notée sur les explants seuls. Malgré ces contradictions, l'explant rétinien était facilement manipulé et montrait les cibles cellulaires de la LPV et des activations des cellules gliales, ils peuvent continuer servir à la recherche des effets de la LPV sur la rétine. La LPV seule pourrait induire une inflammation rétinienne après avoir ciblé spécifiquement les cellules neuronales.

Résumé en anglais

Staphylococcus aureus is a ubiquitous pathogen and second bacteria responsible for nosocomial infections. It secretes various virulence factors. Panton-Valentine leucocidin (PVL) is a virulent leukotoxin from *S. aureus* and presents active effects towards leukocytes and neuronal cells. It reacts via the C5a receptor (C5aR). The effects of PVL on retina is little known. Could PVL incite inflammation after targeting neurons? We explored PVL retinal cell target and early retinal inflammation and tried to find the processes of bacterial toxins aggravating bacterial endophthalmitis.

We employed two different rabbit models to study the PVL effects on retina: intravitreal injection of PVL *in vivo* and retinal explant *ex vivo*. We showed that retinal ganglion cells were the only retinal neurons which express C5aR and the major cell targets of PVL. PVL induced Müller and microglial cell activation. Two models showed somehow different results: In *in vivo* animal model, PVL transiently colocalized with displaced amacrine cells, nitrotyrosine and IL-6 expression increased in retina. In *ex vivo* explant, PVL colocalized later with some horizontal cells and possibly with a subpopulation of amacrine cells. Some neuronal apoptosis was noticed only on retinal explants after PVL treatment. Despite these inconsistencies, the retinal explants were easily manipulated and showed obvious cellular targets of PVL and glial cell activations, they can contribute to research the effects of PVL on retina. PVL alone without *S. aureus* could induce great inflammation in retina after targeting retinal neurons.